NASA Contractor Report 4740

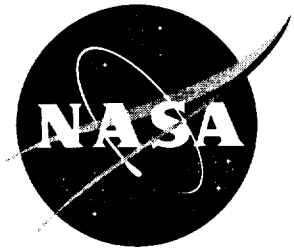

Contamination Control Engineering Design Guidelines for the Aerospace Community

A.C. Tribble, B. Boyadjian, J. Davis, J. Haffner, and E. McCullough
Rockwell International Corporation
Downey, CA

National Aeronautics and Space Administration
Marshall Space Flight Center • MSFC, Alabama 35812

Prepared for Goddard Space Flight Center
under Contract NAS5–32876 and sponsored
by the Space Environments and Effects Program
managed at the Marshall Space Flight Center

May 1996

FOREWORD

This report describes work accomplished under contract NAS5-32876 from the NASA Goddard Space Flight Center as part of the NASA Space Environment Effects Program.

Prior to 1 October 1995, the Space Environment Effects Program Manager was Ms. Joan Funk, NASA Langley Research Center. Subsequent to 1 October 1995, the Space Environment Effects Program Manager was Mr. Steve Pearson, NASA Marshall Space Flight Center. Dr. Philip Chen, NASA Goddard Space Flight Center, was the Technical Monitor. The following Rockwell International personnel provided support during this program:

Dr. Alan Tribble	Principal Investigator
Mr. Berge Boyadjian	Expert Systems Software
Mr. John Davis	Optical Sensor Design
Dr. James Haffner	Contamination Control
Mr. Edward Mc Cullough	Hypertext Software

Questions or comments on this manuscript should be directed to:

Dr. Alan Tribble
Rockwell International
P.O. Box 7009
Downey, CA 90241-7009

Phone: 310-922-4763
Fax: 310-922-5822
Email: *actribbl@ssd.rockwell.com*

TABLE OF CONTENTS

FIGURES

TABLES

ACRONYMS

AGE	Aerospace Ground Equipment
ASTM	American Society for Testing and Materials
BOL	Beginning of Life
CCB	Contamination Control Board
CCE	Contamination Control Engineering
CVCM	Collected Volatile Condensable Material
DF	Degradation Factor
EOL	End of Life
FED	Federal
FPA	Focal Plane Array
GC	Generally Clean
GN_2	Gaseous Nitrogen (N_2)
HDBK	Handbook
HEPA	High Efficiency Particle Air
IES	Institute of Environmental Sciences
IR	Infrared; Impact Rate
JSC	Johnson Space Center
MIL	Military
MLI	Multi-Layer Insulation
MWIR	Midwave Infrared
NASA	National Aeronautics and Space Administration
NVR	Non-Volatile Residue
OSR	Optical Solar Reflector
PAC	Percent Area Coverage
QCM	Quartz Crystal Microbalance
SC	Sticking Coefficient
SNR	Signal to Noise Ratio
SO	Surface Obscuration
STD	Standard
TBD	To Be Determined
TBR	To Be Reviewed
TML	Total Mass Loss
ULPA	Ultrahigh Efficiency Particle Air
UV	Ultraviolet
VC	Visibly Clean
VCM	Volatile Condensable Material

1. Introduction

1.1 Objective

Contamination may be simply defined as any foreign matter. In general, contamination is grouped into two broad categories labeled *molecular* and *particulate*. Molecular contamination refers to the cumulative buildup of individual molecules of foreign matter. An example of molecular contamination is the familiar odor of plastics or the "new car smell". These are indications of volatile molecules being generated by organic materials. Molecular contamination may occur during ground processing, but is usually of more concern on orbit, (H_2O especially). Particulate contamination refers to the deposition of visible, (μm sized), conglomerations of matter. Surfaces that become dusty and eyeglasses that require periodic wiping are an indication of the presence of particles in the atmosphere. These particles, which are deposited mainly during ground operations, will fall from the air onto exposed surfaces.

Effective contamination control is essential for the success of most aerospace programs because the presence of contamination, even in miniscule quantities, can degrade the performance of spacecraft hardware. The presence of contamination on thermal control surfaces will alter absorptance/emittance ratios and change thermal balance, while contamination on solar arrays will decrease power output. Contamination in optical instruments will decrease signal throughput and can scatter the signal beyond the diffraction design, thus further decreasing performance. The end result of contamination may be intuitively obvious. What is not obvious, however, is how one: a) quantifies the critical level of contamination, and b) enforces contamination control to ensure compliance with requirements. Consequently, the objective of this document is two-fold. First, to furnish spacecraft system engineers and payload providers with a means of quantifying the contamination cleanliness levels required for proper performance of their equipment, and second, to provide insight into what procedures and processes will have to be maintained during fabrication, assembly, integration, test, launch and operation in order to maintain those levels on orbit.

As illustrated in Figure 1-1, contamination control for a space program is an iterative process that flows from the mission objective directly into design and operations.

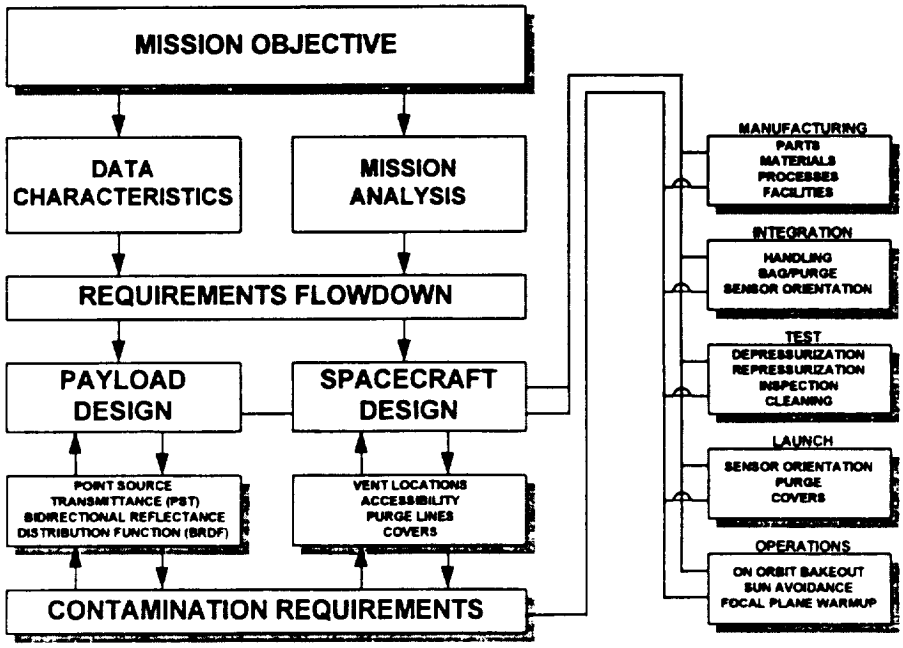

Figure 1-1. Contamination control and its relation to spacecraft design.

Most spacecraft flying remote sensing instrumentation are exceptionally sensitive to contamination. A mission objective that involves gathering remote sensing data would first define the type of optical data that is needed in terms of the waveband of interest, signal strength, resolution, and related parameters. The constraints that these values place on the design of a payload will be traded as a function of other mission parameters such as orbital altitude, inclination, eccentricity, relation to other satellites in the constellation (if applicable), and so on. Once a suitable optimum has been achieved, the system level trades flow down requirements onto the design of the payload and the spacecraft. Once a point design is developed, the design margin between requirements and capabilities help determine the contamination requirements of the payload, thermal control surfaces, and solar arrays. These contamination limitations then place requirements on: choices of materials, vent paths, location of propulsion system thrusters, integration and test plans, orbital operations plans, power consumption profiles, duty cycles, payload temperatures, and so on. It may be necessary to iterate the design of the payload and subsystems several times in order to obtain a design that can be implemented economically.

This document is designed to provide insight into the contamination control process through descriptions of the basic physics governing the various contamination processes, illustrations of the steps that must be taken to prevent contamination from becoming a problem, and the inclusion of realistic examples from past programs. Terms and nomenclature are reviewed in this chapter, molecular contamination is examined in Chapter 2, and particulate contamination is examined in Chapter 3. The fourth chapter, Contamination Control, examines the various methodologies and procedures that may be required to enforce cleanliness levels. The fifth and final chapter provides a bibliography of applicable documents for those readers desiring more in depth knowledge on a particular subject. In total, the document is intended to provide a comprehensive view of contamination control and its importance to aerospace programs.

1.2 Nomenclature

1.2.1 Symbols

A = area (m^2); absorbed energy (W)
C = normalization constant
d = diameter (m)
E = energy (W)
f = frequency function
F = radiative view factor (m^2)
I = incident energy (W); spectral response (A/W)
IR = impact rate (Å/hr)
L = length (m); radiance (W m^{-2} sr^{-1})
m = mass (kg)
M = exitance (W m^{-2})
n = surface density of particles (m^{-2})
N = surface density of particles $\geq x$ (m^{-2}); air class
p = air flow parameter
P = pressure (N m^{-2})
q = heat flux (W)
Q = heat flux (W)
r = radius (m)
R = gas constant (kcal/mole); reflected energy (W)
S = solar flux (W m^{-2})
t = time (s)
T = temperature (K)
U = binding energy (W)
V = volume (m^3)
VF = view factor
x = contaminant thickness (μm); particle size (μm)
X = particle size (μm)

α = absorptance
β = angle (deg.)
ε = emittance
ϕ = angle (deg.)
γ = sticking coefficient
λ = wavelength (μm)
θ = number of molecular monolayers; angle (deg.)
ρ = reflectance; density (g cm^{-3})
σ = Boltzmann's constant
τ = transmittance; residence time (s)
ω = solid angle (sr^{-1})

1.2.2 Subscripts/Superscripts

a = activation
c = contamination
s = solar
n = normal

1.3 Definitions

1.3.1 Preferred Units of Measure

Microgram (μg) 10^{-6} gram = 3.5×10^{-8} ounce.
One microgram per square centimeter is approximately one milligram per square foot or 1.4×10^{-8} pound per square inch.

Micrometer (μm) 10^{-6} meter = 10^{-4} cm = 3.94×10^{-5} in. = 0.0394 mils.

Milligram (mg) 10^{-3} gram = 3.5×10^{-5} ounce.

Nanogram (ng) 10^{-9} gram = 3.5×10^{-11} ounce.

1.3.2 Alternative Units of Measure

Angstrom (Å) 10^{-10} meter = 10^{-8} cm = 10^{-4} μ = 3.94×10^{-9} in. = 3.94×10^{-6} mils.
A water molecule is approximately 3 Å in diameter. A film of water 100 Å thick provides a film of one microgram per square centimeter and is approximately 33 molecular layers thick.

Micron (μm) 10^{-6} meter. An older term for micrometer.

1.3.3 Terms

Air Quality

Air quality classifications, as defined by FED-STD-209E, are specified by the maximum allowable number of particles per cubic foot, (or cubic meter), of air. The name of the class in English units, (the usual convention in the U.S.), is taken from the maximum allowable number of particles, 0.5 μm and larger, per cubic foot. *Class 350,000* air is typically referred to as a "good housekeeping area" and is suitable for most integration and assembly operations. *Class 100,000 – Class 1,000* air is referred to as a "cleanroom" and is required for installation of most space system hardware. Within the cleanroom, a laminar flow bench may provide *Class 100* air which is required for operations involving the exposure of sensitive optical surfaces. In SI units, the name is taken from the logarithm, base 10, of the maximum allowable number of particles, 0.5 μm and larger, per cubic meter. *Class M5.5* is equivalent to *Class 10,000*, and so on. (For more information on FED-STD-209E, see section 3.3.1.)

Bidirectional Reflectance Distribution Function (BRDF)

The ratio of reflected radiance off a scattering surface to the incident irradiance. BRDF may be a function of the angle of incidence, angle of reflection, irradiance, and wavelength. (For more information on BRDF, see section 3.2.3.)

Cleanliness Level

An established maximum allowable amount of contamination in a given are or volume or on a component. See also *Air Quality* and *Surface Cleanliness*.

Clean Work Station

A limited area over which more stringent cleanliness levels are maintained within a larger cleanroom, e.g., *Class 100* laminar flow clean benches within a *Class 100,000* cleanroom.

Cleanroom

A cleanroom is an enclosed area employing control over the particle and molecular matter in the air in addition to controls on temperature, humidity, and pressure, as required. A cleanroom may be described as *Class 100,000*, *Class 10,000*, etc., in accordance with FED-STD-209E. In addition to air cleanliness, the cleanroom class also defines design and operating requirements (air filtration, air flow rates, etc.) as well as the maximum allowable contamination in the air. General guidelines and operational constraints for cleanrooms are contained in Air Force T.O. 00-25-203.

Collected Volatile Condensable Material (CVCM)

The quantity of outgassed matter from a test specimen that condenses on a collector maintained at a specific constant temperature for a specified time. CVCM is expressed as a percentage of the initial specimen mass and is calculated from the condensate mass determined from the difference in mass of the collector plate before and after the test. The test conditions ASTM E 595, or ASTM E 1559, may be used to determine CVCM. (For information on ASTM E 595 or ASTM E 1559, see sections 2.3.1.1.1 or 2.3.1.1.2, respectively.)

Contaminant

A specific type of contamination.

Contamination

Any foreign material. More explicitly, undesired foreign material (particles or molecular films) lying on the surface of a solid material or incorporated in a gas or liquid. On orbit, this may also include particles floating within the field of view of a sensor.

Contamination Control

Any organized action to control the level of contamination.

Contamination Control Board (CCB)

Organized body of individuals charged with enforcing contamination control for a given program. The board is usually chaired by the lead contamination control engineer and contains representatives from: design, materials & processes, manufacturing, test, quality assurance, and others as deemed necessary.

Controlled Work Area

A manufacturing, assembly, or test area for which controls and procedures are implemented that result in the control of contamination when proper procedures are incorporated. Airborne hydrocarbon, temperature, humidity, and particle distribution are controlled. Good housekeeping practice and selected cleanroom controls and procedures are imposed, but full cleanroom requirements may not be met.

Conventional Industrial Area

An area where contamination is not controlled.

Demonstrated Equivalence

The condition where a method of measurement has passed a series of tests to show that it gives equivalent results to those of a standard measurement.

Fiber

A particle whose length-to-width ratio is in excess of 10:1, with a minimum length of 100 μm.

Generally Clean (GC)

Freedom from manufacturing residue, dirt, oil, grease, debris or other extraneous contamination. This level can be achieved by washing, wiping, vacuuming, brushing, or rinsing. This level shall not be designated for hardware that is sensitive to contamination.

Good Housekeeping Area

An enclosed area used for detail fabrication and operations where parts can be subsequently cleaned. The following criteria are used:

1) Enclosed area with cleanable floors and walls.

2) Operations which generate NVR are prohibited.

3) Particles are not allowed to accumulate to visible levels; temperature and particle count are controlled.

4) Limited shop operations (no heavy machining, grinding, welding, degreasing, rinsing, paint spraying, etc.).

5) Limited access to personnel and equipment. Training in cleanliness required for personnel. No smoking or eating.

6) *Class 350,000* air or better.

Gross Cleaning

General cleaning to remove contaminants such as weld scale, heat treat scale, corrosion, oils, grease, shop films and deposits. The cleanliness level achieved by gross cleaning normally does not require inspection other than visual. Gross cleaning is considered normal shop practice and is defined by applicable Process Specifications.

HEPA Filter

High efficiency particle air (HEPA) filter used in cleanrooms, clean benches, and in other places where low airborne particle counts are required. Sometimes referred to as a "99.97% filter" because it removes 99.97% or more of the particles 0.3 μm or larger.

Laminar Flow

Flow in which the clean air moves in defined streamlines from inlet to outlet without eddies or areas of turbulence which would carry contamination upstream

Molecular Contamination

Undesired foreign film matter without definite dimension. This includes corrosive and noncorrosive films resulting from oil, greases, chemical residues, fingerprints, heat and vacuum applications, chemical action and incompatible materials. Such films often arise from a process called outgassing. Molecular contamination films can sometimes form into droplets or beads which can be better treated as particles.

Nonvolatile Residue (NVR)

Soluble material remaining after controlled evaporation of a volatile liquid or determined by special purpose analytical instruments, usually measured in milligrams per unit volume, or per unit area for surfaces. Generally applies to residue from ground operations, rather than on orbit outgassing. (See MIL-STD-1246C, section 2.2.1, for more information.)

Particle
Matter with observable length, width, and thickness usually measured in μm. This includes fibers.

Particle Size
The apparent maximum linear dimension or diameter of the particle.

Particulate Contamination
Undesired foreign material of miniature size with observable length, width, and thickness.

Percent Area Coverage
An alternative method of specifying particle levels on a surface, found by dividing the total surface area of all particles on a surface by the area of the clean surface.

Purge
To flow gas through a system, (e.g., a line, pipe, or tube), for the purpose of removing a residual fluid, (a gas or liquid), or to provide a positive flow of gas from some opening in the system to prevent the entry of contamination.

Precision Cleaning
Cleaning of hardware surfaces to meet a specific surface cleanliness level. Precision cleaning is accomplished by ultrasonic cleaning and/or solvent flush, by solvent wipe, or by vacuuming and/or nitrogen purge or other methods currently in development, in a controlled area. Precision cleaned articles shall be packaged, protected, or shall be kept in an appropriate clean area after cleaning.

Sensitive Surface (also, Critical Surface)
A surface of an item or structure w contamination beyond a given degree will degrade end of life performance to less than that sp ied for the mission.

Significant Surface
Any surface of an item or product which is required to meet established cleanliness level requirements.

Solvent Flushing
A method of cleaning surfaces with a stream of filtered solvent under pressure, directed against a surface to dislodge and flush away contamination.

Surface Cleanliness
Surface cleanliness may be usefully specified by MIL-STD-1246C. Particulate levels are specified by the size of the largest particle, in μm, per square foot, (or per 0.1 square meters), of significant surface area. That is, surface level 100 implies that there is at most one 100 μm particle per square foot of surface area. Molecular contamination levels are specified in milligrams per 0.1 square meters of significant surface area. The molecular contamination level may be converted to contamination thickness if the density of contaminants is known. (A density of one gram per cubic centimeter may be assumed for most non-volatile residue, molecular contaminants.) Cleanliness level 100 refers just to particles, cleanliness level A refers just to molecular, while cleanliness level 100A refers to both. (For more information on molecular cleanliness, see section 2.2.1. For more information on particle cleanliness, see section 3.2.1.)

Surface Defect
Voids or undesired foreign material incorporated into the surface of a solid material in the course of production operations.

Total Mass Loss (TML)

Total amount of material that is outgassed from a specimen that is maintained at a specified constant temperature and operating pressure for a specified time. TML is calculated from the mass of the specimen as measured before and after the test and is expressed as a percentage of the initial specimen mass. The test conditions specified by ASTM E 595 may be used to determine TML. (For more information on ASTM E 595, see section 2.3.1.1.1.)

ULPA Filter

Ultrahigh efficiency particle air (ULPA) filter used in areas requiring the most stringent controls. It removes 99.9995% of the particles 0.12 μm or larger.

Visibly Clean (VC)

The absence of all particle and molecular contamination when viewed by a normal unaided, (except corrected vision), eye. VC levels are quantified by NASA-SN-C-0005, (sections 3.2.4 and 4.2.3.1.)

Volatile Condensable Material (VCM)

The outgassed matter from a material that may condense on a collector, usually one at a lower temperature. See also, *collected volatile condensable material.*

2. Quantifying Molecular Contamination Level Requirements

2.1 Effects of Molecular Films

Consider a ray of light that is incident upon a surface that is designed to be partially reflective and partially transmissive, Figure 2-1. Conservation of energy requires that the total of the energy that is reflected back to space, R, absorbed by the surface, A, and transmitted through the surface, T, be equal to the incident energy, I. In terms of the normalized energies, this is

$$\rho + \alpha + \tau = 1, \qquad \textbf{Equation 2-1}$$

where $\rho = R/I$ is the reflectance, $\alpha = A/I$ is the absorptance, and $\tau = T/I$ is the transmittance. Because of the fundamental nature of materials, ρ, α, and τ will be functions of the angle of incidence, polarization, and wavelength of the incident energy. In general, absorptance may be inferred from experimentally determined values of reflectance and transmittance or from properties of bulk materials. Surfaces serving as mirrors or thermal radiators are usually made of materials that maximize reflectance and minimize transmittance. Baffles in optical and thermal systems require materials which absorb, or reflect, with a minimum of scattering. Other surfaces, such as solar array coverslides (broad band) or optical waveband filters (narrow band), are designed to maximize transmittance and minimize reflectance. As shown by Equation 2-1, the absorptance of a clean surface satisfies the relation

$$\alpha(\lambda) = 1 - \rho(\lambda) - \tau(\lambda). \qquad \textbf{Equation 2-2}$$

As will be seen shortly, in many problems of interest a surface is often designed so that either $\rho(\lambda)$ or $\tau(\lambda)$ is effectively zero.

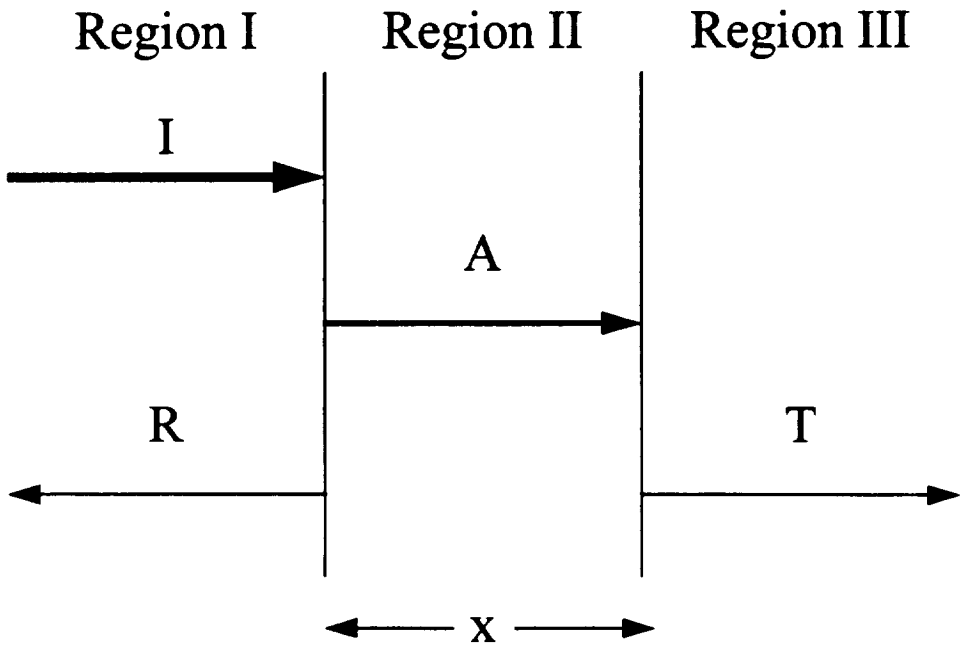

Figure 2-1. Incident (I), reflected (R), absorbed (A), and transmitted (T) energy.

In general, the energy drop over a region of thickness Δx is given by

$$\Delta I(\lambda,0) = I(\lambda,\Delta x) - I(\lambda,0), \qquad \textbf{Equation 2-3}$$

where $I(\lambda,\Delta x)$ is defined as the energy flux of wavelength λ reaching depth Δx. The amount of absorption can be expected to be directly proportional to the thickness of the region, Δx, and the amount of incident energy, $I(\lambda,0)$, so that

$$\Delta I(\lambda,0) = -\alpha_c(\lambda) I(\lambda,0)\Delta x, \qquad \textbf{Equation 2-4}$$

where $\alpha_c(\lambda)$ is defined to be the experimentally determined absorption coefficient of the contaminating layer. Solving Equation 2-4 it is seen that

$$I(\lambda,x) = I(\lambda,0)\exp\left[-\alpha_c(\lambda)x\right]. \qquad \textbf{Equation 2-5}$$

From the definition of absorption, the absorptance of a contaminated surface is therefore given by

$$\alpha^x(\lambda) = \alpha(\lambda)\left\{1 - \exp\left[-\alpha_c(\lambda)x\right]\right\}. \qquad \textbf{Equation 2-6}$$

Consider the specific case of a surface that is designed to be totally reflective, such as a mirror or a thermal radiator, but is covered with a thin layer of a contaminant film. That is, Region I of Figure 2-1 is free space, Region II is the contaminant layer, and Region III is a material that, (when clean), effectively salsifies the constraint $\tau(\lambda) = 0$. Substituting Equation 2-6 into Equation 2-2 produces an expression for the decrease in surface reflectance as a function of contamination thickness

$$\rho^x(\lambda) = \rho(\lambda)\exp\left[-2\alpha_c(\lambda)x\right]. \qquad \textbf{Equation 2-7}$$

Note that the factor of 2 is present in the exponential of Equation 2-7 because a ray of light would have to transverse the contaminant film, be reflected, and transverse the contaminant film a second time to avoid being absorbed. The equivalent expression for a surface that is designed to be totally transmissive, such as a solar array coverslide, is

$$\tau^x(\lambda) = \tau(\lambda)\exp\left[-\alpha_c(\lambda)x\right]. \qquad \textbf{Equation 2-8}$$

The factor of 2 does not appear in the exponential of Equation 2-8 because the ray of light need only transverse the contaminant film a single time before being transmitted.

2.1.1 Effects on Reflecting or Radiating Surfaces

Two important classes of surfaces that are degraded by molecular contamination are thermal control surfaces and mirrors, which would be part of the optical train of a telescope. As implied by Equation 2-6 through Equation 2-8, the effect of molecular contamination will be to alter surface properties.

2.1.1.1 Thermal Control Surfaces

In space, the primary source of heat energy to a spacecraft is usually the Sun. The air mass zero (AMO) solar flux as a function of wavelength, $S(\lambda)$, is illustrated in Figure 2-2. Integrating $S(\lambda)$ over all wavelengths gives the average value for the total solar flux, S, as 1350 ± 5 W/m^2 at the nominal Earth-Sun distance of 1 AU.[1]

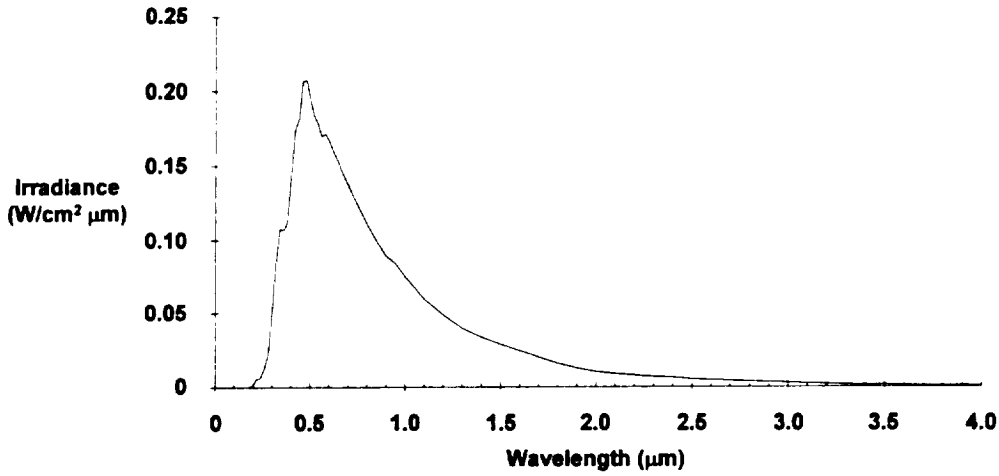

Figure 2-2. Solar flux as a function of wavelength.

An object will absorb heat, Q (W), from the Sun according to the relation

$$Q_{in} = \alpha_s A_n S, \qquad \textbf{Equation 2-9}$$

where A_n (m^2) is the surface area normal to the solar flux and α_s is the solar absorptance of the surface, which is defined by

$$\alpha_s = \frac{\int \alpha(\lambda) S(\lambda) d\lambda}{\int S(\lambda) d\lambda}. \qquad \textbf{Equation 2-10}$$

In space there is no air to aid in convective cooling, so a spacecraft can lose heat only by conducting it to cooler parts of the spacecraft, often with heat pipes, or by radiating it back to space. Radiation loss to space, assuming an unobstructed view, is described by the relation

$$Q_{out} = \varepsilon A_{tot} \sigma T^4, \qquad \textbf{Equation 2-11}$$

where ε is the emittance, (a fundamental property of the surface material), A_{tot} (m^2) is the total surface area, T (K) is the object temperature, and $\sigma = 5.67 \times 10^{-8}$ W/m^{2}K^4 is Boltzmann's constant. (Note that

[1] ASTM E 490, *Standard Solar Constant and Air Mass Zero Solar Spectral Irradiance Tables*, 27 September 1973.

ε may be a function of wavelength, but can usually be treated as a constant for a broadband radiating source.) An object will either heat up or cool down until the heat gain, (Equation 2-10), is balanced by an equivalent heat loss, (Equation 2-11). In a first approximation, one can assume that the material temperature is much greater than that of the surrounding space environment so that radiation to the vehicle from sources other than the Sun are small in comparison. (This is not always a valid assumption for a thermal engineer, especially in low Earth orbit where Earth albedo may be significant.) Subject to this constraint, the equilibrium temperature of the surface is approximated by

$$T = \left(\frac{\alpha_s}{\varepsilon}\right)^{1/4}\left(\frac{SA_n}{\sigma A_{tot}}\right)^{1/4} \approx \left(\frac{\alpha_s}{\varepsilon}\right)^{1/4}\left(\frac{A_n}{A_{tot}}\right)^{1/4}(392.8\ \mathrm{K}). \qquad \textbf{Equation 2-12}$$

As an example, consider the case of a sphere which produces no internal energy with $A_n = \pi r^2$ and $A_{tot} = 4\pi r^2$. The blackbody ($\alpha_s/\varepsilon = 1$) temperature of a sphere at the distance of the orbit of the planets is shown in Figure 2-3. For comparison, the equilibrium temperature of a sphere and of an inclined plane, as a function of α_s/ε, is shown in Figure 2-4.

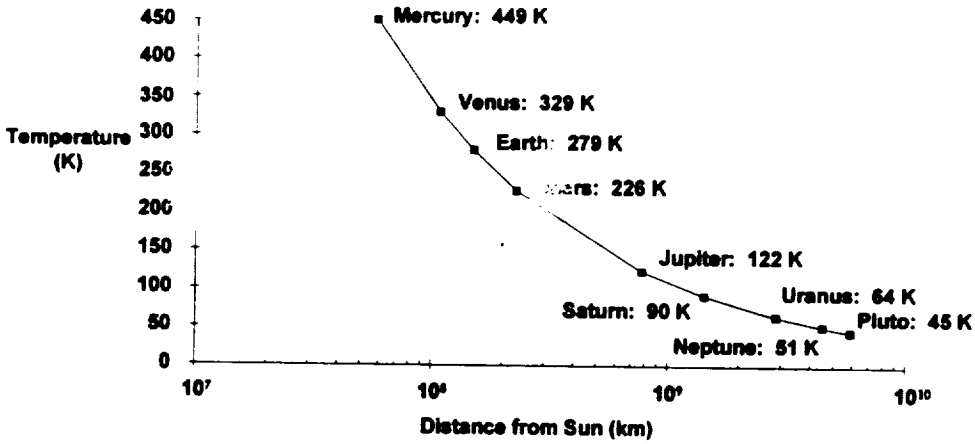

Figure 2-3. Equilibrium temperature of a blackbody sphere.

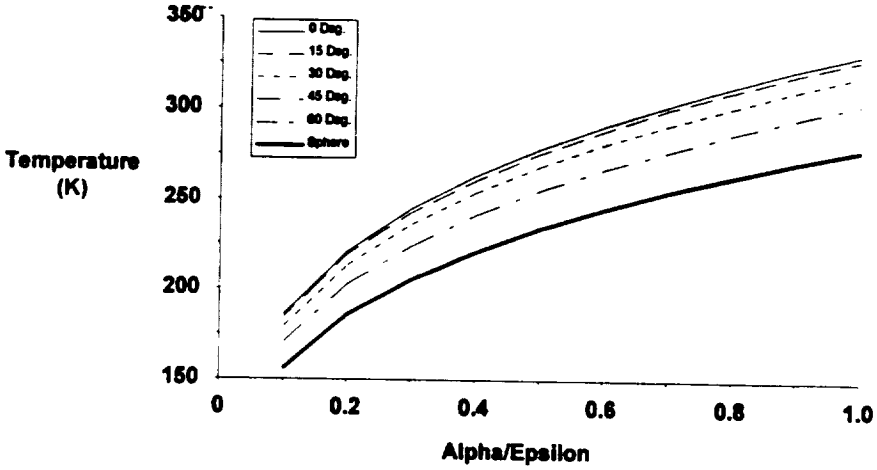

Figure 2-4. Equilibrium temperature of an inclined plane and a sphere in AMO solar flux.

As shown in Figure 2-4, if the value of either α_s or ε is altered by contamination, either molecular or particulate, the result will be a change in the equilibrium temperature of the surface given by

$$\frac{\Delta T}{T} = \frac{1}{4}\left[\frac{\Delta(\alpha_s/\varepsilon)}{(\alpha_s/\varepsilon)}\right] = \frac{1}{4}\left[\left(\frac{\Delta\alpha_s}{\alpha_s}\right) - \left(\frac{\Delta\varepsilon}{\varepsilon}\right)\right]. \qquad \textbf{Equation 2-13}$$

Thermal control surfaces usually fall into one of two categories. Sun facing surfaces are oftentimes designed to be highly reflective to minimize the amount of heat that is absorbed by the spacecraft. If the low initial value of α_s is increased by contamination, the heat load to the spacecraft will increase. Deep space facing surfaces, (and many Sun facing surfaces as well), are often designed to be highly emissive, so that radiation heat loss to space is maximized and certain parts of the spacecraft, (such as infrared focal plane detectors), can be passively cooled. Because they radiate heat more effectively than they absorb it, these surfaces are usually called radiators. If radiators are contaminated with a material that lowers their effective emissivity the heat loss will decrease and the "cold" parts of the spacecraft will warm up. Each of these scenarios is discussed separately in the following sections.

2.1.1.1.1 Effects on Solar Absorptance

To minimize spacecraft mass and volume, materials having low values of α_s are often used for reflective surfaces designed to minimize heat absorption. Thermal balance can be maintained over the spacecraft's lifetime only if the reflector maintains its thermal properties, (its initial α_s value, or equivalently, its α_s/ε ratio). Three examples of materials used for this application are: i) optical solar reflectors (OSR's), essentially a mirror protected by a thin quartz coverglass, ii) S13GLO, a white paint, and iii) Teflon with a 2 mil coating of silver. The experimentally determined reflectance of these materials is illustrated in Figure 2-5. Assuming that $\tau(\lambda)$ is effectively zero, these values of $\rho(\lambda)$ can be used to determine $\alpha(\lambda)$ which in turn can then be used to determine α_s. Typical values of α_s and ε are listed in Table 2-1 for these, and other, common spacecraft materials.[2]

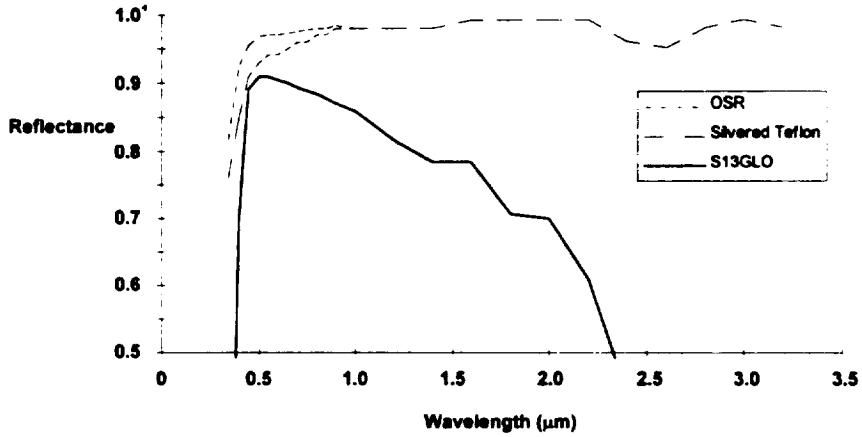

Figure 2-5. Reflectance values for three typical spacecraft thermal control materials.

[2] Hall, D. F., and Fote, A. A., "α_s/ε Measurements of Thermal Control Coatings on the P78-2 (SCATHA) Spacecraft," in *Heat Transfer and Thermal Control*, ed. A. L. Crosbie, Vol. 78, p. 467, Progress in Aeronautics and Astronautics (1981).

Henninger, J. H., "Solar Absorptance and Thermal Emittance of Some Common Spacecraft Thermal Control Coatings", NASA RP 1121, (1987).

Table 2-1. Absorptance/emittance of typical spacecraft materials.

Material	α_s	ε	α_s/ε	Material	α_s	ε	α_s/ε
Aluminum - polished	0.35	0.04	8.75	Kapton/Al	0.48	0.81	0.6
Beryllium - polished	0.4	0.05	8.0	In_2O_3/Kapton/Al	0.4	0.71	0.56
Copper - polished	0.28	0.13	2.2	Quartz Fabric/Tape	0.19	0.6	0.3
Stainless Steel - polished	0.5	0.13	3.85	OSR (quartz mirror)	0.06	0.81	0.07
Gold - on Al	0.26	0.03	6.5	FEP (5 mil)/Silver	0.11	0.8	0.14
Grafoil	0.66	0.34	1.9	FEP (2 mil)/Silver	0.08	0.62	0.13
Silicon Solar Cell				Black Paint			
- bare	0.82	0.64	1.3	- Epoxy	0.95	0.85	1.12
- Si cover	0.82	0.81	1.0	- Acrylic	0.97	0.91	1.07
- Si cover, blue filter	0.78	0.81	0.96	White Paint			
- Si cover, red filter	0.7	0.81	0.86	- Silicone (S13GLO)	0.24	0.88	0.27

As shown by Equation 2-7, the presence of a thin contaminant film on the surface of a material will alter its solar absorptance according to the relation

$$\alpha_s^x = \alpha_s + \Delta\alpha_s = \frac{\int\left\{1-\rho(\lambda)\exp\left[-2\alpha_c(\lambda)x\right]\right\}S(\lambda)d\lambda}{\int S(\lambda)d\lambda}. \qquad \textbf{Equation 2-14}$$

The absorption coefficient that was determined from a mixture of "typical" spacecraft contaminants is shown in Figure 2-6.[3] Note that the absorption profile of a single contaminant may be noticeably different, especially in different wavebands, Figure 2-7.[4] Also, the absorption profile of contaminants that have been baked on through a photochemical deposition process may be significantly darker, see Section 2.4.1. A contaminant layer with the absorption coefficient shown in Figure 2-6 would increase the solar absorptance of a reflecting surface, (possibly upsetting the thermal balance of the spacecraft), as shown in Figure 2-8. Historically, most spacecraft experience some degradation in α_s after reaching orbit, Figure 2-9. Some spacecraft have end of life (EOL) increases in α_s as great as 0.15 – 0.20.[5]

---

[3] Champetier, R., "Effects of Contamination on Optical Characteristics of Surfaces," Spacecraft Contamination from Propulsion Systems Workshop, The Aerospace Corporation, El Segundo, CA, 22 September 1981.

[4] Wood, B. E., Bertrand, W. T., Bryson, R. J., Seiber, B. L., Falco, P. M., and Cull, R. A., "Surface Effects of Satellite Material Outgassing Products," *J. Thermophys. Heat Trans.*, Vol. 2, No. 4, pp. 289 - 295, Oct., (1988).

Muscari, J. A., "Nonmetallic Materials Contamination Studies Final Technical Report," Martin Marietta TR MCR-80-637, 16 December 1980, (NASA JPL Contract NAS7-100).

[5] Ahern, J. E., Belcher, R. L., and Ruff, R. D., "Analysis of Contamination Degradation of Thermal Control Surfaces on Operational Satellites," AIAA Paper 83-1449, AIAA 18th Thermophysics Conference, Montreal, Canada (1983).

Curan, D. G. T., and Millard, J. M., "Results of Contamination/Degradation Measurements on Thermal Control Surfaces of an Operational Satellite," AIAA Paper 77-740, AIAA 12th Thermophysics Conference, Albuquerque, NM, (1977).

Mossman, D. L., Bostic, H. D, and Carlos, J. R., "Contamination Induced Degradation of Optical Solar Reflectors in Geosynchronous Orbit," Society of Photo Optical Instrumentation Engineers, *Optical System Contamination Effects, Measurement*, Control, Vol. 777, p. 12, (1987).

Pence, W. R., and Grant, T. J., "α_s Measurements of Thermal Control Coatings on Navstar Global Positioning System Spacecraft," in *Spacecraft Radiative Transfer and Temperature Control*, ed. T. E. Horton, Vol. 83, p. 234, Progress in Aeronautics and Astronautics, (1984).

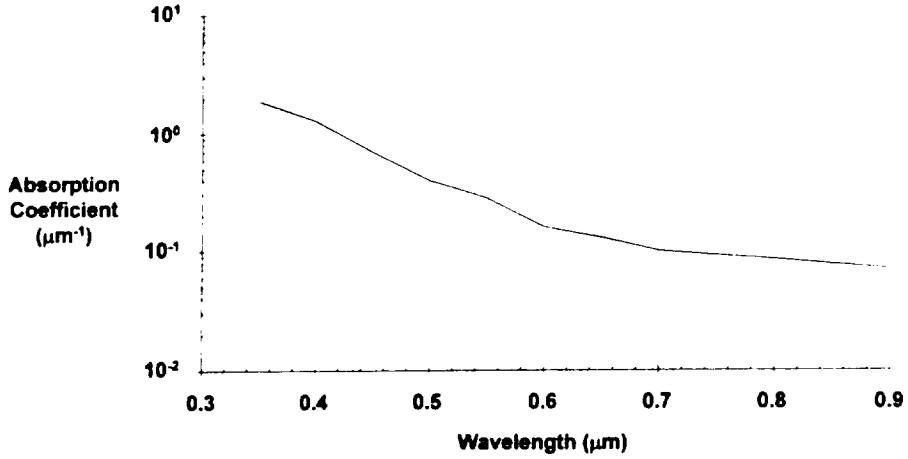

Figure 2-6. Absorptance profile of "typical" spacecraft contaminants in the visible.

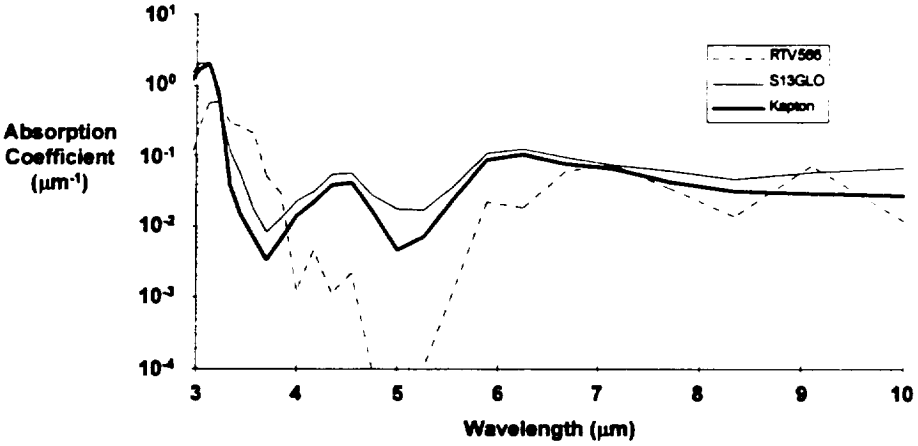

Figure 2-7. Absorptance profile of specific contaminants in the infrared.

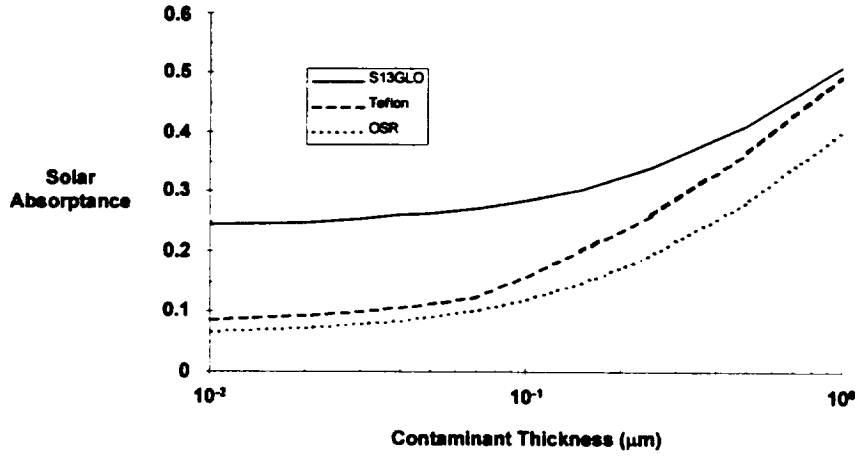

Figure 2-8. Solar absorptance as a function of contaminant thickness.

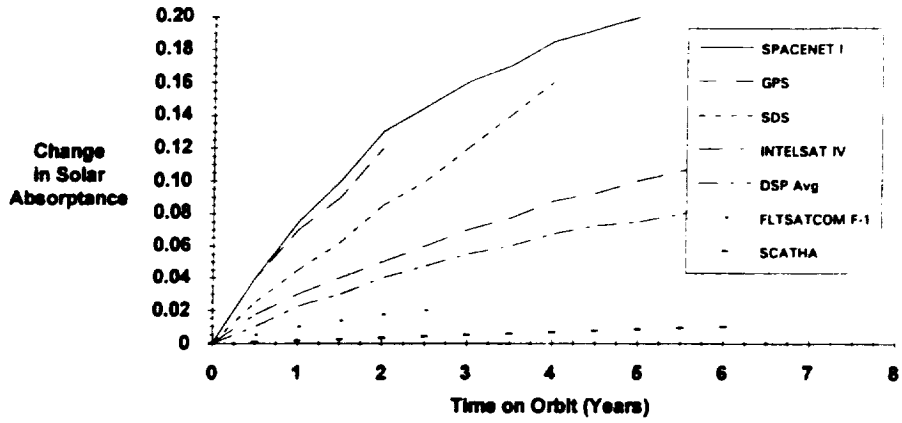

Figure 2-9. Thermal control surface solar absorptance changes.

In situ observations of thermal control coating degradation on the GPS Block I satellites are shown in Figure 2-10. Much of this degradation is associated with photochemical deposition of contamination, which will be discussed in section 2.4.1. Depending on the orbit, there are a variety of other mechanisms that may contribute to degradation of surface materials, such as the Solar ultraviolet, atomic oxygen, nuclear radiation, and micrometeoroids/orbital debris impact.

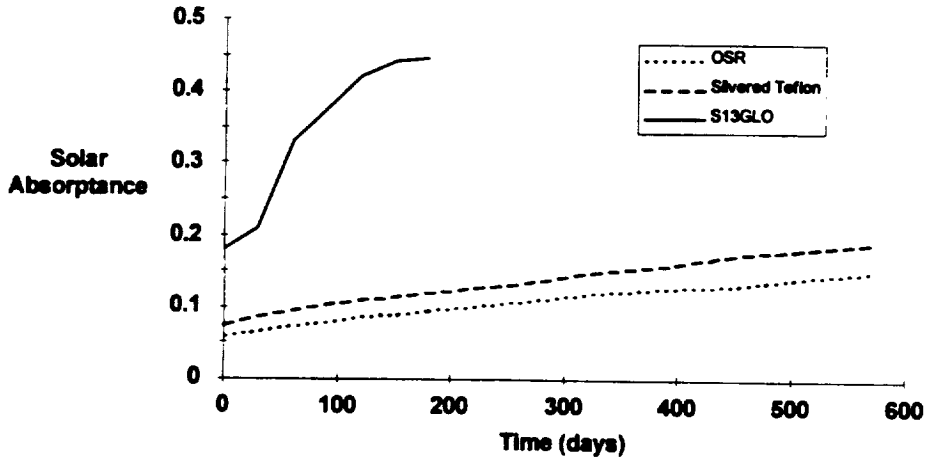

Figure 2-10. Degradation in thermal control materials seen on the GPS Block I spacecraft.

Recall that for OSR's a typical beginning of life (BOL) value is 0.08. In order to maintain thermal control and still allow for a large degradation in α_s, the thermal engineer would have to provide some means of eliminating the excess heat load at EOL, most probably by oversizing a thermal radiator at BOL. Oversizing radiators at BOL may require the designer to take active steps, (such as providing heater power, controlling the radiator area through the use of louvers, placing requirements on spacecraft orientation, etc.), to offset the increased heat loss at BOL when heat absorption by the OSR's is low. Consequently, controlling contamination to minimize the change in α_s can also minimize spacecraft size, weight, and cost.

2.1.1.1.2 Effects on Emittance

For many aerospace applications, particularly infrared remote sensing, the spacecraft must maintain a payload at very cold temperatures. The temperature of liquid nitrogen, 77 K, is not uncommon for many telescopes while others, like the Space Infrared Telescope Facility (SIRTF),

make use of liquid helium, 4 K. In order to achieve these temperatures the payload must be provided with sufficient radiator space so that the steady state heat loss from the radiator is sufficient to balance the heat load from the spacecraft and the payload electronics. If the emittance of the radiator were to decrease, the radiator would not be able to radiate heat as effectively and the temperature of the payload would increase. Many electro-optical focal plane detectors lose sensitivity or cease to function entirely when warmed above a threshold value of temperature, consequently maintaining high emissivity on radiator surfaces is critical for mission success. Fortunately, the effects of contamination on emissivity are usually not as severe as the effects on solar absorptance.

Typical emissivity values for most materials, (contamination included), are high, in the range $0.8 < \varepsilon < 1.0$. For any surface, the critical emissivity is its value near wavelengths in the vicinity of the Wein displacement law maximum, found from $\lambda T \sim 0.29$ cm-K. For room temperatures, $T \sim 300$ K and $\lambda \sim 10$ μm. The maximum wavelength increases as temperature decreases. For such wavelengths, ε is usually > 0.8 with the exception of some polished metals, for which ε may be < 0.2 far into the IR. However, even visible white paints have $\varepsilon \sim 0.8$ at the IR wavelengths of interest for spacecraft designers.

Molecular contamination will predominately be either transparent or opaque at radiating wavelengths. If transparent, the radiating surface is basically unaffected; if opaque it takes over the job of the radiator. Only if there is a significant decrease in the thermal conductivity leading to the radiating surface will the equilibrium temperature of the underlying surface be changed. For thin (< 1 μm) layers of molecular contamination this is not usually the case. Therefore, to a first approximation molecular surface contamination should have little thermal effect on high emissivity surfaces at < 300 K.

The effects of molecular contamination on low emissivity surfaces, such as polished metals, can be dramatic. While molecules which are transparent to wavelengths > 10 μm will not increase the surface emissivity, and therefore not decrease the surface temperature, molecules which are opaque at these wavelengths, which most molecules are, will increase emissivity and decrease temperature. For many situations this can be desirable, if the extra energy is radiated to space and not to some other temperature sensitive spacecraft surface. However, for some spacecraft components, such as batteries, a low temperature, (< 0° C), results in a reduced output. If the battery temperature drops below a critical value, on the order of –50° C, failure will result. Moving parts, such as tape recorders, steerable sensors, antennas, propulsion tanks, etc. are more likely to "freeze up" if temperatures get too low. Most semiconductor devices, which depend upon dopants for their charge carriers, should not be affected. However, any intrinsic semiconductors will have their charge carrier populations reduced as temperature decreases. Thus, for some spacecraft materials and components, a reduced temperature due to contamination on low emissivity surfaces is undesirable.

There have been only a few studies of the effects of molecular contamination on emissivity. Henninger found that ε for black surfaces, ($0.84 < \varepsilon < 0.94$), was not affected, while dark surfaces, ($\varepsilon \sim 0.75$), experienced a small increase.[6] Stechman measured the effects of pulsed rocket exhausts on both black, ($\alpha_s \sim 0.8$), and white, ($\alpha_s \sim 0.2$), surfaces.[7] The effective α_s values increased, but ε values actually decreased. The α_s increase was 2% – 50% for the white surfaces, and 2% – 4% for the black surfaces. The ε decreases were $< \sim 4\%$ for all non-metallic surfaces, and > 300% for the one metallic surface, (Mistic Tape), reported. Thus, high ε surface were little effected, but surfaces with low values of either α_s and/or ε had those values appreciably increased by the deposited molecular contamination.

Note that an additional contamination concern in thermal control pertains to thermal radiator baffles which are highly specular. These surfaces are used to shield the radiator from external heat sources and can cause significant back scatter into the radiator when illuminated by the Sun or Earth. Often the thermal designer is more concerned with the baffles than with the initial radiator, since the radiator is protected from the Sun.

---

[6] Henninger, J. H., "Solar Absorptance and Thermal Emittance of Some Common Spacecraft Thermal Control Coatings", NASA RP 1121, (1987).

[7] Stechman, R. C., "Space Shuttle Plume Contamination," Proceedings of the USAF/NASA International Spacecraft Contamination Conference," NASA CP-2053, AFML-TR-78-204, pp. 401 - 411, 7 - 9 March 1978.

2.1.1.2 Optical Elements - Mirrors

A mirror is often used as the first optical element of a remote sensing telescope. The mirror is designed to reflect light energy, of the proper wavelength, from a distance target - through the optical train - and eventually onto an electro-optical detector. As shown by Equation 2-7, the effect of contamination on the mirror would be to decrease the signal strength, (the number of photons), reflected by the mirror. This would, in turn, decrease the signal to noise ratio (SNR) at the focal plane array.

As shown by Figure 2-6, molecular contamination is generally more absorptive in the ultraviolet then in the infrared. The effect on SNR for a given sensor would depend on the absorption coefficient of the contaminants in question and also on the waveband of interest. Narrowband measurements may be totally compromised by a localized peak in the absorption coefficient, while broadband measurements may only see a slight decrease in SNR. Note that most optical references do not deal with the absorption coefficient $\alpha_c(\lambda)$ directly, but use an extinction coefficient k, where

$$\alpha_c(\lambda) = \frac{4\pi k}{\lambda}. \qquad \textbf{Equation 2-15}$$

The extinction coefficient also forms the imaginary part of the complex index of refraction

$$n^* = n + ik. \qquad \textbf{Equation 2-16}$$

In addition to absorbing the signal, molecular contamination may also cause an increase in thermal emissivity of the mirror surface or scattering from the mirror surface. Both of these effects may give rise to additional noise, and decrease the sensor SNR. Because scattering is usually more of a concern with particulate contamination, the issue of scattering is discussed separately in section 3.1.3.

2.1.2 Effects on Transmitting Surfaces

2.1.2.1 Solar Array Coverslides

If a contaminant film builds up the coverslide over a solar cell less light will be transmitted to the cell and the power output of the cell will degrade according to the relation

$$DF(x) = \frac{\int S(\lambda) I_s(\lambda) \exp[-\alpha_c(\lambda) x] d\lambda}{\int S(\lambda) I_s(\lambda) d\lambda}, \qquad \textbf{Equation 2-17}$$

where $I_s(\lambda)$ (W/m) is the spectral response of the cell, a measure of how effectively the cell converts a particular wavelength of light into power. A typical solar cell response curve is shown in Figure 2-11 and the resulting degradation in cell output due to contamination is shown in Figure 2-12. (This figure has assumed the contaminant absorptance profile shown in Figure 2-6.) As with previous examples, the specific result is slightly dependent on the nature of the contaminant and the response curve of the cell in question.

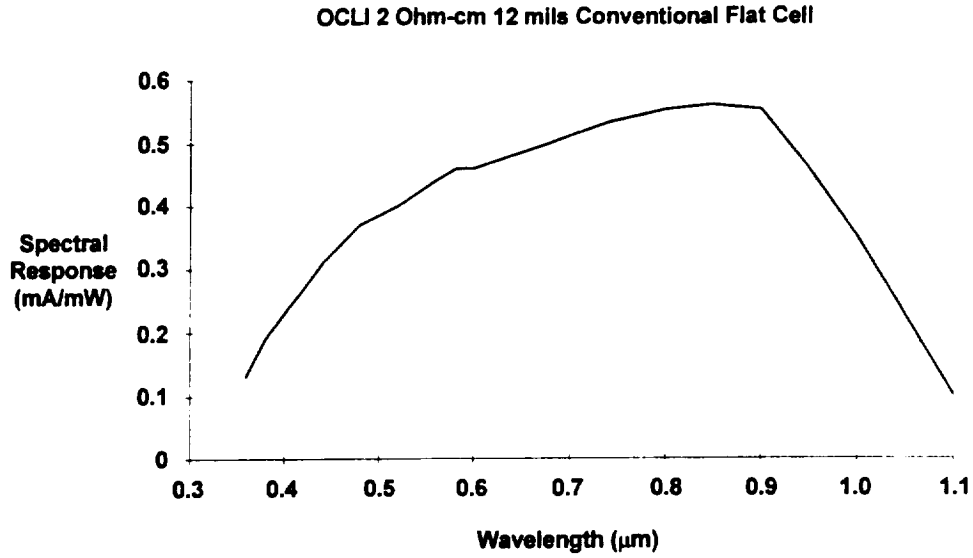

Figure 2-11. A typical solar cell response curve.

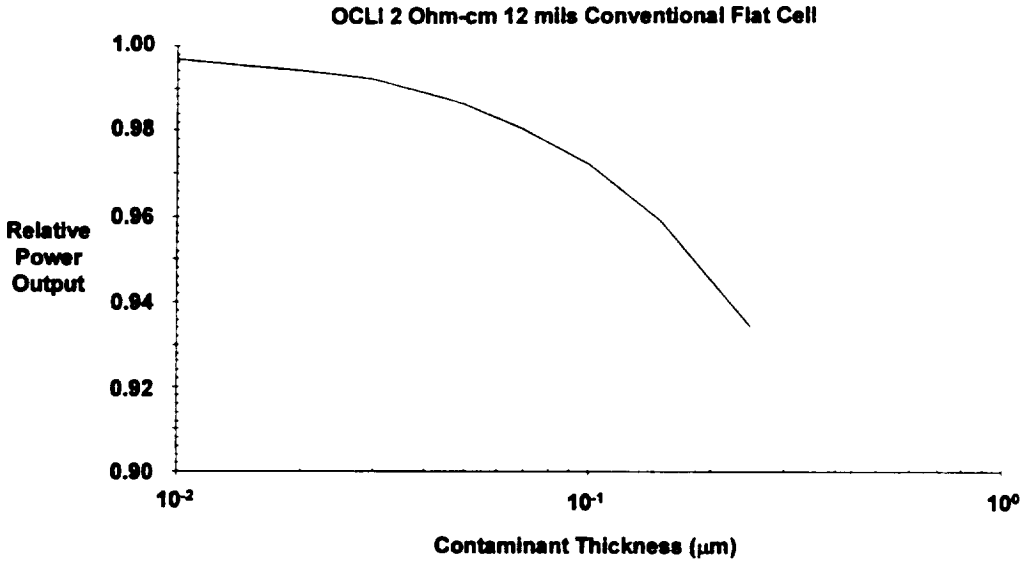

Figure 2-12. Effect of contamination on solar cell output.

2.1.2.2 Optical Elements - Lenses, Focal Plane Arrays

As with a mirror, the presence of a contaminant film on a lens or a focal plane will decrease the intensity of the signal by decreasing the amount of energy transmitted, (Equation 2-8). Because of the factor of two difference between the exponent of Equation 2-7 and Equation 2-8, contamination on a lens would be less damaging to SNR than contamination on a mirror. That is, a contaminant film on a lens would only have to be traversed once, while a contaminant film on a mirror would have to be traversed twice. The design of an optical telescope usually leaves the inner optical elements protected from external contamination. Similarly, the deposition of molecules tends to be by direct path which would yield a favored side to the contamination, (see section 2.3.1.2). For this reason, it is primarily the external components of a telescope which are most contamination critical. However, this must be evaluated on a case by case basis.

2.1.3 Additional Concerns

2.1.3.1 Cryogenic Surfaces

Many modern space-based sensors operate in the infrared (IR) portion of the electromagnetic spectrum, defined as wavelengths greater than ~ 0.7 μm. There are at least two reasons for this. First, many objects radiate either completely or partially at these wavelengths, primarily because they are relatively cool. T < 1000 K). Second, the transmission of infrared radiation through the Earth's atmosphere (including clouds, dust, etc.) is better (at selected wavelengths) than for visible or UV light. For some applications, e.g. observing objects in space against an Earth background, selecting the proper IR wavelength has the advantage of almost eliminating background radiation emitted and/or scattered by the Earth. For any space-based optical sensors the choice of wavelength(s) and its associated bandwidth are critical. For many applications those wavelengths lie in the infrared.

An optical sensor which operates in the IR, especially MWIR ($\lambda > \sim 5$ μm) must generally be cooled in order to limit the background noise produced by the sensor itself. That background will consist of photons emitted by the mirrors, lenses, and other parts of the sensor, and may also consist of thermal (Johnson) noise in the sensor electronics (associated with the sensor focal plane). The optical IR background will have a Planck wavelength distribution. Fortunately its intensity will be reduced by the low emissivity of most optical surfaces to ~ 5% of that of a blackbody, or less. The electronic noise may have several non-thermal components such as 1/f noise (due to electron quantum mechanical tunneling at the boundary), generation-recombination (GR) noise if the number of charge carriers in sensitive circuits fluctuates, shot noise (due to the random arrival of charge carriers at barriers), in addition to the Johnson noise. Since it is desirable to maximize the SNR in any sensor, cooling the sensor (especially an IR sensor) accomplishes this by reducing the optical and usually the electronic noise. This cooling is often necessary to obtain a detectable signal.

The contamination issue associated with cooling any part of a spacecraft, especially an IR sensor, is that the average molecular residency times are exponential functions of temperature, see section 2.3.1.3. Molecules which would not stick to a warm surface will have lengthy residence times on a cold surface. For example, water (the most common outgassing molecule from spacecraft surfaces) resides less than a microsecond, on average, at room temperatures, but will have a residence time on the order of the age of the universe (~ 10^{17} s) on a surface at a temperature of ~ 77 K. Thus, cold surfaces act as "getters" for most molecules which strike them.

The consequences of molecular contamination on cold spacecraft surfaces depend on the nature of the contamination as well as the sensitivity of the surface. Molecules which do not scatter, reflect or absorb IR photons at the wavelength of interest are of little concern. This is true of one atom gas molecules, (e.g. Ne, Ar) and often true of two atom gas molecules (e.g., N_2, O_2). This is because one atom molecules have no vibration modes, and two atom molecules have only one vibration mode. (Rotational modes lie in the microwave portion of the spectrum and are of little concern in contamination studies.) However, three atom molecules, (e.g., H_2O, CO_2, ...) and four atom molecules (e.g., NH_3, ...) have several vibrational modes, some of which could lie in the IR regions of interest and be and additional source of noise. Hence, molecular contamination on cooled optical surfaces are a special problem for IR sensors.[8]

---

[8] Bertie, J. E., Labbe, H. J., and Whalley, E., "Absorptivity of Ice I in the Range 4000 - 30 cm-1," *J. Chem. Phys.*, Vol. 50, No. 10, pp. 4501 - 4520, 15 May 1969.

Pipes, J. G., Roux, J. A.., Smith, A. M and Scott, H. E., "Infrared Transmission of Contaminated Cryocooled Optical Windows," *A Journal*, Vol. 16, No. 9, pp. 984 - 990 Sept., (1978).

Pipes, J. G., Sherrill, F. G., Wood, ' ., and Clark, W. L., "Cryocooled Opti.. and Contamination," *Optical Engineering*, Vol. 18, No. 6, pp. 620 - 625, Nov. - Dec., (1979).

Thompson, S. B., Arnold, F., and Sanderson, R. B., "Optical Effects of Cryodeposits on Low Scatter Mirrors," AIAA Paper 73-732, 8th Thermophysics Conference, Palm Springs, CA, July 1973.

Wood, B.E., and Roux, J.A., "Infrared Optical Properties of Thin H2O, NH3, and CO2 Cryofilms," *J. Opt. Soc. Am.*, Vol. 72, No. 6, pp. 720-728, June, (1982).

There is also the concern that a frozen contaminant layer would appear more opaque than its unfrozen counterpart. Freezing a clear liquid, such as water, can often produce a much more opaque solid. As a result, the presence of cryogenic surfaces are a sure indication that contamination control will be a significant factor in the design, development, and operation of a space system.

2.1.3.2 Thin Molecular Films - Interference and Scattering

One property associated with thin films is an effect known as interference. As is well known, thin films whose thickness are $\lambda/4$, $3\lambda/4$, ... tend to be non-reflecting at those wavelengths. A ray of light being reflected by a film of thickness $\lambda/4$ would exit the film exactly out of phase with the incoming ray. They would interfere destructively and cancel. Thin films of thickness $\lambda/2$, λ, ... tend to reflect well because the incoming and outgoing rays would be in phase. For the problem at hand, the following observations can be made. If λ = 1 μm, (the near IR), then $\lambda/4$ is 0.25 μm, or about 100 molecular monolayers. This is a fair amount of contamination, especially for sensitive optical surfaces such as mirrors and lenses. As will be quantified in the next section, maintaining surface cleanliness to level A or B should be sufficient to prevent thin film effects from occurring on most surfaces. When combined with the fact that contaminant layers are typically more absorptive in the UV than in the IR, Figure 2-6, this conclusion is even more true for MWIR ($\lambda \sim 5$ μm) and LWIR ($\lambda > 10$ μm). Consequently, this phenomena is of more concern at visible and ultraviolet wavelengths.

A second concern arises from that fact that molecular contamination does not deposit itself in uniform layers, but in clumps. This is especially true for the first 100 monolayers or so. If the molecules are not transparent at the wavelengths of interest, scattering rather than reflection will usually be the primary effect of concern. Because scattering is usually of more concern from particulates, the discussion of scattering from molecular films will be postponed until section 3.1.3.

2.2 Quantifying Molecular Contamination

2.2.1 MIL STD 1246C

Both molecular and particulate contamination levels are quantified by MIL STD 1246C. Molecular contaminant films are referred to as Non-Volatile Residue (NVR), which is defined as the soluble material remaining after evaporation of a volatile liquid or determined by special purpose analytical instruments. NVR is usually measured in milligrams per unit volume, such as milligrams per 100 milliliters of fluid sample, but may also be measured in milligrams per 0.1 square meters of surface area. The NVR levels quantified by MIL STD 1246C are specified in Table 2-2. A requirement that a surface must be clean to level "C" means that molecular films cannot exceed 3 mg per 0.1 m^2, or 3 $\mu g/cm^2$, on that surface. If the density of the contaminant is known, (1 g/cm^3 is a reasonable value), the MIL STD level can be converted to a contaminant thickness, Table 2-3.

Table 2-2. MIL-STD-1246C molecular contamination levels.

Level	NVR Limit mg/0.1 m^2 ($\mu g/cm^2$)	NVR Limit mg/liter	Level	NVR Limit mg/0.1 m^2 ($\mu g/cm^2$)	NVR Limit mg/liter
A/100	0.01	0.1	C	3.0	30.0
A/50	0.02	0.2	D	4.0	40.0
A/20	0.05	0.5	E	5.0	50.0
A/10	0.1	1.0	F	7.0	70.0
A/5	0.2	2.0	G	10.0	100.0
A/2	0.5	5.0	H	15.0	150.0
A	1.0	10.0	J	25.0	250.0
B	2.0	20.0			

Table 2-3. Molecular contamination thickness versus MIL-STD-1246C cleanliness level.

"Level"	NVR ($\mu g/cm^2$)	Contamination Thickness (nm) $\rho_c = 0.75$ g/cm^3	$\rho_c = 1.0$ g/cm^3	$\rho_c = 1.5$ g/cm^3	$\rho_c = 2.0$ g/cm^3
A/100	0.01	0.13	0.10	0.07	0.05
A/50	0.02	0.27	0.20	0.13	0.10
A/20	0.05	0.67	0.50	0.33	0.25
A/10	0.1	1.33	1.00	0.67	0.50
A/5	0.2	2.67	2.0	1.33	1.00
A/2	0.5	6.67	5.00	3.33	2.50
A	1.0	13.33	10.00	6.67	5.00
B	2.0	26.67	20.00	13.33	10.00
C	3.0	40.00	30.00	20.00	15.00
D	4.0	53.33	40.00	26.67	20.00
E	5.0	66.67	50.00	33.33	25.00
F	7.0	93.33	70.00	46.67	35.00
G	10.0	133.33	100.00	66.67	50.00
H	15.0	200.00	150.00	100.00	75.00
J	25.0	333.33	250.00	166.67	125.00

Note that contamination thicknesses of 0.01 μm, (10 nm), corresponds to cleanliness level A (assuming ρ = 1 g/cm^3). As shown in Figure 2-8 and Figure 2-12, less than 0.01 μm of molecular contamination will have little effect on thermal control surfaces and solar arrays. As will be discussed in Chapter 3, maintaining cleanliness level A is, relatively speaking, not that difficult. This is an indication of the fact that optical surfaces are often the most susceptible to contamination.

2.3 Generation, Transportation and Deposition of Molecular Contaminants

Even if a spacecraft's surfaces are clean when installed in the launch vehicle, the spacecraft itself will be a source of contamination during launch or on orbit operations. All but the purest organic materials will contain fractional amounts of "volatile" chemicals, either on the surface or dispersed through the material, Table 2-4.[9] These volatile chemicals, which may be simply excess chemicals left over from improper catalyst/resin ratios, improper curing, etc., may, over time, migrate to the surface and escape into the local environment. This process, called *outgassing*, is responsible for the familiar odor of plastics or rubber. In addition, thruster plumes are a potentially serious threat if the backflow is capable of reaching sensitive surfaces. Similarly deploying or operating mechanisms, releasing covers, or conducting proximity operations are all potential sources of contamination once on orbit.

Table 2-4. Examples of common spacecraft contamination sources.

Structures	Epoxies, polycarbonates, polyurethanes, polyamines, polyimides, flourocarbons
Potting/Encapsulation	Polyurethanes, epoxies, silicones
Conformal Coatings	Polyurethanes, epoxies, silicones
Adhesives	Epoxies, silicones, polyurethanes
Tapes	Polyesters, acrylics, polyamides, flourocarbons
Other	Acetates, epoxies, acetals, polyamides

[9] Vest, C. E., Buch, R. M., and Lenkevich, M. J., "Materials Selection as Related to Contamination of Spacecraft Surfaces," *SAMPE Quarterly*, Vol. 19, No. 2, pp. 29 - 35, (1988).

2.3.1 Contamination due to Materials Outgassing

Experimental data indicate that outgassing is seen to vary either: i) as an exponential function of time, ii) inversely as a power of time, or iii) independently of time, depending on the mechanism responsible for the outgassing process. These three outgassing processes are known as *desorption*, *diffusion*, and *decomposition*, respectively. Desorption is the release of surface molecules that are held by electrical (chemical) forces. Diffusion is the homogenization that occurs from random thermal motions. Contaminants that diffuse to the surface of a material may have enough thermal energy to escape the surface forces and simply evaporate into the local environment. Finally, decomposition is a type of chemical reaction where a compound divides into two or more simpler substances, which may then outgas through desorption or diffusion.

In addition to the time dependency, each process is seen to depend exponentially on a unique range of activation energies, E_a, (the energy required to initiate the process), and temperature, T, (the measure of the available thermal energy), according to the relation $\exp^{(-E_a/RT)}$. The activation energies define a temperature range over which the various reactions are considered likely, (provided that they are chemically possible in the first place), Table 2-5. Because desorption involves only surface films it will usually contribute comparatively little to total mass loss on orbit, even though it has a low temperature dependence and fast time constant. Note, however, that desorption is the mechanism responsible for removing contaminant layers from metals. Similarly, decomposition usually contributes comparatively little to total mass loss due to its high temperature dependence and time independence. Diffusion, on the other hand, has a mid-range temperature dependence and mid-range time constant. Because diffusion is the mechanism responsible for outgassing from organic materials, and involves the total mass of organic material present, it is the mechanism that is the major source of outgassing on orbit.

Table 2-5. Characteristics of various outgassing mechanisms.

Mechanism	Time Dependence	Activation Energy (kcal/mole)	1/e Temperature Range $T = E_d/R$, (K)
Desorption	t^{-1} to t^{-2}	1 – 10	500 – 5000
Diffusion	$t^{-1/2}$	5 – 15	2500 – 7500
Decomposition	n/a	20 – 80	10,000 – 40,000

2.3.1.1 Contamination Generation - Diffusion

The amount of mass loss due to diffusion can be represented by the relation

$$\frac{dm}{dt}(t,T) = Cm\frac{\exp^{-E_a/RT}}{\sqrt{t}}, \qquad \textbf{Equation 2-18}$$

where C ($s^{1/2}$) is a normalization constant that must be experimentally determined, m (kg) is the amount of mass contributing to the outgassing, E_a (kcal/mole) is the activation energy, R (kcal K/mole) is the gas constant, T (K) is the temperature, and t (s) is the time. Integrating Equation 2-18 provides an expression for the amount of mass outgassed between time t_1 and t_2, which is

$$\frac{\Delta m}{m} = 2C\exp^{-E_a/RT}\left(t_2^{1/2} - t_1^{1/2}\right). \qquad \textbf{Equation 2-19}$$

The amount of matter that is outgassed by a material is dependent on the material's specific outgassing characteristics, which are contained in the normalization constant C and the activation energy E_a.

2.3.1.1.1 ASTM E 595 - Materials Outgassing Test

A standard test of a material's outgassing characteristics, which can be used to determine C, (near room temperature), is ASTM E 595. In this test, a sample of the material being studied is held at a temperature of 125° C for 24 hours at a pressure of less than 7×10^{-3} Pa. Comparing the initial and final mass of the sample yields the change in mass, Δm, which is known as the Total Mass Loss (TML). Because T, t_1, and t_2 are known, once Δm is determined the reaction constant C can be evaluated, provided that the activation energy of the material is known. For most spacecraft organic materials, the activation energy is in the range 5 – 15 kcal/mol. Knowing the specific value for a specific material will infer C. More often, the outgassing will be due to a conglomeration of material so that a rough estimation of the "average" activation energy, (usually taken to be 10 kcal/mole), is all that is available. Note that ASTM E 595 is incapable of deducing C if E_a is unknown. If this is the case, the more robust ASTM E 1559 must be used, section 2.3.1.1.2.

The concern in contamination control is not merely over how much mass will be outgassed, but also over how much of the outgassed mass will condense on a sensitive surface. To determine this second parameter, the ASTM E 595 outgassing test utilizes a collecting plate, held at 25° C, to measure the amount of Collected Volatile Condensable Material (CVCM). That is, CVCM is a measure of the fraction of the TML that could condense on a 25° C plate. Recall that MIL STD 1246C specifies molecular contamination levels in terms of NVR, where NVR is defined as the amount of mass per unit area and is measured by chemical wiping. While NVR and CVCM are closely related, they are distinct quantities. (Note also, that CVCM will typically be a strong function of temperature. This will be discussed in section 2.3.1.3.)

Usually, much of the TML is due to very light chemical species, such as water, which will not condense on room temperature surfaces. ASTM E 595 also measures a third parameter, Water Vapor Regained (WVR), by subjecting the post-test sample to a 50% relative humidity environment at 23° C for 24 hours. The mass gain is used to infer WVR.

As a starting point, the conventional wisdom defines typical pass/fail criteria for most spacecraft materials to be 1% TML and 0.1% CVCM. That is, a material with a TML of 0.5% would pass the screening test, while a material with 0.2% CVCM would fail. Using these criteria alone, without taking into consideration the materials activation energy or its absorption coefficient can be quite misleading. A material with an activation energy of 12 kcal/mole or greater would outgas very slowly and could still pass the test although most of the outgassable matter had yet leave the material. Similarly, a material which has a significant TML value may be quite innocuous if its CVCM is near zero or it is essentially transparent. Conversely, a material may have a small TML and be quite optically black for correspondingly small values of CVCM. If problems are foreseen, more detailed analysis is usually warranted.[10]

Outgassing parameters and activation energies for several typical spacecraft materials are shown in Table 2-6. The mass density of outgassed contaminants is typically on the order of 1 g/cm^3.

---

[10] Campbell, W. A., Jr., and Scialdone, J. J., *Outgassing Data for Selecting Spacecraft Materials*, NASA RP 1124, Rev. 3 (1993).

Glassford, A. P. M., and Liu, C. K., "Outgassing Rate of Multilayer Insulation Materials at Ambient Temperature," *J. Vac. Sci. Tech.*, Vol. 17, No. 3, pp. 696 - 704, (1980).

Muscari, J. A., and O'Donnell, T., "Mass Loss Parameters for Typical Shuttle Materials," Society of Photo Optical Instrumentation Engineers, *Shuttle Optical Environment*, Vol. 287, pp. 20 - 24, (1981).

Scialdone, J. J., "An Estimate of the Outgassing of Space Payloads and its Gaseous Influence on the Environment," *J. Spacecraft*, Vol. 23, no. 4, p. 373 (1986).

Table 2-6. Outgassing parameters for typical spacecraft materials.

Material	TML (%) at 75° C	TML (%) at 125° C	CVCM (%)
Adhesives			
R-2560	1.58	1.53	n/a
RTV-566	0.11	0.26	0.02
DC 93-500	0.07	0.08	0.05
DC 6-1104	0.29	0.58	0.03
Films			
Kapton FEP	n/a	0.25	0.01
Kapton H	n/a	1.17	0.00
Mylar	n/a	0.32	0.04
FEP Teflon	n/a	0.77	0.35
Oils & Greases			
Brayco 815Z	n/a	0.25	0.01
Braycote 803	n/a	0.24	0.13
Krytox 143AD	n/a	28.54	5.71
Vakote MLD73-91	0.40	n/a	n/a
Paints & Coatings			
S13G/LO	0.45	1.00	0.13
Chemglaze Z306	2.40	2.52	0.07
DC Q9-6313	0.40	0.39	n/a
Aremco 569	2.28	3.58	n/a
LMSC 1170	1.88	2.89	n/a

2.3.1.1.2 ASTM E 1559 - Contamination Generation Characteristics of Spacecraft Materials

Because the ASTM E 595 screening test maintains the outgassing source and collector at fixed temperatures, it does not provide complete insight into the outgassing characteristics of a material. For this reason, it is often necessary to conduct more detailed tests in order to determine outgassing characteristics over a wider temperature range and determine relevant time dependencies. This is the purpose of ASTM E 1559, which is capable of determining both the total mass flux outgassed by a material and the deposition of the outgassed by-products on surfaces held at various temperatures.

To obtain more precision, ASTM E 1559 utilizes Quartz Crystal Microbalances (QCM's), (see section 4.2.1.3), to make measurements of outgassed matter at different temperatures. Essentially, a QCM compares the resonance frequency of a shielded quartz crystal, which remains contamination free, with one that is exposed to the environment and experiences a deposition of contamination. By calibrating the QCM the amount of mass deposition can be determined. Two test methods can be utilized. Test method A specifies three QCM's with operating temperatures of 90 K, 160 K, and 298 K. Test method B utilizes the 90 K QCM, and the user selects a temperature for up to three additional QCM's. The test sample is subjected to three different runs, at temperatures of 398 K (125° C), 348 K (75° C), and 323 K (50° C) with the test continuing for 1 – 5 days for each sample. Although this test is more expensive than ASTM E 595 it is capable of providing much more insight into the specific outgassing characteristics of a material. By heating up the QCM's at the end of the test it is also possible to determine the temperature at which many of the outgassed constituents will condense.

2.3.1.2 Contamination Transport

The amount of contamination that is produced by a spacecraft is important, but the amount of contamination that reaches, and sticks to, a sensitive surface is much more important. In general, transport processes are generally either line of sight or non-line of sight as discussed in the following sections.

2.3.1.2.1 Line of Sight

Once the electrical attraction to the surface of the material has been broken, the outgassed molecules are free to follow ballistic trajectories and may randomly impact other surfaces having a line of sight to the point of departure. The contaminant mass may originate interior to a subsystem or payload, such as the outgasing from the baffle coating of an optical sensor, or from its exterior. Spacecraft are typically vented to allow for pressure reduction during launch. Once on orbit any mass that is outgassed interior to the vehicle would be expected to exit from the spacecraft vents in proportion to their geometric area. This will of course be modified by the presence of interior bulkheads and/or the proximity of high outgassing sources to certain vents.

The rate at which mass is outgassed is given by Equation 2-18. The question of interest is, how much of the outgassed material can reach a sensitive surface? The arrival rate of contaminants at a given point is dependent on the rate of outgassing from all potential sources and the physical geometry of the point in question relative to each source. In a vacuum, the arrival rate is the product of the rate at which mass leaves the source, which can be calculated from Equation 2-18, and a geometrical view factor, which is simply a measure of the fraction of matter that leaves the source and impacts a given point of interest. The outgassing view factor bears a strong resemblance to the thermal view factor, or angle factor, used in calculations of radiative heat balance. We will maintain this analogy in the following derivation.

Consider a plate of area dA_1 which is radiating heat (outgassing mass) to space with radiance L_1 (W m^{-2} sr^{-1}). What fraction of this heat (mass) will impact a surface dA_2 located a distance r from the first plate in the relative orientation shown in Figure 2-13?

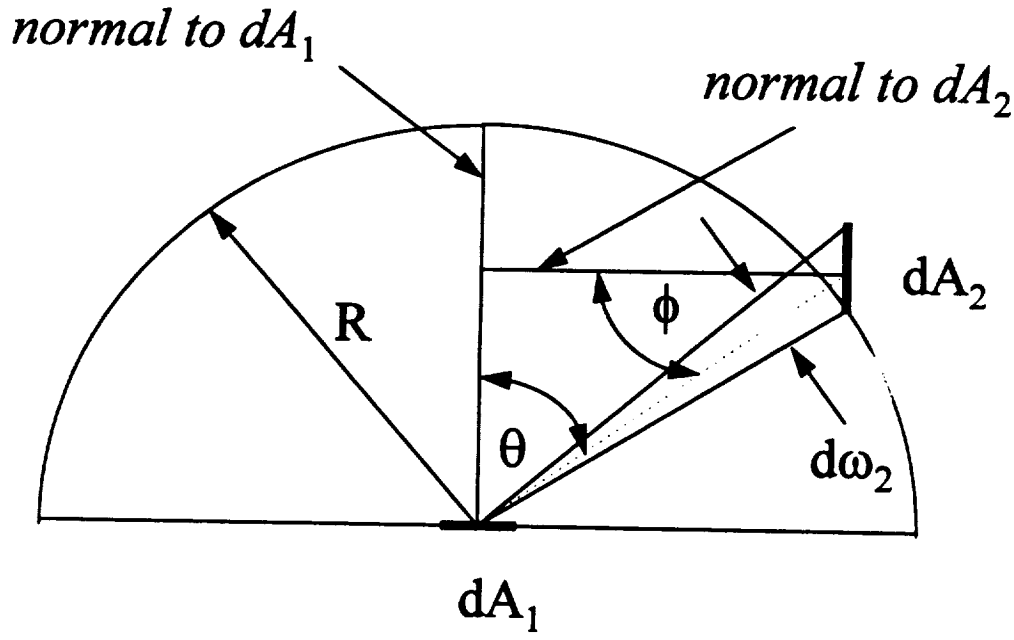

Figure 2-13. View factor geometry.

The rate at which heat (mass) leaves dA_1 in the direction of dA_2 is

$$\Delta q_1 = L_1 \cos\theta dA_1, \qquad \text{Equation 2-20}$$

where θ is the angle between the normal to dA_1 and the radius r connecting the center of the plates. The amount of heat (mass) that leaves dA_1 and is intercepted by dA_2 is

$$\Delta q_{12} = L_1 \cos\theta dA_1 d\omega_2, \qquad \textbf{Equation 2-21}$$

where $d\omega_2$ is the solid angle that dA_2 subtends, with dA_1 as its origin. It is easily seen that

$$d\omega_2 = \frac{\cos\phi}{r^2} dA_2. \qquad \textbf{Equation 2-22}$$

If we consider the case of dA_1 radiating (outgassing) over an entire hemisphere, dA_2, it can be seen that

$$q_1 = L_1 dA_1 \int_0^{\pi/2} \int_0^{2\pi} \cos\theta \sin\theta d\theta d\alpha = \pi L_1 dA_1 = M_1 dA_1, \qquad \textbf{Equation 2-23}$$

where M (W m^{-2}) is defined as the exitance. Consequently, in terms of the exitance of the radiating source, Equation 2-21 reduces to

$$\Delta q_{12} = M_1 \frac{\cos\theta\cos\phi}{\pi r^2} dA_1 dA_2. \qquad \textbf{Equation 2-24}$$

The total heat (mass) transfer between the two surfaces is found by integrating over dA_1 and dA_2. The radiative view factor, F_{12}, is defined by

$$F_{12} = \iint \frac{\cos\theta\cos\phi}{\pi r^2} dA_1 dA_2, \qquad \textbf{Equation 2-25}$$

so that the total heat (mass) transfer from dA_1 to dA_2 is given by

$$q_{12} = M_1 F_{12}. \qquad \textbf{Equation 2-26}$$

As previously seen, the thermal exitance, M, has units of W m^{-2}, or J s^{-1} m^{-2}. We confirm that Equation 2-24 and Equation 2-26 are equally applicable to the case of outgassing, provided that the mass exitance is measured in units of mass per unit time per unit area. By analogy, the mass exitance is defined by

$$M_1 = \frac{dm_1}{dt} \frac{1}{dA_1}, \qquad \textbf{Equation 2-27}$$

where dm_1/dt is obtained from Equation 2-18 and dA_1 is the area of the outgassing source, (for example, the cross sectional area of a vent). Using this expression in Equation 2-26 would produce an expression for the mass per unit time which left dA_1 and impacted dA_2.

Recall that MIL STD 1246C defines molecular contamination levels in terms of mass per unit area. What is oftentimes more useful than the amount of mass distributed over dA_2 is simply mass per unit area at a specific point within dA_2. For this reason, we define the view factor used in many outgassing calculations a

$$VF_{12} = \int \frac{\cos\theta\cos\phi}{\pi r^2} dA_1 . \qquad \textbf{Equation 2-28}$$

Note that the values of θ and ϕ are defined by the point of impact within dA_2. Using this expression, the mass of contaminants per unit area per unit time which arrive at a specific point in dA_2, after having originated from dA_1, is given by

$$\left[\frac{\Delta m}{\Delta t \Delta A}\right]_2 = M_1 VF_{12} . \qquad \textbf{Equation 2-29}$$

The thickness of contaminants at a specific point in dA_2 is obtained by simply dividing Equation 2-29 by the density of the contaminant, ρ_c (g/cm^3). Explicitly, the thickness of contamination that is outgassed by dA_1 and impacts a specific point within dA_2 is given by

$$\frac{\Delta x_2}{\Delta t} = \frac{1}{\rho_c}\left(\frac{dm_1}{dt}\frac{1}{dA_1}\right)\int \frac{\cos\theta\cos\phi}{\pi r^2} dA_1 , \qquad \textbf{Equation 2-30}$$

where θ is the angle between the normal to the outgassing source and the radius vector to the collection point, ϕ is the angle between the normal to the collection point and the radius vector from the collection point, and r is the distance between source and collector as illustrated in Figure 2-13.

If there are numerous sources contributing to outgassing, the total mass reaching a given point of interest is simply the sum of the parts. If a source does not have a direct line of sight to the collection point of interest, its view factor for direct deposition is zero. An outgassing source may be an extended surface, such as a thermal control panel covered with an outgassing paint, or may be quite localized, such as outgassing through a spacecraft vent or from a single electrical component. Contamination may also come from thermal blankets or multilayer insulation. If two or more payloads are carried into orbit on the same launch vehicle, one payload may be degraded by contamination from the other payload. Any material that may outgas is a potential source of contamination.

2.3.1.2.2 Non-Line of Sight

2.3.1.2.2.1 Desorptive Transfer and Scattering

It is not always necessary for a contaminant source to have a direct line of sight to a sensitive surface in order for the source to contaminate the surface. A source may outgas matter onto an intermediate surface, which will in turn desorb matter onto the surface of concern. Consequently, reflection, or desorptive transfer, may also need to be considered in a comprehensive contamination

analysis.[11] Contaminants may also exit a vehicle and be scattered back through collisions with ambient atmospheric molecules. Obviously, this phenomenon is of greater concern in LEO where the atmospheric density is greatest. Scialdone reports a 50% return flux at 160 km altitude, but only a 0.0001% return at 1000 km.[12] For extremely sensitive surfaces, these non-line of sight transfer mechanisms may be significant.

2.3.1.2.2.2 *Electrostatic Reattraction During Spacecraft Charging*

One non-line of sight deposition mechanism that may be of concern even in the absence of extremely sensitive surfaces is electrostatic reattraction during periods of intense spacecraft charging.[13] Under certain orbital conditions the ambient plasma environment may charge a spacecraft to large negative voltages, (–20,000 volts was seen on ATS-6).[14] Spacecraft charging to high voltages is a phenomena that is usually associated with higher altitudes, or polar orbits. If a molecule is outgassed during a spacecraft charging event, and if the molecule is ionized while within the Debye sheath, (the plasma shielding distance), it may be electrostatically reattracted to the vehicle, Figure 2-14.

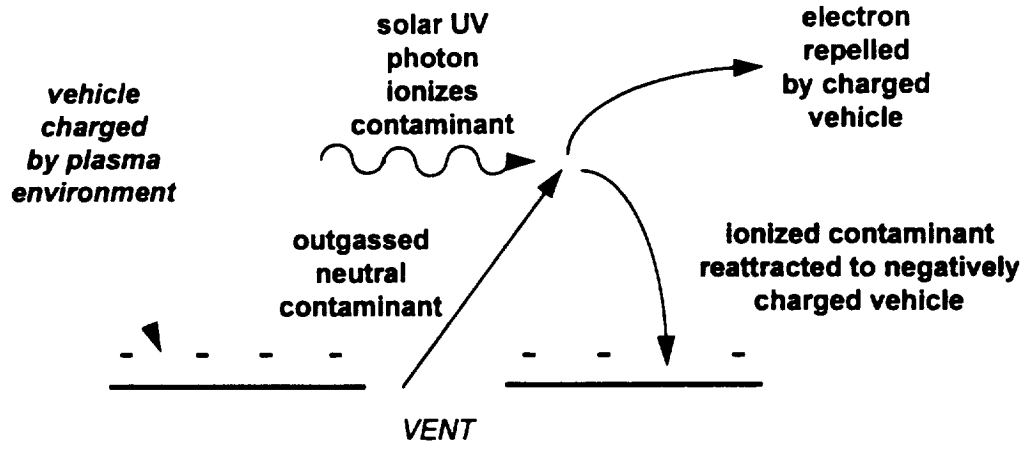

Figure 2-14. Electrostatic reattraction of ionized contaminants.

In situ measurements of molecular contamination made on the Spacecraft Charging at High Altitudes (SCATHA) spacecraft indicated that as much as 31% of the contamination received was deposited during periods of spacecraft charging. This phenomena is of greater concern at higher orbits where the plasma screening distances are greater. This provides the contaminant molecule more time to become ionized as it exits the vehicle. In low Earth orbit, the plasma screening distances are on the order of 1 cm and this phenomena is not expected to be an issue. In geosynchronous orbits, where plasma

[11] Alan Kan, H. K., "Desorptive Transfer: A Mechanism of Contamination Transfer in Spacecraft," *J. Spacecraft*, Vol. 12, No. 1, pp. 62 - 64, (1975.)

[12] Scialdone, J. J., "Self-Contamination and Environment of an Orbiting Satellite," *J. Vac. Sci. Tech.*, Vol. 9, No. 2, pp. 1007 - 1015, (1972).

[13] Clark, D. M., and Hall, D. F., "Flight Evidence of Spacecraft Surface Contamination Rate Enhancement by Spacecraft Charging Obtained with a Quartz Crystal Microbalance, " *Spacecraft Charging Technology Conference 1980*, NASA CP-2182, AFGL-TR-81-0270, (1981).

Hall, D. F., and Wakimoto, J. N., "Further Flight Evidence of Spacecraft Surface Accommodation Rate Enhancement by Spacecraft Charging," AIAA Paper 84-1703, 19th Thermophysics Conference, Snowmass, CO, 25 June 1984.

Liemohn, H. B., Tingey, D. L., Stevens, G. G., Mahaffey, D. W., and Wilkinson, M. C., "Charging and Contamination During Geosynchronous Orbit Insertion," Society of Photo-Optical Instrumentation Engineers, *Optics in Adverse Environments*, Vol. 216, pp. 80 - 86, (1980).

[14] Olsen, R. C., McIlwain, C. E., and Whipple, E. C., Jr., "Observations of Differential Charging Effects on ATS-6," *J. Geophys. Res.*, Vol. 86, No. A8, pp. 6809 - 6819, (1981).

screening distances are on the order of meters, reattraction is a much greater concern. It is important to note that reattraction is only possible during periods of time when 1.) the contaminant flux is sunlit, (so that it may be ionized by the solar UV), and 2.) the vehicle is charged negatively.

2.3.1.3 Contamination Deposition - Surface Residence Time/Accumulation Rate

If an outgassed molecule impacts a surface, experimental evidence confirms that, in most cases, the outgassed molecule will adhere to the surface and establish thermal equilibrium. The contaminant molecule will then remain attached to the surface until, following the random probabilities of quantum mechanics, it acquires enough energy to escape the electrical attraction to the surface. The average residence time on the surface is therefore related to the surface temperature and is approximated by the expression

$$\tau(T) = \tau_o \exp^{E_a/RT}, \qquad \text{Equation 2-31}$$

where τ_o is the oscillation period of the molecule on the surface.[15] Scialdone reports oscillation times on the order of 10^{-14} to 10^{-12} s, with 10^{-13} s being average.[16] Conversely, Naumann reports an oscillation period for water of 10^{-16} s.[17] For most applications, the actual value of τ_o is not that critical as most outgassed contaminants will have a very short residence time on all but cryogenically cooled surfaces. For example, water with an activation energy of ~ 11 kcal/mole, has a residence time of 1×10^{11} s on a surface at 100 K, but only 10 μs on a 300 K surface, Figure 2-15. If a contaminant molecule has a residence time long in comparison to the life of the mission, it can be assumed to remain permanently.

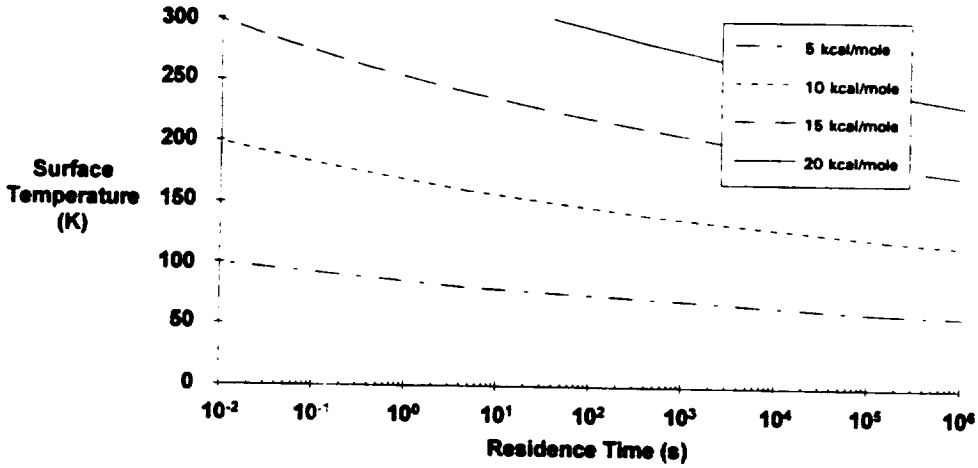

Figure 2-15. Residence time of molecules as a function of surface temperature.

A contaminant layer may build up on a surface provided that the arrival rate of contaminants exceeds the rate of departure. That is, contamination will accumulate if at least some of the incident

---

[15] Chen, P. T., Hedgeland, R. J., and Thomson, S. R., "Surface Accommodation of Molecular Contaminants," Society of Photo-Optical Instrumentation Engineers, *Optical System Contamination: Effects, Measurement, Control II,* Vol. 1329, pp. 327 - 336, (19[illegible]).

[16] Scialdone, J. J., "Characterization of the Outgassing of Spacecraft Materials," Society of Photo-Optical Instrumentation Engineers, *Shuttle Optical Environment*, Vol. 287, pp. 2 - 9, (1981).

[17] Naumann, R. J., "Contamination Assessment and Control in Scientific Satellites," NASA TN-D-7433, October, (1973).

contaminant molecules have a residence time that is long in comparison to the time period of interest. The accumulation rate is approximated by

$$x_2(t,T) = \int \gamma(T)\left(\frac{\Delta x_2}{\Delta t}\right) dt, \qquad \textbf{Equation 2-32}$$

where γ (T) is the sticking coefficient, i.e., the fraction of incident molecules that attach "permanently" to the surface, and $\Delta x_2/\Delta t$ is the arrival rate given by Equation 2-30. γ may be assumed to be 1.0 for worst-case predictions or for cryogenic surfaces where the residence time of most contaminants is long. However, the ASTM E 595 results would predict a sticking coefficient of 0.1 for room temperature surfaces, in agreement with the fraction of TML that remains as CVCM. If more detailed calculations are required, the evaporation rate can be estimated from the accumulation rate and the residence time or from the BET equation.

In 1938, Brunauer, Emmett, and Teller developed an expression to describe multilayer adsorption, and their equation has become known as the BET equation.[18] In essence, the BET theory assumes that adsorption sites are independent and may each accommodate an unlimited number of molecules. That is, adsorption occurs by the formation of piles of molecules on each site. Without derivation, (which would involve the Fermi-Dirac distribution function and other expressions from statistical mechanics), the volume of gas present on a surface V, (normalized to the volume required to form one monolayer V_m), is

$$\frac{V}{V_m} = \frac{\left(\frac{P}{P_o}\right)\exp^{\left[\frac{(U_1-U_2)}{RT}\right]}}{\left[1-\left(\frac{P}{P_o}\right)\right]\left[1+\left(\exp^{\left[\frac{(U_1-U_2)}{RT}\right]}-1\right)\left(\frac{P}{P_o}\right)\right]}, \qquad \textbf{Equation 2-33}$$

where U_1 is the binding energy of the contaminant molecule to the surface, U_2 is the binding energy of contaminant molecules to one another, P is the ambient pressure, and P_o is the saturating vapor pressure of the contaminant gas. The form of the BET equation is illustrated in Figure 2-16. As shown, only contaminants with extremely low vapor pressures, so that P/P_o is large, and/or high surface binding energies, could be expected to form condense in layers on a surface.

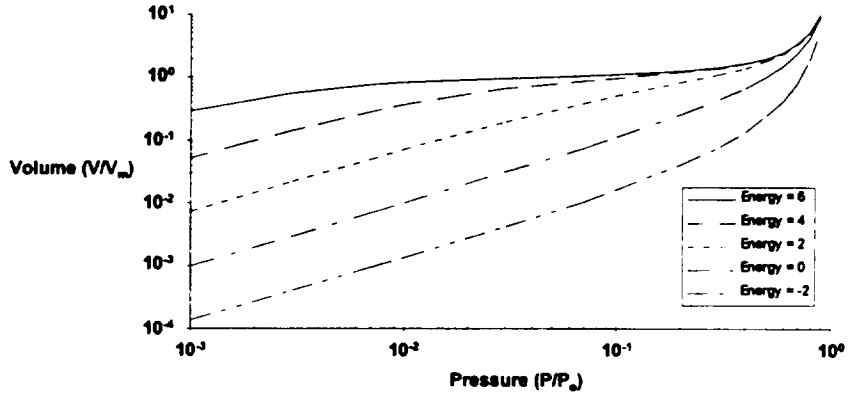

Figure 2-16. The form of the BET equation. Energy = $(U_1 - U_2)/RT$.

[18] Brunauer, Emmett, and Teller, *J. Am. Chem. Soc.*, Vol. 60, p. 309 (1938).

2.3.2 Contamination due to Thruster Plumes

Studies of thruster exhaust plumes indicate that thrusters are known to scatter a very small fraction of the ejected mass at angles greater than 90° off of the thruster axis, Figure 2-17.[19] Typically the amount of mass ejected at the higher angles is less than one part in 10^3, but this is dependent on the specific thruster design. Because mass ejection at high off-axis angles is a real possibility, there is often a concern that firing a spacecraft's propulsion system could cause contaminants from the exhaust plume to impact sensitive surfaces. (This is particularly of concern during rocket stage separation.[20]) Plume impingement could be the indirect result of ejection at high off-axis angles, which would be due to scattering within the plume itself, or the result of scattering from ambient molecules near the spacecraft. (This last scenario is highly unlikely to begin with due to the mass difference between ambients and fuel products, and would also decrease in probability with altitude as atmospheric density decreases.) Hydrazine monopropellant and bipropellant fuels are commonly used for nominal on-orbit station-keeping maneuvers. Both on-orbit measurements and laboratory tests have indicated that hydrazine exhaust does not collect on surfaces warmer than about –45° C.[21] Analine impurity decomposition products were witnessed at –101° C, water was collected at –129° C, and ammonia was detected at –167° C. Consequently, deposition from hydrazine thruster plumes will not be a problem for most non-cryogenic surfa. Bipropellant exhaust constitutes a larger contamination concern. The predominant species in th. bipropellant plume resulting from incomplete combustion of MMH and N_2O_4 is monomethylhydrazine nitrite (MMH-HNO_3). With an activation energy of 20.48 kcal/mole, MMH-HNO_3 is a ntamination concern for cooled surfaces.[22] That is, it would have a residence time longer than th. of the universe on a 100 K surface.

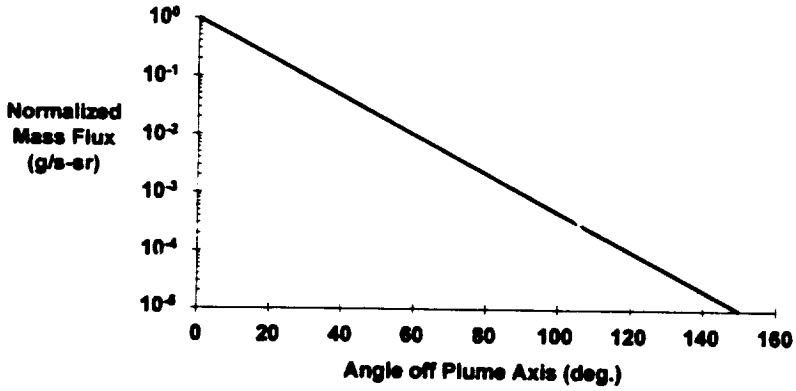

Figure 2-17. Thruster plume off-axis scattering.

[19] Etheridge, F. G., Garrard, G. G., and Ramirez, P., "Plume Contamination Measurements," Rockwell International, SSD84-0073, June (1984).

[20] Allegre, J., Raffin, M., and Lengrand, J. C., "Experimental Study of the Plume Impingement Problem Associated with Rocket Stage Separation," *J. Spacecraft*, Vol. 23, No. 4, pp. 368 - 372, July - August (1986).

Arnold, G. S., Doi, J. A., and Sinsheimer, F. B., "Estimates of Environmental Interactions of Contaminant Films from Titan IV Staging," The Aerospace Corporation, TOR-93(3409)-3, 15 April 1993.

[21] Fote, A. A., and Hall, D. F., "Contamination Measurements during the Firing of the Solid Propellant Apogee sertion Motor on t '78-2 (SCATHA) Satellite," in Society of Photo Optical Instrumentation Engineers, *Seattle Optical Environment*, Vol. 287, p. 95 (1981).

Carre, D. J., and Hall, D. F., "Contamination Measurements during Operation of Hydrazine Thrusters on the P78-2 (SCATHA) Satellite," *J. Spacecraft*, Vol. 20, no. 5, p. 444 (1983).

[22] Liu, C.-K., and Glassford, A. P. M., "Contamination Effect of MMH/N2O4 Rocket Plume Product Deposition," *J. Spacecraft*, Vol. 18, no. 4, p. 306 (1981).

2.4 Synergistic Effects

2.4.1 Photochemically Enhanced Deposition

As with many space environment effects there is often the possibility that synergistic interactions between two or more effects may result in a total degradation that is greater than the sum of its parts. An excellent example is the interaction between the solar UV and molecular contamination. On orbit, illuminated solar arrays would be thought to be too warm, (~ 60° C), to allow for the buildup of molecular contamination due to the very short residence times anticipated for most contaminants, (« 1 s). However, it is well documented in the laboratory that the presence of UV light can cause contamination to condense on surfaces that would otherwise remain clean.[23] Presumably, the UV light initiates a polymerization process that either: i) binds the contaminant molecule to the surface, or ii) binds several contaminant molecules into a larger molecules with a correspondingly longer residence time. It is now accepted that this photochemical deposition process was responsible for an accelerated degradation in solar array output noted on the GPS Block I satellites, Figure 2-18.[24] As a result, even warm surfaces may be subject to the deposition of contaminant layers if they are exposed to the solar UV. The rate of photochemical deposition of contaminants is seen to increase as the molecular arrival rate decreases, Figure 2-19.[25] Consequently, the photochemical sticking coefficient will increase as outgassing rates decrease. The sticking coefficient, *SC*, is related to the impact rate, *IR* (Å/hr), by

$$\log SC = -0.797 \log IR - 1.156. \qquad \textbf{Equation 2-34}$$

The result may be a fairly linear buildup of contamination and photochemical deposition may continue to create problems long after outgassing rates have subsided to low values. The contamination related power degradation from the GPS Block I satellites did not become noticeable until after about 3 years on orbit. At this point in a mission the majority of the outgassing has long since ceased and contamination concerns, if not already apparent, have faded.

Another important consideration for the case of photodeposited films is the issue of contaminant absorptance. As shown in Figure 2-20, laboratory investigations confirm that photodeposited films may be much darker than the "typical" contaminant film used in Figure 2-6.[26] Consequently, when estimating contamination effects on sunlit surfaces the use of the more pessimistic absorptance profile is advised.

---

[23] Stewart, T. B., Arnold, G. S., Hall, D. F., and Marten, H. D., "Absolute Rates of Vacuum-Ultraviolet Photochemical Deposition of Organic Films," *J. Phys. Chem.*, Vol. 93, No. 6, pp. 2393 - 2400, (1989).

Stewart, T. B., Arnold, G. S., Hall, D. F., Marvin, D. C., Hwang, W. C., Young Owl, R. C., and Marten, H. D., "Photochemical Spacecraft Self-Contamination: Laboratory Results and Systems Impacts," *J. Spacecraft*, Vol. 26, No. 5, pp. 358 - 367, (1989).

[24] Tribble, A. C., and Haffner, J. W., "Estimates of Photochemically Deposited Contamination on the GPS Satellites," *J. Spacecraft*, Vol. 28, No. 2, pp. 222 - 228, (1991).

[25] Hall, D. F., Stewart, T. B., and Hayes, R. R., "Photo-Enhanced Spacecraft Contamination Deposition," AIAA Paper 85-0953, 20th Thermophysics Conference, Williamsburg, VA, June (1985).

[26] Judeikis, H. S., Arnold, G. S., Young Owl, R. C., and Hall, D. F., "Design of a Laboratory Study of Contaminant Film Darkening in Space," Aerospace Report No. TR-94 (4935)-3, 1 October 1993.

Arnold, G. S., and Luey, K., "Photochemically Deposited Contaminant Film Effects: Data Archive, Vol. 2 - Appendices A through D.," Aerospace Report No. TR-94 (4935)-13, 15 September 1994.

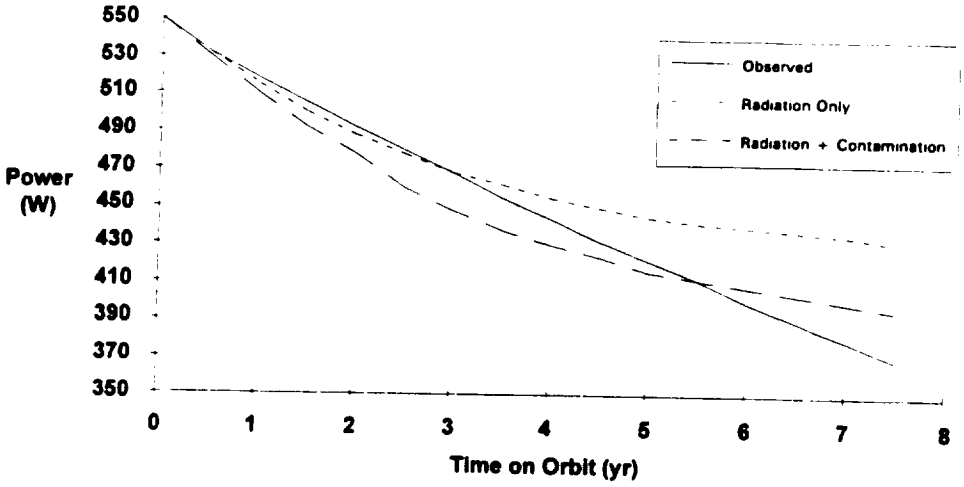

Figure 2-18. Evidence of photochemically deposited contamination on GPS Block I.

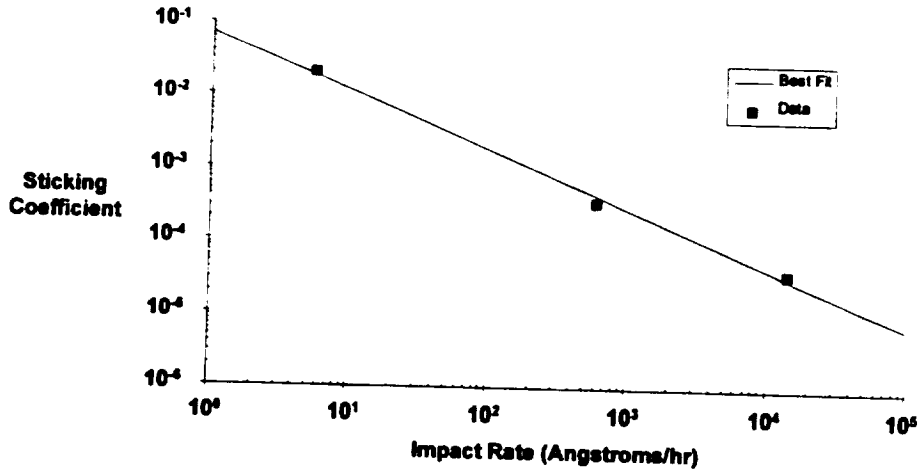

Figure 2-19. Photochemical deposition absorption ratio vs. impact rate.

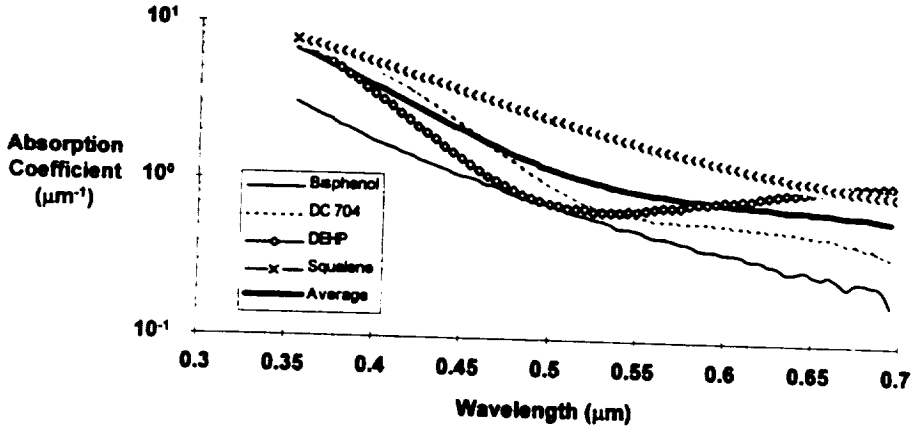

Figure 2-20. Absorptance profile of photochemically deposited films.

2.5 Estimating End of Life Molecular Cleanliness Levels

In order to establish allowable contamination levels for sensitive surfaces it is necessary to know: i) how contamination will affect the performance of the spacecraft subsystem, and ii) what performance degradation the subsystem can tolerate. With this information it will be possible to quantify how much contamination the subsystem can tolerate. This is usually done for end of life conditions, since a more stringent contamination limit has cost and schedule impacts, while a less stringent limit may shorten mission life.

2.5.1 Solar Arrays

Using the solar output shown in Figure 2-2, the spectral response shown in Figure 2-11, and the absorptance profile shown in Figure 2-20, (because films resident on a illuminated solar array would most likely be due to photochemical deposition), the resulting power output is shown in Figure 2-21. As shown, A 1% power margin equates to roughly level A depending on the specific nature of the contaminant. Note that the degradation due to photochemically deposited films, Figure 2-20, is much greater than that associated with non-photochemically deposited films, Figure 2-12.

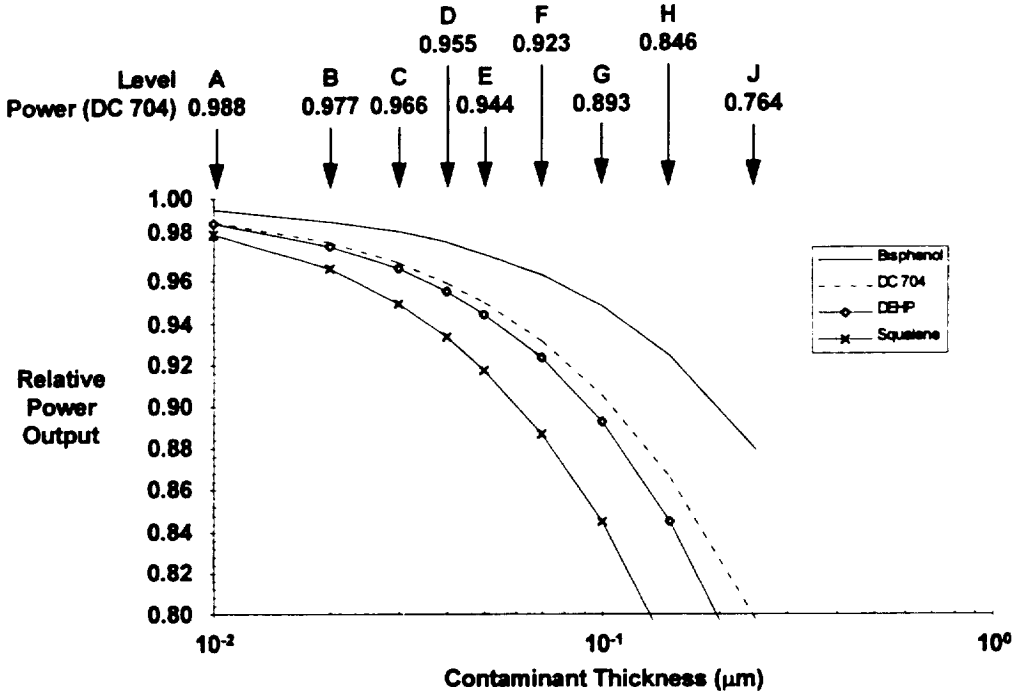

Figure 2-21. Solar array power as a function of MIL STD 1246C cleanliness levels.

The preceding example has made two key assumptions that may or may not be justified, depending on the problem at hand. First, the power degradation in Figure 2-12 is based on the spectral response characteristics of a solar cell as specified in Figure 2-11 and a contaminant absorptance profile as illustrated in Figure 2-20. If the values for the problem in question are noticeably different, it may have an effect on the required surface cleanliness.

More importantly, the surface cleanliness requirement requires interpretation to understand if it is viewed as an "average" contamination requirement or "worst case" contamination requirement. The answer depends on the actual spacecraft design. A solar array is manufactured by connecting the individual solar cells in series into a "string" of cells that produces the required voltage. A single cell usually produces ~ 1 volt, while the spacecraft bus requires much more, (28 volts is typical for most U.S. spacecraft). The number of cells in a string, and the number of strings in the panel, is therefore determined by the power requirement. Because of the nature of solar cells, if a single cell in a string is

degraded by contamination the power output of the entire string will be effected. That is, the power output from a single string of solar cells is governed by the "worst case" deposition on that string. The power production from the entire array is simply the sum of the power produced by the individual strings.

Consider the two options illustrated in Figure 2-22. A solar array that has its strings of solar cells oriented parallel to the spacecraft boom presents a high view factor between the spacecraft body, and all of its contamination sources, and one cell in each string. This design is vulnerable to contamination as a single outgassing source could contaminate every string on the panel. Conversely, a design which orients its strings perpendicular to the spacecraft boom presents a high view factor for the string nearest the body and a much lower one for the string farthest away. This option will be much more tolerant to contamination since an outgassing source on the vehicle would be expected to deposit most of its contaminants on the string nearest the body, and proportionately less on the strings further away. For this reason, the end of life surface cleanliness requirement that is specified for a solar array must also factor in the orientation of the strings in order to be meaningful.

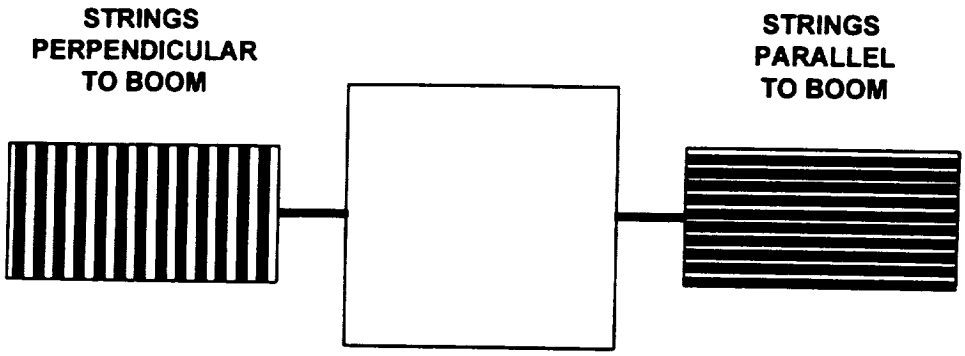

Figure 2-22. Solar array design options.

2.5.2 Thermal Control Surfaces

Consider the example of a thermal control surface, assumed to be an optical solar reflector (OSR), with an end of life α_s/ε requirement of 0.12. The data shown in Table 2-5 indicate a contamination free value for solar absorptance of 0.06. As shown in Figure 2-23, an end of life α_s/ε value of 0.12 equates to a contaminant thickness of about 0.1 μm, or surface cleanliness level G. This contamination requirement is interpreted as the "average" contamination value. The radiator will absorb heat from space in proportion to its solar absorptance and its area. Consequently, it may be acceptable for certain portions of the radiator to be degraded below the level G requirement, provided that the remaining portions of the radiator are clean enough to compensate for the dirty parts.

This result is predicated on a surface reflectance as specified in Figure 2-5 and a nominal contaminant absorptance profile as shown in Figure 2-6. Consequently, this result is more applicable to surfaces that are not illuminated by the Sun. Using the photochemically deposited contaminant absorptance profile from Figure 2-20 would produce a greater degradation in α_s for a given value of contaminant thickness.

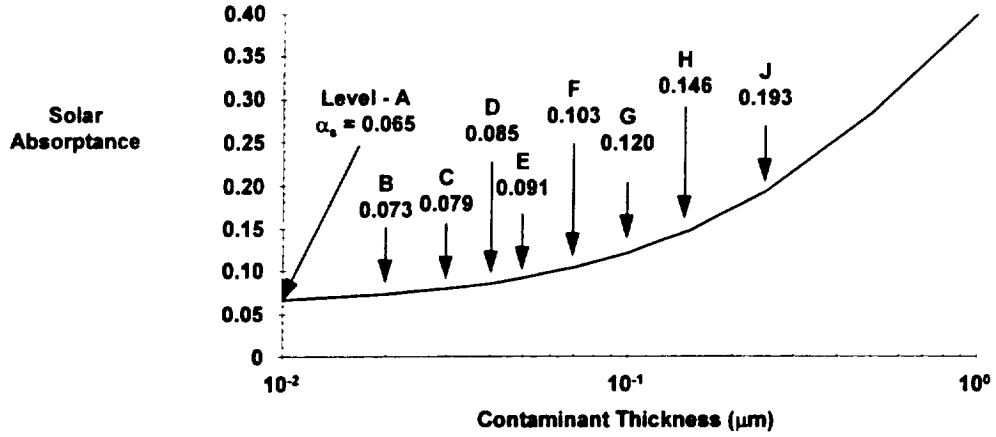

Figure 2-23. Degradation of an optical solar reflector (OSR) with initial α_s = 0.06 as a function of MIL STD 1246C cleanliness levels.

2.5.3 Optical Surface Contamination

Consider the example of a visible sensor, composed of 3 reflective mirrors, 2 transmissive lenses, and a focal plane, operating in the 0.35 - 0.90 μm waveband. We will assume that the sensor has an initial signal to noise ratio (SNR) of 10.0 and requires a value of at least 9.0 for acceptable operation. The contaminant absorptance profile shown in Figure 2-6 would reduce the signal strength in this waveband as shown in Figure 2-24.

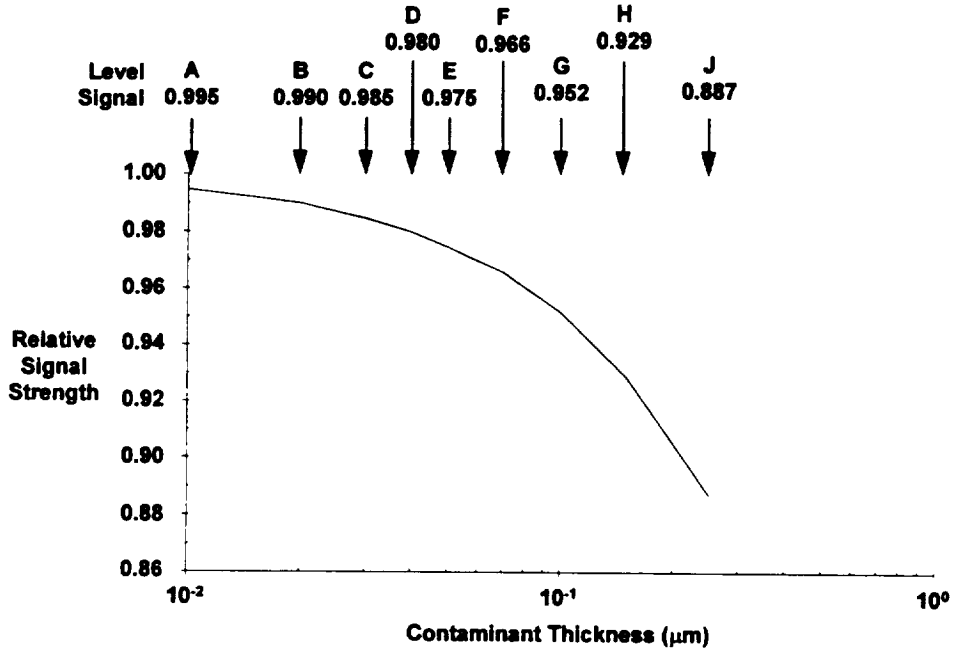

Figure 2-24. Degradation in signal strength as a function of MIL STD 1246C cleanliness level for a broadband visible sensor.

A signal strength reduction by 9.0/10.0 = 0.90 equates to a surface cleanliness requirement of about 0.2 μm, or level H. However, this is a total contamination requirement to be distributed between all

elements of the optical train. That is, the total contaminant thickness that the signal can traverse, and still have the minimum required strength, is 0.2 μm. The signal will not care whether all of the contamination is present on the first optical element or evenly dispersed over all elements. As a result, the requirement must be interpreted before it can be flowed down to specifications. Evenly distributing this requirement between three mirrors, two lenses, and a focal plane array would imply an "average" surface cleanliness of 0.2 μm/11 = 0.018 μm, or level A. (Note that the factor of 11 arises because a light ray would have to traverse each mirror surface twice, plus the front and back of each lens. This is not necessarily physically accurate in that the outer surface of a lens will usually act as a contamination barrier, protecting the inner surface of the lens and other elements "downstream" in the optical train, from contamination which originates "upstream".)

Obviously, the waveband of interest, the contaminant absorptance profile in that waveband, and the design of the sensor are all a critical part of determining the contamination requirement.[27] Note that, as illustrated in Figure 2-6 and Figure 2-20, most contaminants are more absorptive in the ultraviolent than in the visible or infrared. For this reason, UV sensors are much more sensitive to contamination. It is not unusual for many sensors to go "blind" in the UV before even leaving the ground, due to the build up of contaminant films that are too small to noticeably affect visible or IR operations. The Earth Radiation Budget (ERB) instrument on Nimbus 6 and 7 experienced a 45% transmission loss in the 0.3 – 0.4 μm waveband after 3.5 years on orbit. Similarly the Strategic Aerosol and Gas Experiment (SAGE) instrument on AEM-B experienced between 5.5% and 11% transmission loss in four wavebands between 0.385 and 1.0 μm.[28]

2.6 Design Guidelines for Controlling Molecular Contamination

As summarized in Table 2-7, while many spacecraft elements are sensitive to contamination, the actual amount of contamination that an element can tolerate is highly dependent upon its function. As shown, UV sensor elements are the most sensitive to contamination, while IR sensor elements are least sensitive. This Table ignores the effects of particulate contamination, and the issue of contamination control, and should not be taken out of context. As will be seen in the next two chapter, visible and IR sensors are extremely sensitive to particulate contamination. For these elements, the required particulate contamination levels often drive the design of the entire spacecraft. The effects of molecular contamination can best be controlled by minimizing the amount of contamination that is: i) generated, ii) transported, and iii) deposited on a surface. The effects of contamination would also be reduced if the absorptance profile of the contaminants were minimized, but since this is rarely (if ever) an option it is not seriously discussed here.

As shown in Table 2-8, design options to minimize contamination fall into four categories: materials, design, operations, and margin. Most organic materials on board a spacecraft can be a source of outgassing. For this reason, simply choosing materials that do not generate many outgassed by-products is the simplest solution. Due to the diverse nature of materials on the vehicle, (RTV adhesives, cabling, wiring, paints, ...), eliminating all outgassing is simply not possible. However, the mass properties list can provide information for pre-flight analysis to identify those materials which will be expected to be the greatest sources. When possible, selecting low outgassing versions from a list of candidates can prevent many problems from occurring. If this is not an option, pre-flight

---

[27] Chen, A. T., Abe, N.D. Mullen, C. R., and Gilbert, C. C., "Contamination Sensitivity and Control of Optical Sensors," Society of Photo-Optical Instrumentation Engineers, *Optical Sensor Contamination: Effects, Measurement, Control*, Vol. 777, pp. 97 - 126, (1987).
Ostantowski, J. F., "Contamination Sensitivity of Typical Mirror Coatings - A Parametric Study," Society of Photo-Optical Instrumentation Engineers, *Spacecraft Contamination Environment*, p. 80, (1982).

[28] Mouldin, L. E., III, and Chu, W. P., "Optical Degradation due to Contamination on the SAGE/SAGE II Flight Instruments," Society of Photo-Optical Instrumentation Engineers, *Spacecraft Contamination Environment*, pp. 58 - 64, (1982).

treatment of the material may be necessary to reduce its on orbit outgassing.[29] Vacuum baking of materials will force outgassing to occur on the ground, rather than in space, and reduce the amount of volatiles that will be generated on orbit. Because this method is costly and the material will undoubtedly reabsorb water and other contaminants from the atmosphere between the bakeout and launch, it is used only when pre-flight analysis indicates it is the best systems level, (lowest cost), solution.

Table 2-7. Summary of molecular contamination concerns.

Element	Affected Parameter	Operational Criteria	Required Cleanliness: *If Single Surface*	Required Cleanliness: *If 5 Optical Surfaces*
UV Sensor[a]	Signal Strength	< 10% Absorption (0.2 - 0.3 μm)	~ 0.05 μm (Level B)	~ 0.004 μm (~ Level A/20)
Solar Arrays[b]	Power Production	< 2% Power Loss	~ 0.015 μm[a] (Level A)	N/A
Thermal Control Surfaces	α_s/ε Ratio	$\Delta\alpha_s$ < 2.0 initial α_s (Initial OSR α_s = 0.06)	~ 0.2 μm (Level H)	N/A
Visible Sensor	Signal Strength	< 10% Absorption (0.35 - 0.90 μm)	~ 0.2 μm (Level H)	~ 0.04 μm (Level D)
IR Sensor[c]	Signal Strength	< 10% Absorption (1.0 - 2.0 μm)	~ 1.5 μm (>> Level J)	~ 0.3 μm (~ Level J)

[a]assumes nominal contaminant absorptance profile - highly absorptive in the UV
[b]assumes darker, photochemically deposited contaminant absorptance profile
[c]requires cryogenic surfaces that retain contaminants

Table 2-8. Design guidelines to minimize molecular contamination.

Materials	*Selection* Choose low outgassing materials for all applications, (adhesives, paints, coatings, ...) *Pre-Treatment* Consider vacuum bakeout of critical materials before installation in the vehicle
Design	Locate vents and thrusters with minimal view factors to sensitive surfaces
Operations	*Ground* Insure good contamination control procedures during assembly and test, provide for inspection and cleaning of sensitive surfaces *Flight* Allow time for on orbit bake out during early operations, provide cooler surfaces the opportunity to warm up and outgas condensed films
Margin	Allow for degradation in both ground and flight operations

Although multi-layer insulation (MLI) blankets, paints, and other materials on the exterior surfaces of a vehicle will be sources of outgassing, most of the outgassed mass originates internal to the vehicle where the electronic boxes and cabling are located. The matter that is outgassed interior to the vehicle will undergo multiple scatterings until it can locate a vent path and escape. Consequently, the design and location of the vents, and thrusters, are an equally critical part of contamination control. Designing a vehicle so that view factors from possible spacecraft sources to sensitive surfaces are minimal is straightforward, but does require a conscious effort on the part of the designer.

[29] O'Donnell, T., "Evaluation of Spacecraft Materials and Processes for Optical Degradation Potential," Society of Photo-Optical Instrumentation Engineers, *Spacecraft Contamination Environment*, Vol. 338, p. 65, (1982).

The last stage in the process, deposition, is rarely anything that the designer can control directly. The fundamental chemical nature of the contaminant, and the nature of the surface material and its temperature, will control the deposition rate. This rate can only be indirectly affected by warming the surface, to minimize deposition, and keep them pointed away from the Sun, to minimize photochemical deposition. Obviously, the mission objective must be considered before designing these alternatives into a system.

Once the design has been cast, ground operations will still play an important role in determining the surface cleanliness of the vehicle when ready for launch. Outgassing from test equipment or surrounding facilities can contaminate a spacecraft while it is being assembled. Periodic inspection and, if necessary, cleaning will be required to verify beginning of life cleanliness levels. End of life performance can often be extended through proper on orbit flight operations. Allowing a spacecraft several days, or weeks, to outgass upon reaching orbit, and before opening sensor covers, is one means of insuring that contaminants dissipate before sensitive surfaces are exposed. Cooled surfaces, such as IR focal planes, can be allowed to warm up in an attempt to "boil off" condensed contaminants. However, this example would subject the focal plane to thermal stresses, would render the sensor useless during the procedure, and would require recalibration after the procedure. For this reason it is viewed as a last resort option.

The final, and often most critical, step that a design engineer can take to ensure proper on orbit performance is to allocate a proper margin. As we have seen, contaminant thicknesses on the order of 0.1 μm are sufficient to cause noticeable degradation of many surfaces. Therefore, some allocation must be made for the degrading effects of molecular contamination on most surfaces. The actual value to be used will be dependent on the nature of the surface, criticality of the subsystem, mission objective, cost and schedule. As a general rule, the more sensitive a surface is to contamination, the more costly and time consuming it will be to insure that it performs properly on orbit. Providing a generous margin, if possible, will minimize cost, schedule, and risk.

3. Quantifying Particulate Contamination Level Requirements

3.1 Effects of Particles

By definition, particles are visible (μm-sized) conglomerations of matter that deposit onto surfaces exposed to the environment. In the colloquial sense, they are simply "dust". Particles are a natural part of the environment as is familiar to anyone who has ever dusted a mantlepiece or washed a windshield. Modeling a particle as a sphere of arbitrary size, as shown in Figure 3-1, we see that the effect of the dust on the surface may be twofold.

First, the dust will prevent some light from reaching the underlying surface. Some effects of particulate contamination are therefore proportional to the surface obscuration, or the percent area coverage (PAC). Solar arrays, thermal control surfaces, and optical surfaces may all be degraded due to surface obscuration. Secondly, the particles may scatter light off of its original direction of travel. This is a critical concern for many optical systems.

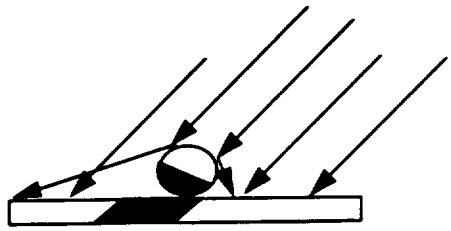

Figure 3-1. A particle on a surface.

3.1.1 Surface Obscuration - Effects on Reflecting Surfaces

3.1.1.1 Optical Elements - Mirrors

The presence of particles on a reflecting mirror will reduce the strength of the signal that is reflected to the next optical element. Normally, particles would be expected to have a rather high absorptivity, consequently any light from the signal which falls on a piece of dust, rather than the actual mirror, will be lost to the optical system. The magnitude of the loss in signal strength is therefore expected to be proportional to the fractional surface area that is obscured by the particles.

3.1.1.2 Thermal Control Surfaces

The presence of particles on a thermal control surface will have the net effect of altering its effective solar absorptance and/or emissivity.[1] By design, many thermal control surfaces are chosen to have a low value of solar absorptance. Particles, which would typically have a higher solar absorptance than the underlying surface, would block some light from reaching the radiator directly. However, most of the obscured solar flux would be absorbed by the particles rather than reflected back to space. As a result, the particles would seek a higher equilibrium temperature than the surface on which they are sitting. The particles would then radiate, and conduct, more heat to the surface than they receive in return and the end result would be an increase in the equilibrium temperature of the surface. By inspection, the change in solar absorptance due to particles is given by

$$\alpha_s^* = \alpha_s + \Delta\alpha_s = \alpha_{s,surf.}(1 - PAC) + \alpha_{s,part.}(PAC), \qquad \textbf{Equation 3-1}$$

or

[1] Hamberg, O., and Tomlinson, F. D., "Sensitivity of Thermal Surface Solar Absorptance of Particulate Cointamination," AIAA 71-473, 6th Thermophysics Conference, Tullahoma, TN, April (1971).

$$\Delta\alpha_s = PAC(\alpha_{s,part.} - \alpha_{s,surf.}), \qquad \text{Equation 3-2}$$

where $\alpha_{s,surf}$ and $\alpha_{s,part}$ refer to the solar absorptance of the clean surface and particles, respectively, and *PAC* is the percent area coverage of the particles. Similarly, particles will also change the effective emissivity of a surface according to the relation

$$\varepsilon^* = \varepsilon + \Delta\varepsilon = \varepsilon_{clean}(1 - PAC) + \varepsilon_{part.}(PAC), \qquad \text{Equation 3-3}$$

or

$$\Delta\varepsilon = PAC(\varepsilon_{surf.} - \varepsilon_{part.}). \qquad \text{Equation 3-4}$$

Consequently, it is seen that the effective increase in solar absorptance, emissivity, and equilibrium temperature, (Equation 2.13), is directly proportional to the *PAC*. Note that the biggest concern is to be expected if black (highly absorptive) particles are deposited on white (highly reflective) surfaces, or if white (low emissivity) particles deposit on black (high emissivity) surfaces. Most particulate contamination is dust, with some sand and soil particles, especially out of doors. Lint, pieces of thread, and hairs may also be present where people are active. Most of these particles are a dull gray having $\alpha_s > \sim 0.5$, $\varepsilon > \sim 0.5$, and are optically opaque. Gray particles would have little effect on gray surfaces.

3.1.2 Surface Obscuration - Effects on Transmitting Surfaces

3.1.2.1 Solar Arrays

Because solar cells are non-imaging devices, surface obscuration at the wavelengths of interest, (~ 0.4 - 1.1 μm), is the only effect of surface particles. At first glance it would appear that the power reduction would be exactly equal to the *PAC* of those particles. However, individual solar cells are less sensitive to surface particles that expected. Experiments indicate that a 1% *PAC* produces only a 0.2% power loss, Figure 3-2.[2] A *PAC* of ~ 2.2% was required to produce a 1% power loss. While some of the particles may be partially tramsmissive, the major effect is believed to be scattering around the particles. Consequently, the power degradation is almost invariably less than the *PAC*.

As with molecular contamination, the effect of surface particle contamination on a string of solar cells depends upon the manner in which the contamination is deposited. If each cell in a string is equally contaminated the overall effect will be as shown in Figure 3-2. However, if one cell were to receive all of the contamination the power reduction will be much greater. That is, if all of the particles were collected to form a sheet obscuring 1% of the solar cell, a power decrease on the order of 1% would be expected. This is due to the fact that the contaminated cell not only produces less power, but also becomes a resistive load also, (neglecting temperature effects, which can be important if the cells are not all at the same temperature). As discussed in section 2.5.1 of this report, string orientation is important if the cells in that string are not equally contaminated.

[2] Raab, J. H., *Particulate Contamination Effects on Solar Cell Performance*, MCR-86-2015, Rev A, Final Report for F04701-83-C-0045, January (1987).

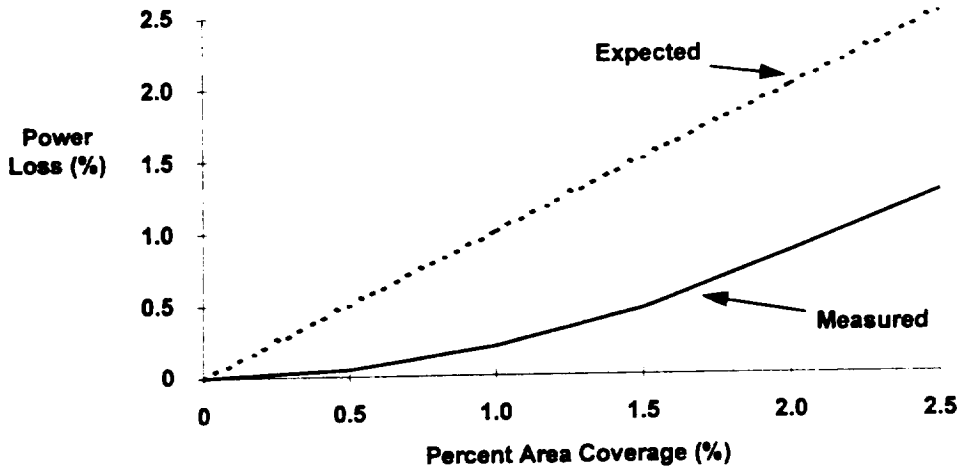

Figure 3-2. Solar array power loss due to surface obscuration by particles.

3.1.2.2 Optical Elements - Lenses, Focal Plane Arrays, and Concentrated Optics

As with the optical mirror, any particulate contamination which resides on a lens or a focal plane array would prevent the optical element from transmitting the signal and reduce its signal strength in proportion to the *PAC*. A critical difference for most lenses, and especially focal planes, is that these locations are typically where the signal from a wide collecting area, (the primary mirror), has been focused into a much smaller cross section. The end result is that particulate contamination on the final optical element, or the focal plane, will be much more damaging than would particles on the primary mirror. For example, if the primary mirror is 1 m^2 in area, but the focal plane is only 10 cm^2, the signal gathered by the primary mirror has been focussed by a factor of 1000 before reaching the focal plane. Absorption at this last location is therefore 1000 times as damaging to the signal strength. More importantly, because of the small size of modern focal plane detector elements even small particles, < 5 μm in diameter, can block one or more focal plane pixels which are of the same order. This effectively blinds the pixel permanently. Because of the magnification of the telescope, even a small particle on the focal plane blocks more of the signal that many large particles on the primary mirror or lens. Since particles are comparable to the wavelengths for many IR sensors, they can also scatter light to other pixels not directly obscured.

3.1.2.2.1 Additional Concerns for Focal Planes

If the particle is even partially electrically conducting it may short out one or more pixels unless the focal plane is covered by a non-conducting filter, (which is often the case). As for particles on the primary optical surface, mechanical or chemical damage is seldom a problem. It is possible for a particle to produce a thermal problem since focal planes for IR sensors typically operate at low temperatures (< 77 K). The cooling requirements for these focal planes are typically a few milliwatts. If a particle were to be located where it produces a thermal "short" to a warmer sensor component close to the focal plane, the refrigeration may be unable to maintain the focal plane temperature. If the focal plane is cooled by onboard cryogen, the result would be a reduced mission life. Incidentally, molecular contamination, such as ice), can also form thermal shorts near the focal plane with similar results.

While focal planes are nearly always protected against external contamination, they are vulnerable to internal contamination. It is very important that all components of optical sensors be fabricated from materials which do not outgas, flake, or otherwise produce contamination. The launch environment may shake particles loose from some part of the sensor which could land on the focal

plane. While small particles are difficult to remove by "g" forces, (it takes a force several thousand times the acceleration due to gravity to dislodge μm-sized particles), the possibility should not be overlooked.

3.1.3 Scattering

In addition to surface obscuration, which effectively reduces signal strength, the presence of particles on optical surfaces can induce other disastrous consequences into an optical train. By design, a baffle is intended to block extraneous signals from off axis sources and prevent them from being able to reach the focal plane. A perfectly absorptive surface would prevent all incident light from the Sun, for example, from reaching the focal plane. Consider the effects of dusting this surface with particles that are less than 100% absorptive. If particles on an optical baffle are even partially reflective they may scatter light from the Sun, (or other off-axis source), back into the optical train. Because of the large intensity of the Sun, 1350 W m^{-2}, if even a small fraction of this energy were scattered into the optical train and able to reach the focal plane it could be sufficient to overwhelm the signal from the sensors intended target and possibly even damage the focal plane itself. For this reason, keeping any surface within an optical element clean is of utmost importance.

As a first step in relating surface cleanliness to surface scattering it is appropriate to emphasize some of the key objectives of optical design.[3] We first define stray light to mean light from any source other than the object that the sensor is interested in observing. Typically, the biggest sources of stray light for an orbiting sensor are the Sun, Earth, and Moon. A system can be designed to reject stray light by forcing the stray light out of the optical train, so that it cannot reach the detector, or by causing it to make the maximum number of reflections off of absorbing surfaces before reaching the detector. For example, a baffle surface with a reflectance of 0.01 would attenuate the signal by a factor of $(0.01)^n$ after n bounces. The amount of stray light radiation reaching a detector due to scattering off a small element of an internal surface, such as a baffle or a mirror, is the product of three factors: i) the amount of radiation incident upon the surface, (the strength of the stray light source), ii) the reflectivity of the surface for the particular incoming and outgoing directions, and iii) the projected solid angle of the detector as seen from the element.

The amount of radiation incident upon a given surface will be determined primarily by operations. That is, the geometry between the Sun and the object of interest will determine the amount of sunlight that can strike a given location within the baffle, Figure 3-3. For this reason, one requirement flowing from the design characteristics of the sensor will be an operational constraint on the Sun exclusion angle, (and possibly also an Earth/Moon exclusion angle). Surface reflectivity is ultimately related to surface cleanliness. A surface with a reflectance of 0.01, (an absorptance of 0.99), will be a better attenuator of stray light when it is clean than it will be when dirty. When dirty each and every particle of dust will act as a separate scattering source and will increase the reflectance of absorbing surfaces. One challenge of stray light analysis is to relate surface cleanliness requirements to sensor design and operational constraints. Finally, the projected solid angle of the detector from a given element within the sensor is a factor that is fixed by design. Once the design of the sensor has been fixed based on the characteristics of the target, and the operations geometry has determined the strength of off-axis sources, surface cleanliness remains the last barrier to ensuring effective operations. This is seen as follows.

3.1.3.1 Mie Scattering

The first systematic study of scattering by larger particles was done by Mie.[4] These studies were aimed at understanding the scattering by spherical, colloidal metal particles. The results provide a qualitative understanding of scattering by non-spherical particles, and reduce to Rayleigh's theory

[3] Race, L. B., personal communication from "Stray Radiation Analysis of the Brilliant Eyes Line of Sight Pointing Mirror Assembly and Alternative Configuration Designs," Rockwell International, 21 September 1993.

[4] Mie, G., *Ann. Phys.*, Vol. 25, no. 4, pp. 377 - 445, (1908).

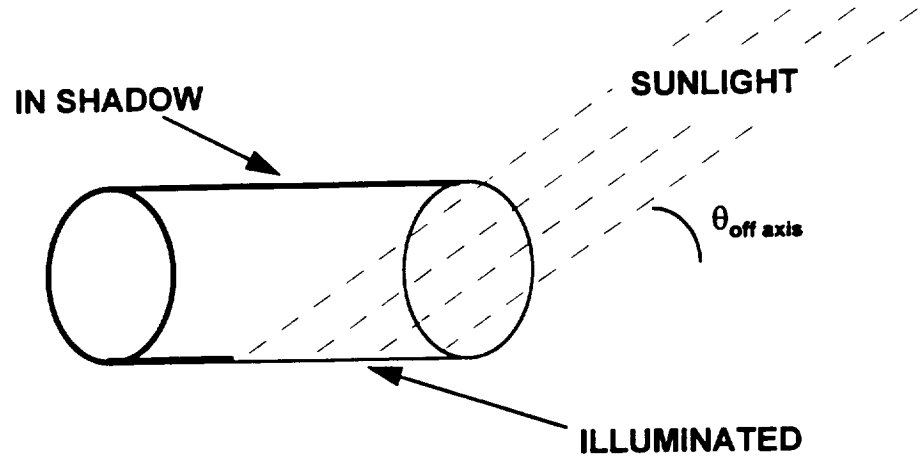

Figure 3-3. Geometry determines scattering on baffle surfaces.

when the spheres are very small. Rayleigh scattering is the name applied to the incoherent scattering of light by particles of dimension smaller than the wavelength of the light.[5] Mie theory shows that the ratio of scattered energy to the incident energy intercepted by the geometrical cross section of the particles is given by

$$2\left(\frac{\lambda}{2\pi d}\right)^2 \sum_{j=1}^{\infty}(2j+1)\left\{|a_j|^2+|b_j|^2\right\}, \qquad \textbf{Equation 3-5}$$

where a_j and b_j are functions of spherical Bessel functions and Hankel functions of the second kind with complex arguments.. This is illustrated in Figure 3-4.

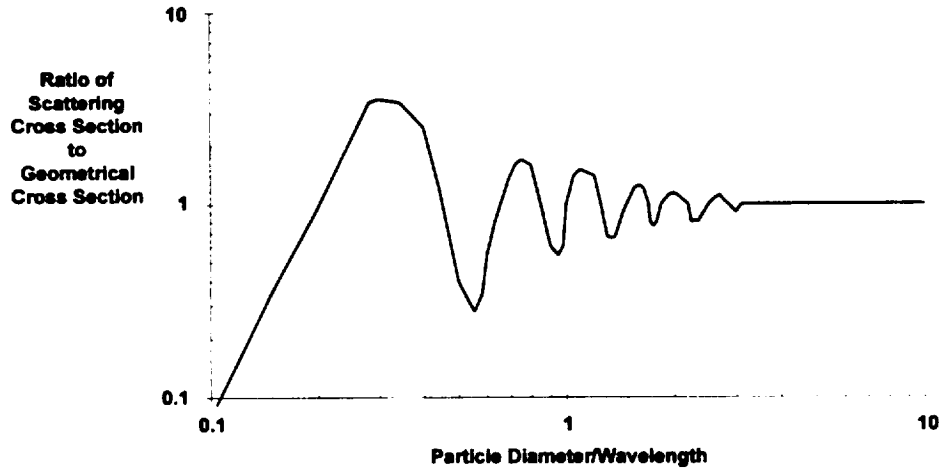

Figure 3-4. Ratio of scattered energy to incident energy as predicted by Mie theory.

[5] Rayleigh, J. W. S., *Philos. Mag.*, Vol. λ. , pp. 107 - 120, (1871).

For $d/\lambda << 1$ the behavior is $(d/\lambda)^{-4}$. This is the Rayleigh scattering which accounts for the blue color of the sky. For $d/\lambda \sim 1$ the scattering cross section oscillates between about 0.4 and 4.0 times the geometrical cross section, so that Mie theory is necessary for particles of this size and larger. For d/λ greater than about 3, the scattered energy is not strongly dependent on λ and the methods of geometrical optics are used. Experimental observations of scattering typically indicate fairly good agreement with Mie theory.[6]

3.1.3.2 Bidirectional Reflectance Distribution Function (BRDF)

Based on conservation of energy and momentum, a perfectly smooth surface would satisfy the condition that the angle of incidence θ_i is equal to the angle of reflection θ_r. Because no physical surface can ever be perfectly smooth, all real optical devices will have surface imperfections due to cracking, pitting, or particulate contamination. One effect of these imperfections is to scatter a small fraction of the incident light at angles other than $\theta_r = \theta_i$. One measure of the scatter of optical components is the bidirectional reflectance distribution function (BRDF), which is the scattered surface radiance divided by the incident surface irradiance.[7] BRDF is a function of many variables and is defined by

$$\text{BRDF} = f_s(\theta_i,\phi_i:\theta_s,\phi_s) = \frac{dL_s(\theta_i,\phi_i:\theta_s,\phi_s:E_i)}{dI_i(\theta_i,\phi_i)}, \qquad \textbf{Equation 3-6}$$

where L_s (W m^{-2} sr^{-1}) is the scattered radiance measured at (θ_s, ϕ_s) and I_i (W/m^2) is the incident irradiance from (θ_i, ϕ_i) as illustrated in Figure 3-5. The units of BRDF are sr^{-1}. Intuitively, BRDF can be defined as the ratio of the scattered power measured by a detector to the incident power on the sample, divided by the projection of the solid angle of the detector on the sample surface.

Closed form solutions for BRDF are difficult to obtain, but there is general agreement that BRDF can be deconvolved into three independent terms. That is,

$$\text{BRDF} = F_\lambda F_o F_s, \qquad \textbf{Equation 3-7}$$

where F_λ is the wavelength, or spectral, factor given by

$$F_\lambda = \frac{k^4}{\pi^2} = \left(\frac{2\pi}{\lambda}\right)^2 \frac{1}{\pi^2} = \frac{16\pi^2}{\lambda^4}, \qquad \textbf{Equation 3-8}$$

---

[6] Schade, H., and Smith, Z. E., "Mie Scattering and Rough Surfaces," *Applied Optics*, Vol. 24, No. 19, pp. 3221 - 3226, (1985).

[7] Bartell, F. O., Dereniak, E. L., and Wolfe, W. L., "The Theory and Measurement of Bidirectional Reflectance Distribution Function (BRDF) and Bidirectional Transmittance Distribution Function (BTDF)," Society of Photo-Optical Instrumentation Engineers, *Radiation Scattering in Optical Systems*, Vol. 257, pp. 154 - 160, (1980).

Nicodemus, F. E., "Directional Reflectance and Emissivity of an Opaque Surface," *Applied Optics*, Vol. 4, No. 7, pp. 767 - 776, (1965).

Nicodemus, F. E., Richmond, J. C., Hsia, J. J., Ginsberg, I. W., and Limperis, T., "Geometrical Considerations and Nomenclature for Reflectance," Department of Commerce, PB-273 439, October (1977).

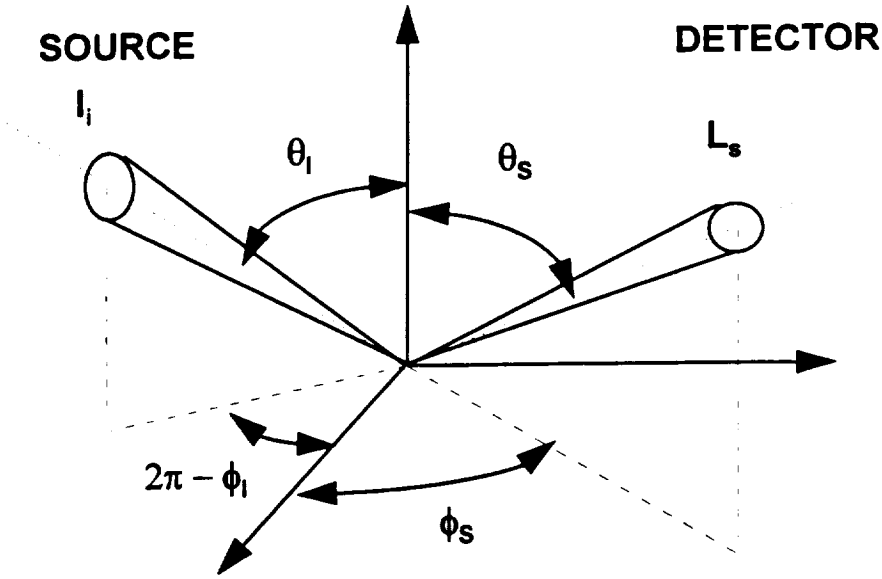

Figure 3-5. BRDF geometry.

F_o is the optical factor, which includes information about the surface material and geometry, and F_s is the surface factor, which includes the measure of surface roughness. The form of F_o and F_s vary depending on the theory used to obtain them.[8] Because no real materials or surface finishes can ever reach their theoretical values experimental measurements of BRDF are relied upon in most applications. Emperically, BRDF is seen to agree with the expression

$$\text{BRDF} = b\left[\frac{|\sin\theta_s - \sin\theta_i|}{0.01}\right]^m = b\left[\frac{|\beta_s - \beta_i|}{0.01}\right]^m, \qquad \textbf{Equation 3-9}$$

or equivalently

$$\log\text{BRDF} = \log b + m\log\left[\frac{|\beta_s - \beta_i|}{0.01}\right], \qquad \textbf{Equation 3-10}$$

where θ_s is the angle of scattering, θ_i is the angle of incidence (usually 0° in a test configuration), m is the observed slope, and b is the BRDF when $\sin\theta - \sin\theta_o = 0.01$. For smooth surfaces, m is typically between –1 and –3.

In practice, the theoretical BRDF cannot be reached even for non-symmetric telescope designs. Figure 3-6 shows what has been achieved for eight sensors which have been built. It is seen that off-

[8] Beckmann, P., and Spizzichino, A., *The Scattering of Electromagnetic Waves from Rough Surfaces*, Pergamon Press, (1963).
Davies, H. O., "The Reflection of Electromagnetic Waves from a Rough Surface," *Proc. IEEE*, Vol. 101, p. 209, (1954).
Wolfe, W. L., "Induced Angle Invariance in Surface Scatter," Society of Photo-Optical Instrumentation Engineers, *Scatter from Optical Components*, Vol. 1165, pp 10 - 17, (1989).

axis (non-symmetric) designs can achieve lower BRDF values at the expense of design and fabrication complexity. These measurements were on clean mirrors under controlled conditions and were achieved by super-polishing techniques. It will be noted that achieving these low BRDF numbers require an almost-perfect mirror figure, which is more easily done if the mirror is to be used at IR wavelengths.

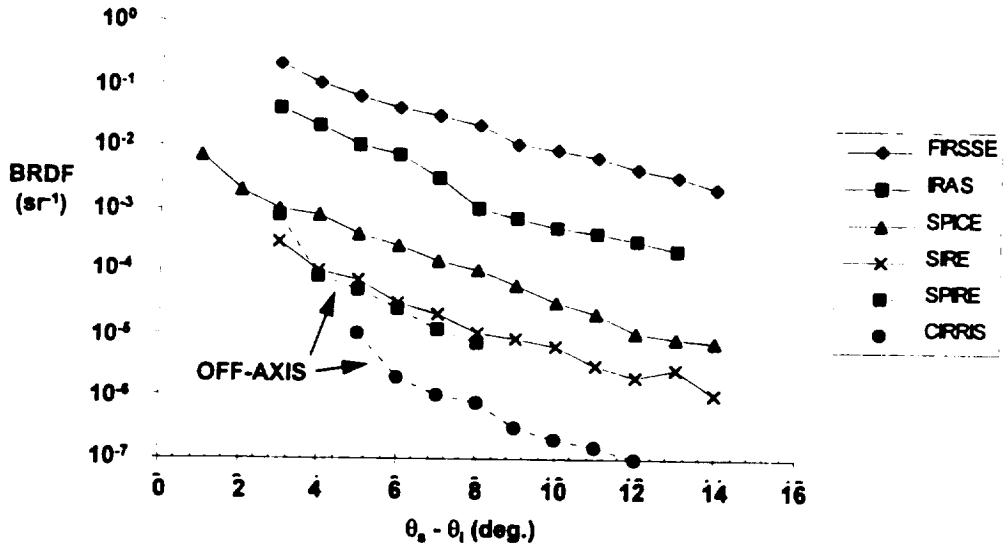

Figure 3-6. BRDF measurements for selected space sensors.

Often a BRDF of 10^{-4} at an angle of 1°, (i.e., the off axis source is 1° out of the sensors field of view), is taken as the idealized goal for reflecting telescopes. The smaller the λ/D ratio, the ratio of the wavelength to the telescope diameter, the easier this is to attain if the primary mirror has a perfect figure. However, the smaller the λ/D ratio, the more difficult it is to achieve even with an almost perfect figure. Considering that small λ/D ratios increase signal to noise ratio and also dramatically increase sensor weight, the sensor designer has a serious optimization problem.

As will be seen, even a little contamination on the mirror will increase its BRDF dramatically. Especially, if that contamination can scatter light. This is especially true for particles, but even a small amount of molecular contamination will increase the BRDF of a good mirror (however, if the mirror figure is bad, it takes more contamination of any kind to make it worse.) In essence, the presence of contaminantion acts to alter the surface factor F_s.[9] The presence of particles, or molecular films, will increase the surface roughness and, consequently, the BRDF. It should be pointed out that BRDF values add linearly. That is,

$$BRDF_{total} = BRDF_{mirror} + BRDF_{contam.}. \qquad \textbf{Equation 3-11}$$

Beyond about 8° off axis, the scatter is dominated by dust, not surface roughness.[10] Because of difficulties associated with manufacturing ideal surfaces, BRDF values for "perfect" surfaces can rarely be less than 10^{-6} at 1°. Machined surfaces may be in the range 10^{-5} to 10^{-3} at 1°, while a

[9] Bennett, H. E., and Porteus, J. O., "Relation Between Surface Roughness and Specular Reflectance at Normal Incidence," *J. Opt. Soc. Am.*, Vol. 51, No. 2, pp. 123 - 129, (1961).
Elson, J. M., and Bennett, J. M., "Relation Between the Angular Dependence of Scattering and the Statistical Properties of Optical Surfaces," *J. Opt. Soc. Am.*, Vol. 169, No. 1, pp. 31 - 47, (1979).

[10] Dowling, J. M., Hills, M. M., Arnold, G. S., Kan, A. K. A., "Contamination Effects on Surveillance Telescopes," The Aerospace Corporation, TR 93(3935)-14, 22 October 1993.

complete optical train may be more on the order of 10^{-2} at 1°. Note that the BRDF values required of a completed optical train must be decoupled in order to identify the required surface cleanliness requirement for individual surfaces.

3.1.3.2.1 Point Source Transmittance (PST)

BRDF is closely tied to sensor performance characteristics. For example, one measure of sensor performance is Point Source Transmittance (PST). PST is defined as the fraction of the signal strength from an off-axis point source that is transmitted to the focus of the optical train. The relation between BRDF and PST is

$$\mathrm{PST} = \frac{\pi}{4\left(\frac{L}{D}\right)^2}\frac{\cos\theta}{\theta^s}\left[1 - \frac{\theta}{\tan^{-1}\left(\frac{L}{D}\right)}\right]\mathrm{BRDF},$$

Equation 3-12

where L is the focal length of the optical train, D is the aperture diameter, θ (rad) is the angle between the normal and the point source, and s is a parameter that varies from 1, for typical optics, to 2, for superpolished mirrors. Consider the example of a space-borne sensor, such as the Hubble Space Telescope, that is pointing at a faint star cluster that lies within a few degrees of a bright object such as the Sun. The fraction of energy from the Sun that reaches the focal plane will be the product of the total solar output, 1350 W/m^2, and the sensor PST. The PST value, and consequently the BRDF value, would have to be quite small in order for the reflected solar radiation not to overwhelm the faint signal from the star cluster, or possibly even damage the sensor itself. This places a dual constraint on both the Sun exclusion angle (the minimum angular separation between the Sun and object of interest) and surface cleanliness levels.

3.2 Quantifying Particulate Contamination

3.2.1 MIL STD 1246C

As with molecular contamination, surface particle cleanliness is quantified by MIL STD 1246C, Table 3-1 and Figure 3-7. The surface cleanliness is specified by a numerical value, which is interpretted as the size, in μm, of the largest particle that has an average distribution of one per ft^2. Larger particles would occur less frequently than once per ft^2, while smaller particles occur more frequently. Emperical observations indicate that particle size distributions on surfaces exhibit a geometric mean near 1 μm, and are described by the relation

$$\log N(x) = C'\left[\log^2 X_1 - \log^2 x\right],$$

Equation 3-13

where $N(x)$ is the number of particles/ft^2 greater than or equal to x, x (μm) is the particle size, X_1 is the surface cleanliness level, and C' is a normalization constant approximated in the MIL STD by 0.9950. It is important to note that the value of C' is based on measurements of precision cleaned parts and is therefore representative of cleaned products. As shown in Table 3-2, (and Figure 4.8), the coefficients that were measured on uncleaned surfaces in a variety of cleanrooms disagree

Table 3-1. Particulate contamination as quantified by MIL-STD-1246C.

Cleanliness Level	Particle Size (μm)	Count per ft^{-2}	Count per 0.1 m^{-2}	Count per Liter
1	1	1.0	1.08	10
5	1	2.8	3.02	28
	2	2.3	2.48	23
	5	1.0	1.08	10
10	1	8.4	9.07	84
	2	7.0	7.56	70
	5	3.0	3.24	30
	10	1.0	1.08	10
25	2	53	57	530
	5	23	24.8	230
	15	3.4	3.67	34
	25	1.0	1.08	10
50	5	166	179	1,660
	15	25	27.0	250
	25	7.3	7.88	73
	50	1.0	1.08	10
100	5	1,785	1,930	17,850
	15	265	286	2,650
	25	78	84.2	780
	50	11	11.9	110
	100	1.0	1.08	10
200	15	4,189	4,520	41,890
	25	1,240	1,340	12,400
	50	170	184	1,700
	100	16	17.3	160
	200	1.0	1.08	10
300	25	7,455	8,050	74,550
	50	1,021	1,100	10,210
	100	95	103	950
	250	2.3	2.48	23
	300	1.0	1.08	10
500	50	11,817	12,800	118,170
	100	1,100	1,190	11,000
	250	26	28.1	260
	500	1.0	1.08	10
750	50	95,807	105,000	958,070
	100	8,900	9,630	89,190
	250	214	231	2,140
	500	8.1	8.75	81
	750	1.0	1.08	10
1000	100	42,658	46,100	426,580
	250	1,022	1,100	10,220
	500	390	42.1	390
	750	4.8	5.18	48
	1000	1.0	1.08	10

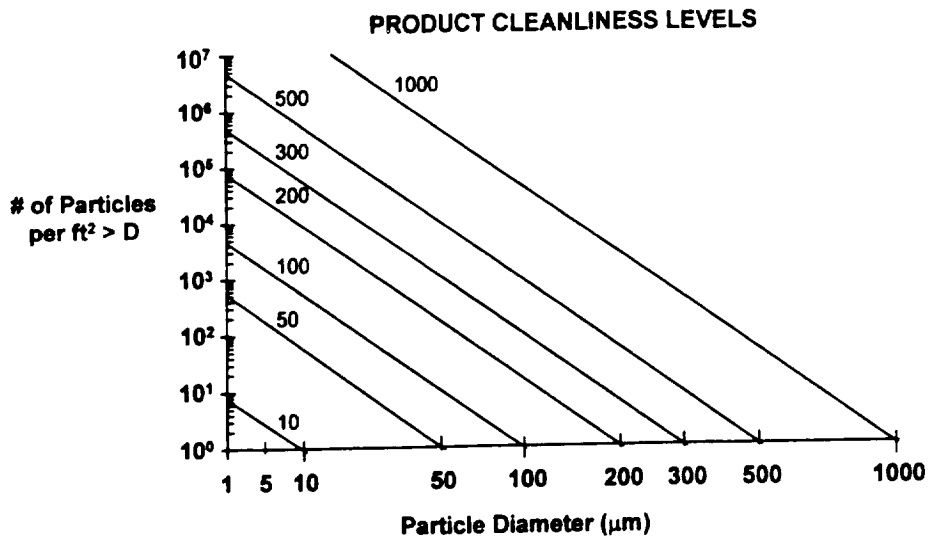

Figure 3-7. MIL STD 1246C surface particle cleanliness levels.

Table 3-2. Measured surface cleanliness values from various cleanroom facilities.

Source	Coefficient C'
MIL-STD-1246C	*0.926*
NASA/KSC	0.311
Aerospace Corp./KSC	0.380
Martin Marietta/KSC	0.315
TRW Factory	0.354
JPL/Eastern Test Range	0.557
Average	*0.383*
Std. Dev.	*0.101*

significantly from the value of 0.9260 assumed by the MIL STD.[11] For uncleaned surfaces a coefficient of 0.383 may agree better with observations. That is, the particle fallout from the air produces a size distribution weighted toward large particles, while surface cleaning is more effective at removing large particles than small particles. Consequently, when using the MIL STD to specify cleanliness levels it is important to limit its use to surfaces that have been cleaned after exposure to fallout. Note that the metric equivalent to Equation 13, where $N(x)$ is defined as the number of particles per 0.1 m^2 greater than or equal to x, is obtained by adding a second variable to the equation

$$\log N(x) = C'\left[\log^2 X_1 - \log^2 x\right] + C'', \qquad \textbf{Equation 3-14}$$

where C'' has the value 0.03197. $N(x)$ is related to the frequency function $n(x)$, defined as the frequency of particles of size x per m^{-2}, by the relation

[11] Hamberg, O., "Particle Fallout Predictions for Cleanrooms," *J. Env. Sci.*, Vol. 25, No. 3, p. 15, (1982).

$$N(x) = \int_{x}^{\infty} n(x')dx' . \qquad \textbf{Equation 3-15}$$

Note that while air quality can be added linearly, surface cleanliness cannot.

3.2.2 Percent Area Coverage

The geometrical *PAC* of a particle on a surface is simply the area of that particle, viewed normally to that surface, divided by the area of the surface. The total *PAC* of a collection of particles is simply the sum total of the area for each particle, assuming that particles do not lie on top of each other.

In principle, the *PAC* should be discernible from the number density, or frequency function, of particles on a surface. However, attempting to derive this information from Equation 3-14 proves difficult, as this equation actually predicts negative numbers of particles for sizes smaller than 1 μm. That is, the MIL STD was apparently intended to describe larger particles and will require modification for *PAC* calculations.[12]

As shown by Kelley, this modification can be obtained by assuming a frequency function of the form

$$n(x) = K(X_1)f(x), \qquad \textbf{Equation 3-16}$$

subject to the constraints

$$\int_{0}^{\infty} f(x)dx = 1, \qquad \textbf{Equation 3-17}$$

the statement that $f(x)$ is normalized, and

$$\int_{0}^{\infty} xf(x)dx = 1\,\mu m, \qquad \textbf{Equation 3-18}$$

to agree with observations that indicate a geometric mean in the size distribution near 1 μm. The solution to $f(x)$ which satisfies these constraints is

$$f(x) = \frac{a}{x}\exp\left[-\frac{\ln^2 x}{b}\right], \qquad \textbf{Equation 3-19}$$

where $a = 0.3578$ and $b = 2.4866$. (Note that the constants are determined both by a need to match the constraints in Equation 3-17 and Equation 3-18, and by a need to match the slope of the MIL STD particle distribution for larger particles.) By definition,

---

[12] Barengoltz, J. B., "Calculating Obscuration Ratios of Contaminated Surfaces," *NASA Tech. Briefs*, Vol. 13, No. 8, Item 2, August (1989).
Kelley, J. G., "Measurement of Particle Contamination," *J. Spacecraft*, Vol. 23, No. 6, p. 641, Nov. - Dec., 1986.

$$. \ (X) = K(X_1)\int_X^\infty f(x)dx \,. \qquad \textbf{Equation 3-20}$$

From Equation 3-14, X_1 will retain its definition from the MIL STD only if

$$N(X_1) = 10^{C^*} = 11. \qquad \textbf{Equation 3-21}$$

Combining the previous two Equations, it is seen that

$$K(X_1) = \frac{11}{\int_{X_1}^\infty f(x)dx}. \qquad \textbf{Equation 3-22}$$

If we assume that particles can be modeled as spheres of diameter x, the total surface area of particles on a surface is given by

$$A_{part.} = \int_0^\infty n(x)\left(\frac{\pi x^2}{4}\right)dx \,. \qquad \textbf{Equation 3-23}$$

The fractional surface area, or *PAC*, is therefore given by

$$PAC = \left(10^{-12}\right)\frac{\pi}{4}K(X_1)\int_0^\infty f(x)x^2dx. \qquad \textbf{Equation 3-24}$$

where the factor of 10^{-12} is needed to covert the units of x from μm to m. Evaluating the integral it is seen that the expression for *PAC* reduces to

$$PAC = \left(9.5\times10^{-12}\right)K(X_1), \qquad \textbf{uation 3-25}$$

and, from Equation 3-19 and Equation 3-22, $K(X_1)$ reduces to

$$K(X_1) = \frac{22}{erfc\left(\frac{\ln X_1}{1.5769}\right)}. \qquad \textbf{Equation 3-26}$$

This analysis modifies the results of MIL STD 1246C as shown in Figure 3-8. The original expression for $N(x)$, Equation 3-14, has been modified to the form

$$\log N(x) = C'\left[\log^2 X_1 - \log^2 x\right] + \log\left(\frac{\log X_1}{\log x}\right), \qquad \text{Equation 3-27}$$

where the last term approaches zero for large X_1 and large x. Surface cleanliness as a function of *PAC* is illustrated in Figure 3-9. As shown, a *PAC* of 1% equates to surface cleanliness level of about 500.

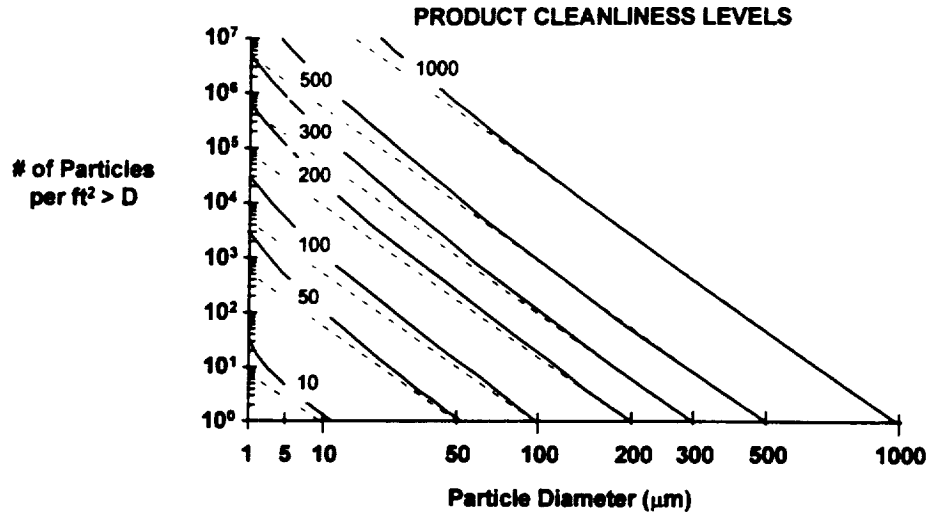

Figure 3-8. Surface cleanliness levels with the inclusion of submicron sized particles.

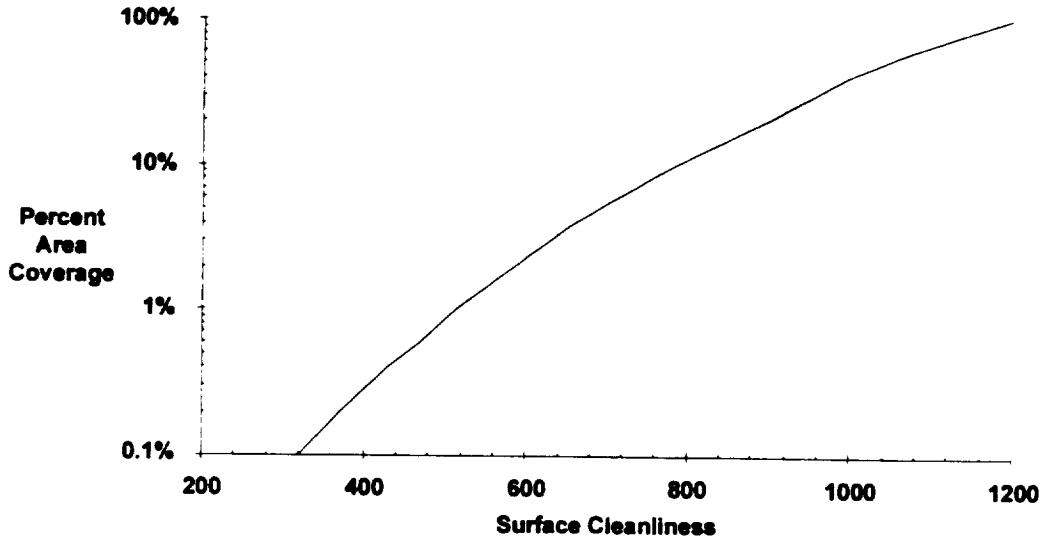

Figure 3-9. Percent area coverage as a function of surface cleanliness.

Based on the relationship between *PAC* and surface cleanliness the *PAC* may be estimated by counting particles of various sizes on the surface in question as shown in Table 3-3.[13]

[13] Ma, P. T., Fong, M. C., and Lee, A. L., "Surface Particle Obscuration and BRDF Predictions," SPIE Vol. 1165, *Scatter from Optical Components*, pp. 381 - 391, (1989).

Table 3-3. Calculating particle percent area coverage.

Particle Size Range	Particles per 0.1 m^2	×	Coefficient	=	Percent Area Coverage
>1 - 10 μm	_____	×	1.737×10^{-8}	=	_____
>10 - 25 μm	_____	×	1.528×10^{-7}	=	_____
>25 - 50 μm	_____	×	7.078×10^{-7}	=	_____
>50 - 100 μm	_____	×	2.435×10^{-6}	=	_____
>100 - 150 μm	_____	×	5.186×10^{-6}	=	_____
>150 - 250 μm	_____	×	7.484×10^{-6}	=	_____
>250 - 500 μm	_____	×	6.522×10^{-6}	=	_____
>500 - 750 μm	_____	×	1.048×10^{-5}	=	_____
>750 μm	_____	×	1.922×10^{-5}	=	_____
Sum all values to obtain total percent area coverage					_____

3.2.2.1 Additional Concerns

In reality, the effective *PAC* due to a collection of particles is a function of viewing angle and wavelength. If the relevant viewing direction is not normal to the surface, or is an integration over many angles, the effective *PAC* may be affected, especially if the particles are not spherical which is usually the case. Also, any directional properties of the surface itself must be taken into consideration. Similarly, if the particles are not large compared to the wavelengths of interest, the effective obscuration will be less than the geometrical obscuration of the particle. This is usually the case. Since the surface characteristics are nearly always determined by how the surface interacts with electromagnetic radiation, these are usually the major areas of concern. However, if the particles interact mechanically, (e.g., abrasively, like rocket exhaust), or chemically, (e.g., like an acid etch), with the surface, these factors may be paramount. In the usual case, the particles are deposited gently, by fallout from the air, and do not interact chemically with the surface. Because the particles have values of α, and ε which differ from those of the underlying surface, the effective *PAC* is usually the parameter of interest.

3.2.2.1.1 Directional Effects

The directions at which electromagnetic radiation arrives at or leaves a surface are different for different spacecraft surfaces. For solar cell arrays, the electromagnetic radiation, (sunlight), is usually normal to the surface. By orienting the solar cells in this way the maximum electrical power output is attained. However, spinning spacecraft with body mounted solar cells are exposed to sunlight at various arrival angles. This angular dependence must be taken into account in evaluating effective surface particle contamination since such particles, usually dust, are irregular in shape and do not necessarily project the same geometrical cross sections in different directions.

Spacecraft radiators are generally placed where they do not view the Sun and where they have a clear view of space. For a Lambertian surface the effective *PAC* would be independent of direction only for spheres, because emissivity has a cos θ dependence, (with θ being the angle relative to the surface normal). While many dust particles are quasi-spherical, some are fiber segments with *l/d*, length to diameter ratio, > 10. The orientations of such fibers generally average out over angle, but if the radiator is a second surface mirror, which has a non-Lambertian ε, the fiber effects may not average out.

Some optical sensors have exposed mirrors, gratings, lenses, baffles, etc. which are very directionally sensitive to the incoming electromagnetic radiation. In addition, they are usually designed to accommodate that radiation from different directions. Whether the contaminating surface particles act diffusively or specularly upon that fraction of the incoming radiation which they reflect can be as important as how large that reflected component is.

In practice, the only practical way to deal with the directional effects of surface particle contamination is to measure the performance of the sensitive spacecraft components, (usually these are solar cell panels, radiators, or optical sensors), with and without contamination present. It is usually

too time consuming to try to calculate such directional effects except in simple cases, and the required input parameters for the surface particles may not be available. This conclusion is reinforced once the other effects, wavelengths and composition, are considered.

3.2.2.2 Wavelength Effects

The wavelengths of interest for spacecraft are usually 0.4 – 1.1 μm for solar cells, and 0.5 – 20 μm for radiators. In addition, ultraviolet light sensors may operate at < 0.4 μm and RF antennas at > 1000 μm. For comparison, the particles of interest generally lie in the 0.5 – 500 μm diameter range. Thus, the particles have dimensions right in the middle of the range of the wavelength of interest. This means that Mie scattering effects must be considered.

3.2.3 Bidirectional Reflectance Distribution Function (BRDF)

3.2.3.1 The Effects of Particulate Contamination on BRDF

Mie scattering theory can be used to relate BRDF to surface cleanliness levels as shown in Figure 3-10 for 10.6 μm wavelength.[14] BRDF increases as surface contamination levels increase because each particle is able to scatter light away from the desired angle of reflection. Note that more exact calculations of BRDF predict roughly double the value obtained from Mie theory.[15] This emphasizes the fact that the scatter from a smooth mirror may dominated by the scatter from surface particles.[16] Typically, BRDF measurements of materials are measured directly in the laboratory and are fed into stray light analysis programs such as APART/PADE for systems level analysis.[17] For this reason, it is often suggested that BRDF be used as the direct measure of surface cleanliness, rather than MIL STD 1246C.

---

[14] Young, R. P., "Low-Scatter Mirror Degradation by Particulate Contamination," *Optical Eng.*, Vol. 15, no. 6, pp. 516 - 520, Nov. - Dec., (1976).

[15] Johnson, B. R., "Exact Calculation of Light Scattering from a Particle on a Mirror," SPIE Vol. 1754, *Optical System Contamination*, pp. 72 - 83, (1992).

Johnson, B. R., and Arnold, G. S., "Radiation Scattering from Particulate Contaminated Mirrors," Aerospace Report No. ATR-94 (7281)-1, 1 March 1994.

[16] Spyak, P. R., and Wolfe, W. L., "Scatter from Particulate-Contaminated Mirrors. Part I: Theory and Experiment for Polystyrene Spheres and λ = 0.06328 μm," *Opt. Eng.*, Vol. 31, No. 8, pp. 1746 - 1756, (1992).

Spyak, P. R., and Wolfe, W. L., "Scatter from Particulate-Contaminated Mirrors. Part 2: Theory and Experiment for Dust and λ = 0.632 μm," *Opt. Eng.*, Vol. 31, No. 8, pp. 1757 - 1763, (1992).

Spyak, P. R., and Wolfe, W. L., "Scatter from Particulate-Contaminated Mirrors. Part 3: Theory and Experiment for Dust and λ = 10.6 μm," *Opt. Eng.*, Vol. 31, No. 8, pp. 1764 - 1774, (1992).

Spyak, P. R., and Wolfe, W. L., "Scatter from Particulate-Contaminated Mirrors. Part 4: Properties of Scatter from Dust for Visible and Infrared Wavelengths," *Opt. Eng.*, Vol. 31, No. 8, pp. 1775 - 1784, (1992).

[17] Arizona's Paraxial Analysis of Radiation Transfer/Program for the Analysis of Diffracted Energy, Breault Research Organization.

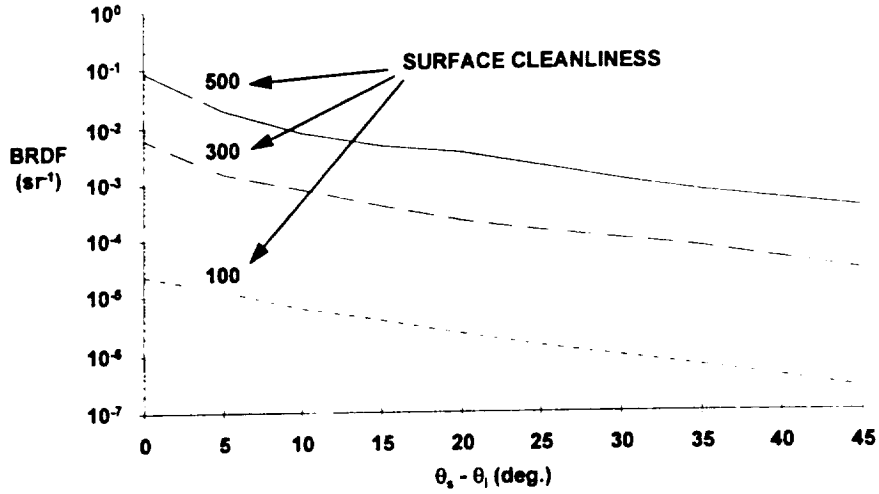

Figure 3-10. BRDF as a function of surface cleanliness at 10.6 μm wavelength - Mie theory.

BRDF values at 1° for very clean surfaces are listed in Table 3-4. These values must be added to the BRDF for the clean surface to obtain the total BRDF for a dirty surface. BRDF as a function of radiation wavelength is shown in Figure 3-11. The decreasing values of BRDF at larger wavelengths, for a given angle, are due to the fact that more of the particle lies in the Rayleigh scattering region ($\lambda > r$) where the Mie scattering cross sections are smaller than their geometrical cross sections.

Table 3-4. Approximate BRDF at 1° due to surface particles - Mie theory.

Surface Level	Fractional Area Obscured	BRDF at 1°
115	3×10^{-6}	1×10^{-4}
145	1.2×10^{-5}	3×10^{-4}
165	2.3×10^{-5}	5×10^{-4}
195	5.0×10^{-5}	1×10^{-3}
250	1.5×10^{-4}	3×10^{-3}
280	2.2×10^{-4}	5×10^{-3}
330	4×10^{-4}	1×10^{-2}

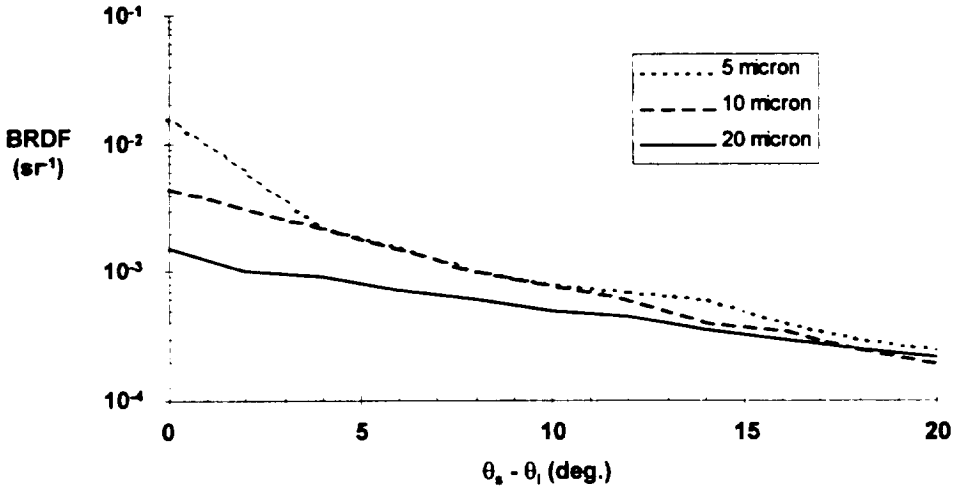

Figure 3-11. BRDF as a function of wavelength for a level 300 surface - Mie theory.

3.2.3.2 The Effects of Molecular Contamination on BRDF

In many circumstances molecular contamination may also be a source of scattering. One reason that molecular contamination effects the BRDF of a mirror is that the molecules tend to form clumps on the mirror's surface rather than depositing themselves in a smooth layer. The tendency to clump is the result of the fact that the contaminant molecules are usually more strongly attracted to each other than to the mirror molecules. Thus, a mirror with molecular contamination will look spotty if examined in detail.

There have been relatively few experimental studies of the effects of molecular contamination on mirror BRDF since, in general, particulate contamination is a far more serious problem. At the same time, scatter from molecular films is difficult to analyze theoretically, difficult to evaluate by simple observation, and difficult to correct.[18] Williams and Lockie exposed a SiC mirror to dust and, separately, to hydrocarbon diffusion pump oil and compared the contaminated BRDF readings to those of the clean surface.[19] As indicated by Figure 3-12, dust degrades BRDF by the largest factor at larger angles while oil degrades the BRDF by by largest factor at smaller angles. Williams and Lockie did not quantify the contamination levels after exposing the mirror to a "contaminating" environment, but Somers and Muscari report no change in BRDF up to 0.11 μm of CVCM.[20]

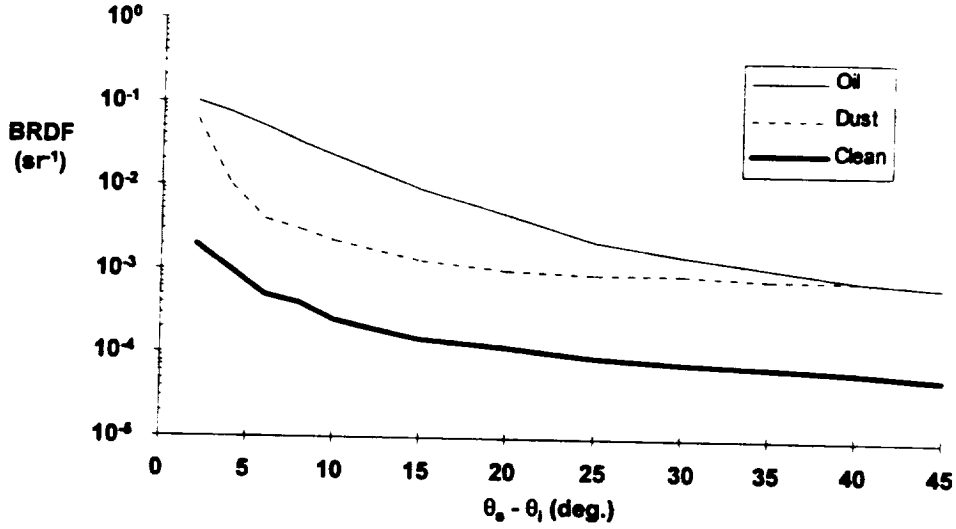

Figure 3-12. Experimentally determined BRDF change of a contaminated SiC mirror.

The Arnold Engineering Development Center has examined the effects of condensed gases on cryogenic surfaces.[21] BRDF measurements on an 18 K surface were obtained for films of: air, N_2, O_2, H_2O, CO_2, CO, and Ar. BRDF measurements on a 68 K surface were obtained for films of: H_2O,

[18] Bousquet, P., Flory, F., and Roche, F., "Scattering from Multilayer Thin Films: Theory and Experiment," *J. Opt. Soc. Am.*, Vol. 71, No. 9, pp. 1115 - 1123, (1981).

[19] Williams, V. L., and Lockie, R. T., "Optical Contamination Assessment by Bidirectional Reflectance Distribution Function (BRDF) Measurement," *Optical Eng.*, Vol. 18, No. 2, pp. 152 - 156, (1979).

[20] Somers, R., and Muscari, J. A., "Effects of Contaminants on Bidirectional Reflectance Distribution Function," Society of Photo-Optical Instrumentation Engineers, *Spacecraft Contamination Environment*, Vol. 338, pp. 72 - 79, (1982.)

[21] Seiber, B. L., Bryson, R. J., Bertrand, W. T., and Wood, B. E., "Cryogenic BRDF Measurements at 10.6 μm and 0.63 μm on Contaminated Mirrors," Arnold Engineering Development Center, AEDC-TR-94-16, February (1995).

RS12M polycyanate resin, Nusil CV2500 Silicone, Solihane 113/C113-300 Urethane, and RTV 560 Silicon. As shown in Figure 3-13, there was little effect on BRDF for very thin layers of H_2O. However, as the film thickness increased beyond 3 μm there was a two order of magnitude increase in the visible scatter. This effect is attributed to a shattering or fracturing of the contaminant film surface.[22] This fracturing is observed to occur near 20 K for water (ice) films. Similar effects are noted for other cryogenic films.

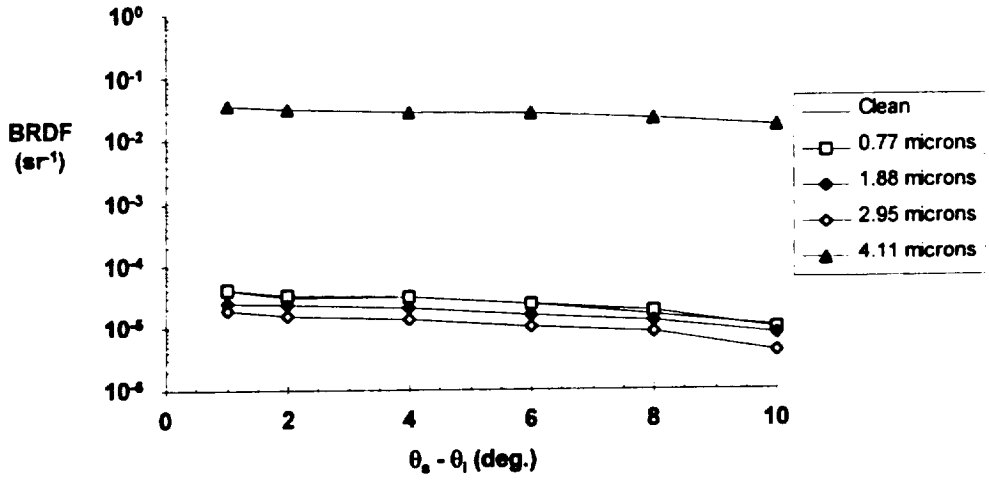

Figure 3-13. Effect of H_2O deposition on 16K mirror BRDF - 10.6 μm.

3.3 Generation, Transportation, and Deposition

3.3.1 Air Quality: FED STD 209E

The buildup of particles on a surface is directly related to the amount of particles in the surrounding air. Viscous drag will balance the fall of particles under the influence of gravity, but over time more and more particles will fall out of the atmosphere onto exposed surfaces. FED-STD-209E defines air quality in terms of the maximum allowable number of particles per cubic meter, or cubic foot, of air. In SI units, the name of the air class is taken from the base 10 logarithm of the maximum allowable number of particles, 0.5 μm and larger, per cubic meter. In English units, the name of the class is taken from the maximum allowable number of particles, 0.5 μm and larger, per cubic foot. The concentration limits are approximated by

$$\text{particles} / \text{m}^3 = 10^M \left(\frac{0.5\mu\text{m}}{x} \right)^{2.2}, \qquad \text{Equation 3-28}$$

$$\text{particles} / \text{ft}^3 = N_c \left(\frac{0.5\mu\text{m}}{x} \right)^{2.2},$$

[22] Arnold, F., "Degradation of Low Scatter Metal Mir , by Cryodeposit Contamination," Arnold Engineering Development Center, AEDC-TR-75-128, Octrober (1975).

where M is the numerical designation of the class in SI units and N_c is the numerical designation of the class in English units. Class limits are illustrated in Figure 3-14 and Table 3-5. Class 10,000 (M 5.5) cleanrooms are typical of most spacecraft manufacturing cleanrooms. Nominal industrial quality air may be class 3,500,000, (M 8), or worse, while class 100, (M 3.5), laminar flow benches may be required for the assembly of sensitive optical components. Note that air class is specified in terms of the maximum allowable. Air quality in operational cleanrooms is generally well below maximum.

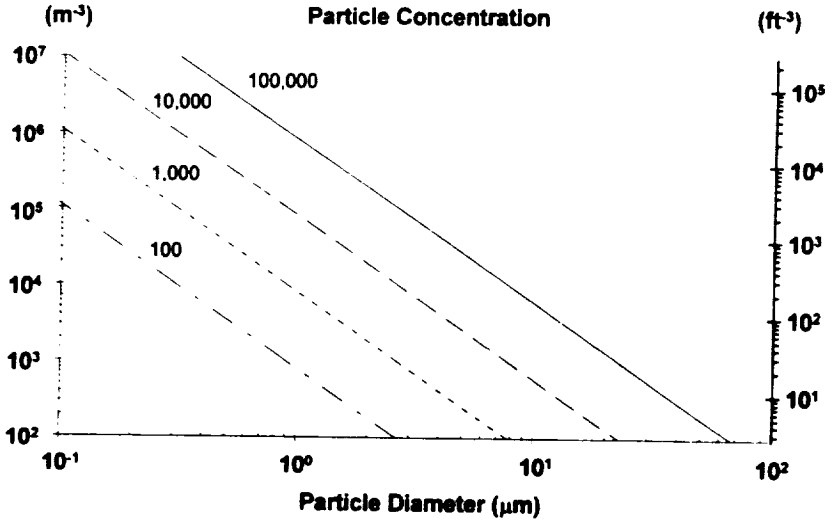

Figure 3-14. FED STD 209E air quality classifications.

Table 3-5. Air quality as defined by FED-STD-209E.

Air Class		Class Limits							
		0.1 μm		0.3 μm		0.5 μm		5 μm	
		Volume		Volume		Volume		Volume	
SI	English	(m^3)	(ft^3)	(m^3)	(ft^3)	(m^3)	(ft^3)	(m^3)	(ft^3)
M 1		350	9.91	30.9	0.875	10.0	0.283	-	-
M 1.5	1	1,240	35.0	106	3.00	35.3	1.00	-	-
M 2		3,500	99.1	309	8.75	100	2.83	-	-
M 2.5	10	12,400	350	1,060	30.0	353	10.0	-	-
M 3		35,000	991	3.090	87.5	1,000	28.3	-	-
M 3.5	100	-	-	10,600	300	3,530	100	-	-
M 4		-	-	30,900	875	10,000	283	-	-
M 4.5	1,000	-	-	-	-	35,300	1,000	247	7.00
M 5		-	-	-	-	100,000	2,830	618	17.5
M 5.5	10,000	-	-	-	-	353,000	10,000	2,470	70.0
M 6		-	-	-	-	1,000,000	28,300	6,180	175
M 6.5	100,000	-	-	-	-	3,530,000	100,000	24,700	700
M 7		-	-	-	-	10,000,000	283,000	61,800	1,750

As shown in Figure 3-15, emperical observations indicate that the average fallout rate of 5 μm particles onto a horizontal surface, (the floor), is given by

$$\frac{dN(5\mu m,t)}{dt} = cp\tilde{N}_c^{\,0.773}, \qquad \text{Equation 3-29}$$

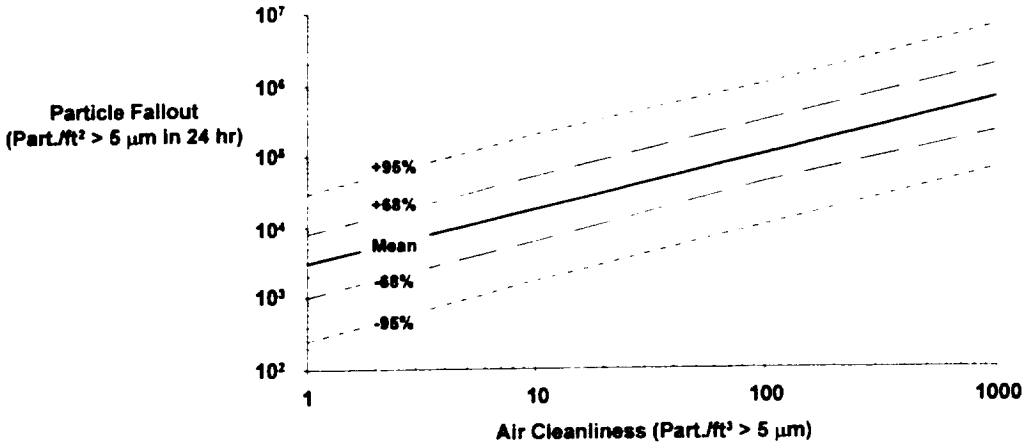

Figure 3-15. Particle fallout rates as a function of air cleanliness.

where c and p are normalization constants, $\tilde{N}_c$ is the number of particles > 5 μm in size per ft^3 of air, and dN/dt, the fallout rate is interpreted as the number of particles > 5 μm settled per unit area per day.[23] The coefficient c is chosen for consistency with the desired units. The value $c = 1$ is used if dN/dt is measured in particles per square feet per day, while the value $c = 1.076$ is used if dN/dt is measured in particles per 0.1 square meters per day. Suggested values for p, as a function of cleanroom characteristics, are listed in Table 3-6.

Table 3-6. Air quality parameters for various air classes.

Air Characteristics	Criteria	p
Still or low velocity air	< 15 air changes/hr	28,510
Normal cleanroom	15-20 air changes/hr	2,851
Laminar flow bench	air velocity > 90 ft/min.	578

Integrating Equation 3-29 gives the total number of particles > 5 μm present on a surface as a function of time,

$$N(5\mu\text{m},t) = cp\tilde{N}_c^{\,0.773}t\,. \qquad \textbf{Equation 3-30}$$

From the definition of air quality, Equation 3-28, it is seen that

$$\tilde{N}_c = N_c\left(\frac{0.5}{5}\right)^{2.2}. \qquad \textbf{Equation 3-31}$$

[23] Hamberg, O., "Particulate Fallout Predictions for Clean Rooms," *J. Env. Sci.*, pp. 15 - 20, May/June (1982).

Inserting Equation 3-31 and Equation 3-30 into Equation 3-27 allows one to solve for particle surface level as a function of exposure time in a given air-class environment.[24] The expression for surface cleanliness, (in English units), becomes

$$\log\left((0.02)cpN_c^{0.773}t\right) = C'\left[(\log X_1)^2 - (\log 5)^2\right] + \log\left[\frac{\log X_1}{\log 5}\right]. \qquad \textbf{Equation 3-32}$$

Solving this expression gives surface cleanliness as a function of time as illustrated in Figure 3-16. Note that particle buildup on vertical surfaces should be about 1/10 of the horizontal value while downward facing surfaces may see a buildup of only 1/100 the horizontal value, Figure 3-17.

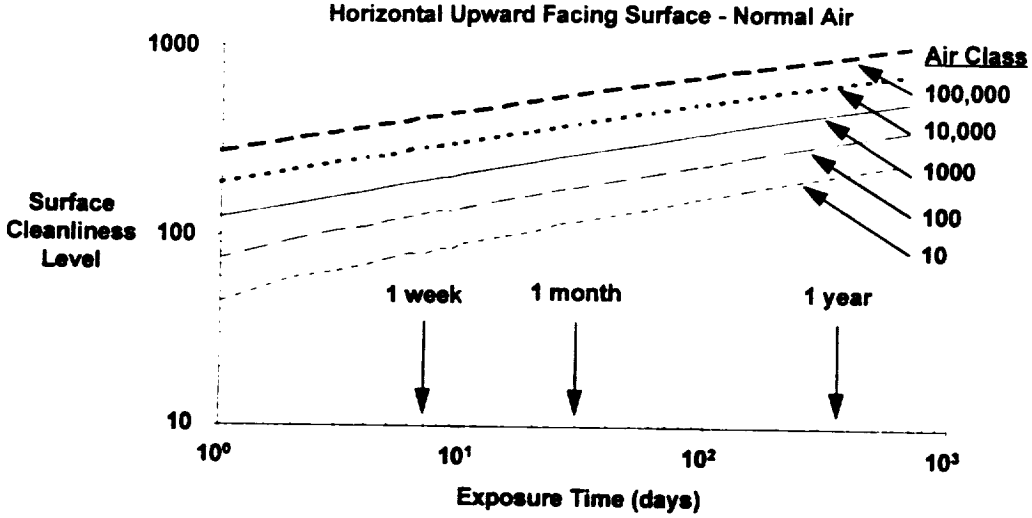

Figure 3-16. Horizontal upward facing surface cleanliness - normal air.

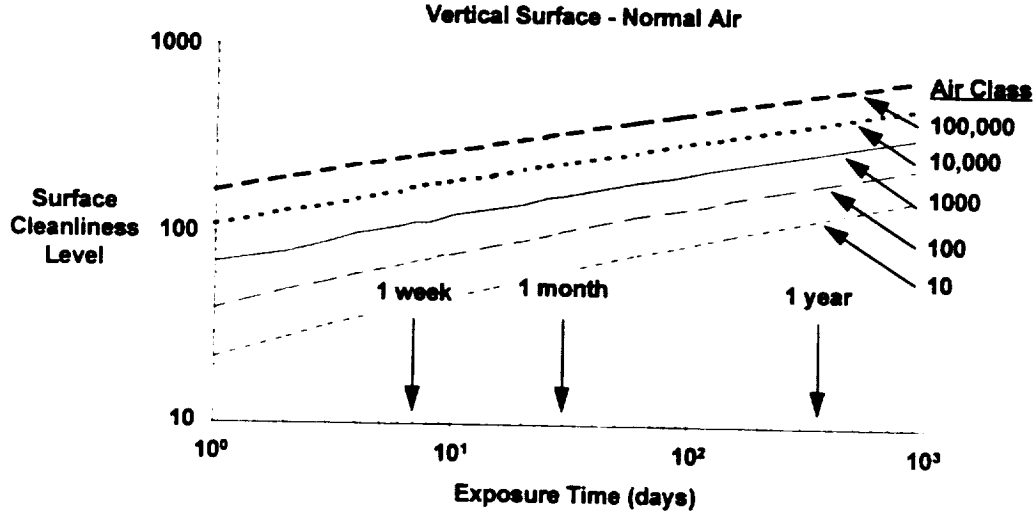

Figure 3-17. Vertical surface cleanliness - normal air.

[24] Buch, J. D., and Barsh, M. K., "Analysis of Particulate Contamination Buildup on Surfaces," Society of Photo-Optical Instrumentation Engineers, *Optical System Contamination: Effects, Measurement, Control*, Vol. 777, pp. 43 - 54, (1987).

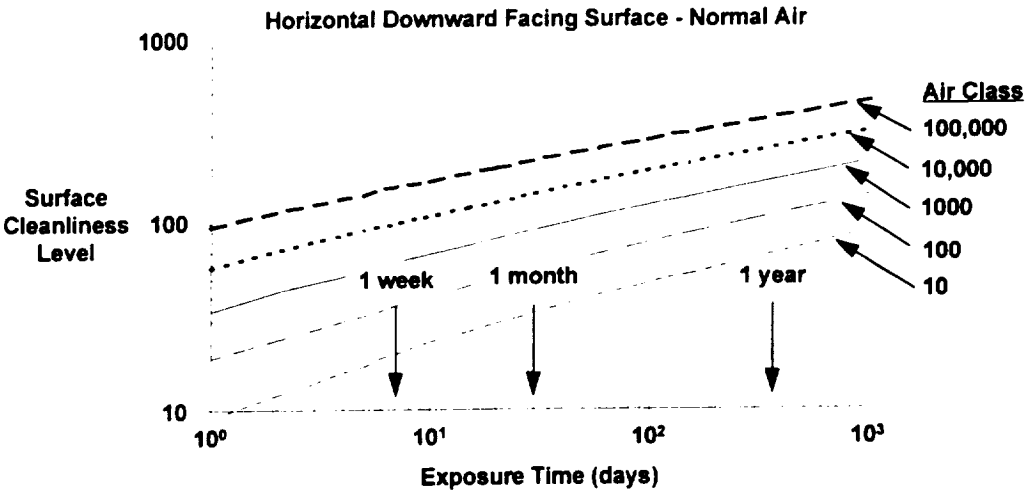

Figure 3-18. Horizontal downward facing surface cleanliness - clean air.

Based upon Equation 3-32, 10 days in class 100,000 air will produce level 445 on a horizontal upward facing surface. Vertical surfaces can expect to receive about 10% the buildup of horizontal upward facing surfaces, (or level 275), while horizontal downward facing surfaces can expect to receive about 1% as much, (or level 165). Scaling these results for air class, which is linear, and pre-launch time will yield the expected surface particle levels which are non-linear, at launch. Because the air in any given facility will be perturbed by the day to day operations, it is appropriate to estimate particle levels on spacecraft surfaces prior to launch using Hamberg's statistical relationships between particle air class and particle surface level, Figure 3-15.

An example of the magnitude of surface degradation that an optical sensor may encounter during assembly, test, and launch is provided in Table 3-7. As shown, good housekeeping practices alone (class 10,000 air) can rarely provide beginning-of-life surface cleanliness values better than level 550 unless plans are made to clean the surfaces during launch-processing operations. Reducing on-orbit contamination below level 450 will require stricter attention to detail, such as limiting exposure to class 1000 or better air. Finally, reducing beginning-of-life surface cleanliness below level 300 will require near heroic contamination control measures. As a benchmark, the Hubble Space Telescope primary mirror requirement was level 300, while the external surfaces of the spacecraft were level 950.

3.4 Particle Redistribution During Launch and On Orbit

Most particles are deposited on surfaces during ground operations. However, these particles may be released on orbit during nominal spacecraft operations and allowed to redeposit on sensitive surfaces. On unmanned spacecraft this may occur due to articulation of solar arrays, thermal expansion/contraction, the release of covers, etc. On manned missions, like the shuttle, venting and water dumps may generate particles. Sudden collisions with micrometeorites or orbital debris may also dislodge particles, and could also generate new particles from the impact site. Regardless of the source, particles released on orbit may interfere with optical operations.

3.4.1 The Shuttle Launch Environment

Consider the example of the Shuttle. For virtually all spacecraft, it is possible to quantify the expected pre-launch and launch induced contamination levels. (This information is discussed in Chapter 4.) The particles that are deposited during ground operations may be redistributed during launch and/or on orbit operations. Optical measurements taken by a photometer in the Shuttle bay having a 32° field of view during STS missions 2, 3, 4, and 9 reported particles during every available

viewing opportunity during the first 13 hours of a mission.[25] After about 24 hours on orbit the particle viewing rate decayed to a quiescent rate of about 500 particles of size > 10 μm per orbit. Other experimenters have reported detecting 1100 particles from 4 hours of data taken early in the Spacelab 2 mission (STS-54F).[26] The particles were slow-moving and had temperatures in the range 190 to 350 K. As expected, the size distribution was in agreement with that observed at the shuttle preparation facilities.

Table 3-7. Sample surface cleanliness calculations.

		Surface Particle Level		
	Exposure	Air Quality		
Sensor Location	Time	100	1000	10,000
Manufacturing	n/a	100	100	100
Telescope Assembly				
Focal plane integration	1 week	130	195	290
Assembly alignment	2 weeks	165	145	355
Install covers	1 week	180	270	390
Spacecraft Assembly				
Integration	3 months	245	360	510
Test				
Subsystem tests	4 months	285	410	535
Thermal vacuum tests	1 month	295	420	537
Final preparations	1 month	300	430	538
Launch Processing				
Inspection/check out	1 week	302	433	539
Load propellant	1 week	304	435	540
Vehicle closeouts	1 week	305	437	541
Install in launch vehicle	2 weeks	307	440	542
Ready for launch	1 day	307	441	542
Launch				
Ascent	10 min	320	445	545
Initial On-Orbit Checkout				
Instrument deployment	2 weeks	325	450	550

3.4.2 Micrometeoroid & Orbital Debris Impact

Because spacecraft travel at extremely high velocities, ~ 8 km/s is typical for circular low Earth orbit, collisions with even small pieces of matter can have disastrous consequences. In support of the shuttle program, studies of micrometeoroid and orbital debris (MMOD) impact have found that small MMOD, which are numerous, are able to dislodge large particles from surfaces quite easily but do not,

[25] Clifton, K. S., and Owens, J. K., "Optical Contamination Measurements on Early Shuttle Missions," *App. Optics*, Vol. 27, No. 3, p. 603, (1988).

[26] Simpson, J. P., Witteborn, F. C., Graps, A., Fazio, G. G., and Koch, D. G., "Particle Sightings by the Infrared Telescope on Spacelab 2," *J. Spacecraft*, Vol. 30, No. 2, p. 216, (1993).

in general, remove submicron-sized particles.[27] Larger MMOD, which are less frequent, are able to remove both large and small particles. However, because of the nature of the hypervelocity impact particles will be generated by the backsplash of material from the crater produced by the impact. It is predicted that 5.7×10^3 particles of size ≥ 5 μm would be liberated from the surface of the shuttle each day by MM impact alone. Conversely, between 6.9×10^5 and 1.4×10^7 particles of size ≥ 2 μm, or $2.0 - 3.3 \times 10^5$ particles ≥ 10 μm in size, would be generated from the crater backsplash. If OD impacts are factored in, (the OD environment is a function of altitude and inclination), these numbers may increase significantly for certain orbits.

3.5 Estimating End of Life Particle Cleanliness Levels

3.5.1 Solar Array Contamination

As shown in Figure 3-2, the actual power degradation from a contaminated solar array is seen to be less than the *PAC*. This is presumably because the particles do scatter some light into the coverslide itself, rather absorbing it all or scattering it back to space. In any case, a 1% power degradation due to particles equates to a 2.25% *PAC*. This *PAC* in turn equates to a surface cleanliness of level 520, Figure 3-9. As will be seen in the next section, this is sufficiently dirty to be easily seen during pre-launch inspection. We can therefore conclude that this level of pre-launch contamination would be seen and removed before flight. Given that the particle levels deposited on orbit should be small enough to be of concern only to optical sensors, particulate contamination should not produce any noticeable power losses on orbit. Consequently, as a rule almost the entire contamination budget for a solar array may be allocated to molecular contamination.

3.5.2 Thermal Control Surface Contamination

As shown in Equation 3-1 and Equation 3-3, the change in α_s/ε due to particles is a function of *PAC*. While experimental values of temperature increase due to surface particle contamination are not found in the open literature, a little calculation shows that the effect will be small. Consider an extreme case where the emissivity of a radiator is altered by the particles. If $\varepsilon_{clean} = 1$ and $\varepsilon_{part.} = 0$, it can be shown that a surface particle level of ~ 650 will be required to increase the temperature by 1%, Table 3-8. The other extreme would be contamination with $\varepsilon_{part.} = 1$ on a surface which has a low emissivity, ($\varepsilon_{clean} \sim 0.1$ is about as low as ε_{clean} can reasonably be for infrared wavelengths). In this case, it can be shown that a surface particle level of ~ 450 would be required to have a 1% effect on radiator temperature, Table 3-9. Facey and Nonnenmacher report that black particles on light surfaces appear to have to have an effective emittance of approximately 0.50, not 1.0.[28] This is presumably due to thermal conductance between the particle and the surface. This implies that the surface particle levels where the 1% effect would be noticed can be raised to ~ 775 and ~ 600, for the two cases just discussed, respectively. It is noted that the effect of dark contamination on a light surface is to lower the temperature. This can cause problems if the contamination causes a fuel tank to freeze, for example.

Additionally, problems can arise due to mismatch of solar absorptance. Again, dark contamination on a light colored surface would lead to undesirably high temperatures. Here $\alpha_{s,clean}$ can be as low as 0.05, while ε_{clean} cannot exceed 1.0. If the contamination has $\alpha_{s,part.} = 1.0$ the effect on the temperature of a passive sphere will be as shown in Table 3-10. A surface particle level of ~ 350 is required to increase the temperature by 1%. This confirms the fact that effects on solar absorptance are usually more critical than effects on emissivity.

---

[27] Barengoltz, J., "Particle Release Rates from Shuttle Orbiter Surfaces due to Meteoroid Impact," *J. Spacecraft*, Vol. 17, No. 1, p. 58 (1980).

[28] Facey, T. A., and Nonnenmacher, A. L., "Measurement of Total Hemispherical Emissivity of Contaminated Mirror Surface," Society of Photo-Optical Instrumentation Engineers, *Stray Light and Contamination in Optical Systems*, Vol. 967, pp. 308 - 313, (1988).

Table 3-8. Effect of white ($\varepsilon = 0$) particles on a dark ($\varepsilon = 1$) radiator facing deep space.

Particle Level	Percent Area Coverage (*PAC*)	Effective Emitting Area (1 – *PAC*)	$\Delta T/T_o$
200	0.0002	0.9998	-5×10^{-5}
300	0.0008	0.9992	-2×10^{-4}
400	0.0026	0.9974	-6.5×10^{-4}
500	0.0080	0.9920	-2×10^{-3}
600	0.025	0.975	-6×10^{-3}
700	0.053	0.947	-1.3×10^{-2}
800	0.11	0.89	-2.75×10^{-2}
900	0.20	0.80	-5×10^{-2}
1000	0.36	0.64	-9×10^{-2}

Table 3-9. Effect of black ($\varepsilon = 1$) particles on a light ($\varepsilon = 0.1$) radiator facing deep space.

Particle Level	Percent Area Coverage (*PAC*)	Effective Emitting Area [0.1(1 – *PAC*) + 1(*PAC*)]	$\Delta T/T_o$
200	0.0002	~ 0.1	$+5 \times 10^{-5}$
300	0.0008	~ 0.1	$+2 \times 10^{-3}$
400	0.0026	0.102	$+6 \times 10^{-3}$
500	0.0080	0.107	$+2 \times 10^{-2}$
600	0.025	0.123	$+6.2 \times 10^{-2}$
700	0.053	0.148	$+1.3 \times 10^{-1}$
800	0.11	0.199	$+2.7 \times 10^{-1}$
900	0.20	0.280	$+5.0 \times 10^{-1}$
1000	0.36	0.424	$+8.9 \times 10^{-1}$

Table 3-10. Effect of black ($\alpha_s = 1$) particles on a light ($\alpha_s = 0.05$) radiator facing the Sun.

Particle Level	Percent Area Coverage (*PAC*)	Effective Absorptance [0.05(1 – *PAC*) + 1(*PAC*)]	$\Delta T/T_o$
200	0.0002	0.05019	$+9.5 \times 10^{-4}$
300	0.0008	0.05076	$+3.8 \times 10^{-3}$
400	0.0026	0.05247	$+1.2 \times 10^{-3}$
500	0.0080	0.0576	$+3.8 \times 10^{-2}$
600	0.025	0.0738	$+1.18 \times 10^{-1}$
700	0.053	0.1004	$+2.52 \times 10^{-1}$
800	0.11	0.1545	$+5.23 \times 10^{-1}$
900	0.20	0.240	$+9.50 \times 10^{-1}$
1000	0.36	0.392	$+1.71 \times 10^{0}$

The effects of contamination on thermal control coatings thus depends on the nature of the surface and whether or not it faces the Sun, as well as upon the differences in α_s and ε between the coating and the surface. Since most contamination has $\alpha_s \sim \varepsilon \sim 0.5$, the effects are not severe unless particle levels become high, $> \sim 600$. It is also important to note that while effective values of α_s or ε may change, the ratio of α_s/ε may remain usable.[29]

[29] Adlon, G. L., Rusert, E. L., and Slemp, W. S., "Effects of Simulated Mars Dust Erosion Environment on Thermal Control Coatings," *J. Spacecraft*, Vol. 7, No. 4, pp. 507 - 510, (1970). Dyhouse, G. R., "Martian Sand and Dust Storms and Effects on Spacecraft Coatings," *J. Spacecraft*, Vol. 5, No. 4, pp. 473 - 475, (1968).

Because a *PAC* of a few percent should be visible before launch, section 4.2.3.1, one can assume that beginning of life particle levels for thermal control surfaces correspond to surface obscurations of, at most, a few percent. A degradation in α_s/ε of a few percent should not be noticeable for most surfaces as end of life α_s/ε margins are usually more on the order of 100% for critical surfaces. In general, particles should pose no credible threat to thermal control surfaces and their entire contamination budget may be allocated to molecular contamination.

3.5.3 Optical Surface Contamination

As was previously discussed, the effect of *PAC* on optical surfaces is to reduce signal throughput. This effect becomes more pronounced as one moves through the optical train to the focal plane, where the concentrated signal can be completely absorbed by a single particle sitting atop a pixel. To avoid this problem, optical elements are, for the most part, enclosed so that external contamination cannot reach the inner surfaces. This is done through a combination of design, and by bagging the elements and connecting them to a filtered purge when not in use. However, this still leaves the first surface vulnerable to both surface obscuration and scattering. Scattering effects, which are not important for solar arrays or thermal control surfaces, are often paramount here. Not only does scattering degrade the image quality, but (for strong off-axis sources) may mask it completely.

Recall that the BRDF is a measure of the ability of a mirror or a lens to discriminate against off axis sources, section 3.1.3.2. BRDF can have a value of 10^{-3} sr^{-1} to 10^{-4} sr^{-1} at 1°, for clean, high quality surfaces, Figure 3-6. This can easily be degraded to 10^{-2} sr^{-1} or worse at 1° by contamination. It is seen that these particle levels are far lower than those which produce 1% effects on solar panels or thermal control surfaces, even under extreme conditions. It should be mentioned that surface roughness of optical surfaces is also important to BRDF. Lower quality surfaces may have BRDF values of 10^{-2} sr^{-1} at 1°, (or even 5°), when clean. It takes correspondingly more contamination to affect the off-axis rejection of poor quality surfaces as compared to good quality surfaces.

Once the BRDF requirement for an optical sensor has been established, the amount of surface particle contamination which can be tolerated on the primary surface can be estimated. As Figure 3-6 shows, even clean off-axis sensors have trouble achieving 10^{-4} sr^{-1} at 1°, with 10^{-3} or 10^{-2} being more typical. Therefore, unless the mission requirements are rather relaxed, very few particles can be tolerated. Attaining and maintaining such requirements on orbit is difficult.

Consider the example of a sensor that is viewing a target an angle θ off axis from the Sun, (Figure 3-3). Because the PST of the sensor will be nonzero, some of the energy from the Sun will be scattered onto to the focal plane. (This is the definition of PST.) As shown by Equation 3-12, the number of photons reaching the detector will be a function of surface cleanliness, (BRDF), as well as the angle between the Sun and the optical axis. The purpose of the detector, or focal plane, is to convert the light from the signal into electrons. These signal electrons are stored in a capacitor in the focal plane for some predetermined integration time that is necessary to build up the signal strength to a level that can insure detection with a high level of probability. During the processing of the signal, the signal will be "contaminated" with electrons from sources other than the signal, called noise. A detailed discussion of all noise sources is beyond the scope of this work, but an example calculation of noise terms is shown in Table 3-11. The critical parameter in optical design is the signal to noise ratio. If the "usual" noise sources are supplemented by noise, (stray light), from the Sun, the strength of the noise will increase and the signal to noise ratio will decrease.

Consider the example of a sensor with a primary mirror having an area of 1 m^2; a *L/D* ratio of 2.0; operating in the 1.95 – 2.05 μm waveband. We assume that the initial SNR for an undefined target, given the noise sources listed in Table 3.10, is 10.0. (This will ensure detectivity of the signal.) By inspection, the number of focal plane electrons, (noise), generated by off-axis scatter from the Sun is approximated by

$$n_{e,OAS} = A_{pixel}\left(\frac{S_{\Delta\lambda}}{E_{\lambda}}\right)PST\eta\Delta t\,, \qquad \text{Equation 3-33}$$

Table 3-11. Sample noise calculations for an arbitrary sensor.

Noise Souce	Focal Plane Electrons
Background	200
Clutter	100
Johnson	100
1/f	30
Readout	250
ADC/Preamp	175
Total Noise (without off-axis scatter)	855

where A_{pixel} (m^2) is the area of the primary mirror that contributes light to a single pixel, (equal to the area of the primary mirror divided by the number of pixels in the focal plane array), $S_{\Delta\lambda}$ (W m^{-2}) is the solar intensity in the waveband of interest, PST is defined by Equation 3-12, η is the fraction of solar radiation reaching the focal plane that produces an electron, and Δt is the integration time of the sensor. It is easily seen that in the waveband of interest $S_{\Delta\lambda}$ is 10 W m^{-2} and $E_\lambda = 9.91 \times 10^{-20}$ J.[30] For this example we will arbitrarily assume: the number of pixels is 256 × 256 so that $A_{pixel} = 15.26 \times 10^{-6}$ m^2; $s = 1.5$; $\eta = 0.5$; and $\Delta t = 1 \times 10^{-6}$ s. Utilizing these parameters, and the BRDF values provided in Figure 3-10, the signal to noise ratio of the detector, as a function of cleanliness and off-axis angle, is illustrated in Table 3-12 and Figure 3-19. With a Sun exclusion angle of 30° the surface must be kept at cleanliness level ~ 200 or better to maintain a signal to noise ratio of ~ 8.0. If the surface is dirtier than this, the Sun exclusion angle must increase. If the surface is cleaner, the Sun exclusion angle may decrease. Increasing the area of the primary mirror, *L/D*, or the integration time of the sensor will relax the cleanliness requirement, (by raising the minimum value of cleanliness required), for a fixed value of SNR. (Unfortunately, these first two options invariably add mass and volume to the sensor and are not always viable options. Similarly, the sensor integration time must be kept small enough to avoid blurring of the image and will be fixed depending on the processing requirements and operational constraints of the system.) Conversely increasing the number of pixels in the focal plane or increasing the surface polish on the mirror, (the value of *s*), will make the cleanliness requirement more stringent, (by lowering the minimum value of cleanliness required.)

Note that there are a family of curves, as shown in Figure 3-19, for various surface cleanliness values and Sun-exclusion angles, that can ensure a minimum SNR value is met. For this reason, when specifying surface cleanliness for an optical sensor the requirement must be tied to not only sensor design characteristics, (waveband of interest, *L/D*, *s*, minimum SNR, ...), but also operational constraints, (signal strength, Sun-exclusion angle, ...) so that the required surface cleanliness level may be properly identified.

Table 3-12. SNR increase due to particulate contamination.

Off-Axis Angle (deg.)	Surface Cleanliness	Off-Axis Electrons	Signal to Noise Ratio
15	100	333	7.20
	300	33,285	0.25
	500	374,455	0.02
30	100	18	9.79
	300	1,821	3.20
	500	27,313	0.30
45	100	1	9.99
	300	178	8.28
	500	2,231	2.77

[30] Wolfe, W. L., and Zissis, G. J., *The Infrared Handbook*, 2d Ed., Office of Naval Research, Washington, DC (1985).

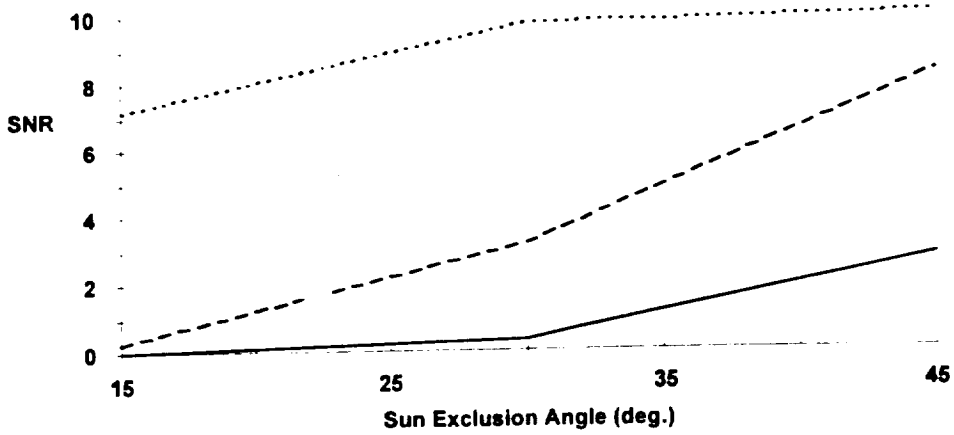

Figure 3-19. SNR increase due to particulate contamination.

3.6 Design Guidelines for Controlling Particulate Contamination

As shown in Table 3-13, the amount of particulate contamination that a spacecraft element can tolerate is highly dependent upon its function, as well as spacecraft mission objectives and operational constraints. In general, concerns for the effects of particulate contamination on the performance of optical elements drive contamination control for the spacecraft. Particle cleanliness levels for thermal control surfaces or solar arrays are, even in worst case scenarios, significantly relaxed in comparison. In most cases, particulate contamination on thermal control surfaces and solar arrays can be controlled below critical levels by pre-launch cleanings so that the entire contamination budget for these surfaces may be allocated to molecular contamination. (This is definitely not the case for optics, however.)

Table 3-13. Summary of particulate contamination concerns.

Element	Affected Parameter	Operational Criteria	Required Cleanliness
IR Sensor	Signal to Noise Ratio	SNR > 8.0	200[a]
Thermal Control Surfaces	absorption	$\alpha_s \sim 0.05$	350[b]
	emittance	$\varepsilon \sim 0.05$	450[b]
		$\varepsilon \sim 1.0$	650[b]
Solar Arrays	Power Production	< 1% Power Loss	520

[a] based on the design/operational constraints of the example in Table 3.12.
[b] assumes worst possible mismatch in α_s or ε between contamination and surface

As with molecular contamination, the effects of particulate contamination can be minimized by minimizing the amount of contamination that is: i) generated, ii) transported, and iii) deposited on a surface. As shown in Table 3-14, design options to minimize particulate contamination fall into the categories: air quality, design, operations, and margin.

Because particulate contamination during ground operations is ultimately related back to air quality, maintaining surfaces in as clean an environment as possible will minimize the buildup of particles on a surface. Because it is not feasible to maintain an entire spacecraft in a class 10 environment for long periods of time, it is usually accepted that sensitive surfaces will be covered and maintained in their own mini-cleanroom environment until needed. By covering, or bagging, sensitive components and connecting them to their own filtered air supply they will not be exposed to the usual "dirty" environment of the assembly area. When needed, the assembly can be moved to a laminar flow bench or other clean area for removal from its covers. Maintaining sensitive surfaces in an environment free from contamination sources is costly, but will minimize inspection and cleaning costs downstream.

Table 3-14. Design guidelines to minimize particulate contamination.

Materials	Choose paints, coatings, etc. that do not flake or chip
Design	Orient sensitive surfaces facing downward during launch
Operations	*Ground* Insure good contamination control procedures duing assembly and test, provide for inspection and cleaning of sensitive surfaces *Flight* Allow time for launch related particles to disperse before opening covers on sensitive surfaces
Margin	Allow for degradation in both ground and flight operations

Although it is usually only optical systems that are sensitive to particulate contamination, the entire spacecraft design must reflect this sensitivity. Particles carried aloft on other parts of the vehicle may dislodge, float around, and redeposit on sensitive surfaces after launch. Consequently, care must be taken to minimize particulate contamination on all surfaces. As with molecular contamination, providing for some time after reaching orbit for particles within the launch shroud to dissipate can help.

Finally, the last step in effective contamination control is always margin. Providing for a significant difference between the amount of contamination that the surface can tolerate and the amount of contamination that analysis predicts will be deposited, will minimize risk and enable operations even if on orbit performance is below pre-flight worst case predictions.

4. Contamination Control

Once the cleanliness requirement for a surface has been quantified, the issue becomes "Can this level of cleanliness be maintained and verified?" If a surface can tolerate a large amount of contamination no special procedures, other than pre-launch visual inspection and cleaning, may be warranted. In the other extreme, analysis may indicate that the required cleanliness level is too clean to be maintained on orbit. This would force the program to relax the contamination requirements by either: a) redesigning the hardware, or b) altering the mission operations profile. In most cases, the required cleanliness level lies between these two extremes and can be maintained only through enforcement of the proper contamination control processes and procedures.[1]

The sections that follow provide a discussion of the various methods that can be used to prevent, detect, and remove contamination from sensitive surfaces, as well as methods to help maintain surface cleanliness. These sections may be tailored to specific program objectives and utilized in a contamination control plan as part of the overall contamination control effort. Finally, the specific case of the Shuttle Orbiter examined in order to provide the designer with a feel for the type of environment a spacecraft will be exposed to during launch processing and early on orbit operations.

4.1 Preventing Contamination

To be effective, the contamination control process must start with conceptual design and proceed through on orbit operations. There are a variety of steps that the designer can take to minimize both the contamination generated by a subsystem and the effects of contamination on a subsystem. Often these steps impose no added effort to the program and can simplify problems during the later stages, when solutions are more costly and time consuming.

4.1.1 Spacecraft Design

4.1.1.1 Configuration

The space vehicle design must reflect an understanding of the importance of minimizing view factors between outgassing sources and sensitive surfaces and to facilitate inspection and cleaning, where possible. The majority of the outgassing mass generated by a space vehicle originates interior to the vehicle, from black boxes, cable harnesses, wire bundles, etc. The space vehicle configuration should provide vent paths that direct contaminants away from sensitive surfaces. Thrusters that are part of the propulsion and/or attitude determination and control subsystems may also be a source of contamination. In order of decreasing risk: solid fuel, liquid bipropellant, liquid monopropellant, and cold gas thrusters may all pose risks to sensitive surfaces. The design should reflect an understanding of this concern by minimizing view factors between thrusters and sensitive surfaces.

4.1.1.1.1 Honeycomb Panels

Honeycomb panel should be vented to the interior of the vehicle. From there the exhaust products should be conducted to well defined spacecraft vents, as discussed above, for release. Honeycomb panel may require vacuum baking, if supported by program specific analysis, to minimize the quantity of outgassed products.

4.1.1.2 Materials and Processes

All parts, materials and processes should be reviewed and approved before use. Examples of commonly used spacecraft materials which may be a source of contamination are listed in Table 4.1. The quantity and outgassing characteristics of these items should be documented.

---

[1] Borson, E. N., "Contamination Control Documents for Use in Statements of Work and Contamination Control Plans for Spacecraft Programs," The Aerospace Corporation, TOR-93(3411)-5, 30 September 1993.

Table 4-1. Examples of potential sources of molecular contamination.

Assembly/Application	Outgassing Source
Adhesives	Epoxies, silicones, acrylics, ...
Conformal Coatings	Polyurethanes, epoxies, silicones, ...
Encapsulation/Potting	Polyurethanes, epoxies, silicones, ...
Small Hardware	Acetates, acetals, polyamides, phenolics, ...
Structural Components	Epoxies, polycarbonates, polyurethane, polyamides, polyamines, flourocarbons, ...
Tapes	Polyesters, fluorcarbon acrylics, fluorcarbons, polyamides, ...

4.1.1.2.1 Metals

Metallic surfaces are typically not a source of significant contamination, but may become a source of both outgassing and particulates if allowed to corrode. To prevent this, cadmium, zinc and unfused electrodeposited tin, and dissimilar metal combinations as defined by MIL-STD-889, should be avoided. Metallic materials should be corrosion resistant or be suitably protected from corrosive environments.

4.1.1.2.2 Non-Metals

Materials used in flight and qualification unit hardware should be selected to minimize outgassing and should, in general, not include any which have a TML exceeding 1.0 percent or produce CVCM in excess of 0.1 percent when tested in accordance with ASTM E 595, or equivalent. Deviations from this rule may be granted if: i) no materials which perform the intended function and pass the screening test are available, or ii) it can be shown that the amount of mass outgassed by these materials is insignificant in comparison with that generated by other sources. In these cases vacuum baking should be used to the maximum extent feasible to precondition the material. Materials used in large quality or in close proximity to sensitive surfaces, even through they meet the TML and CVCM requirements, should be analyzed thoroughly to ensure the maintenance of minimum contamination levels.

Note that materials that are permanently housed in hermetically sealed containers are not required to meet outgassing requirements. However, the possibility of container fracture or leakage must be evaluated and shown not to be single point failure. Similarly, materials which fail the outgassing requirements, but are overcoated with a material that does meet the requirements, are considered acceptable if the overcoat is shown to prevent all outgassing. The possibility of pinholes, chipping and other mechanisms for overcoat failure leakage should be evaluated and shown not to be a single point failure.

Whenever feasible, all hardware should be vacuumed during assembly to remove particulate contamination from the surface and, as far as feasible, from the materials interior. Materials which require baking should be baked after their last exposure to molecular contamination, lubricants, machining oils, etc., and before integration with more temperature sensitive components. Materials should be baked at as high a temperature as they can tolerate to speed the migration of outgassing components to the surface. Materials are to be baked at a temperature at least 10°C higher than the highest temperature to be experienced thereafter. Baking should be continued until a monitor collects less than 1 nanogram/cm^2/hr for 24 hours. At this time witness plates should be exposed and the baking continued for at least 24 hours more.

4.1.1.2.3 Processes

Assembly and integration should be performed in controlled work areas to maintain cleanliness at all times. Optical elements should not be exposed in areas less clean than *Class 100*. Further, exposure times for these surfaces should be minimized.

At the time of integration, each detail or subassembly should be visibly free of particulate contamination to the level specified. Each part should be free of oils and other molecular

contaminants at the start of assembly; preferably all parts will have been vacuum baked at this point unless otherwise required. Existing joints should be covered to prevent the entrance of chips and debris during subsequent operations. Parts drilled at assembly should be separated, deburred and cleaned prior to actual assembly. Cleaning shall consist of such operations as vacuuming, dry wiping, solvent wiping, or ultrasonic cleaning, as applicable, to remove shop oils and other contamination. Any shaking, blowing, drilling, or deburring operations which generate or transfer particulates should be done outside the cleanroom assembly areas and prior to the integration of the payload with the satellite.

Visible particulate or other contamination should not be allowed to accumulate on assemblies during integration, and should be removed whenever detected. Suitable removal methods include vacuuming and/or blowing, dry wiping and solvent wiping. The objective is to minimize the accumulation of contamination in joints and recesses where it might evade final cleaning.

Every effort should be made to avoid performing particle generating operations, (drilling cutting, turning of screws or bolts, etc.), in the presence of a clean surface. If such operations must be performed, a suitable vacuuming fixture must be used with each tool to collect the particles generated.

All rivets, bolts, nuts, washers, and similar fasteners and hardware used in integration should be free of any oils, greases, etc., which fail to meet the required outgassing standards. Oil or grease lubricated fasteners should be cleaned by an approved solvent and method prior to use. All assemblies incorporating lubricated fasteners or upon which operations requiring the use of lubricants have been performed must be subsequently vacuum baked to remove all outgassing products.

When subassemblies or parts are transported from a less controlled to a better controlled area, they should be inspected and cleaned to the requirements of the cleanest part to be exposed in the more highly controlled area.

Covers and bags should be used to maintain cleanliness during transportation and/or storage. Outer covers and bags should be inspected for integrity and removed in the anterooms just prior to cleanroom entry. If only one cover or bag is required, its outer surface should be vacuumed, and wiped if required, just prior to cleanroom entry. Inner covers and bags should remain in place, except when partial or complete removal is essential to the accomplishment of operations. They should remain in place as late into the operation as possible without causing undue interference to the operations.

In controlled work areas, a cleanroom-qualified portable vacuum cleaner should be used. If it is impossible to exhaust it outside of the cleanroom, the exhaust should be connected to a HEPA, or better, filter.

4.1.1.3 The Vehicle Interior - Electronic Boxes, Cable Harnesses. ...

Electronic boxes and other closed, non-sensitive compartments are of concern because they will vent particles and outgas products upon exposure to vacuum. The electronics and wiring are the primary source of outgassing on most spacecraft. Analysis should be performed to determine if pre-treatment of boxes and wiring harnesses by vacuum baking is necessary to minimize outgassing. Exterior surfaces should be inspected and cleaned before closeout.

4.1.1.4 Electrical Power System - Solar Arrays

Contamination will reduce the power output generated by a solar array. It is necessary that the solar arrays be kept as clean as possible in order to provide maximum margin for losses due to radiation damage. Power losses from contamination and radiation damage will usually define system lifetime. Three contamination control measures should be planned. During ground operations the solar arrays should be periodically inspected and cleaned. Inspections must be performed before and after shipment and immediately before installation in the launch vehicle. During launch, the solar arrays will be protected from fairing fallout by orienting them vertically in the launch vehicle shroud and by shielding them from sources of particulates or outgassing. (Vertical surfaces collect much less particles that upward facing surfaces do.) Molecular contaminants will stick to the warm solar panels if polymerized by the solar ultraviolet. Consequently, on orbit outgassing from the spacecraft must be directed away from solar panels.

4.1.1.5 Thermal Control Surfaces

The chief impact of contamination on thermal control surfaces is to increase their solar absorptance. A secondary concern is that contamination can also alter thermal emittance. Thus contamination of thermal radiators may upset thermal balance and lead to overheating of critical components. In many cases this is an issue only if the radiator surface is sunlit. If the surface is deemed to be sensitive one will employ the same precautions noted above for the solar arrays. MLI should be embossed to eliminate the need for a spacer net between the layers. The vent holes should be punched and the MLI thoroughly cleaned before the aluminum coating is applied.

4.1.1.6 Attitude Determination & Control - Attitude Sensors

There are two concerns for optics: i) to maximize signal throughput, and ii) to minimize bidirectional reflectance distribution function (BRDF). The subsystem designer and supplier should determine EOL requirements for all attitude sensors and compare their requirements to those required for thermal radiators and solar arrays. If they are of the same order, employ the same precautions noted above for the solar arrays. If they are more stringent, employ the precautions noted below for payloads.

4.1.1.7 Propulsion - Thrusters

Exhaust from thrusters, whether used for orbit insertion, drag makeup, or attitude control, should be directed away from the vehicle in such a manner that view factors to sensitive surfaces are minimized. If feasible, the use of thrusters for attitude control should be avoided in favor of momentum wheels, torque rods, or similar technologies which do not generate potential contaminants.

4.1.1.8 Other Exterior Surfaces

Exterior surfaces of the spacecraft, which have line of sight to solar arrays, optical sensors or payloads, must be thoroughly cleaned and outgassed. Structural panels and MLI should be fabricated of low outgassing materials and vacuum baked, at the highest tolerable temperature for each, until: i) there is no detectable outgassing, or ii) analysis indicates that the outgassing rate observed, when multiplied by the view factor to any applicable sensitive surfaces and evaluated against the space system operational concept, is not predicted to pose a contamination threat.

4.1.2 Optical Payload Accommodation

Optical payloads are often the most contamination sensitive surfaces on the space vehicle, and drive contamination control for the entire system. When this is the case, contamination control must start with the payload manufacturer. The payload should be assembled and tested; then disassembled and thoroughly cleaned. This cleaning should, unless analysis indicates otherwise, include vacuum baking. The payload module will then be reassembled and protected. The protection may be provided by sealing in a clean, inert atmosphere, by purging with GN_2, or by evacuating and sealing. Analysis and testing will be required to determine the best approach. Testing and other exposure after reassembly must be minimized; exposure will only occur in *Class 100* or better environment. Provision will be made for "aliveness" testing without opening the sensor module.

The upward facing surface, presumably the front of the satellite which includes the payload cover, will collect the fairing fallout. During launch shocks, especially the cover opening, can scatter these particles to surfaces in the line of sight. The cover opening will be directed to avoid exposing the solar arrays or radiators. Unless otherwise indicated by analysis, all exterior payload surfaces will be inspected and cleaned before launch.

4.1.3 Ground Equipment

Aerospace Ground Equipment (AGE) elements which are brought into the presence of flight or qualification hardware should meet the cleanliness requirements of the exposed flight or qualification hardware surfaces at that time. Any such elements which contact the flight or qualification hardware

surfaces should use materials meeting the requirements of section 4.1.1.2 to avoid contamination transfer. Any AGE exposed to in a low pressure or vacuum environment in proximity to flight or qualification hardware shouldl also meet the requirements of section 4.1.1.2 to avoid transfer of outgassed products.

4.1.4 Manufacturing, Assembly, and Test

Most fabrication will be performed in general factory or good housekeeping areas and subsequently cleaned to visibly clean. Subassembly, assembly, integration and test should be performed in *Class 100,000* or better cleanrooms with periodic inspections and cleanings. Optics must be delivered clean to the specified level and should thereafter be exposed to only *Class 100* or better environments. Exposure after receipt must be minimized.

4.1.4.1 Parts Fabrication

Unless otherwise specified, parts fabrication may be performed in general factory or good housekeeping area, as appropriate. During fabrication, cleanliness provisions of standard cleaning specifications should be observed. Corrosion, all oils and greases, and gross particle contamination must be removed and parts must be protected before moving to subassembly areas.

4.1.4.2 Subassembly, Assembly, and Test

Except as otherwise specified, parts should be cleaned to visibly clean level II (VC-II) or better and brought into *Class 100,000* cleanroom for subassembly. Subassembly, assembly, and test should be conducted in *Class 100,000* cleanrooms unless otherwise noted. When not undergoing assembly, or test operations, components must be covered or otherwise protected. Operations involving the use of uncured or partially cured silicones must be performed in isolated area as they are a notorious source of contamination during ground operations.

4.1.4.2.1 Test Chambers

Test chambers in which flight or qualification hardware will be exposed must be precleaned and maintained at the cleanroom class specified for the hardware. In addition, after cleaning, the test sequence should be prerun with all support equipment present but without flight or qualification hardware. QCMs and/or witness plates should be installed to monitor the contamination deposition at the location to be occupied by the flight or qualification hardware. If the monitors show excessive contamination, the chamber must be recleaned and the test repeated until contamination deposition is shown to be within the limits specified.

4.1.4.3 Controlled Work Areas

4.1.4.3.1 Access

As shown in Figure 4-1, the presence of people, (or more specifically activity performed by people), in a cleanroom will greatly increase the quantity of contaminants in the air. Consequently, access to controlled work areas should be strictly limited. Any individual entering a controlled work area must undergo training to ensure familiarization with proper contamination control procedures. The correct cleanroom gowning of each person entering the area must also be verified. The number of persons permitted in the area should be restricted to the minimum required to perform the operation in progress.

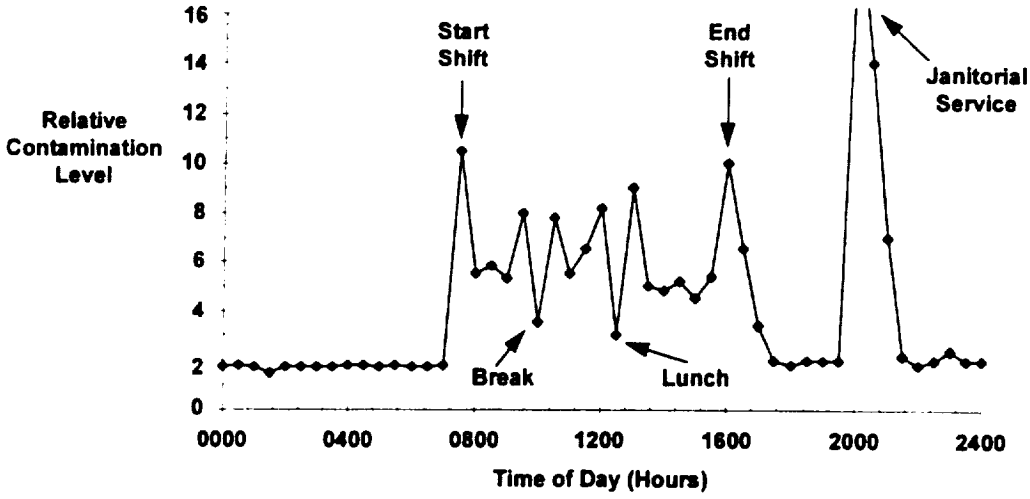

Figure 4-1. Relative contamination levels in a cleanroom during daily operations.

4.1.4.3.2 Cleanroom Training

All personnel requiring access to controlled work areas, and their line supervision as deemed necessary, should receive indoctrination in the purposes and practices of cleanroom operation, and any additional training as is deemed necessary for their specific tasks, before being certified for entry to controlled work areas. Additional contamination training and briefings should be conducted at appropriate intervals to supplement the initial certification training. Suggested topics include:

1) A general introduction concerning the significance of contamination control to the success of the program.

2) The significance of contamination control in all phases of design, fabrication, assembly, integration, storage, shipment, test, and launch integration. Emphasize that anyone can get it dirty; it requires full effort by all to keep it clean.

3) The importance of dress and discipline in cleanroom operations.

4) Specific techniques of cleaning, clean assembly and packaging.

5) Monitoring procedures.

6) Review the Contamination Control Plan.

7) Familiarization with other appropriate documentation.

4.1.4.3.3 Before Entering the Controlled Work Area

Before entering the cleanroom, personnel should check to verify that they comply with the following guidelines.

1) Do not eat, smoke, or chew gum in the smocking areas or controlled work areas.

2.) Do not bring food, beverages, gum, candy, cigarettes, tissue, pencils, or handkerchiefs into the controlled work area.

3) Avoid wearing clothes that generate particles, such as: fuzzy sweaters, velour, terry cloth, or dirty clothing.

4) All jewelry, including watches, must be covered.

5) Take only lint-free paper and non-retractable ball-point pens into the controlled work area.

6) Avoid wearing cosmetics in any controlled work area. This includes: lipstick, blush, eyeshadow, eyebrow pencil, mascara, hairspray, etc. These items will be prohibited in the stricter areas as appropriate.

7) Smokers should take a drink of water before entering a controlled work area. Drinking water will help reduce the particulates in the breath after smoking.

4.1.4.3.4 Entering the Garment Room and Controlled Work Areas

The purpose of the cleanroom garment is to protect hardware from contaminants generated by people. Cleanroom garments should be selected based on hardware cleanliness requirements and the types of operations that must be performed in the cleanroom. Smocks do not provide good isolation of hardware from people generated contaminants. Fibers from street clothes worn under the smock will fall out from under the smock. These fibers will generally be larger and will settle out of the air close to where they are generated. There may be places and operations in a cleanroom where this is acceptable, but only a full coverall will provide the required isolation when people are working in, around, and above spacecraft hardware

Requirements for entry into the garment room and controlled work areas include:

1) Shoes should be cleaned with cleaning machine and mats at entry. Additional shoe covering may be required.

2) Cleanroom garments should be donned in the anteroom. Caps should be worn to cover as much hair as possible.

3) Beards and mustaches should be covered. Do not groom hair in the smock room or controlled work areas.

3) Garments should be inspected before donning to ensure they are clean, there are no rips or open seams and all fasteners are usable.

4) Cleanroom garments should not be worn outside the controlled area and anteroom. When not being worn they should be stored according to instructions.

4.1.4.4 General Area Regulations

General area regulations include:

1) Outer garments designed and maintained for cleanroom use will be worn by all personnel any time they are in these areas.

2) Smoking and eating is forbidden in these areas and in adjacent anterooms and entries. Notice of this restriction should be displayed at entrances and in the anteroom areas.

3) Entry of paper in these areas will be limited and only approved types (limited-linting, plastic coated, plastic covered, etc.) will be used.

4) Only approved wipers will be allowed into these areas.

5) Only approved ball point pens will be allowed into thee areas. Pencils and erasers are forbidden.

6) Depending on the severity of the contamination concer, sources of particulate matter and volatile materials, e.g., cosmetics and lotions, shall not be worn or carried into these area.

7) Each person working in these areas shall clean his assigned work area before and after each activity.

8) All hardware, tools and equipment shall be covered or packaged when not in use.

9) Lint-free gloves (cleanroom latex gloves unless otherwise specified) shall be worn at all times when near critical surfaces.

10) No aerosol cans or mercury thermometers shall be allowed in these areas.

11) Personnel with a temporary physical condition which can generate contamination (e.g., head or chest cold, hay fever, or other cause of coughing, skin or hair condition which produces flaking) shall report it promptly to the supervisor. They shall be assigned work outside the controlled area until the condition is cleared up.

4.1.4.4.1 Receiving Area Entry

Entry of items directly into the receiving area should be done so as to minimize any contamination of the area. All exposed parts should be protected by drapes and covers. A temporary floor covering and drapes may be used to construct an anteroom area. The anteroom should be so constructed that open doors are isolated from the area. The doors may then be opened and the bagged parts moved in. The doors should then be closed and the outer cover inspected, vacuumed and wiped. The outer covering may then be removed and the part brought to the receiving area. Upon completion of the receiving activities, the floor covering should be completely vacuumed and the drapes removed. The floor covering should again be vacuumed and then removed. The whole area should then be vacuumed and inspected.

4.1.4.4.2 Movement Between Areas

Personnel must be cognizant of the cleanliness classification of areas they are entering, leaving, and passing through. Cleanroom garments must be appropriate for the area being entered; color coding may be appropriate. Special care must be taken when entering the laminar flow areas; entry must always be from the downstream end.

All items transported between areas must be cleaned to the requirements of the area being entered and must be appropriately covered or packaged. This includes handcarried fixtures and tools which shall be bagged or placed in precleaned and covered trays.

4.1.4.4.3 Area Monitoring

Initial and periodic measurement of particulate levels and airflow characteristics in areas of controlled cleanliness shall be recorded for predetermined locations. Additional measurements may be taken as required whenever necessary to assure cleanliness levels before and after critical operations and tests.

4.1.4.4.4 Janitorial Service

A janitorial schedule should be developed for each controlled area. The schedule should be updated as necessary and should include any temporary activities. Janitorial equipment (vacuum cleaner, mops, buckets, etc.) should be cleanroom certified items and should not be used outside the area. As shown in Figure 4-1 janitorial service is often the most contamination producing activity

performed in the cleanroom. It is important that janitorial personnel be educated on methods that can reduce the amount of contaminants "stirred up" by their activities.

4.1.4.5 Laminar Flow Area Regulations

All operations, access and training requirements listed in sections 4.1.4.3 and 4.1.4.4 above apply to laminar flow areas as well. In addition,

1) Personnel will receive additional training and be specifically certified for these areas. Only personnel so certified will be allowed in these areas.

2) Special cleanroom garments will be reserved for use in these areas. These garments may be stored and donned in the same entry room as those for the less clean areas, and may be worn while passing through those areas to reach the laminar flow areas. However, no work will be performed in less clean areas while wearing these garments, nor will they be worn in close proximity to operations in the less clean area.

3) Always keep in mind that anything that goes under a laminar flow hood will contaminate the air.

4) Move slowly and avoid unnecessary activity at or around a laminar flow hood. Stand away from the hood unless you are working there.

5) Do not cough or sneeze into or under a laminar flow station.

6) Exposed parts will be kept as near the filter bank as possible. In no event will personnel pass between the filter bank and exposed parts.

7) Clean operations will be conducted upstream from dirty ones.

8) Particle generating operations are to be avoided in these areas. If such operations must be performed they will be performed as far from the filter bank as possible.

4.2 Monitoring Contamination

The amount of contamination which can be tolerated on each sensitive surface will also determine what monitoring techniques must be employed. The method of inspection, and frequency, are ultimately determined by surface cleanliness levels and mission objectives. For minimal contamination requirements, visual inspection may be sufficient. If it looks dirty, clean it. Otherwise, leave it alone. For somewhat more stringent requirements, witness plates, (a small plate similar to the sensitive surface that is placed next to that surface), may be required. Every so often the witness plate is examined with some degree of care. If the plate is contaminated it is assumed that the adjacent surface is also contaminated. If the contamination levels are unacceptable, or even borderline, the surface and the witness plate are cleaned. For more stringent requirements, the sensitive surface are examined directly and cleaned if borderline. Finally, for the most sensitive surfaces, component (or full subsystem) tests may be run to verify that contamination has not impaired their performance.

Every spacecraft component should have some margin of safety, even though each subsystem specialist may be reluctant to admit it. A little probing will usually elicit a power decrease, a temperature rise, or a signal attenuation which can be tolerated without compromising mission success. However, contamination is only one of the effects which must be considered in allocating this margin. Among the other effects to be considered are manufacturing tolerances, storage, handling and testing effects, launch and deployment factors, as well as on orbit environments. It is usually necessary to reach a compromise so that no one effect is favored in setting the performance margins.

No matter how good the contamination control planning and procedures, there is always the risk of accidents and there are schedule requirements which limit how clean an on orbit spacecraft can be. In the process flow prior to launch, there is some point beyond which it will be impossible to clean the

spacecraft and, usually, a later point after which it will be impossible to even inspect the surface. Whatever contamination the spacecraft has then will only increase after that, with the launch process often being the most contamination producing event in the life of the surface.

4.2.1 Molecular Contamination

As shown in Table 4-2, these are a variety of techniques that may be used to deduce surface cleanliness. The actual method to be used in a given application depends on the surface cleanliness requirement, the accuracy desired, and other program factors such as cost and schedule. Each of these methods are discussed in the sections that follow.

Table 4-2. Molecular contamination monitoring options.

Method	Sensitivity	Pro's	Con's	Application
Gravimetric	0.2 mg/ft^2	Generally Accepted	24 hr Turn Around; Handling Errors; Low Sensitivity	Ground Processing Only
OSEE	0.1 mg/ft^2	Fast Response	Requires Calibration; Low Sensitivity on Some Surfaces	Ground Processing Only
QCM	0.005 mg/ft^2	Real Time; High Sensitivity	Only Measures Mass Deposition	Ground Processing & On Orbit
Calorimetry	0.01 mg/ft^2	Real-Time	Only Measures Absorptance Changes	On Orbit Only

4.2.1.1 Gravimetric

Gravimetric procedures may used to determine the amount of molecular contamination, non-volatile residue (NVR), remaining on a surface. These procedures are based on ASTM E 1234, ASTM E 1235 or their derivatives.[2] In essence, the surface is solvent wiped and the NVR is extracted from the wipers with additional solvent, which is either evaporated in a vacuum oven or in a *Class 100* unidirectional air-flow hood. The mass of the residue minus the mass of a blank sample, divided by the area wiped, is equal to the mass per unit area of NVR on the surface. ASTM E 1235 recommends using Soxhlet-extracted wipers and methylene chloride. Because of potential toxicity, methylene chloride is not recommended for use in a cleanroom. More environmentally friendly methods recommend using ethyl acetate and/or ethyl acetate/cyclohexane azeotrope.[3] Because gravimetric methods are so well characterized they are a standard means of measuring molecular contamination during ground processing. The disadvantages of this method are that it does not provide real time answers, it is unsuitable for use on optics or other easily damaged surfaces, and is not adaptable to on orbit cleaning.

4.2.1.2 Optically Stimulated Electron Emission (OSEE)

A metallic surface that is subjected to a flux of UV light will emit electrons through the photoelectric effect. This process forms the basis for one means of measuring surface contamination called optically stimulated electron emission (OSEE).[4] A clean surface that is subjected to a UV flux of a known strength and distribution will produce a certain measure of photoelectrons which can be

[2] Borson, E. N., Watts, E. J., and To, G. A., "Standard Method for Measurement of Nonvolatile Residue on Surfaces," The Aerospace Corporation, SD-TR-89-63, 10 August 1989.

[3] Arnold, G. S., and Uht, J. C., "Nonvolatile Residue Solvent Replacement," The Aerospace Corporation, SMC-TR-95-28, 1 March 1995.

[4] Arora, A., "Surface Contamination Measurement and Control by Nondestructive Techniques," *J. Env. Sci.*, p. 30, Nov./Dec. 1985.

Gause, R. L., "A Noncontacting Scanning Photoelectron Emission Technique for Bonding Surface Cleanliness Inspection," NASA TM-100361, February 1989.

monitored. If the surface is contaminated, the contaminant layer will absorb some fraction of the incident UV and reduce the strength of the UV that can reach the metallic surface. Consequently, the number of photoelectrons will also be reduced. As shown in Figure 4-2, if the instrumentation is properly calibrated it may be used to infer surface NVR levels. The advantages of this method are that it provides real time answers and does not require direct contact with the surface. This last factor alone makes it suitable for use on optical devices. The disadvantage is that the instrumentation must be calibrated for the surface in question, (large variabilities may be seen when level A is approached), and may not be usable on all surfaces, (i.e., when the photoelectron current from the surface is too small). As with gravimetric methods this technique is suitable only during ground operations.

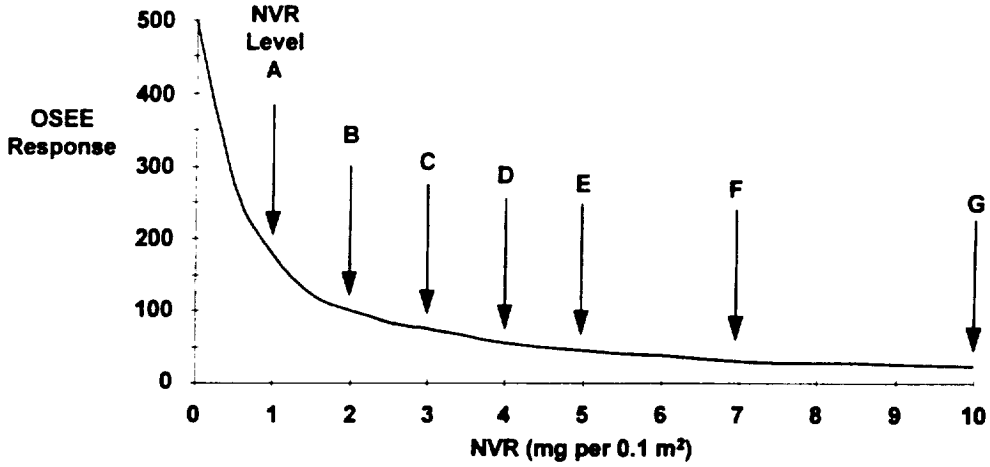

Figure 4-2. Optically stimulated electron emission response as a function of NVR.

4.2.1.3 Quartz Crystal Microbalance's (QCM's)

One device that is capable of directing measuring the deposition of contaminating material on a surface is a *Quartz Crystal Microbalance (QCM)*. Essentially, a QCM operates by comparing the resonant frequencies of two quartz crystals. One crystal is exposed to the environment and the other is shielded. The resonant frequency of the exposed crystal will change if mass is deposited on its surface. Consequently, by examining the change in resonant frequency, mass deposition can be inferred. The sensitivity of the device depends on the actual design, but is on the order of 4.43×10^{-9} g/cm^2 Hz at 10 MHz and 25° C.[5] One big advantage of QCM's is that the temperature of the outer surface may be controlled so that mass deposition as a function of surface temperature may be determined. Conversely, heating the device gives knowledge of the temperature at which contaminants will "boil off". Devices with this capability are kr wn as temperature controlled QCM's or simply TQCM's. QCM's are used routinely in applications where direct deposition of mass is needed. Because QCM's can be manufactured in very small packages, (~ 3 cm diameter × 3 cm length; 100 g; 140 mW at 10 Vdc), they are suitable for use as flight experiments.[6] Note however that QCM's are incapable of relaying information about the absorptive nature of the mass that has been collected.

---

[5] Wallace, D. A., and Wallace, S. A., "Realistic Performance Specifications for Flight Quartz Crystal Microbalance Instruments for Contamination Measurement on a Spacecraft," AIAA Paper 88-2727, (1988).

[6] Bryson, R. J., Seiber, B. L., Bertrand, W. T., Jones, J. H., Wood, B. E., and Lesho, J. C., "Pre-Flight Testing of Thermoelectric Quartz Crystal Microbalances (TQCM) for Midcourse Space Experiment," Arnold Engineering Development Center, AEDC-TR-93-24, February 1994.
Mark 9 Contamination Sensor Specifications, QCM Research, Laguna Beach, CA.

4.2.1.4 Calorimetry

In order to measure degradation of thermal control materials on orbit, spacecraft may be instrumented with devices called *calorimeters*. Essentially, a calorimeter is a thermistor that is calibrated to operate over the predicted range of temperatures. By isolating a sample material from the spacecraft and allowing it to establish thermal equilibrium, its temperature will be indicative of its α_s/ε ratio. Changes in α_s/ε will be indicated by a change in temperature of the sample. If the thermistor has been properly calibrated, the change in α_s can be inferred. The relative uncertainty in absorptance is dependent on the uncertainty in emittance, temperature, solar irradiance, and heat loss due to coupling to the surrounding material. Because of this coupling, the absorptance is given by

$$\alpha_s = \frac{\varepsilon\sigma T^4 A_{tot} + \dot{Q_L}}{SA_n}, \qquad \text{Equation 4-1}$$

where Q_L" is the heat loss due to coupling between the sample materials and its surrounding supports. Differentiating this equation will provide the relative uncertainty in α_s. If preflight calibration is performed, a sensitive design may be able to infer changes in absorptance as low as 0.0005. Although calorimeters do not relay information about the mass of the material that has been deposited, they do provide information on the absorptive nature of the contamination. In comparison to QCM's, calorimeters are smaller, lighter, and require fewer spacecraft resources.

4.2.2 Air Quality

As has been previously seen, air quality and exposure time are the key factors that determine particle fallout onto surfaces. For this reason, it is important to monitor air quality in the cleanroom in order to validate exposure conditions. As shown in Table 4-3, two accepted methods of doing this are membrane filter sampling and light scattering.

Table 4-3. Air quality monitoring techniques.

Method	Sensitivity	Pro's	Con's	Application
Membrane Filter Sample	~ 5 μm	Statistical Analysis of Particle Sizes	Not Real Time	Ground Processing
Light Scattering	~ 0.1 μm	Real Time; Statistical Analysis of Particle Size	Calibration Required; Limited Dynamic Range	Ground Processing
Dark Field Photography	~ 0.1 μm	Statistical Analysis of Particle Size	Not Real Time	On Orbit

4.2.2.1 Membrane Filter Sampling: ASTM F 25

The ASTM F 25 particle sizing methodology is based on the microscopical examination of particles impinging on a membrane filter with the aid of a vacuum. Essentially, a membrane filter is connected to a vacuum system which is used to gather samples of air at various locations in the cleanroom. Subsequent examination of the membrane filter under magnification will provide particle size distribution data for larger, ~ 5 μm, particles. This information, when combined with knowledge of the volume of air sampled, can be used to infer air quality in accordance with FED STD 209E.

4.2.2.2 Light Scattering: ASTM F 50

Continuous sizing and counting of airborne particulates can be conducted as described in ASTM F 50. In essence, the air in a controlled environment is sampled at a known flow rate. Particles contained in the sampled air are passed through an illuminated sensing zone in the optical chamber of

the instrument. Light scattered by individual particles in the air is received by a photodetector and converted into electrical signals. The signal pulse height can be related to particle size. The number of particles of a given size can be registered or displayed. The advantage of ASTM F 50 over ASTM F 25 is that ASTM F 50 can operate continuously, without a human operator.

4.2.2.3 Dark Field Photography

The last measure of air quality, and one most suited for on orbit operations, is dark field photography. Essentially, illuminating any particulates near a spacecraft with a flash bulb, and taking a picture against the dark background of space, will yield a count of particulates near the spacecraft. By making a time exposure the particulates will leave a trail in the photographs that can be used to induce velocity and point of origin. The strength of the signal from a given particulate will, presumably, be proportional to its reflectance and geometrical size. Although this technique is not very accurate for measuring particulate sizes, it is capable of quantifying the near spacecraft environment. Obviously, flying such instruments on most spacecraft are unnecessary and their use is usually restricted to applications, such as the Shuttle, where measurements during one flight will have application to future flights.

4.2.3 Particulate Contamination

As shown in Table 4-4, several procedures have been developed to determine the distribution of particulates on a surface. Visual techniques are

Table 4-4. Particle contamination monitoring techniques.

Method	Sensitivity	Pro's	Con's	Application
Visual Inspection	~ 5 μm	Standard Method	Not Real Time	Ground Processing
Scattering	N/A	High Sensitivity; Fast Turnaround	Statistical Analysis Difficult	Ground Processing & On Orbit

4.2.3.1 Visual Inspection

4.2.3.1.1 ASTM "Statistical" Procedures

ASTM E 1216 and ASTM F 24 are procedures for measuring and counting particulate contamination on surfaces. In essence, a tape sample is applied to a surface in order to cause any particulates present to bond to the tape. The tape sample is then removed and examined under a microscope. Provided that the sample is large enough to be statistically significant, the results will yield surface cleanliness in accordance with MIL STD 1246C.

4.2.3.1.2 NASA "Appearance" Procedures

Rather than perform an intensive, detailed statistical count of particles on a surface to determine surface cleanliness in accordance with MIL STD 1246C, one would like to be able to correlate appearance with cleanliness. Some of the first studies of surface cleanliness were performed in order to quantify the fallout of dust from chimney gases.[7] In these studies, the objective was to determine the maximum amount of deposition that would go unnoticed by a casual observer. In aerospace applications, one is usually interested in determining the minimum amount of contamination that would go undetected by a trained observer. In any case, the conclusions of this initial study remain valid:

[7] Carey, W. F., "Atmospheric Deposits in Britain - A Study of Dinginess," *Int. J. Air Poll.*, Vol. 2, pp. 1 - 26, 1959.

- Surfaces that receive deposits of particulates appear dusty when the cover is sufficiently dense to reduce the reflection of light perceptibly. Consequently, a surface will often appear dusty even though individual particles are too small to be distinguished.

- Particles less than 1 mm (1000 μm) will not be visible on the ground from the standing position. When viewed from a distance of 25 cm, a circle of 0.1 mm (100 μm) in diameter subtends an angle of just over 1/60th of a degree and is the smallest dot visible to the human eye. This would imply that, depending on the contrast, the human eye should be able to verify surface cleanliness of about level 1000 at a distance of 2 m, and surface cleanliness 100 at a distance of 25 cm.

- Contrast between the color of the particle and the background is a critical factor in distinguishing decreased reflectance. The response of the human eye to color is illustrated in Figure 4-3. High contrast makes it easier to detect contamination, (black particles on a white surface), while low constrast makes it much more difficult, (gray particles on a gray surface). If viewed from a distance too great to perceive individual particles, highly contrasting particles can be detected by the human eye when 0.2% of the area is covered, (level 370). Weakly contrasting particles require 0.4% coverage, (level 430), before the particulates could be noticed.

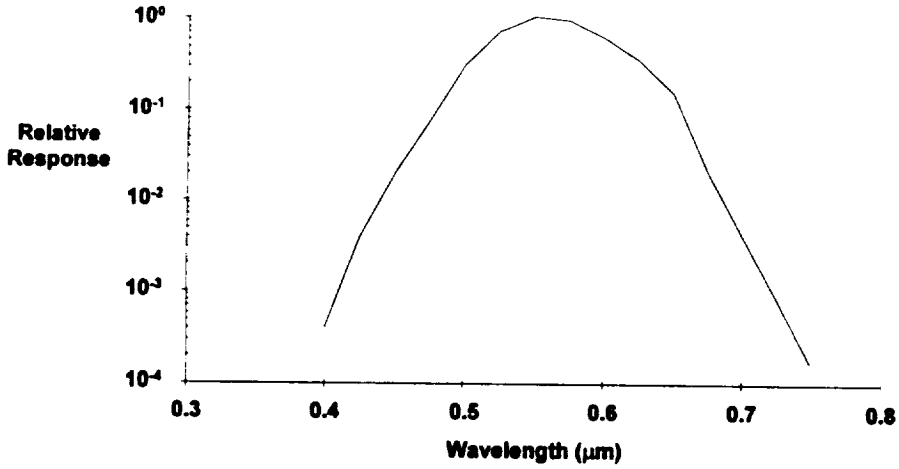

Figure 4-3. Response of the human eye to colors.

While visual inspection is a relatively unscientific way to evaluate cleanliness, some studies have made progress in quantifying it. Levels of illumination, viewing distance, and other parameters, have been quantified, Table 4-5.[8] The calculated resolution limits are based on diffraction and assume a wavelength of 0.5 μm and a human eye with a 0.3 cm pupil. It is seen that while the standard VC-I is not especially discerning, the more sensitive VC-I½, and sensitive VC-II should detect many of the surface particles. Using ultraviolet light aided by visual magnification, VC-III and VC-IV, can improve the results even further.

[8] Anon, "Specifications - Contamination Control Requirements for the Space Shuttle Program," NASA-SN-C-0005, Rev. A, Jan. 1982.
Raab, J. H., "Qualification of Shuttle Orbiter Payload Bay Cleanliness Levels," Martin Marietta, MCR-86-2004, January, 1984.

Table 4-5. Visually clean levels.

Level		Illumination (ft candles)	Inspection Distance	Magnification	UV Light	Resolution Limit (μm)
Standard	VC-I	50	5–10 ft	1	no	600–1200
Sensitive	VC-I½	50	2–4 ft	1	no	240–480
Highly Sensitive	VC-II	100	6–18 in	1	no	60–180
	VC-III	100–200	6–18 in	2–7	no	10–90
	VC-IV	100–200	6–18 in	2–7	yes	~ 10

When these inspection criteria are applied to sensitive surfaces they yield information about the cleanliness levels that may be verified during ground processing. Haffner reports that the quantization of the levels of visually clean is primarily a function of contrast and only secondarily a function of the percent area coverage (*PAC*).[9] Experiments conducted with dots of different sizes and colors on a cathode ray tube indicate that at a distance of one foot, white particles on a black surface can be detected by the human eye at a *PAC* of 0.1% (level 320), Table 4-6. Conversely, black particles on a white surface require a *PAC* of 1% (level 515) to ensure detection. Note that these values represent the upper bound to surface obscuration detection while the diffraction limit of 120 μm represents the lower bound. Similar results for 5 feet viewing distance are shown in Table 4-7.

Table 4-6. Visual detectivity at 1 foot viewing distance (VC-II).

Backgnd Color	Particle Color	Contrast	PAC Detected	Backgnd Color	Particle Color	Contrast	PAC Detected
Black	White	102.6	0.1%	Green	White	34	0.3%
	Blue	15.6	0.1%		Blue	-53	0.1%
	Green	68.6	0.1%		Yellow	14	0.3%
	Yellow	82.6	0.1%		Red	-50	0.1%
	Red	18.6	0.1%		Black	-68.6	0.1%
Red	White	84	0.1%	Blue	White	87	0.1%
	Blue	-3	0.1%		Green	53	0.1%
	Green	50	0.1%		Yellow	67	0.1%
	Yellow	64	0.1%		Red	3	0.1%
	Black	-18.6	0.1%		Black	-15.6	0.1%
Yellow	White	20	0.3%	White	Blue	-87	1.0%
	Blue	-66	0.1%		Green	-34	1.0%
	Green	-14	3.0%		Yellow	-20	3.0%
	Red	-64	0.1%		Red	-84	1.0%
	Black	-82.6	0.1%		Black	-102.6	1.0%

Contrast = (Particle Intensity - Background Intensity)/100
Diffraction Limit of Human Eye at 1 Foot ~ 120 μm

Plotting the data shown in Table 4-6 it is possible to construct a curve fit to the data as shown in Figure 4-4. The interpretation of this is that if surface cleanliness level and contrast are plotted and found to lie above the line the cleanliness can, with a high level of confidence, be verified by the inspection criteria of VC-II. Values lying below the line may be detectable, but with a lower level of confidence. A similar process quantifies the visual inspection criteria for VC-I, VC-I , and VC-II as shown in Figure 4-5. As a point of departure, VC-I can verify to level 625, VC-I½ can verify to level 450, and VC-II can verify level 320.

[9] Haffner, J. W., "Contamination Study of GPS Spacecraft," Rockwell International, SSD86-0104, 30 May 1986.

Table 4-7. Visual detectivity at 5 feet viewing distance (VC-I).

Backgnd Color	Particle Color	Contrast	PAC Detected	Backgnd Color	Particle Color	Contrast	PAC Detected
Black	White	102.6	0.1%	Green	White	34	1.0%
	Blue	15.6	0.1%		Blue	-53	0.3%
	Green	68.6	0.1%		Yellow	14	3.0%
	Yellow	82.6	0.1%		Red	-50	1.0%
	Red	18.6	0.1%		Black	-68.6	1.0%
Red	White	84	0.1%	Blue	White	87	0.1%
	Blue	-3	1.0%		Green	53	0.3%
	Green	50	1.0%		Yellow	67	0.1%
	Yellow	64	0.3%		Red	3	3.0%
	Black	-18.6	1.0%		Black	-15.6	1.0%
Yellow	White	20	1.0%	White	Blue	-87	3.0%
	Blue	-66	1.0%		Green	-34	3.0%
	Green	-14	3.0%		Yellow	-20	6.0%
	Red	-64	1.0%		Red	-84	1.0%
	Black	-82.6	1.0%		Black	-102.6	3.0%

Contrast = (Particle Intensity - Background Intensity)/100
Diffraction Limit of Human Eye at 5 Feet ~ 600 μm

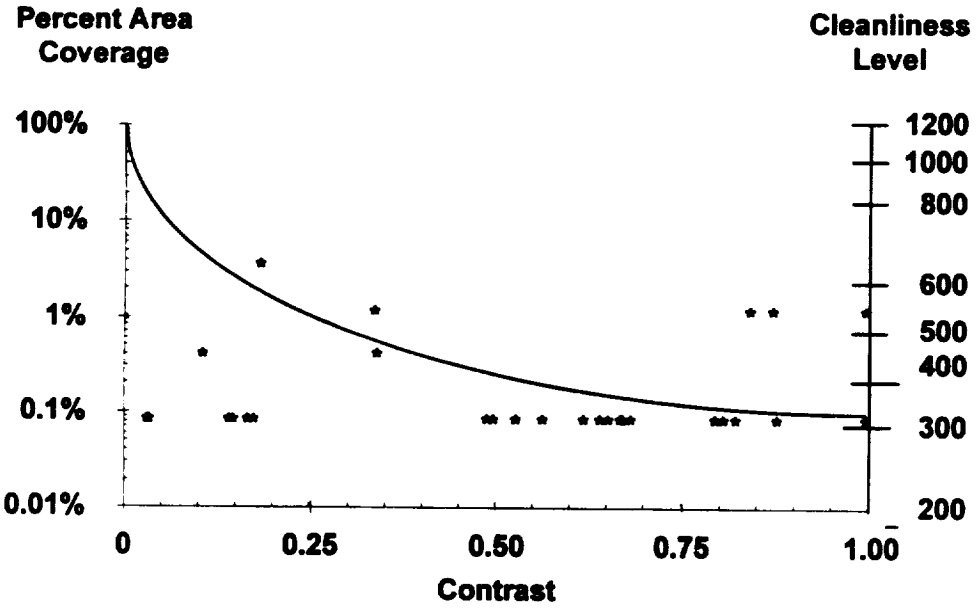

Figure 4-4. Visual cleanliness as a function of contrast for 1 foot inspection distance.

When these results are compared to previous studies the results show some agreement for solar cells, which are blue, less for beta cloth, which is white, and considerable disagreement for black paint, Table 4-8.[10] The degree of gloss is probably a factor for painted surfaces.

[10] Raab, J. H., "Qualification of Shuttle Orbiter Payload Bay Cleanliness Levels," Martin Marietta, MCR-86-2004, January 1986.
Maag, C. R., "The Contamination Environment of STS Mission 51-C as Measured by the Interim Operational Contamination Monitor (IOCM)," NASA JPL, DD-00023, August 1985.

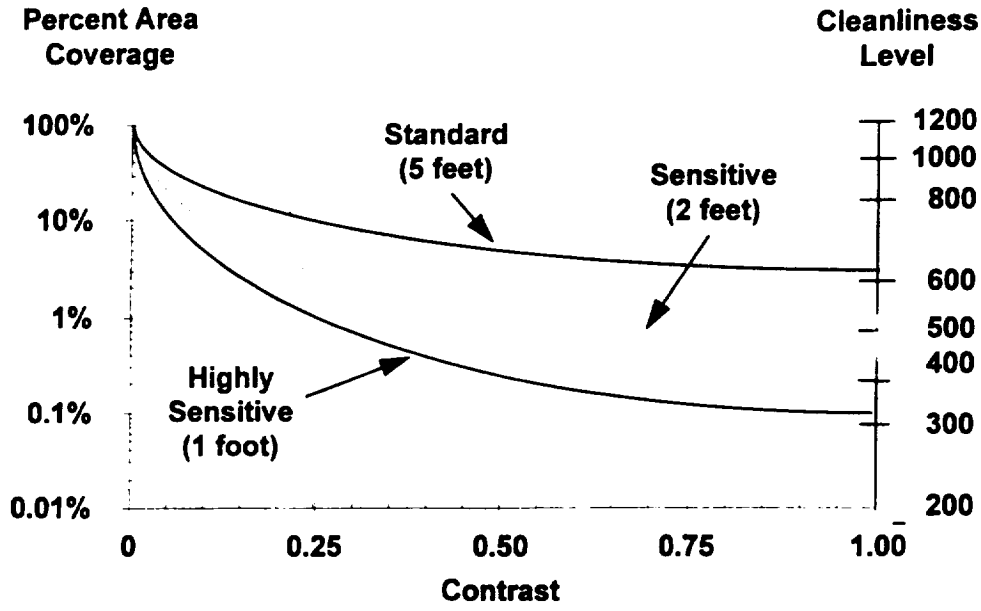

Figure 4-5. Generalized visual inspection performance criteria.

Table 4-8. Comparison of visual detection of particles.

		Measured Obscuration					
		Martin		JPL		Rockwell	
Surface	Illumin. (ft candles)	Particle Level	PAC	Particle Level	PAC	Particle Level	PAC
Beta Cloth	100	385	1×10^{-3}	750	3×10^{-2}	615	1×10^{-2}
(white)	50	560	6×10^{-3}	-	-	750	3×10^{-2}
Black Paint	150	-	-	100	3×10^{-6}	385	1×10^{-3}
(black)	50	-	-	-	-	385	1×10^{-3}
Solar Cells	100	320	5×10^{-4}	-	-	385	1×10^{-3}
(blue)	50	485	3×10^{-3}	-	-	485	3×10^{-3}
Aluminized	100	365	7×10^{-4}	-	-	485	3×10^{-3}
Kapton	50	-	-	-	-	615	1×10^{-2}
(yellow)							

4.2.3.1.3 Solar Arrays

Solar cells appear to the human eye to be blue. Fortunately, both solar cells and the human eye are sensitive to approximately the same portion of the electromagnetic spectrum. Consequently, if the cells are visually clean to the eye they are probably not contaminated enough to be operationally affected. The results of various attempts to quantify visually clean levels yield the best agreement for solar cells, Table 4-8. Thus solar cells clean to VC-I can be verified to have surface particle levels < 485, while those clean to VC-II have surface particle levels of ~ 350. Interpolating yields a VC-I½ surface particle level of ~ 420. The corresponding surface obscurations are 3×10^{-3} (VC-I), 1.5×10^{-3} (VC- I½), and 8×10^{-4} (VC-II).

Fortunately, all of these surface particle levels will result in power losses, (for individual cells), of < 0.1%. Even adding pre-launch (10 days in *Class 100,000* air) and launch (Shuttle Cargo bay) contributions to surface particle levels of 625 and 600, respectively, would produce an on orbit level of 675, (SO ~ 1.8×10^{-2}). This would produce a solar cell power loss of ~ 0.5%. This is a conservative

number which assumes that the solar cells were facing up both before and during launch. While solar panels performance may be affected more than this if the particle fallout is not distributed uniformly, it is apparent that most solar panels should arrive on orbit with not enough particle contamination to seriously degrade their power output.

4.2.3.1.4 Thermal Control Surfaces

Thermal control surfaces are usually white, if they face the Sun, or black, if they face deep space. Some spacecraft body surfaces are wrapped with multi-layer insulation (MLI) which is sometimes yellow in appearance, but more often appears silver as the result of aluminum deposited on the inside of the inside layers. Since the main appearance difference between white and silver is the specular component in the optical reflectance, white and silver surfaces are sometimes grouped together in their sensitivities to visual inspection.

As shown in Table 4-8, diffuse white surfaces do not show visual particle contamination as well as darker surfaces, especially if the dark surfaces are shiny. While there is disagreement between the various researchers in what particle levels can be visually detected on white surfaces, VC-I is apparently sensitive to a ~ 700 level, while VC-II is apparently sensitive to a ~ 600 level. Interpolating, yields a 640 particle level possible for VC-I½. The corresponding surface obscurations are: ~ 8×10^{-3} (VC-I), ~ 1.3×10^{-2} (VC- I½), and ~ 2×10^{-2} (VC-II). Assuming the thermal control surfaces are just at the point of being visually contaminated by particles, adding the typical pre-launch (10 days in *Class 100,000* air) and launch (~ 600 particle level) will produce on orbit levels of ~ 790 (VC-I), ~ 765 (VC- I½), and ~ 740 (VC-II). The corresponding surface obscuration ratios are 3.8×10^{-2} (VC-I), 3.1×10^{-2} (VC- I½), and 2.6×10^{-2} (VC-II), respectively.

Since dust particles are generally gray, their relative lack of contrast is responsible for their being hard to see on white surfaces. However, this lack of contrast in the visual wavelength region also reduces their effect on thermal control surfaces in the infrared region if their relative lack of contrast extends into the far infrared ($l > \sim 10$ μm).

As discussed in Chapter 2, under extreme conditions the thermal control surface and the contaminating particles are assumed to have opposite limiting values of α_s or ε. Black particles on a white radiator which do not face the Sun produce a 1% temperature decrease if the particle level exceeds ~ 520, (~ 0.35% obscuration), while a 1% temperature rise will be produced if the particle level exceeds ~ 450, (0.2% obscuration). These levels are considerably below the dust particle levels which can be detected on white surfaces. Fortunately, dust particles are grey, not black, and many radiators do not face up during launch. The white particles on a black surface is a better approximation here, which analysis shows requires a ~ 830 surface particle level to produce a 1% effect. Because of this relative lack of contrast, radiators are almost always very tolerant to contamination, both molecular and particulate.

4.2.3.1.5 Optical Surfaces

As has been pointed out, optical surfaces are very sensitive to particulate contamination. Fortunately, such sensors are always fabricated in special cleanrooms, (usually *Class 10,000* or better), kept covered when in storage, and sealed up between the time they are incorporated into a spacecraft and when they are deployed on orbit. Even on orbit, if they are used only intermittently, it is not unusual to re-cover them, especially if thruster operations are conducted nearby.

It is obvious that the usual visual inspection techniques are inadequate and even the stringent visual inspection levels, (VC-III or VC-IV), may not be sufficient even if such inspections are possible and they almost never are. Consequently, special test fixtures are usually constructed to verify the performance of the optical sensor through direct measurements of the sensors scattering characteristics. This is the subject of the next section.

4.2.3.2 Scattering: ASTM E 1392

For many applications involving sensitive optics, the only true measure of a sensors cleanliness is a direct measurement of its scattering characteristics. The general procedure for meaasuring BRDF is

ASTM E 1392. Because scatter measurements on aerospace optics must invariably be tailored to the specific program at hand, the details of ASTM E 1392 will not be discussed. Essentially, light from a source, (such as a laser), is scattered off of the surface in question and collected by a detector at some predetermined off axis angle. The graph of energy received/energy input vs. scattering angle yields BRDF. Because the test equipment necessary to make these measurements is usually quite sophisticated it is appropriate to discuss some of the unique requirements of these test fixtures.

Scattering test fixtures will often have their own vacuum chamber, may be cryogenically cooled, and are sensitive instruments in their own right. In this chamber, it is possible to simulate the on-orbit opening of the sensor, test its response to various simulated targets, and verify its calibration. Once this has been done the sensor is resealed, ready for incorporation into the spacecraft. Once incorporated within the spacecraft, the usual testing is mainly electrical and thermal. Voltages, currents, and waveforms are verified using laboratory generated signals which simulate the output from the optical sensor. Temperatures, especially under thermal vacuum conditions, are monitored for 30 or more days to verify the calculated heat loads, the on board refrigerator performance, or the cryogen use rate. During this time solar array performance, activation operations etc., will be measured. During this time the optical sensor will often be sealed up, protected from all external contamination.

With the optical sensors, especially cooled IR sensors, so well protected from external environments, the main threats can be internal environments. The particle contamination which may result is due to flakes of paint, metal or plastic burrs, and the like. For this reason the sensor is shaken very vigorously before its final tests to make certain that no launch induced particulates will be generated. In addition, the sensitive optical surfaces are not allowed to face up except when necessary. As expected, the on-orbit particle levels for optical sensors should be very low.

While measurements of the scattering characteristics of an optical surface are usually performed only on the ground, it is possible to design calibration devices into space sensors. Alternatively, the mission operations profile may allow for the sensor to periodically point toward the Sun, or other off-axis source, in order to back BRDF and surface cleanliness out of the resulting SNR.

4.3 Cleaning Contaminated Surfaces

The issue of how dirty a system gets during ground processing is of somewhat academic interest if the surface can be restored, with minimal effort, to the desired cleanliness before beginning orbital operations. Any cleaning techniques used must satisfy certain general criteria. The process must not be damaging to the underlying surface, must not leave a surface residue, and must be effective on a variety of surfaces and substrates. While chemical solvent wiping, the most obvious cleaning process, is effective at removing both molecular and particulate contamination, other processes are effective at removing only one or the other . Consequently, they are best discussed separately.

4.3.1 Removing Molecular Films

Various approaches have been considered to deal with molecular contamination on sensitive surfaces. Where contact with the surface is allowed solvent wiping is perhaps the most obvious method available, and relies on the chemical properties of a solvent to dislodge the molecular film from a contaminated surface. Obviously, this method can only be used on accessible parts during ground processing. Optical surfaces, or any device where direct contact with the surface is prohibited, must approach the problem in a different manner. As a rule noncontact techniques attempt to impart a large amount of energy into the film so that either: i) the recoil force that results from the absorption of the energy dislodges the film, or ii) the film heats to a sufficiently high temperature that its residence time is small and it can escapes the surface. At the same time noncontact techniques must minimize the energy input to the underlying surface to avoid damaging the surface finish. Both categories are capable of cleaning a surface to better than level A (< 1 mg per .1 m^2 NVR). In general, solvent wiping is relied upon as the standard method of choice for non-optical surfaces during ground processing, while noncontact techniques continue to be evaluated for use on optical surfaces during both ground processing and on orbit operations.

4.3.1.1 Solvent Wiping

The solvent wipe method used for surface cleaning and preparation is identical to that described in the gravimetric methods used to monitor surface cleanliness. The only difference is that when "cleaning" is the objective, rather than "verifying" surface cleanliness, there is no need to keep track of used wipes. The surface is wiped until a wiper appears clean under visual inspection, then a test wipe is made to verify surface cleanliness. This is the standard method for cleaning during ground processing. The only exception is made for optical surfaces which may be damaged by direct contact with a wiper. However, since the larger concern for optical surfaces is from particulates the discussion of cleaning polished optics will be reexamined in section 4.3.2.

4.3.1.2 Noncontact Techniques

As shown in Table 4-9, there are a variety of energy deposition techniques that may be used to "evaporate" molecular contaminants from surfaces. For the majority of these techniques, the energy absorbed by the contaminant layer is rapidly diffused throughout the layer, and then conducted to the underlying surface. The problem is that the inter-molecular forces, (Van der Waals forces), are so strong for molecular masses that techniques capable of removing molecules also damage optical surfaces. These techniques are not normally used on solar arrays or thermal control surfaces in that these surfaces may be cleaned via solvent wiping without damaging their finish.

Table 4-9. Noncontact techniques for removing molecular contamination.

Method	Pro's	Con's	Application
Thermal Heating	Standard Method Simplicity	May not be 100% Effective	Ground Processing & On Orbit
Charged Particle Beam	Standard Method	May Damage Finish	Ground Processing & On Orbit
Plasma Sputtering	Can Remove all Contaminants	May Damage Finish	Ground Processing & On Orbit
Laser Beam	High Energy/Area; High Cross Section	Wavelength Dependent	Ground Processing & On Orbit

4.3.1.2.1 Thermal Heating

The simplest method to stimulate evaporation of a condensed molecular film is simply thermal heating. Connecting the optical surfaces to a heater and raising the temperature can be effective at driving off much of the contaminants. This method can be used during ground processing or during on orbit operations. On orbit, heating of the optical surfaces may also be accomplished by reorienting the vehicle to point in the general direction of, (but not directly at), the Sun. The downside to this technique is that it is not easily adaptable to cryogenic surfaces. Many IR focal planes require cryogenic temperatures to operate properly. As discussed in Chapter 2, these cold focal planes often serve as "getters" for contamination. These contaminants may be removed by heating the focal plane to near room temperature, but this implies that the sensor will not be usable during the heating and subsequent cooling periods and will require recalibration after the operation. It also subjects the focal plane to significant thermal stresses. In theory, this practice can be repeated as often as is necessary, (on orbit degradation of signal intensity would indicate when "cleanings" are needed), but in practice focal planes may usually only be cycled a few times before they are damaged and cease to function.

4.3.1.2.2 Charged Particle Beams

The effectiveness of charged particle beam, (electron or ion), cleaning of contaminated surfaces is a function of many variables, including: beam species, beam energy, beam current density, and

contaminant.[11] This technique has proven effective for removing contaminants from cryogenic surfaces, but one area of concern is the lack of a priori knowledge of the beam intensity that will damage the underlying surface. Piper et. al report that heat source fluences should be at least 10 kW cm^{-2}. Lower fluences allow the needed energy to be dissipated into the underlying surface via thermal conduction.

4.3.1.2.3 Plasma Sputtering

Plasma sputtering has been shown to be an effective cleaning technique in many semiconductor applications. In essence, accelerated gas ions are projected onto the contaminated surface at low pressure. The collisions between the ions and the surface atoms result in the ejection, or sputtering, of surface atoms that are highly dependent on the ion energy and flux. Ion sputtering has proven effective at rmoving virtually any contaminant, but it has proven difficult to find an ion energy that will both: a) remove the contaminants, and b) leave the underlying surface undamaged.[12] RF plasma sputtering can remove contaminants without damaging metallic surfaces, provided a DC bias is applied to the metal. This method has also been shown to remove water on 120 K surfaces.

4.3.1.2.4 Laser Beams

Both ultraviolet and Infrared laser heating appear to offer the opportunity for contaminant removal without optical damage.[13] Pulsed CO_2 lasers are efficient energy sources, (conversion efficiency ~ 10%), and many important contaminants, such as ice, are highly absorping at CO_2 wavelengths. CO2 lasers have proven capable of removing films in excess of 5 mm thick, whereas Nd:YAG lasers are only useful on films < 0.1 mm. This is a function of contaminant absorptance. If the contaminating layer is absorptive to the laser light, the film absorbs the energy and can be vaporized more easily. If the film is more transparent, (as is the case for Nd:YAG), much of the light is absorbed by the underlying substrate so that the heating of the film comes from thermal diffusion. This is ineffective on thicker films. The semiconductor industry utilizes UV lasers in certain cleaning operations. Contaminant layers are typically very absorbing at UV wavelengths and energy densities on the order of 0.5 J cm^{-2} have proven effective for cleaning mirrors.

4.3.2 Removing Particulates

Many of the methods utilized to clean molecular contamination may also be used to remove particulate contamination. Solvent wiping, for example, is highly effective at removing particulates. Many of the noncontact, molecular techniques will also work on particulates. The "shock" of

---

[11] Fisher, R. F., George, P. M., Flammang, S. M., and Howard, T. L., "Ion Beam Cleaning of Contaminated Optics, SPIE Vol. 1329, *Optical System Contamination: Effects, Measurement, Control II*, pp. 86 - 97, 1990.

George, P. M., Lindquist, J. M., and Hankins, M., "Ion Beam Removal of Water and Dioctyl Phthalate from Cryogenic Mirrors," *J. Spacecraft*, Vol. 27, No. 3, pp. 253 - 257, 1990.

Piper, L. G. Spencer, M. N., Woodward, A. M., and Green, B. D., "CROSS: Contaminant Removal off Optic Surfaces in Space," Rome Air Development Center, Interim Technical Report, June 1987.

[12] Shaw, C. G., "Contamination Removal by Ion Sputtering," SPIE Vol. 1329, *Optical System Contamination: Effects, Measurement, Control II*, pp. 98 - 109, (1990).

[13] Piper, L. G., Frish, M. B., Pierce, V. G., and Green, B. D., "Laser Cleaning of Cryogenic Optics," SPIE Vol. 1329, *Optical System Contamination: Effects, Measurement, Control II*, pp. 110 - 126, (1990).

Osiecki, R. A. and Magee, T. J., "Ultraviolet Laser Cleaning of Mirrored Surfaces," SPIE Vol. 1329, *Optical System Contamination: Effects, Measurement, Control II*, pp. 127 - 133, (1990).

Pierce, V. G., Frish, M. B., Green, B. D., Piper, L. G., Guregian, J., and Anapol, M., "Laser-Mirror Cleaning in a Simulated Space Environment," SPIE Vol. 1329, *Optical System Contamination: Effects, Measurement, Control II*, pp. 134 - 140, (1990).

absorbing energy from a charged particle beam or laser, for example, can often dislodge surface particulates as well. However, as shown in Table 4-10, where particulates are the main concern there are other noncontact cleaning techniques available. Stowers and Patton report that solvent wiping will leave only 2 - 40 particles/cm^2 (> 5 μm), whereas spraying with high velocity liquid jets leaves 2 - 60 particles/cm^2, and strippable adhesive coatings leave ~ 500/cm^2.[14] Strippable adhesive coatings will be examined in the next section as a means of preventing surface contamination, rather than as a means of cleaning a contaminated surface.

Table 4-10. Noncontact techniques for removing particulate contamination.

Method	Pro's	Con's	Application
Shaking/Agitation	Simple	Not Effective on Smaller Particles	Ground Processing
Jet Spray	Simple	Not Effective on Smaller Particles	Ground Processing & On Orbit

4.3.2.1 Noncontact Techniques

The forces adhering particulates to a surface are ultimately electrical in nature.[15] In an air environment, the attractive forces between a 1 μm glass particle and a wafer surface are estimated at 71% capillary (0.045 dynes), 22% van der Waals – London (0.014 dynes), 7% electrical double layer (0.003 dynes), and 1% electrostatic image (0.001 dynes). In general, particle adhesive forces vary widely with particle size, shape, and material characteristics. Some particles may fall off under the influence of gravity, while others will remain attached under the influence of 1000 g's. In order to clean particulates from a surface, an external force must be applied to the particulates in order to overcome the adhesive forces. One method is to simply shake the "contaminated" device so that the particulates are dislodged. The spacecraft will be subjected to significant vibrations during launch, so prelaunch shake testings are one way to verify system integrity as well as remove contamination. This is also the reason that launch typically initiates particulate redistribution within the launch vehicle shroud. Ultrasonic and megasonic agitation methods are often used in the semiconductor industry, but these are obviously unsuitable for bulk cleaning of assembled optics.

Another noncontact cleaning method is to simply blow air, or other fluid, across the surface. If the shear force exceeds the adhesion force holding the particle, the particle will be removed and suspended in the turbulent fluid. Increasing the fluid density and local velocity, and lowering the fluid viscosity, increases the effectiveness of this cleaning method. In general, liquids are more effective than gases. Ninety percent cleaning efficiencies associated with the removal of 10 μm-sized particles have been reported for > 150 psi cold gas jets.[16] Flushing or blowing with low pressure gas is largely ineffective due to the surface adhesion forces involved. Pressures required to remove particles vary as 1/D, making particulates smaller than 0.5 μm extremely difficult to remove. CO_2 jet spray techniques have been used in commercial applications for some time, and also prove to be effective at removing surface particulates.[17] The expansion of liquid CO_2 will produce a CO_2 "snow" which can transfer momentum to surface particulates, disloding and sweeping them off of the surface. Post cleaning

[14] Stowers, I. F., and Patton, H. G., "Techniques for Removing Contamination from Optical Surfaces," *Surface Contamination*, K. L. Mittal, Ed., pp. 341 - 349, Plenum Publishing, (1979).

[15] Feicht, J. R., Blanco, J. R., and Champetier, R. J., "Dust Removal from Mirrors: Experiments and Analysis of Adhesive Forces," SPIE Vol. 967, *Stray Light and Contamination in Optical Systems*, pp. 19 - 29, (1988).

[16] Haffner, J. W., and Wang, J. J., "Dust Removal from Mirrors," Rockwell International, SSD-785-240-005-87, 30 September 1987.

[17] Motyl, K. M., "Cleaning Metal Substrates using Liquid/Supercritical Fluid Carbon Dioxide," NASA Tech Briefs, MFS-29611, 18 March 1979.

Peterson, R. V., and Bowers, C. W., "Contamination Removal by CO2 Jet Spray," SPIE Vol. 1329, *Optical System Contamination: Effects, Measurement, Control II*, pp. 72 - 85, (1990).

inspection indicates that this method should be capable of cleaning a surface to about level 250. While these processes are adaptable to on orbit operations, these cleaning techniques are mainly used during ground processing.

4.4 Maintaining Surface Cleanliness

4.4.1 Storage

Any time that clean components are not being processed, they should be covered with an antistatic bag in a *Class 100,000* or better cleanroom. During extended storage the system should be connected to an air, or preferably dry nitrogen, purge supplied to the interior of the bag at a slight positive pressure relative to the surrounding area. This will prevent particulates or other contaminants from entering the enclosed atmosphere. The air (or nitrogen) should be filtered by HEPA filters, or better, and contain no detectable hydrocarbons. Optical components must be similarly protected in a *Class 100* environment unless doubly protected, e.g., under purge or inside a spacecraft housing and bagged. Extremely sensitive optics may need to continue the purge up until launch, or even through early on orbit operations.[18] Temperature and humidity should be controlled and monitored.

Optical devices may be further protected through the use of strip coating materials.[19] The strip coating is poured on the surface as a viscous liquid and will dry within a matter of hours. The coating will then protect the underlying surface until it is removed. These strip coatings will typically leave a small residue of molecular contaminants behind, but can totally mitigate other contamination concerns while they are in place.

4.4.2 Transportation

Precision cleaned parts, subassemblies, assemblies, etc., should be doubly protected with bags or suitable containers for shipping. Relative humidity should be 50% maximum. Desiccants, witness plate, and temperature and humidity monitors should be used as required. Any air supplied to the interior of the shipping container, should be filtered with HEPA filters, or better. Prior to entry to the cleanroom, the shipping container should be cleaned and the outer protection examined for integrity. The package should then be brought to a clean anteroom where the outer enclosure will be removed and the cleanliness of the inner wrapping checked. Any discrepancies should be noted and resolved at this time.

4.4.3 Accident Recovery

A note concerning accidents is appropriate here. While extreme precautions are being followed to limit the contamination of optical sensors from design through on orbit operations, some thought must be given to recovery from accidents. Such accidents may be as benign as a cleanroom which has filters that have not been changed as scheduled, or as catastrophic as the dropping of the sensor onto a concrete floor. All accidents have the potential to produce contamination, especially particulate contamination, and must be minimized through proper contamination control procedures. When they occur, accidents should be documented so that the proper recovery plans can be made.

4.5 Launch Processing

Years of careful prelaunch planning and testing can be rendered useless if the proper procedures and cautions are not followed at the launch site. Specific processing procedures for each launch vehicle are different, with the time between shroud closeout and launch, the availability of purge in the shroud, and nominal shroud cleanliness being some of the variables that must be examined. If

[18] Scialdone, J. J., ,"Abatement of Gaseous and Particulate Contamination in a Space Instrument," AIAA 83-1567, (1983).

[19] Fine, J., and Pernick, B. J., "Use of Strippable Coatings to Protect and Clean Optical Surfaces," *App. Optics*, Vol. 26, No. 16, pp. 3172 - 3173, 15 August 1987.

standard procedures are not sufficient, the contamination control engineer must work with the launch vehicle provider to ensure that the proper environment is maintained. Because it is one of the most well-studied examples, the specific case of the Shuttle Orbiter is examined in the sections that follow. These sections provide an example of a typical launch processing flow, along with the associated cleanroom environments, and early on orbit contamination environments.

4.5.1 Eastern Test Range Shuttle Processing Facilities

While each Shuttle payload is serviced in its own pre-launch facilities, they all pass through the Shuttle access platform before installation in the Shuttle payload bay. These facilities usually have *Class 100,000* air, Figure 4-6 and Figure 4-7, respectively. Measurements of particle fallout in these facilities show a relatively large fraction of big particles, Figure 4-8. However, these big particles are more readily removed by cleaning than are small particles. They are also more likely to be dislodged by the launch environment than are smaller particles. Lastly, they do not account for as large a fraction of obscured area as smaller particles, which are more numerous.

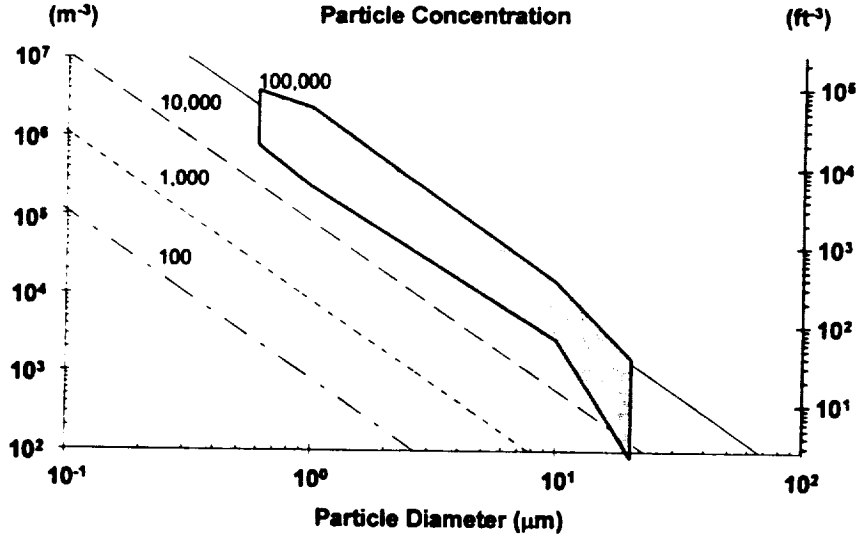

Figure 4-6. Prelaunch shuttle access platform air cleanliness.

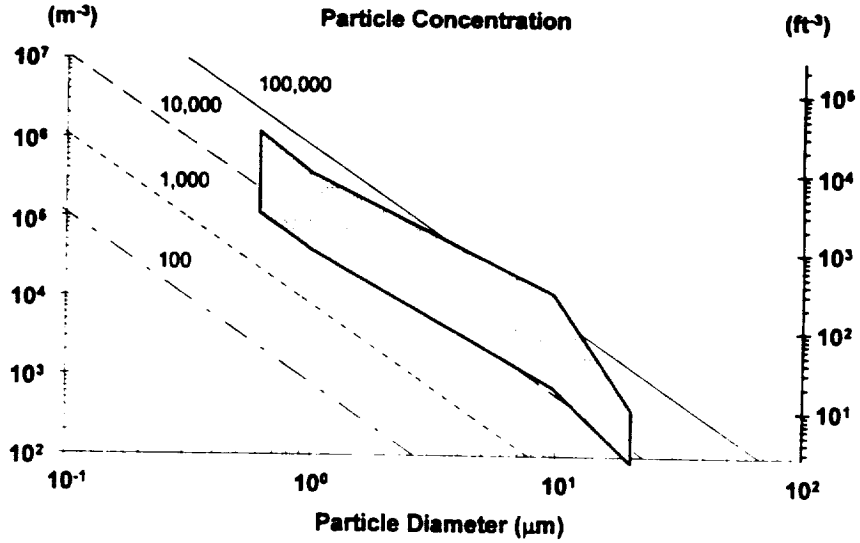

Figure 4-7. Prelaunch shuttle bay air cleanliness.

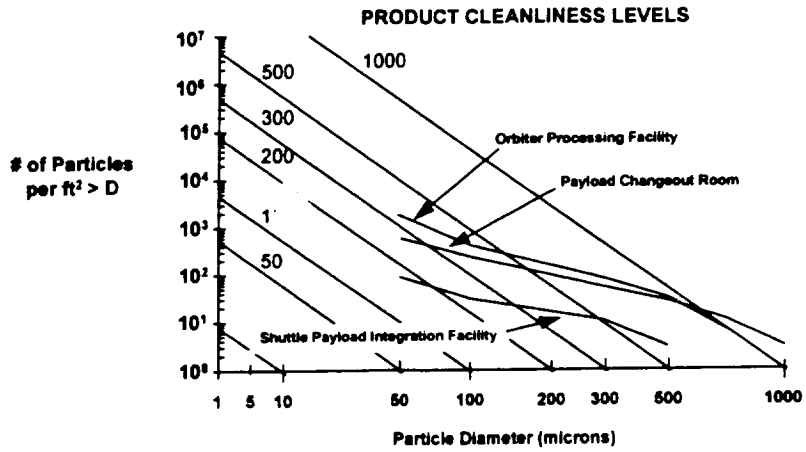

Figure 4-8. Measurement of surface particles in Eastern Test Range (ETR) facilities.

The story for other launch vehicles will be similar, but will vary depending on the specific launch processing environment. Each launch vehicle has different rules about the minimum time from shroud closeout to launch, the availability of filtered purge within the shroud, and so on. Despite the best laid plans, nature is also capable of introducing uncertainty into an otherwise controlled situation. When the Mars Observer spacecraft was on the launch vehicle at the launch pad, the area was struck by a Hurricane. The gale force winds forced humidity and debris into the shroud and forced NASA to return the spacecraft to the launch processing facility for a thorough cleaning before launch operations could resume.

4.5.2 Early on Orbit Contamination Environment

The launch induced surface particle levels must be added, on an obscured area basis, to the pre-launch surface particle levels. For the Shuttle these have been two sets of measurements of the launch induced contamination in the cargo bay. The Passive Optical Sample Assembly (POSA) and the Induced Environment Contamination Monitor (IECM).[20] The POSA consisted of witness plates, some of which faced upward during launch, while the IECM consisted of various sensors including QCM's which did not always work. The cargo bay liner was not in place for any of these measurements. The POSA measurements suggest a 600 particle level on horizontal upward facing surfaces, while the IECM date approximate a 550 level. Both sets of measurements show a flatter particle size distribution that than predicted by MIL STD 1246C. It is reasonably conservative to assume that a launch in the shuttle cargo bay will produce a 600 particle level on horizontal facing surfaces and a 325 level on vertical surfaces. (Keeping in mind that the Shuttle is standing on its tail when launched.) Both the POSA and IECM experiments indicated a molecular level A for the NVR deposited. Many of the observed outgassed species were common solvents used in cleaning processes and appear to be from spacecraft-related sources.

[20] Miller, E. R., "STS-2, -3, -4 Induced Environment Contamination Monitor (IECM) Summary Report," NASA TM-82524, February 1983.

5. Bibliography

5.1 Government Documents

FED-STD-209E, *Airborne Particulate Cleanliness Classes in Cleanrooms and Clean Zones*, 11 September 1992.

MIL-HDBK-406, *Contamination Control Technology*, 31 October 1971.

MIL-STD-889B, *Dissimilar Metals*, 7 July 1976.

MIL-STD-1246C, *Product Cleanliness Levels and Contamination Control Program*, 11 April 1994.

MIL-STD-1568A, *Materials and Processes for Corrosion Prevention and Control in Aerospace Weapons Systems*, 24 October 79

NASA-JSC-08962, *Compilation of VCM Data of Nonmetallic Materials Addendum*, 5 July 1981.

NASA-RP-1124, *Outgassing Data for Selected Spacecraft Materials, Rev. R*, August 1987.

NASA-SN-C-0005, *Specifications - Contamination Control Requirements for the Space Shuttle Program, Rev. A.*, January 1982.

NASA-SP-5076, *Contamination Control Handbook*, 1969.

NASA-SP-R-0022A, *Vacuum Stability Requirements of Polymeric Material for Spacecraft Applications*, 9 September 1974.

T.O. 00-25-203, *Contamination Control of Aerospace Facilities*, U.S. Air Force, 1 March 1985.

5.2 Industrial Standards

5.2.1 American Society for Testing and Materials (ASTM)

ASTM D 4597, *Practice for Sampling Workplace Atmospheres to Collect Organic Gases or Vapors with Activated Charcoal Diffusion Samplers*, 1992.

ASTM D 4598, *Practice for Sampling Workplace Atmospheres to Collect Organic Gases or Vapors with Liquid Sorbent Diffusional Samplers*, 1987.

ASTM D 5466, *Methods for the Determination of Volatile Organic Chemicals in Atmosphers (Canister Sampling Methodology)*, 1993

ASTM E 168, *Practices for General Techniques of Infrared Quantitative Analysis*, 1992.

ASTM E 169, *Practices for General Techniques of Ultraviolet-Visible Quantitative Analysis*, 1993.

ASTM E 204, *Practices for Identification of Material by Infrared Absorption Spectroscopy Using the ASTM Coded Band and Chemical Classification Index*, 1992

ASTM E 334, *Practices for General Techniques of Infrared Microanalysis*, 1990

ASTM E 595, *Total Mass Loss and Collected Volatile Condensable Materials from Outgassing in a Vacuum Environment*, 1993.

ASTM E 673, *Terminology Relating to Surface Analysis*, 1993.

ASTM E 1216, *Standard Practice for Sampling for Surface Particle Contamination by Tape Lift*, 1987.

ASTM E 1234, *Standard Practice for Handling, Transporting, and Installing Non-Volatile Residue (NVR) Sample Plates used in Environmentally Controlled Areas for Spacecraft*, 1995.

ASTM E 1235, *Standard Test Method for Gravimetric Determination of Non-Volatile Residue (NVR) in Environmentally Controlled Areas for Spacecraft*, 1995.

ASTM E 1548, *Practice for Preparation of Aerospace Contamination Control Plans*, 1993.

ASTM E 1549, *Specification for ESD Controlled Garments Required in Cleanrooms and Controlled Environments for Spacecraft for Non-Hazardous and Hazardous Operations*, 1995.

ASTM E 1559, *Standard Test Method for Contamination Outgassing Characteristics of Spacecraft Materials*, 1993.

ASTM E 1560, *Method for Gravimetric Determination of Nonvolatile Residue from Cleanroom Wipers*, 1993.

ASTM F 24, *Standard Test Method for Measuring and Counting Particulate Contamination on Surfaces*, 1965.

ASTM F 25, *Standard Test Method for Sizing and Counting Airborne Particulate Contamination in Cleanrooms and Other Dust Controlled Areas Designed for Electronics or Other Applications*, 1968.

ASTM F 50, *Practice for Continuous Sizing and Counting of Airborne Particles in Dust Controlled Areas and Cleanrooms Using Instruments Capable of Detecting Single Sub-Micrometer and Larger Particles*, 1992.

ASTM F 51, *Method for Sizing and Counting Particulate Contaminant in and on Cleanroom Garments*, 1989.

ASTM F 301, *Practice for Noncryogenic Fluid Systems, Open-Bottle Tap Sampling of*, 1991

ASTM F 302, *Practice for Field Sampling of Aerospace Fluids in Containers*, 1989.

ASTM F 303, *Practices for Sampling Aerospace Fluids from Components*, 1989.

ASTM F 306, *Practice for Sampling Particulates from Man-Accessible Storage Vessels for Aerospace Fluids by Vacuum Entrainment Technique (General Method)*, 1988.

ASTM F 307, *Practice for Sampling Pressurized Gas for Gas Analysis*, 1988.

ASTM F 308, *Practice for Sampling Gas Blow-Down Systems and Components for Particle Contamination by Manual Method.*

ASTM F 311, *Practice for Processing Aerospace Liquid Samples for Particulate Contamination Analysis Using Membrane Filters*, 1983.

ASTM F 312, *Microscopic Sizing and Counting Particles from Aerospace Fluids on Membrane Filters*, 1969.

ASTM F 318, *Practice for Airborne Particulate Contamination in Cleanrooms for Handling Aerospace Fluids*, 1989.

ASTM F 322, *Method for Determining the Quality of Calibration Particles for Automatic Particle Counters*,

ASTM F 324, *Method for Nonvolatile Residue of Volatile Cleaning Solvents Using the Solvent Purity Meter*, 1980.

ASTM F 327, *Practice for Sampling Gas Blowdown Systems and Components for Particulate Contamination by Automatic Particle Monitor Methods*, 1989.

ASTM F 328, *Practice for Determining Counting and Sizing Accuracy of an Airborne Particle Counter Using Near-Monodisperse Spherical Particulate Materials*, 1989.

ASTM F 329, *Practice for Sampling and Measurement of Particulate Contamination in Liquids Using an in-Line Automatic Monitor*, 1983.

ASTM F 331, *Method for Nonvolatile Residue of Halogenated Solvent Extract from Aerospace Components (Using Rotary Flash Evaporator)*, 1989.

ASTM F 649, *Practice for Secondary Calibration of Airborne Particle Counter Using Comaprison Procedures*, 1992.

ASTM F 658, *Practice for Defining Size Calibration, Resolution, and Counting Accuracy of a Liquid-Borne Particle Counter Using Near-Monodisperse Spherical Particulate Mateiral*, 1992.

ASTM F 660, *Practice for Comparing Particle Size in the use of Alternative Types of Particle Counters*, 1988.

ASTM F 1227, *Method for Total Mass Loss of Materials and Condensation of Outgassed Volatiles on Microelectronics-Related Substrates*, 1989.

ASTM F 1471, *Method for Evaluating the Air Cleaning Performance of a High-Efficiency Particulate Air-Filter System*, 1993.

5.2.2 Institute of Environmental Sciences (IES)

IES-RP-CC001.3, *Recommended Practice, HEPA and ULPA Filters*, 1995.

IES-RP-CC002-86, *Recommended Practice, Laminar Flow Clean Air Devices*, 1986.

IES-RP-CC003.2, *Garment System Consdierations for Cleanrooms and Other Controlled Environments*, 1993.

IES-RP-CC004.2, *Evaluating Wiping Materials Used in Cleanrooms and Other Controlled Environments*, 1992.

IES-RP-CC005.2, *Cleanroom Gloves and Finger Cots*, 1994.

IES-RP-CC006.2, *Testing Cleanrooms*, 1993.

IES-RP-CC007.1, *Testing ULPA Filters*, 1992.

IES-RP-CC008-84, *Recommended Practice, Gas-Phase Adsorber Cells*, 1984.

IES-RP-CC009.2, *Compendium of Standards, Practices, Methods and Similar Documents Relating to Contamination Control*, 1993.

IES-RP-CC011.2, *A Glossary of Terms and Definitions Relating to Contamination Control*, 1995.

IES-RP-CC012.1, *Considerations in Cleanroom Design*, 1992

IES-RP-CC013-86-T, *Recommended Practice, Equipment Calibration or Validation Procedures*, 1986.

IES-RP-CC015-87-T, *Recommended Practice, Cleanroom Product and Support Equipment*, 1987.

IES-RP-CC016.1, *The Rate of Deposition of Nonvolatile Residue in Cleanrooms*, 1992.

IES-RP-CC018.2, *Cleanroom Housekeeping - Operating and Monitoring Procedures*, 1992.

IES-RP-CC020-88-T, *Recommended Practice, Substrates and Forms for Documentation in Cleanrooms*, 1988.

IES-RP-CC021.1, *Testing HEPA and ULPA Filter Media*, 1994.

IES-RP-CC022.1, *Electrostatic Charging in Cleanrooms and Other Controlled Environments*, 1992.

IES-RP-CC023.1, *Microorganisms in Cleanrooms*, 1993.

IES-RP-CC024 1, *Measuring and Reporting Vibration in Microelectronic Facilities*, 1993.

IES-RP-CC025, *Swabs in Cleanrooms*, 1994.

IES-RP-CC026, *Cleanroom Operations*, 1994.

5.3 Selected Public Domain References

5.3.1 Molecular Contamination

5.3.1.1 Effects of Molecular Films

Ahern, J. E., and Karperos, K., Calorimetric Measurements of Thermal Control Surfaces on Operational Satellites, J. A. Roux and T. D. McKay, eds, *Progress in Astronautics and Aeronautics*, Vol. 91, AIAA, pp. 235 - 260, 1984.

Ahern, J. E., Belcher, R. L., and Ruff, R. D., Analysis of Contamination Degradation of Thermal Control Surfaces on Operational Satellites, J. A. Roux and T. D. McKay, eds, *Progress in Astronautics and Aeronautics*, Vol. 91, AIAA, pp. 96 - 107, 1984.

Azzam, R. M. A., Bu-Habib, E., Casset, J., Chassaing, G., and Gravier, P., Antireflection of an Absorbing Substrate by an Absorbing thin film at Normal Incidence, *Applied Optics*, Vol. 26, No. 4, pp. 719 - 722, February, 1987.

Curran, D. G. T., and Millard, J. M., Results of Contamination/Degradation Measurements on Thermal Control Surfaces of an Operational Satellite, *AIAA 77-740*, AIAA 12th Thermophysics Conference, Albuquerque, NM, 27 - 29 June 1977.

Curran, D. G. T., and Millard, J. M., Results of Contamination/Degradation Measurements on Thermal Control Surfaces of an Operational Satellite, *AIAA 77-740*, AIAA 12th Thermophysics Conference, Albuquerque, NM, 27 - 29 June 1977.

Facey, T. A., and Nonnemacher, A. L., Measurement of Total Hemispherical Emissivity of Contaminated Mirror Surfaces, *Stray Light and Contamination in Optical Systems*, SPIE Vol. 967, pp. 308 - 313, 1988.

Hall, D. F., and Fote, A. A., Alpha/Epsilon Measurements of Thermal Control Coatings on the P78-2 (SCATHA) Spacecraft, *Heat Transfer and Thermal Control*, A. L. Crosbie, ed., *Progress in Astronautics and Aeronautics*, Vol. 78, AIAA, pp. 467 - 486, 1981.

Hall, D. F., and Fote, A. A., Alpha/Epsilon Measurements of Thermal Control Coatings over Four Years at Geosynchronous Altitude, J. A. Roux and T. D. McKay, eds, *Progress in Astronautics and Aeronautics*, Vol. 91, AIAA, pp. 215 - 234, 1984.

Hall, D. F., and Fote, A. A., Long Term Performance of Thermal Control Coatings at Geosynchronous Altitude, *AIAA 86-1356*, AIAA/ASME 4th Joint Thermophysics and Heat Transfer Conference, 2 - 4 June 1986.

Hass, G., and Hunter, W. R., Laboratory Experiments to Study Surface Contamination and Degradation of Optical Coatings and Materials in Simulated Space Environments, *Applied Optics*, Vol. 9, No. 9, pp. 2101 - 2110, September, 1970.

Heinemann, M., Shuttle Contamination Modeling: The Plasma Wave Field of Spacecraft, *Air Force Geophysics Laboratory*, AFGL-TR-85-0300, 22 November 1985.

Heu, R., Steakley, J. M., and Petrosky, E. J., Ambient Pressure Offgassing Apparatus for Screening Materials Utilized in Environment Supporting Optical Spaceborne Systems, *Optical System Contamination: Effects, Measurement, Control II*, SPIE Vol. 1329, No. 1329-26, pp. 299 - 304, 10 - 12 July 1990.

Joy, P., OSR Degradation, *The Aerospace Corporation*, Proceedings of the Spacecraft Thermal Control Technology Workshop, Section 3.9, 3 3 - 5 February 1993.

Liu, C. K., and Glassford, A. P. M., Contamination Effects of Some Spacecraft Materials and Rocket Plume Products, *Proceedings of the USAF/NASA International Spacecraft Contamination Conference*, NASA CP-2075, AFML-TR-78-226, pp. 1066 - 1088, 7 - 9 March 1978.

Maag, C. R., Effects of the Contamination Environment on Surfaces and Materials, *NASA/SDIO Space Environmental Effects on Materials Workshop*, NASA CP-3036, pp. 353 - 366, 28 June - 1 July 1988.

Montgomery, E. E., Development of a Spacecraft Materials Data Base, *Air Force Wright Aeronautical Laboratory*, AFWAL-TR-85-4047, May, 1985.

Mossman, D. L., Bostic, H. D., and Carlos, J. R., Contamination Induced Degradation of Optical Solar Reflectors in Geosynchronous Orbit, *Optical System Contamiantion: Effects, Measurment, Control*, SPIE Vol. 777, No. 777-02, pp. 35052, 19 - 22 May 1987.

Neff, J. A., Mullen, C. R., and Fogdall, L. B., Effects of a Simulated Synchronous Altitude Environment on Contaminated Optical Solar Reflectors, *J. Spacecraft*, Vol. 23, No. 4, pp. 386 - 390, July - August, 1986.

Osantowski, J. F., Contamination Sensitivity of Typical Mirror Coatings - A Parametric Study, *Spacecraft Contamination Environment*, SPIE Vol. 338, No. 338-08, pp. 80 - 86, 4 - 6 May 1982.

Pence, W. R., and Grant, T. J., Alpha-sub-s Measurements of Thermal Control Coatings on Navstar Global Positioning System Spacecraft, *Spacecraft Radiative Transfer and Temperature Control*, T. E. Horton, ed., Vol. 83, Progress in Astronautics and Aeronautics, pp. 234 - 246, 1982.

Seiber, B. L., Bertrand, W. T., and Wood, B. E., Contamination Effects of Satellite Material Outgassing Products on Thermal Surfaces and Solar Cells, *AEDC-TR-90-27*, December, 1990.

Simonson, R. J., Thornberg, S. M., and Liang, S. Y., Outgassing Detection, *Cleanrooms*, Vol. 9, No. 2, p. 23, February, 1995.

Tribble, A. C., Quantifying the Effects of Molecular and Particulate Contamination on Thermal Control Systems, *The Aerospace Corporation*, Proceedings of the Spacecraft Thermal Control Technology Workshop, Section 3.10, 3 - 5 February 1993.

Vest, C. E., Bucha, R. M., and Lenkevich, M. J., Materials Selection as Related to Contamination of Spacecraft Critical Surfaces, *SAMPE Quarterly*, Vol. 19, No. 2, pp. 29 - 35, January, 1988.

Wood, B. E., Bertrand, W. T., Kiech, E. L., Holt, J. D., and Falco, P. M., Surface Effects of Satellite Material Outgassing Products, *AEDC-TR-89-2*, June, 1989.

Wood, B. E., Bertrand, W. T., Seiber, Kiech, E. L., Falco, P. M., and Holt, J. D., Satellite Material Contaminant Optical Properties, *Scatter from Optical Components*, SPIE Vol. 1165, No. 11163-35, pp. 392 - 400, 8 - 10 August 1989.

5.3.1.1.1 Cryogenic Surfaces

Ahmadjian, J., Conley, T., Huppi, R., and Baker, K., Cryogenic Infrared (IR) Spectral Measurements on Board the Space Shuttle - CIRRIS, *Shuttle Optical Environment*, SPIE Vol. 287, No. 287-12, pp. 102 - 107, 23 - 24 April 1981.

Arnold, F., Degradation of Low-Scatter Metal Mirrors by Cryodeposit Contamination, *Arnold Engineering Development Center*, AEDC-TR-75-128, October, 1975.

Arnold, F., Sanderson, R. B., and Mantz, A. W., Infrared Spectral Reflectance of Plume Species on Cooled Low-Scatter Mirrors, *Air Force Rocket Propulsion Laboratory*, AFRPL-TR-73-52, September, 1973.

Barengoltz, J. B., Millard, J. M., Jenkins, T., and Taylor, D. M., Modeling of Internal Contaminant Deposition on a Cold Instrument Sensor, *Optical System Contamination: Effects, Measurement, Control II*, SPIE Vol. 1329, No. 1329-30, pp. 337 - 351, 10 - 12 July 1990.

Bertie, J. E., Labbe, H. J., and Whalley, E., Absorptivity of Ice I in the Range 4000 - 30 cm^{-1}, *J. Chem. Phys.*, Vol. 50, No. 10, pp. 4501 - 4520, May, 1969.

Palmer, K. F., Infrared Optical Properties of Solid Mixtures of Molecular Species at 20 K, J. A. Roux and T. D. McKay, eds, Progress in Astronautics and Aeronautics, Vol. 91, AIAA, pp. 162 - 179, 1984.

Pipes, J. G., Roux, J. A., Smith, A. M., and Scott, H. E., Infrared Transmission of Contaminated Cryocooled Optical Windows, *AIAA Journal*, Vol. 16, No. 9, pp. 984 - 990, September, 1978.

Pipes, J. G., Sherrell, F. G., Wood, B. E., and Clark, W. L., Cryocooled Optics and Contamination, *Optical Eng.*, Vol. 18, No. 6, pp. 620 - 625, November - December, 1979.

Roux, J. A., Wood, B. E., and Smith, A. M., IR Optical Properties of Thin H20, NH3, and CO2 Cryofilms, *AEDC-TR-78-57*, September, 1979.

Thompson, S. B., Arnold, F., and Sanderson, R. B., Optical Effects of Cryodeposits on low Scatter Mirrors,, *AIAA 73-732*, AIAA 8th Thermophysics Conference, Palm Springs, CA, 16 - 18 July 1973.

Wood, B. E., and Roux, J. A., Infrared Optical Properties of Thin H2O, NH3, and CO2 Cryofilms, *J. Opt. Soc. Am.*, Vol. 72, No. 6, pp. 720 - 728, June, 1982.

Wood, B. E., and Roux, J. A., Infrared Optical Properties of Thin CO, NO, CH4, HCl, N2O, O2, N2, and Ar Cryofilms, , J. A. Roux and T. D. McKay, eds, Progress in Astronautics and Aeronautics, Vol. 91, AIAA, pp. 139 - 161, 1984.

Wood, B. E., and Smith, A. M., Infrared Reflectance and Refractive Index of Condensed Gas Films on Cryogenic Mirrors, *AIAA 78-851*, 2nd AIAA/ASME Thermophysics and Heat Transfer Conference, Palo Alo, CA, 24 - 26 May 1978.

Wood, B. E., Smith, A. M., Roux, J. A., and Seiber, B. A., Spectral Infrared Reflectance of H2O Condensed on LN2-Cooled Surfaces in Vacuum, *AIAA Journal*, Vol. 9, No. 9, pp. 1836 - 1842, September, 1971.

5.3.1.2 Generation, Transport and Deposition

5.3.1.2.1 General

Alan Kan, H. K., Desorptive Transfer: A Mechanism of Contaminant Transfer in Spacecraft, *J. Spacecraft*, Vol. 12, No. 1, pp. 62 - 64, January, 1975.

Anon., Compilation of VCM Data of Nonmetallic Materials, *NASA JSC 08962, Rev. R*, December, 1978.

Campbell, W. A., Jr., and Scialdone, J. J., Outgassing Data for Selecting Spacecraft Materials, *NASA RP 1124, Rev. 2*, 1990.

Chen, P. T., Hedgeland, R. J., and Thomson, S. R., Surface Accommodation of Molecular Contaminants, *Optical System Contamination: Effects, Measurement, Control II*, SPIE Vol. 1329, No. 1329-29, pp. 327 - 336, 10 - 12 July 1990.

Chen, Y. H., Update of Aerojaet Mass Analyzer Program for On-Orbit Satellite Contamination Prediction, *Optics in Adverse Environments*, SPIE Vol. 216, No. 216-03, pp. 24 - 30, 4 - 5 February 1980.

Cull, R., Improved Materials Characterization for Spacecraft Applications, *13th Space Simulation Conference*, The Payload - Testing for Success, NASA CP-2340, pp. 341 - 342, 8 - 11 October 1984.

Dyer, J. S., Benson, R. C., Phillips, T. E., and Guregian, J. J., Outgassing Analyses Performed During Vacuum Bakeout of Components Painted with Chemglaze Z306/9922, *Optical System Contamination*, SPIE Vol. 1754, pp. 177 - 194, 23 - 24 July 1992.

Eckert, W. R., Offgassing and Odour Tests of Non-Metallic Materials for Space Cabins, *Spacecraft Materials in Space Environment* SP-145, pp. 34762, 2 - 5 October 1979.

Glassford, A. P. M. and Liu, C. K., Characterization of Contamination Generation Characteristics of Satellite Materials, Volume II - Assessment of Industry Survey and Literature Review, *AFWAL-TR-83-4126*, Vol. 2, July, 1984.

Glassford, A. P. M., Outgassing Behavior of Multilayer Insulation Material, *J. Spacecraft*, Vol. 7, No. 12, pp. 1464 - 1467, December, 1970.

Glassford, A. P. M., and Garrett, J. W., Characterization of Contamination Generation Characteristics of Satellite Materials: Phase 2 - Test Method Development, *AFWAL-TR-85-4118*, December, 1985.

Glassford, A. P. M., and Garrett, J. W., Characterization of Contamination Generation Characteristics of Satellite Materials, *WRDC-TR-89-4114*, 22 November, 1989.

Glassford, A. P. M., and Garrett, J. W., Characterization of Contamination Generation Characteristics of Satellite Materials, *Phase II - Test Method Development*, Air Force Wright Aeronautical Laboratories, AFWAL-TR-85-4118, December, 1985.

Glassford, A. P. M., and Liu, C. K., Characterization of Contamination Generation Characteristics of Satellites, *Vol. II - Assessment of Industry Survey and Literature Review*, Air Force Wright Aeronautical Laboratories, AFWAL-TR-83-4126, July, 1984.

Glassford, A. P. M., and Liu, C. K., Outgassing Rate of Multilayer Insulation Materials at Ambient Temperature, *J. Vac. Sci. Technol.*, Vol. 17, No. 3, pp. 696 - 704, May - June, 1980.

Glassford, A. P. M., and Liu, C. K., Outgassing Rate of Multilayer Insulation, *Proceedings of the USAF/NASA International Spacecraft Contamination Conference*, NASA CP-2040, AFML-TR-78-192, pp. 83 - 106, 7 - 9 March 1978.

Glassford, A. P. M., Osiecki, R. A., and Liu, C. K., Improved Methods for Characterizing Material-Induced Contamination, *Spacecraft Contamination: Sources and Prevention*, J. A. Roux and T. D. McCay, eds, Progress in Astronautics and Aeronautics, Vol. 91, AIAA, pp. . 1984.

Henninger, J. H., Solar Absorptance and Thermal Emittance of Some Common Spacecraft Thermal Control Coatings, *NASA RP 1121*, 1984.

Hughes, T. A., Outgassing of Materials in the Space Environment, *Proceedings of the USAF/NASA International Spacecraft Contamination Conference*, NASA CP-2039, AFML-TR-78-190, pp. 13 - 29, 7 - 9 March 1978.

Kiu, C. K. and Glassford, A. P. M. Characterization of Contamination Generation Characteristics of Satellite Materials, Volume I - Industry Survey and Literature Review, *AFWAL-TR-83-4126*, Vol. 1, November, 1983.

Leger, L., Gaseous Contamination Concerns, *Proceedings of the USAF/NASA International Spacecraft Contamination Conference*, NASA CP-2080, AFML-TR-78-231, pp. 1155 - 1158, 7 - 9 March 1978.

Muscari, J. A., and O'Donnell, T., Mass Loss Parameters for Typical Shuttle Materials, *Shuttle Optical Environment*, SPIE Vol. 287, No. 287-03, pp. 20 - 24, 23 - 24 April 1981.

O'Donnell, T., Taylor, D. M., and Barengoltz, J. B., New Screening Methodology to Select Low-Outgassing Materials for Cold, Spaceborne Optical Instruments, *Optical System Contamination: Effects, Measurement, Control II*, SPIE Vol. 1329, No. 1329-25, pp. 280 - 298, 10 - 12 July 1990.

Peterson, M. A., Evaluation of Free-Molecular Flow Passage Conductances with Thermal Radiation Analysis Software, *J. Spacecraft*, Vol. 23, No. 6, pp. 630 - 634, November - December, 1986.

Phillips, J. R., Fong, M. C., and Panczak, T. D., Monte Carlo Simulation of Contaminant Transport to and Deposition on Complex Spacecraft Surfaces, *Scatter from Optical Components*, SPIE Vol. 1165, No. 1165-32, pp. 370 - 380, 8 - 10 August 1989.

Poehlmann, H. C., Outgassing Tests of Fiber/Epoxy Composite Materials, *SAND78-7075*, February, 1979.

Rantanen, R. O., and Gordon, R. D., Contaminant Buildup on Ram Facing Spacecraft Surfaces, *Optical System Contamiantion: Effects, Measurment, Control*, SPIE Vol. 777, No. 777-04, pp. 26 - 33, 19 - 22 May 1987.

Salik, J., Computer Models of the Growth of Monolayers, *Optical System Contamiantion: Effects, Measurment, Control*, SPIE Vol. 777, No. 777-41, pp. 310 - 315, 19 - 22 May 1987.

Scherr, L. M., and Lee, W. W., Assessment of Condensable Molecular and Particulate Contamination upon Optical Elements in Space Systems, *Optical System Contamiantion: Effects, Measurment, Control*, SPIE Vol. 777, No. 777-11, pp. 127 - 137, 19 - 22 May 1987.

Scialdone, J. J., Abatement of Gaseous and Particulate Contamination in a Space Instrument, J. A. Roux and T. D. McKay, eds, Progress in Astronautics and Aeronautics, Vol. 91, AIAA, pp. 108 - 136, 1984.

Scialdone, J. J., An Estimate of the Outgassing of Space Payloads and its Gaseous Influence on the Environment, *J. Spacecraft*, Vol. 23, No. 4, pp. 373 - 378, July - August, 1986.

Scialdone, J. J., Characterization of the Outgassing of Spacecraft Materials, *Shuttle Optical Environment*, SPIE Vol. 287, No. 287-01, p. 34739, 23 - 24 April 1981.

Scialdone, J. J., Correlation of Self-Contamination Experiments in Orbit and Scattering Return Flux Calculations, *Proceedings of the USAF/NASA International Spacecraft Contamination Conference*, NASA CP-2049, AFML-TR-78-200, pp. 290 - 310, 7 - 9 March 1978.

Scialdone, J. J., Self-Contamination and Environment of an Orbiting Satellite, *J. Vac. Sci. Tech.*, Vol. 9, No. 2, pp. 1007 - 1015.

Scialdone, J., Time-Dependent Polar Distribution of Outgassing from a Spacecraft, *NASA TN D-7597*, April, 1974.

Scott, C., Material Selection for Cleanroom Compatibility, *Microcontamination*, p. 18, April, 1987.

Zeiner, E. A., A Multinodal Model for Surface Contamination Based Upon the Boltzmann Equation of Transport, *Proceedings of the USAF/NASA International Spacecraft Contamination Conference*, NASA CP-2040, AFML-TR-78-191, pp. 34 - 82, 7 - 9 March 1978.

Zeiner, E. A., Measurements of the Kinetics and Transport Properties of Contaminants Released from Polymeric Sources in Space and the Effects on Collecting Surfaces, *Proceedings of the USAF/NASA International Spacecraft Contamination Conference*, NASA CP-2074, AFML-TR-78-225, pp. 1006 - 1065, 7 - 9 March 1978.

5.3.1.2.2 Thrusters

Allegre, J., Raffin, M., and Lengrand, J. C., Experimental Study of the Plume Impingement Problem Associated with Rocket Stage Separation, *J. Spacecraft*, Vol. 23, No. 4, pp. 368 - 372, July - August, 1986.

Alred, J. W., Latest Version of Complete RCS Flowfield, *NASA Johnson Space Center*, ET4/8210-96, 22 October 1982.

Alt, R. E., Bipropellant Engine Plume Contamination Program, *Arnold Engineering Development Center*, AEDC-TR-79-28, Vol I, Chamber Measurements - Phase I, December, 1979.

Barsh, M. K., Jeffrey, J. A., Brestyanszky, P., and Adams, K. J., Contamination Mechanisms of Solid Rocket Motor Plumes, *Proceedings of the USAF/NASA International Spacecraft Contamination Conference*, NASA CP-2051, AFML-TR-78-202, pp. 347 - 384, 7 - 9 March 1978.

Boynton, F., Exhaust Plumes from Nozzles with Boundary Wall Layers, *J. Spacecraft*, Vol. 5, No. 10, pp. 1143 - 1147, October, 1968.

Brook, J. W., Far Field Approximation for a Nozzle Exhausting into a Vacuum, *J. Spacecraft*, Vol. 6, No. 5, pp. 626 - 628, May, 1969.

Carre, D. J., and Hall, D. F., Contamination Measurements During Operation of Hydrazine Thrusters on the P78-2 (SCATHA) Satellite, *J. Spacecraft*, Vol. 20, No. 5, pp. 444 - 449, Sept. - Oct., 1983.

Dettleff, G., Boettcher, R. D., Dankert, C., Koppenwallner, G., and Legge, H., Attitude Control Thruster Plume Flow Modeling and Experiments, *J. Spacecraft*, Vol. 23, No. 5, pp. 476 - 481, Sept. - Oct., 1986.

Etheridge, F. G., and Boudreaux, R. A., Attitude-Control Rocket Exhaust Plume Effects on Spacecraft Functional Surfaces, *J. Spacecraft*, Vol. 7, No. 1, pp. 44 - 48, January, 1970.

Fong, M. C., and Lee, A. L., BGK Method to Determine Thruster Plume Backscatter, *Optical System Contamination: Effects, Measurement, Control II*, SPIE Vol. 1329, pp. 318 - 326, 1990.

Fote, A. A., and Hall, D. F., Contamination Measurements during the Firing of the Solid Propellant Apogee Insertion Motor on the P78-2 (SCATHA) Spacecraft, *Shuttle Optical Environment*, SPIE Vol. 287, No. 287-11, pp. 95 - 101, 23 - 24 April 1981.

Furstenau, R. P., McCay, T. D., and Mann, D. M., U.S. Air Force Approach to Plume Contamination, *Optics in Adverse Environments*, SPIE Vol. 216, No. 216-07, pp. 62 - 70, 4 - 5 February 1980.

Girata, P. T., Jr., and McGregor, W. K., Postfire Sampling of Solid Rocket Motors for Contamination Sources in High-Altitude Test Cells, J. A. Roux and T. D. McKay, eds, Progress in Astronautics and Aeronautics, Vol. 91, AIAA, pp. 312 - 327, 1984.

Greenwald, G. F., Approximate Far-Field Flow Description for a Nozzle Exhausting into a Vacuum, *J. Spacecraft*, Vol. 7, No. 11, pp. 1374 - 1376, November, 1970.

Guernsey, C.S., and McGregor, R. D., Bipropellant Rocket Exhaust Plume Analysis on the Galileo Spacecraft, *AIAA 86-1488*, AIAA/ASME/ SAE 22nd Joint Propulsion Conference, Huntsville, AL, 16 - 18 June 1986.

Heinemann, M., Shuttle Contamination Modeling: Evolution of Ionized Shuttle Exhaust, *Air Force Geophysics Laboratory*, AFGL-TR-86-0023, 22 January 1986.

Hill, J. A. F., and Draper, J. S., Analytical Approximation for the Flow from a Nozzle into a Vacuum, *J. Spacecraft*, Vol. 3, No. 10, pp. 1552 - 1554, October, 1966.

Kinslow, M., and Stephenson, W. B., Bipropellant Engine Plume Contamination Program, *Arnold Engineering Development Center*, AEDC-TR-79-28, Vol III, Performance Predictions for the AJ10-181 Bipropellant Rocket Engine Using the CONTAM/TCC Code, September, 1979.

Kung, R. T. V., Cianciolo, L., and Myer, J. A., Solar Scattering from Condensation in Apollo Translunar Injection Plume, *AIAA Journal*, Vol. 13, No. 4, pp. 432 - 437, April, 1975.

Lawton, E. A., and Moran, C. M., Methylhydrazinium Nitrate, *J. Chem. Eng. Data*, Vol. 29, No. , pp. 357 - 358, 1983.

Leising, C. J., and Greenfield, M. L., Contamination and Heat Transfer Problems Resulting from High Expansion of the Subsonic Boundary Layer Flow in the Voyager TE-M-364-4 Solid Rocket Motor, *Proceedings of the USAF/NASA International Spacecraft Contamination Conference*, NASA CP-2052, AFML-TR-78-203, pp. 385 - 400, 7 - 9 March 1978.

Liu, C.-K., and Glassford, A. P. M., Contamination Effect of MMH/N2O4 Rocket Plume Product Deposit, *J. Spacecraft*, Vol. 18, No. 4, pp. 306 - 311, July - August, 1981.

Maag, C. R., Backflow Contamination from Solid Rocket Motors, *Proceedings of the USAF/NASA International Spacecraft Contamination Conference*, NASA CP-2050, AFML-TR-78-201, pp. 332 - 346, 7 - 9 March 1978.

Maag, C. R., Jeffrey, J. A., and Millard, J. M., Effect of Bipropellant Plume Exhaust Effects on Spaceborne Optical Instruments, *Optics in Adverse Environments*, SPIE Vol. 216, No. 216-08, pp. 71 - 79, 4 - 5 February 1980.

Martinkovic, P. J., Monopropellant Exhaust Contamination Investigation, *AFRPL-TR-69-72*, April, 1969.

McCay, T. D., Powell, H. M., and Busby, M. R., Direct Mass Spectrometric Measurements in a Highly Expanded Rocket Exhaust Plume, *J. Spacecraft*, Vol. 15, No. 3, pp. 133 - 138, May - June, 1978.

McCay, T. D., Weaver, D. P., Williams, W.D., Powell, H. M., and Lewis, J. W. L., Exhaust Plume Contaminants from an Aged Hydrazine Monopropellant Thruster, *Proceedings of the USAF/NASA International Spacecraft Contamination Conference*, NASA CP-2055, AFML-TR-78-206, pp. 456 - 517, 7 - 9 March 1978.

Millard, J. M., Hansen, P. A., Earth Observing System (EOS)/NOAA Candidate Propulsion System Assessment and Instrument Contamination Requirements, *Optical System Contamination: Effects, Measurement, Control*, SPIE Vol. 777, pp. 79 - 90, 1987.

Miller, J. L., and Drygen, E., Front Surface Optic Contamination From Small Rocket Plumes, *Stray Light and Contamination in Optical Systems*, SPIE Vol. 967, pp. 320 - 331, 1988.

Molinari, L. F., Design of a Propulsion System Test Facility to Study Rocket Plumes in the Space Environment, *Proceedings of the USAF/NASA International Spacecraft Contamination Conference*, NASA CP-2056, AFML-TR-78-207, pp. 518 - 532, 7 - 9 March 1978.

Passamaneck, R. S., and Chirivella, J. E., Small Monopropellant Thruster Contamination Measurement in a High-Vacuum Low-Temperature Facility, *J. Spacecraft*, Vol. 14, No. 7, pp. 419 - 426, July, 1977.

Piesik, E. T., Koppang, R. R., and Simkin, D. J., Rocket-Exhaust Impingement on a Flat Plate at High Vacuum, *J. Spacecraft*, Vol. 3, No. 11, pp. 1650 - 1657, November, 1966.

Powell, H. M., Price, L. L., and Alt, R. E., Bipropellant Engine Plume Contamination Program, *Arnold Engineering Development Center*, AEDC-TR-79-28, Vol II, Chamber Measurements - Phase I, November, 1979.

Ramirez, P., The Effect of Bipropellant Thruster Contaminant on Solar Array Performance, *SAE 841526*, Aerospace Congress and Exposition, Long Beach, CA, October, 1984.

Roux, J. A., and Wood, B. E., Infrared Optical Properties of Solid Monomethyl Hydrazine, N2O4, and N2H4 at Cryogenic Temperatures, *J. Opt. Soc. Am.*, Vol. 73, No. 9, pp. 1181 - 1188, September, 1983.

Roux, J. A., Wood, B. E., Smith, A. M., and Stechman, R. C., IR Optical Properties of Bipropellant Cryocontaminants, *Proceedings of the USAF/NASA International Spacecraft Contamination Conference*, NASA CP-2054, AFML-TR-78-205, pp. 412 - 455, 7 - 9 March 1978.

Schmidt, E. W., *Hydrazine and its Derivatives: Preparation, Properties, Applications*, John Wiley & Sons, New York, NY, 1984.

Scott, H. E., Frazine, and Lund, E. G., Bipropellant Engine Plume Study, *Proceedings of the USAF/NASA International Spacecraft Contamination Conference*, NASA CP-2063, AFML-TR-78-214, pp. 682 - 740, 7 - 9 March 1978.

Smith, S. D., Improvements in Rocket Engine Nozzle and High Altitude Plume Computations, J. A. Roux and T. D. McKay, eds, Progress in Astronautics and Aeronautics, Vol. 91, AIAA, pp. 197 - 214, 1984.

Stechman, R. C., Space Shuttle Plume Contamination, *Proceedings of the USAF/NASA International Spacecraft Contamination Conference*, NASA CP-2053, AFML-TR-78-204, pp. 401 - 411, 7 - 9 March 1978.

Takimoto, H. H., and Denault, G. C., Combustion Residues from N2O4-MMH Motors, *The Aerospace Corporation*, TR-0066 (5210-10) - 1, 15 September 1969.

Trinks, H., and Hoffman, R. J., Experimental Investigation of Bipropellant Exhaust Plume Flowfield, Heating, and Contamination and Comparison with the CONTAM Computer Model Predictions, J. A. Roux and T. D. McKay, eds, Progress in Astronautics and Aeronautics, Vol. 91, AIAA, pp. 261 - 292, 1984.

Wu, B. J. C., Possible Water Vapor Condensation in Rocket Exhaust Plumes, *AIAA Journal*, Vol. 13, No. 6, pp. 797 - 802, June, 1975.

Zlotskowski, J., Rocket Plume Contamination, *Proceedings of the USAF/NASA International Spacecraft Contamination Conference*, NASA CP-2082, AFML-TR-78-233, pp. 1162 - 1168, 7 - 9 March 1978.

5.3.1.2.3 Spacecraft Charging Enhancement

Chen, A. T., Shaw, C. G., and Mabe, J. H., Laboratory Study of Electrostatic Charging of Contaminated Ulysses Spacecraft Thermal Blankets, *Optical System Contamination: Effects, Measurement, Control II*, SPIE Vol. 1329, No. 1329-33, pp. 369 - 381, 10 - 12 July 1990.

Clark, D. M., and Hall, D. F., Flight Evidence of Spacecraft Surface Contamination Rate Enhancement by Spacecraft Charging Obtained with a Quartz Crystal Microbalance, *NASA CP-2182*, Spacecraft Charging Technology Conference 1980.

Garrett, H. B., Review of the Near-Earth Spacecraft Environment, *Optics in Adverse Environments*, SPIE Vol. 216, No. 216-13, pp. 109 - 115, 4 - 5 February 1980.

Hall, D. F., Flight Experiment to Measure Contamination Enhancement by Spacecraft Charging, *Optics in Adverse Environments*, SPIE Vol. 216, No. 216-15, pp. 131 - 138, 4 - 5 February 1980.

Hall, D. F., and Wakimoto, J. N., Further Flight Evidence of Spacecraft Surface Contamination Rate Enhancement by Spacecraft Charging, *AIAA 84-1703*, AIAA 19th Thermophysics Conference, Snowmass, CO, 25 - 28 June 1984.

Liemohn, H. B., Tingey, D. L., Stevens, G. G., Mahaffey, D. W., and Wilkinson, M. C., Charging and Contamination During Geosynchronous Orbit Insertion, *Optics in Adverse Environments*, SPIE Vol. 216, No. 216-09, pp. 80 - 86, 4 - 5 February 1980.

Stevens, N. J., and Purvis, C. K., NASCAP Modeling Computations on Large Optics Spacecraft in Geosynchronous Substorm Environments, *Optics in Adverse Environments*, SPIE Vol. 216, No. 216-14, pp. 116 - 130, 4 - 5 February 1980.

Stevens, N. J., Roche, J. C., and Mandell, M. J., NASA Charging Analyzer Program - A Computer Tool That Can Evaluate Electrostatic Contamination, *Proceedings of the USAF/NASA International Spacecraft Contamination Conference*, NASA CP-2048, AFML-TR-78-199, pp. 274 - 289, 7 - 9 March 1978.

5.3.1.2.4 Photochemical Deposition

Arnold, G. S., and Luey, K., Photochemically Deposited Contaminant Film Effects: Data Archive, Vol 2 - Appendices A through D., Aerospace Report No., TR-94 (4935)-13, 15 September 1994.

Arnold, G. S., Young Owl, R. C., and Hall, D. F., Optical Effects of Photochemically Deposited Contaminant Films, *Optical System Contamination: Effects, Measurement, Control II*, Vol. SPIE Vol. 1329, No. 1329-34, pp. 255 - 265, 10 - 12 July, 1990.

Hall, D. F., and Stewart, T. B., Photo-Enhanced Spacecraft Contamination Deposition, *AIAA 85-0953*, AIAA 20th Thermophysics Conference, Williamsburg, VA, 19 - 21 June 1985.

Judeikis, H. S., Arnold, G. S., Hill, M. W., Young Owl, R. C., and Hall, D. F., Design of a Laboratory Study of Contaminant Film Darkening in Space, *Scatter from Optical Components*, SPIE Vol. 1165, No. 1165-37, pp. 406 - 423, 8 - 10 August 1989.

Koontz, S., Leger, L., Albyn, K., and Cross, J., Vacuum Ultraviolet Radiation/Atomic Oxygen Synergism in Materials Reactivity, *J. Spacecraft*, Vol. 27, No. 3, pp. 346 - 348, May - June, 1990.

Stewart, T. B., Arnold, G. S., Hall, D. F., and Marten, H. D., Absolute Rates of Vacuum-Ultraviolet Photochemical Deposition of Organic Films, *J. Phys. Chem.*, Vol. 93, No. 6, pp. 2393 - 2400, , 1989.

Stewart, T. B., Arnold, G. S., Hall, D. F., Marvin, D. C., Hwang, W. C., Young Owl, R. C., and Marten, H. D., Photochemical Spacecraft Self-Contamination: Laboratory Results and Systems Impacts, *J. Spacecraft*, Vol. 26, No. 5, pp. 358 - 367, Sept. - Oct., 1989.

Tribble, A. C., and Haffner, J. W., Estimates of Photochemically Deposited Contamination on the GPS Satellites, *J. Spacecraft*, Vol. 28, No. 2, pp. 222 - 228, March - April. 1991.

5.3.1.3 Program Specific Documents

5.3.1.3.1 Shuttle

Ehlers, H. K. F., Jacobs, S., Leger, L. J., and Miller, E., Space Shuttle Contamination Measurements from Flights STS-1 Through STS-4, *J. Spacecraft*, Vol. 21, No. 3, pp. 301 - 308, May - June, 1984.

Miller, E. R., Shuttle Induced Environment Contamination Monitor, *Proceedings of the USAF/NASA International Spacecraft Contamination Conference*, NASA CP-2057, AFML-TR-78-208, pp. 534 - 566, 7 - 9 March 1978.

Miller, E. R., and Carignan, G. R., Mass Spectrometer, *Spacecraft Contamination Environment*, SPIE Vol. 338, pp. 34 - 38, 4 - 6 May 1982.

Von Zahn, U., and Wulf, E., The Gaseous Environment of the Shuttle, as Observed by Mass Spectrometer Inside the Payload Bay of the Shuttle Orbiter, *AIAA 85-6097*, AIAA Shuttle Environment and Operations II Conference, 13 - 15 November 1985.

5.3.1.3.2 Long Duration Exposure Facility

Blakkolb, B. K., Ryan, L. E., Bowen, H. S., and Kosic, T. J., Optical Characterization of LDEF Contaminant Film, *LDEF - 69 Months in Space*, Second Post-Retrieval Symposium, NASA CP-3196, pp. 1035 - 1040, 1 - 5 June 1992.

Borson, E. N., and Sinsheimer, F. B., Contamination Measurements on Experiment M0003, *LDEF - 69 Months in Space*, Second Post-Retrieval Symposium, NASA CP-3195, pp. 1033 - 1034, 1 - 5 June 1992.

Crutcher, E. R., and Warner, K. J., Molecular Films Associated with LDEF, *LDEF - 69 Months in Space*, First Post-Retrieval Symposium, NASA CP-3137, pp. 155 - 178, 2 - 8 June 1991.

Crutcher, E. R., Nishimura, L. S., Warner, K. J., and Wascher, W. W., Migration and Generation of Contaminants from Launch Through Recovery: LDEF Case History, *LDEF - 69 Months in Space*, First Post-Retrieval Symposium, NASA CP-3135, pp. 121 - 140, 2 - 8 June 1991.

Crutcher, E. R., Nishimura, L. S., Warner, K. J., and Wascher, W. W., Quantification of Contaminants Associated with LDEF, *LDEF - 69 Months in Space*, First Post-Retrieval Symp um, NASA CP-3136, pp. 141 - 154, 2 - 8 June 1991.

Harvey, G. A., Organic Contamination of LDEF, *LDEF - 69 Months in Space*, First Post-Retrieval Symposium, NASA CP-3138, pp. 179 - 198, 2 - 8 June 1991.

Pippin, G., and Crutcher, R., Contamination on LDEF: Sources, Distribution, and History, *LDEF - 69 Months in Space*, Second Post-Retrieval Symposium, NASA CP-3194, pp. 1023 - 1032, 1 - 5 June 1992.

Preuss, L., and Schaefer, W., Coating and Contamination Experiment on LDEF, *Spacecraft Materials in Space Environment*, ESA SP-146, pp. 71 - 80, 2 - 5 October 1979.

Stuckey, W. K., Radhakrishnan, G., and Wallace, D., Post-Flight Analyses of the Crystals from the M0003-14 Quartz Crystal Microbalance Experiment, *LDEF - 69 Months in Space*, Second Post-Retrieval Symposium, NASA CP-3197, pp. 1269 - 1284, 1 - 5 June 1992.

5.3.1.3.3 Other Programs

Arnold, G. S., Doi, J. A., and Sinsheimer, F. B., Estimates of Environmental Interactions of Contaminant Films from Titan IV Staging, *The Aerospace Corporation* TOR-93 (3409) -3, 15 April 1993.

Barengoltz, J. B., and Taylor, I ..., Analysis and Interpretation of Wide-Field Planetary Camera Outgas Data Collected in the Temperature Range -20 C to -100 C, *Optical System Contamination: Effects, Measurement, Control II*, SPIE Vol. 1329, No. 1329-05, pp. 48 - 71, 10 - 12 July 1990.

Facey, T. A., De Filippis, N. A., and Strecker, M. T., Moisture Loss from Graphite Structures for the Hubble Space Telescope, *AIAA 85-6057*, AIAA Shuttle Environment and Operations II Conference, 13 - 15 November 1985.

Haffner, J. W., Contamination Studies on the Teal Ruby Telescope, *AIAA 85-0952*, AIAA 20th Thermophysics Conference, Williamsburg, VA, 19 - 21 June 1985.

Hall, D. F., Current Flight Results from the P78-2 (SCATHA) Spacecraft Contamination and Coatings Degradation Experiment, *Proceedings of the ESA/CNES/CERT International Symposium*, Spacecraft Materials in Space Environment, Toulouse, France, June, 1982.

Hall, D. F., and Fote, A. A., Preliminary Flight Results from P78-2 (SCATHA) Spacecraft Contamination Experiment, *Spacecraft Materials in Space Environment*, ESA SP-147, pp. 81 - 90, 2 - 5 October 1979.

Marvin, D. C., and Hwang, W. C., Anomalous Degradation of Solar Array Performance on GPS Navstar Satellites, *The Aerospace Corporation*, TOR-0088 (3470-01) -1, 1 October 1988.

Mauldin, L. E., and Chu, W. P., Optical Degradation due to Contamination on the SAGE/SAGE II Spaceflight Instruments, SPIE Vol. 338, *Spacecraft Contamination Environment*, pp. 58 - 64, 1982.

Naumann, R. J., Skylab-Induced Environment, *Scientific Investigations of the Skylab Satellite*, M. I. Kent, E. Stuhlinger, and S.-T. Wu, eds., Vol. 48, Progress in Astronautics and Aeronautics, AIAA, pp. 383 - 395, 1975.

Pence, W., GPS Block II Spacecraft Degradation, *The Aerospace Corporation*, Proceedings of the Spacecraft Thermal Control Technology Workshop, Section 3.11, 3 - 5 February 1993.

5.3.1.4 Other Molecular

Facey, T. A., and Nonnenmacher, A. L., Measurement of Total Hemispherical Emissivity of Contaminated Mirror Surfaces, *Stray Light and Contamination in Optical Systems*, SPIE Vol. 967, No. 967-31, pp. 308 - 313, 17 - 19 August 1988.

Hass, G., Ramsey, J. B., Heaney, J. B., and Triolo, J. J., Thermal Emissivity and Solar Absorptivity of Aluminum Coated with Double Layers of Aluminum Oxide and Silicon Oxide, *Applied Optics*, Vol. 10, No. 6, pp. 1296 - 1298, June, 1971.

Holtzclsw, K. W., and Fraser, M. E., Infrared Emission from the Reaction of Orbital Velocity Atomic Oxygen with Hydrocarbon Materials, *Optical System Contamination: Effects, Measurement, Control II*, SPIE Vol. 1329, No. 1329-31, pp. 352 - 361, 10 - 12 July 1990.

Zhang, F. S., Wang, R. H., Macleod, H. A., Parks, R. E., and Jacobson, M. R., Surface Plasmon Detection of Surface Contamination of Metallic Film Surfaces, *Optical System Contamiantion: Effects, Measurment, Control*, SPIE Vol. 777, No. 777-16, pp. 162 - 170, 19 - 22 May 1987.

5.3.2 Particulate Contamination

5.3.2.1 Effects of Particulates

5.3.2.1.1 General

Adlon, G. L., Rusert, E. L., and Slemp, W. S., Effects of Simulated Mars Dust Erosion Environment on Thermal Control Coatings, *J. Spacecraft*, Vol. 7, No. 4, pp. 507 - 510, April, 1970.

Barengoltz, J. B., Calculating the Obscuration Ratio Due to Particle Surface Contamination, *NASA Tech Brief*, Vol. 13, No. 8, August, 1989.

Benninghoven, K. A., Effects of Particulate Contamination on Optical Solar Reflectors, *Optical System Contamiantion: Effects, Measurment, Control*, SPIE Vol. 777, No. 777-09, pp. 91 - 96, 19 - 22 May 1987.

Carey, W. F., Atmospheric Deposits in Britain: A Study of Dinginess, *Int. J. Air Poll.*, Vol. 2, p. 34,725, 1959.

Dowling, J. M., Hills, M. M., Arnold, G. S., and Kan, H. K. A., Contamination Effects on Surveillance Telescopes, *The Aerospace Corporation*, TR-93 (3935) -14, 22 October 1993.

Dyhouse, G. R., Martian Sand and Dust Storms and Effects on Spacecraft Coatings, *J. Spacecraft*, Vol. 5, No. 4, pp. 473 - 475, April, 1968.

Kelley, J. G., Measurement of Particle Contamination, *J. Spacecraft*, Vol. 23, No. 6, pp. 641 - 645, November - December, 1986.

Raab, J. H., Particulate Contamination Effects on Solar Cell Performance, *Martin Marietta*, MCR-86-2005, January, 1986.

Raab, J. H., Particulate Contamination Effects on Solar Cell Performance, *Martin Marietta*, MCR-86-2015, Rev. A, January, 1987.

Saylor, W. P., and Hanichak, M. C., Contamination Effects on Optical Surfaces, *Scatter from Optical Components*, SPIE Vol. 1165, No. 1165-27, pp. 324 - 341, 8 - 10 August 1989.

5.3.2.1.2 Scattering

Bamberg, J. A., and Mount, J., Scattering from Mirror Surfaces, *Ball Brothers Research Corp.*, TR74-04, June, 1974.

Bartell, F. O., Hubbs, J. E., Nofziger, M. J., and Wolfe, W. L., Measurements of Martin Black at ~ 10 Microns, *Applied Optics*, Vol. 21, No. 17, pp. 3178 - 3180, September, 1982.

Bennett, H. E., Specular Reflectance of Aluminized Ground Glass and the Height Distribution of Surface Irregularities, *J. Opt. Soc. Am.*., Vol. 53, No. 12, pp. 1389 - 1402, December, 1963.

Bennett, H. E., and Porteus, J. O., Relation Between Surface Roughness and Specular Reflectance at Normal Incidence, *J. Opt. Soc. Am.*., Vol. 51, No. 2, pp. 123 - 129, February, 1961.

Bennett, J. M., Measurement of the RMS Roughness, Autocovariance Function and Other Statistical Properties of Optical Surfaces using a FECO Scanning Interferometer, *Applied Optics*, Vol. 15, No. 11, pp. 2705 - 2720, November, 1976.

Bousquet, P., Flory, F., and Roche, P., Scattering from MultilayerThin Films: Theory and Experiment, *J. Opt. Soc. Am.*., Vol. 71, No. 9, pp. 1115 - 1123, September, 1981.

Breault, R. P., Stray Light Technology Overview in 1988, *Stray Light Contamination in Optical Systems*, SPIE Vol. 967, pp. 34739, 1988.

Breult, R. P., Scatter Characteristics of Surfaces, *SPIE's 1987 Technical Symposium Southeast on Optics, Electro-Optics, and Sensors*, Tutorial T3, Orlando, FL, 18-May, 1987.

Church, E. L., and Zavada, J. M., Residual Surface Roughness of Diamond-Turned Optics, *Applied Optics*, Vol. 14, No. 8, pp. 1788 - 1795, August, 1975.

Church, E. L., Jenkinson, H. A., and Zavada, J. M., Measurement of the Finish of Diamond-Turned Metal Surfaces by Differential Light Scattering, *Optical Engineering*, Vol. 16, No. 4, pp. 360 - 374, July - August, 1977.

Elson, J. M., and Bennett, J. M., Relation Between the Angular Dependence of Scattering and the Statistical Properties of Optical Surfaces, *J. Opt. Soc. Am.*., Vol. 69, No. 1, pp. 31 - 47, January, 1979.

Elson, J. M., and Ritchie, R. H., Diffuse Scattering and Surface-Plasmon Generation by Photons at a Rough Dielectric Surface, *Phys. Stat. Sol.*, Vol. 62, pp. 461 - 475, 1974.

Elson, J. M., Rahn, J. P., and Bennett, J. M., Light Scattering from Multilayer Optics: Comparison of Theory and Experiment, *Applied Optics*, Vol. 19, No. 5, pp. 669 - 679, 1 March 1980.

Elson, J. M., Rahn, J. P., and Bennett, J. M., Relationship of the Total Integrated Scattering from Multilayer-Coated Optics to Angle of Incidence, Polarization, Correlation Length, and Roughness Cross-Correlation Properties, *Applied Optics*, Vol. 22, No. 20, pp. 3207 - 3219, 15 October 1983.

Greynolds, A. W., Consistent Theory of Scatter from Optical Surfaces, *Stray Light and Contamination in Optical Systems*, SPIE Vol. 967, No. 967-02, pp. 34990, 17 - 19 August 1988.

Guregian, J. J., Benoit, R. T., and Wong, W. K., Overview of Contamination Effects on the Performance of High-Straylight-Rejection Telescopes via Ground Measurements, *Optical System Contamination: Effects, Measurement, Control II*, SPIE Vol. 1329, No. 1329-01, pp. 2 - 15, 10 - 12 July 1990.

Harvey, J. E., Light Scattering Characterization of Optical Surfaces, *University of Arizona*, Ph.D. Dissertation, 1976.

Jarossy, F. J., and Mason, L. W., An Analytical Technique for Predicting the Effect of Particulate Contamination on Direct Scatter in an Optical Sensor, *Stray Radiation*, SPIE Vol. 675, pp. 160 - 166, 1986.

Johnson, B. R., "Light Scattering from a Spherical Particle on a Conducting Plane: I Normal Incidence," *J. Opt. Soc. Am.*, Vol. A9, pp. 1341 - 1351, (1992).

Johnson, B. R., "Exact Calculation of Light Scattering from a Particle on a Mirror," SPIE Vol. 1754, *Optical System Contamination*, pp. 72 - 83, (1992).

Johnson, B. R., "Light Diffraction by Particles on a Surface," Aerospace Report No. ATR-95 (9558)-4, 15 November 1995.

Johnson, B. R., and Arnold, G. S., "Radiation Scattering from Particlulate-Contaminated Mirrors," Aerospace Report No. ATR-94 (7281)-1, 1 March 1994.

Lange, S. R., Breault, R. P., and Greynolds, A. W., APART, A First-Order Deterministic Stray Radiation Analysis Program, *Stray Light Problems in Optical Syst*. , SPIE Vol. 107, No. 107-11, pp. 89 - 97, 18 - 21 April 1977.

Leader, J. C., Analysis and Prediction of Laser Scattering from Rough-Surface Materials, *J. Opt. Soc. Am.*, Vol. 69, No. 4, pp. 610 - 617, April, 1979.

Magee, K. A., and Wolfe, W. L., Near-Specular Performance of a Portable Scatterometer, *Stray Radiation V*, SPIE Vol. 675, pp. 249, 1986.

Masser, C. S., Means of Eliminating the Effects of Particulate Contamination on Scatter Measurements of Superfine Optical Surfaces, *Scatter from Optical Components*, SPIE Vol. 1165, No. 1165-28, pp. 342 - 349, 8 - 10 August 1989.

Nahm, K. B., Spyak, P. R., and Wolfe, W. L., Scattering from Contaminated Surfaces, *Scatter from Optical Components*, SPIE Vol. 1165, No. 1165-24, pp. 294 - 305, 8 - 10 August 1989.

Nahm, K. B., Spyak, P. R., and Wolfe, W. L., Use of a Simplified Model for Particulate Scatter, *Scatter from Optical Components*, SPIE Vol. 1165, No. 1165-25, pp. 306 - 313, 8 - 10 August 1989.

Pezzaniti, J. L., Hadaway, J. B., Chipman, R. A., Wilkes, D. R., Hummer, L., and Bennett, J. M., Total Integrated Scatter Instruments for In-Space Monitoring of Surface Degradation, *Optical System Contamination: Effects, Measurement, Control II*, SPIE Vol. 1329, No. 1329-17, pp. 200 - 210, 10 - 12 July 1990.

Porteus, J. O., Relation Between the Height Distribution of a Rough Surface and the Reflectance at Normal Incidence, *J. Opt. Soc. Am.*, Vol. 53, No. 12, pp. 1394 - 1402, December, 1963.

Rock, D. F., Radiation Transfer via Reflection from Nonimaging Specular Surfaces, *Radiation Scattering in Optical Systems*, SPIE Vol. 257, pp. 104, 1980.

Schade, H., and Smith, Z. E., Mie Scattering and Rough Surfaces, *Applied Optics*, Vol. 24, No. 19, pp. 3221 - 3226, October, 1985.

Schroeder, M. J., Musinski, D. J., Hull-Allen, C. G., Van Milligen, F. J., Bidirectional Reflectance Distribution Function Measurements on Multilayer Dielectric Coatings as a Function of Polarization State, *Scatter from Optical Components*, SPIE Vol. 1165, No. 1165-22, pp. 270 - 282, 8 - 10 August 1989.

Silva, R. M., Orazio, F. D., Jr., and Stowell, W. K., Scatter Evaluation of Supersmooth Surfaces, *Scattering in Optical Materials*, SPIE Vol. 362, No. 362-13, pp. 71 - 76, 25 - 27 August 1982.

Smith, S. M., Specular Reflectance of Optical-Black Coatings in the Far Infrared, *Applied Optics*, Vol. 23, No. 14, pp. 2311 - 2326, July, 1984.

Spyak, P. R., and Wolfe, W. L., Scatter from Particulate-Contaminated Mirrors. Part 1: Theory and Experiment for Polystrene Spheres and Lambda = 0.6328 Microns, *Optical Engineering*, Vol. 31, No. 8, pp. 1746 - 1756, August, 1992.

Spyak, P. R., and Wolfe, W. L., Scatter from Particulate-Contaminated Mirrors. Part 2: Theory and Experiment for Dust and λ = 0.6328 Microns, , Vol. 31, No. 8, pp. 1757 - 1763, August, 1992.

Spyak, P. R., and Wolfe, W. L., Scatter from Particulate-Contaminated Mirrors. Part 3: Theory and Experiment for Dust and λ = 10.6 Microns, , Vol. 31, No. 8, pp. 1764 - 1774, August, 1992.

Spyak, P. R., and Wolfe, W. L., Scatter from Particulate-Contaminated Mirrors. Part 4: Properties of Scatter from Dust for Visible to Far-Infrared Wavelengths, , Vol. 31, No. 8, pp. 1775 - 1784, August, 1992.

Spyak, P. R., and Wolfe, W., Cryogenic Scattering Measurements, *Stray Light and Contamination in Optical Systems*, SPIE Vol. 967, No. 967-15, pp. 144 - 158, 17 - 19 August 1988.

Stover, J. C., Roughness Characterization of Smooth Machined Surfaces by Light Scattering, *Applied Optics*, Vol. 14, No. 8, pp. 1796 - 1802, August, 1975.

Stover, J. C., Scatter from Optical Components: An Overview, *Scatter from Optical Components*, SPIE Vol. 1165, No. 1165-01, pp. 34739, 8 - 10 August 1989.

Stover, J., Advanced Techniques for Measurement and Interpretation of Optical Scatter, *SPIE Tutorial T5*, SPIE's 1987 Technical Symposium Southeast on Optics, Electro-Optics, and Sensors, Orlando, FL, 21 May 1987.

Sullivan, R. C., Patel, R. b., and Murray, B. W., Thermal Cycling Effects on the BRDF of Beryllium Mirrors, *Scatter from Optical Components*, SPIE Vol. 1165, No. 1165-20, pp. 246 - 259, 8 - 10 August 1989.

Thomas, D. A., Light Scattering from Reflecting Optical Surfaces, *Ph.D. Dissertation*, The University of Arizona, 1980.

Warren, A. D., Simplified Techniques for Estimating Out-of-Field Radiation, *Radiation Scattering in Optical Systems*, SPIE Vol. 257, p. 34990, 1980.

Young, R. P., Sr., Mirror-Scatter Degradation by Particulate Contamination, *Optical System Contamination: Effects, Measurement, Control II*, SPIE Vol. 1329, No. 1329-21, pp. 246 - 254, 10 - 12 July 1990.

5.3.2.1.3 BRDF

Arnold, C. B., and Beard, J. L., ERIM Perspective on BRDF Measurement Technology, *Scatter from Optical Components*, SPIE Vol. 1165, No. 1165-09, pp. 112 - 135, 8 - 10 August 1989.

Asmail, C. C., Cleanliness Requirements for the Air in a BRDF Facility, *Scatter from Optical Components*, SPIE Vol. 1165, No. 1165-31, pp. 360 - 369, 8 - 10 August 1989.

Barnes, P. Y., and Hsia, J. J., 45 deg./0 deg. Bidirectional Reflectance Distribution Function Standard Development, *Scatter from Optical Components*, SPIE Vol. 1165, No. 1165-14, pp. 165 - 174, 8 - 10 August 1989.

Bartell, F. O., Dereniak, E. L., and Wolfe, W. L., The Theory and Measurement of Bidirectional Reflectance Distribution Function (BRDF) and Bidirectional Transmittance Distribution Function (BTDF), *Radiation Scattering in Optical Systems*, SPIE Vol. 257, pp. 154 - 160, 1980.

Bartell, F. O., Dereniak, E. L., and Wolfe, W. L., The Theory and Measurement of Bidirectional Reflectance Distribution Function (BRDF) and Bidrectional Transmittance Distribution Function (BTDF), *Radiation Scattering in Optical Systems*, SPIE Vol. 257, pp. 154 - 160, 1980.

Breault, R. P., Lange, S. R., and Fannin, B. B., Cleaning, Coating and Bidirectional Reflectance Distribution Function (BRDF) Measurements of a Two-Meter Low-Scatter Mirror, *SPIE Vol. 216*, Optics in Adverse Environments, pp. 9 - 23, 4 - 5 February 1980.

Breault, R. P., Lange, S. R., and Fannin, W. B., Cleaning, Coating and Bidirectional Reflection Distribution Function (BRDF) Measurements of a Two-Meter Low-Scatter Mirror, *Optics in Adverse Environments*, SPIE Vol. 216, No. 216-30, pp. 34965, 4 - 5 February 1980.

Cady, F. M., Bjork, D. R., Rifkin, J., and Stover, J. C., BRDF Error Analysis, *Scatter from Optical Components*, SPIE Vol. 1165, No. 1165-13, pp. 154 - 164, 8 - 10 August 1989.

Carosso, P. A., and Pugel Carosso, N. J., Role of Scattering Distribution Functions in Spacecraft Contamination Control Practices, *Applied Optics*, Vol. 25, No. 7, pp. 1230 - 1234, 1 April 1986.

Chen, P. T., and Hedgeland, R. J., Cleanliness Correlation by BRDF and PFO Instruments, *Scatter from Optical Components*, SPIE Vol. 1165, No. 1165-26, pp. 314 - 323, 8 - 10 August 1989.

Church, E. L., Takacs, P. Z [illegible]d Leonard, T. A., Prediction of BRDFs from Surface Profile Measurements, *Scatter from Optical Components*, SPIE Vo[illegible]65, No. 1165-10, pp. 136 - 150, 8 - 10 August 1989.

Fernandez, R., Seasholtz, R. G., Oberle, L. G., and Kadambi, J. R., Comparison of the Bidirectional Reflectance Distribution Function of Various Surfaces, *Stray Light and Contamination in Optical Systems*, SPIE Vol. 967, No. 967-29, pp. 292 - 307, 17 - 19 August 1988.

Heinisch, R. P., Infrared Mirror-Scatter Measurements, *J. Opt. Soc. Amer.*, Vol. 61, No. 9, pp. 1225 - 1229, September, 1971.

Howard, T. L., George, P. M., and Fisher, R. F., BRDF Measurements for Contamination Assessment in a Spacecraft Environment, *Optical System Contamination: Effects, Measurement, Control II*, SPIE Vol. 1329, No. 1329-24, pp. 266 - 279, 10 - 12 July 1990.

Howard, T. L., George, P. M., Flammang, S. M., and Mossman, D. L., Vacuum BRDF Measurments of Cryogenic Optical Surfaces, *Scatter from Optical Components*, SPIE Vol. 1165, No. 1165-29, pp. 350 - 359, 8 - 10 August 1989.

Leonard, T. A., and Pantoliano, M., BRDF Round Robin, *Stray Light and Contamination in Optical Systems*, SPIE Vol. 967, pp. 226 - 235, 1988.

Leonard, T. A., Pantoliano, M. A., and Reilly, J., Results of a CO2 BRDF Round Robin, *Scatter from Optical Components*, SPIE Vol. 1165, No. 1165-12, pp. 153, 8 - 10 August 1989.

Ma, P. T., Fong, M. C., and Lee, A. L., Surface Particle Obscuration and BRDF Predictions, *Scatter from Optical Components*, SPIE Vol. 1165, pp. 381 - 391, 1989.

Mastandrea, A. A., Sensor Contamination Degradation Experiment with a Cryogenic in-situ BRDF Monitor, *Optical System Contamination: Effects, Measurment, Control*, SPIE Vol. 777, No. 777-44, pp. 316 - 319, 19 - 22 May 1987.

Nicodemus, F. E., Directional Reflectance and Emissivity of an Opaque Surface, *Applied Optics*, Vol. 4, No. 7, pp. 767 - 773, July, 1965.

Nicodemus, F. E., Reflectance Nomenclature and Directional Reflectance and Emissivity, *Applied Optics*, Vol. 9, No. 6, pp. 1474 - 1475, June, 1970.

Pompea, S. M., Shepard, D. F., and Anderson, S., BRDF Measurements at 6328 Angstroms and 10.6 Microns of Optical Black Surfaces for Telescopes, *Stray Light and Contamination in Optical Systems*, SPIE Vol. 967, No. 967-23, pp. 236 - 247, 17 - 19 August 1988.

Scherr, L. M., Schmidt, J. H., and Sorensen, K., BRDF of Silicon Carbide and Aluminum Foam Compared to Black Paint at 3.39 Microns, *Scatter from Optical Components*, SPIE Vol. 1165, No. 1165-16, pp. 204 - 211, 8 - 10 August 1989.

Seiber, B. L., Bryson, R. J., Bertrand, W. T., and Wood, B. E., Cryogenic BRDF Measurements at 10.6 Microns and 0.63 Microns on Contaminated Mirrors, *Arnold Engineering Development Center*, AEDC-TR-94-16, February, 1995.

Shepard, D. F., Pompea, S. M., and Anderson, S., Effect of Elevated Temperatures on the Scattering Properties of an Optical Black Surface at 0.6328 and 10.6 Micrometers, *Stray Light and Contamination in Optical Systems*, SPIE Vol. 967, No. 967-28, pp. 286 - 291, 17 - 19 August 1988.

Smith, S. M., Far-Infrared (FIR) Opt[illegible] Black Bidirectional Reflectance Distribution Function (BRDF), *Radiation Scattering in Optical Systems*, SPIE Vol. 257, 1980.

Smith, S. M., and Wolfe, W. L., Comparison of Measurements by Different Instruments of the Far-Infrared Reflectance of Rough, Optically Black Coatings, SPIE Vol. 362, pp. 46 - 53, 1982.

Smith, T. F., and Hering, R. G., Surface Roughness Effects on Bidirectional Reflectance, *AIAA 73-152*, AIAA 11th Aerospace Sciences Meeting, Washington, DC, 10 - 12 January 1973.

Smith, T. F., Suiter, R. L., and Kanayama, K., Bidirectional Reflectance Measurements for One-Dimensional, Randomly Rough Surfaces, *AIAA 79-1036*, AIAA 14th Thermophysics Conference, Orlando, FL, 4 - 6 June 1979.

Somers, R., and Muscari, J. A., Effects of Contamination on Bidirectional Reflectance Distribution Function, *Spacecraft Contamination Environment*, SPIE Vol. 338, No. 338-07, pp. 72 - 79, 4 - 6 May 1982.

Somers, R., and Muscari, J. A., Effects of Contamination on Bidrectional Reflectance Distribution Function, *SPIE Vol. 338*, Spacecraft Contamination Environment, pp. 72 - 79, 4 - 6 May 1982.

Spyak, P. R., and Wolfe, W. L., Scatter from Particulate-Contaminated Mirrors. Part 1: Theory and Experiment for Polystyrene Spheres and λ = 0.06328 microns, *Optical Eng.*, Vol. 31, No. 8, pp. 1746 - 1756, August, 1992.

Spyak, P. R., and Wolfe, W. L., Scatter from Particulate-Contaminated Mirrors. Part 2: Theory and Experiment for Dust and λ = 0.6328 microns, *Optical Eng.*, Vol. 31, No. 8, pp. 1757 - 1763, August, 1992.

Spyak, P. R., and Wolfe, W. L., Scatter from Particulate-Contaminated Mirrors. Part 3: Theory and Experiment for Dust and λ = 10.6 microns, *Optical Eng.*, Vol. 31, No. 8, pp. 1764 -1774, August, 1992.

Spyak, P. R., and Wolfe, W. L., Scatter from Particulate-Contaminated Mirrors. Part 4: Properties of Scatter from Dust for Visible and Far-Infrared Wavelengths, *Optical Eng.*, Vol. 31, No. 8, pp. 1775 - 1784, August, 1992.

Stover, J. C., Rifkin, J., Cheever, D. R., Kirchner, K. H., and Schiff, T. F., Comparison of Wavelength Scaling Data to Experiment, *Stray Light and Contamination in Optical Systems*, SPIE Vol. 967, No. 967-05, pp. 44 - 49, 17 - 19 August 1988.

Sullivan, R. C., Murray, B. W., Henion, S. R., and Stribley, G. T., BRDF Measurement Apparatus for Cryogenically Cooled Samples, *Stray Light and Contamination in Optical Systems*, SPIE Vol. 967, No. 967-14, pp. 138 - 143, 17 - 19 August 1988.

Wang, Y., More on Scattering from Dirty Mirrors, *NASA Tech Briefs*, Vol. 13, No. 11, November, 1989.

Wang, Y., Scattering from Mirrors Contaminated by Particulates: A Model, *Applied Optics*, Vol. 25, No. 23, pp. 4222 - 4223, December, 1986.

Williams, V. L., and Lockie, R. T., Optical Contamination Assessment by Bidirectional Reflectance Distribution Function (BRDF) Measurement, *Optical Engineering*, Vol. 18, No. 2, pp. 152 - 156, March - April, 1979.

Wolfe, W. L., and Wang, Y.-J., Comparison of Theory and Experiments for Bidirectional Reflectance Distribution Function (BRDF) of Microrough Surfaces, *Scattering in Optical Materials*, SPIE Vol. 362, No. 362-08, pp. 40 - 45, 25 - 27 August 1982.

Young, R. P., Low-Scatter Mirror Degradation by Particulate Contamination, *Optical Eng.*, Vol. 15, No. 6, pp. 516 - 520, November - December, 1976.

5.3.2.2 Optical Baffle Materials

Birnbaum, M. M., Metzler, E.C., and Cleland, E. L., Electrically Conductive Black Optical Paint, *Scattering in Optical Materials*, SPIE Vol. 362, No. 362-12, pp. 60 - 69, 25 - 27 August 1982.

Booker, R. L., Specular UV Reflectance Measurements for Cavity Radiometer Design, *Applied Optics*, Vol. 21, No. 1, pp. 153 - 157, January, 1982.

Bradford, A. P., Hass, G., Heaney, J. B., and Triolo, J. J., Solar Absorptivity and Thermal Emissivity of Aluminum Coated with Silicon Oxide Films Prepared by Evaporation of Silicon Monoxide, *Applied Optics*, Vol. 9, No. 2, pp. 339 - 344, February, 1970.

Dawbarn, R., Aluminum Oxide Particles Produced by Solid Rocket Motors, *Proceedings of the USAF/NASA International Spacecraft Contamination Conference*, NASA CP-2067, AFML-TR-78-218, pp. 809 - 845, 7 - 9 March 1978.

Henion, S. R., Johnson, E. A., and Johnson, J. A., Particulate Debris from Pulsed Electron Bombardment of Optical Baffle Materials, *Stray Light and Contamination in Optical Systems*, SPIE Vol. 967, No. 967-32, pp. 314 - 319, 17 - 19 August 1988.

Houck, J. R., New Black Paint for Cryogenic Infrared Applications, *Scattering in Optical Materials*, SPIE Vol. 362, No. 362-11, pp. 54 - 56, 25 - 27 August 1982.

Krewinghaus, A. B., Infrared Reflectance of Paints, *Applied Optics*, Vol. 8, No. 4, pp. 807 - 812, April, 1969.

Lompado, A., Murray, B. W., Wollam, J. S., and Meroth, J. F., Characterization of Optical Baffle Materials, *Scatter from Optical Components*, SPIE Vol. 1165, No. 1165-17, pp. 212 - 226, 8 - 10 August 1989.

O'Donnell, T., Evaluation of Spacecraft Materials and Processes for Optical Degradation Potential, *Spacecraft Contamination Environment*, SPIE Vol. 338, No. 338-06, pp. 65 - 71, 4 - 6 May 1982.

Smith, S. M., F- ·frared Reflectance Spectra of Optical Black Coatings, *Scattering in Optical Materials*, SPIE Vol. 362, No. 362-10, pp. 57 - 59, ' August 1982.

Smith, S. M., I ctance of Ames 24E, Infrablack, and Martin Black, *Stray Light and Contamination in Optical Systems*, SPIE Vol. 967, No. 967-24, pp. 248 - 254 17 - 19 August 1988.

Smith, S. M., Specular Reflectance of Optical-Black Coatings in the far Infrared, *Applied Optics*, Vol. 23, No. 14, pp. 2311 - 2326, July, 1984.

Smith, S. M., and Wolfe, W. L., Comparison of Measurements by Different Instruments of the Far-Infrared Reflectance of Rough, Optically Black Coatings, *Scattering in Optical Materials*, SPIE Vol. 362, No. 362-09, pp. 46 - 53, 25 - 27 August 1982.

Stierwalt, D. L., Infrared Spectral Emittance Measurements of Optical Materials, *Applied Optics*, Vol. 5, No. 12, pp. 1911 - 1915. December, 1966.

Stierwalt, D. L., Infrared Absorption of Optical Blacks, *Optical Engineering*, Vol. 18, No. 2, pp. 147 - 151, March - April, 1979.

5.3.2.3 Program Specific Documents

5.3.2.3.1 Shuttle

Clifton, K. S., Camera/Photometer Results, *Spacecraft Contamination Environment*, SPIE Vol. 338, pp. 30 - 33, 4 - 6 May 1982.

Duncan, B. J., Induced Environment Contamination Monitor (IECM) Cascade Impactor, *Spacecraft Contamination Environment*, SPIE Vol. 338, pp. 10 - 15, 4 - 6 May 1982.

Green, B. D ''ates, G. K., Ahmadjian, M., and Miranda, H., Particle Environment Around the Shuttle as Determined by the Particle Analy: amera for Shuttle (PACS) Experiment, *Optical System Contamiantion: Effects, Measurment, Control*, SPIE Vol. 777, No. 777-01, pp. 34741, 19 - 22 May 1987.

Peters, P. N., Hester, H. B., Bertsch, W., Mayfield, H., and Zatko, D., Induced Environment Contamination Monitor (IECM), Air Sampler: Results from the Space Transportation System (STS-2) Flight, *Spacecraft Contamination Environment*, SPIE Vol. 338, No. , pp. 5 - 9, 4 - 6 May 1982.

Pugel, N., Analysis of Prelaunch Particulate Contamination, *Spacecraft Contamination Environment*, SPIE Vol. 338, No. 338-03, pp. 49 - 56, 4 - 6 May 1982.

Schuerman, D. W., and Giovane, F., Coronagraph: The Ultimate Device to Monitor Orbiting Particulates in the Space Transport System TS) Environment, *Spacecraft Contamination Environment*, SPIE Vol. 338, No. 338-15, pp. 114 - 119, 4 - 6 May 1982.

Scialdone, J. J., Particulate Contaminant Relocation During Shuttle Ascent, *Optical System Contamiantion: Effects, Measurment, Control*, SPIE Vol. 777, No. 777-07, pp. 55 - 66, 19 - 22 May 1987.

Simpson, J. P., and Wittebon, F. C., Effect of the Shuttle Contaminant Environment on a Sensitive Infrared Telescope, *Applied Optics*, Vol. 16, No. 8, pp. 2051 - 2073, August, 1977.

5.3.2.3.2 Other Programs

Bush, J., and Aguilar, L., Particulate Redistribution Experiments for the Hubble Space Telescope, *Optical System Contamiantion: Effects, Measurment, Control*, SPIE Vol. 777, No. 777-26, pp. 226 - 235, 19 - 22 May 1987.

Crutcher, E. R., and Wascher, W. W., Particle Types and Sources Associated with LDEF, *LDEF - 69 Months in Space*, First Post-Retrieval Symposiu NASA CP-3134, pp. 121 - 140, 2 - 8 June 1991.

Darnton, L. A., Champetier, R. J., Blanco, J. R., and Garcia, K. J., Ultrasensitive Dust Monitor for the Advanced X-Ray Astrophysics Facility, *Optical System Contamination: Effects, Measurement, Control II*, SPIE Vol. 1329, No. 1329-19, pp. 221 - 232, 10 - 12 July 1990.

Facey, T. A., A Study of Surface Particulate Contamination on the Primary Mirror of the Hubble Space Telescope, *Measurement and Effects of Surface Defects and Quality of Polish*, SPIE Vol. 525, pp. 140 - 146, 1985.

Facey, T. A., Particulate Contamination Control in the Optical Telescope Assembly for the Hubble Space Telescope, *Optical System Contamiantion: Effects, Measurment, Control*, SPIE Vol. 777, No. 777-23, pp. 200 - 202, 19 - 22 May 1987.

Metheney, W., Pope, T., Rosenberg, W., and Sharbaugh, R., Hubble Space Telescope Particulate Optical Test, *Optical System Contamiantion: Effects, Measurment, Control*, SPIE Vol. 777, No. 777-31, pp. 271 - 277, 19 - 22 May 1987.

St. Clair Dinger, A., Stray Light Analysis of an Aperture Shade Off-Set from the SIRTF Optical Axis, *Stray Light and Contamination in Optical Systems*, SPIE Vol. 967, No. 967-09, pp. 64 - 71, 17 - 19 August 1988.

5.3.2.4 Other Particulate

Bareiss, L. E., and Jarossey, F. J., Impact of the STS Ground/Launch Particle Contamination Environment on an Optical Sensor, J. A. Roux and T. D. McKay, eds, Progress in Astronautics and Aeronautics, Vol. 91, AIAA, pp. 73 - 95, 1984.

Buch, J. D., and Barsh, M. K., Analysis of Particulate Contamination Buildup on Surfaces, *Optical System Contamiantion: Effects, Measurment, Control*, SPIE Vol. 777, No. 777-06, pp. 43 - 54, 19 - 22 May 1987.

Curry, B. P., Lewis, J. W. L., Jones, J. H., and Powell, H. M., The Time- and Space-Dependence of Particulate Effluent in the Exhaust Plume of a Pulsed Liquid Bipropellant Engine, *Arnold Engineering Development Center*, AEDC-TR-80-44, 1980.

del Casal, E. P., Debris from Spallation of Foam Insulation of Cryogenic Fuel Tanks in Space Launch Systems, *Spacecraft Contamination: Sources and Prevention*, J. A. Roux and T. D. McCay, eds, Progress in Astronautics and Aeronautics, Vol. 91, AIAA, pp. 39 - 53, 1984.

Girata, P. T., Jr., and McGregor, W. K., Particle Sampling of Solid Rocket Motor Exhausts in High-Altitude Test Cells, J. A. Roux and T. D. McKay, eds, Progress in Astronautics and Aeronautics, Vol. 91, AIAA, pp. 293 - 311, 1984.

Klavins, A., and Lee, A. L., Spacecraft Particulate Contaminant Redistribution, *Optical System Contamiantion: Effects, Measurment, Control*, SPIE Vol. 777, No. 777-27, pp. 236 - 245, 19 - 22 May 1987.

Konopka, W. L., Reed, R. A., and Calia, V. S., Measurements of Infrared Optical Properties of Al2O3 Rocket Particles, J. A. Roux and T. D. McKay, eds, Progress in Astronautics and Aeronautics, Vol. 91, AIAA, pp. 180 - 196, 1984.

Lee, A. L., Particle Dispersion Around a Spacecraft, *Spacecraft Contamination: Sources and Prevention*, J. A. Roux and T. D. McKay, eds, Progress in Astronautics and Aeronautics, Vol. 91, AIAA, pp. 54 - 72, 1984.

Peters, P. J., A Status of the Stray Light Contamination Problem, *Optics in Adverse Environments*, SPIE Vol. 216, No. 216-11, pp. 95 - 101, 4 - 5 February 1980.

Yadlowsky, E. J., Hazelton, R. C., and Churchill, R. J., Puncture Discharges in Surface Dielectrics as Contaminant Sources in Spacecraft Environments, *Proceedings of the USAF/NASA International Spacecraft Contamination Conference*, NASA CP-2072, AFML-TR-78-223, pp. 945 - 969, 7 - 9 March 1978.

5.3.3 Contamination Control

5.3.3.1 Cleanrooms

Banks, D., Cleanroom Fashions of the Future, *Cleanrooms*, Vol. 8, No. 12, p. 30, December, 1994.

Beeson, R. D., Everything you Always Wanted to Know About Cleanroom Garments ..., *Cleanrooms*, p. 27, September, 1989.

Bell, L. L., Cleanroom Cleaning Supplies - Keeping it Clean, *Cleanrooms*, p. 16, January, 1989.

Brandt, B., and Wright, A. L., Analyzing Particle Release of Cleanroom Headcoverings, *Microcontamination*, p. 53, October, 1990.

Burdick, L. A., Jr., Hultquist, A. E., and Mason, K. D., Clean Room for Hubble Space Telescope, *Optical System Contamiantion: Effects, Measurment, Control*, SPIE Vol. 777, No. 777-24, pp. 203 - 210, 19 - 22 May 1987.

Burnett, J., Trends in Cleanroom Selection: Alternatives for Contamination Protection, *Microcontamination*, p. 34, May, 1986.

Cowie, B., Particle Control Technologies Fashioned into Cleanroom Garments, *Cleanrooms*, p. 24, September, 1984.

Devloo, G. H., Design Energy Efficiency into Cleanroom Mechanical Systems, *Cleanrooms*, p. 10, October, 1988.

Dillenbeck, K., Characterization of Air Ionization in the Cleanroom, *Microcontamination*, p. 41, June, 1985.

Dixon, A. M., Guidelines for Clean Room Management and Discipline, *Handbook of Contamination Control in Microelectronics*, D. L. Tolliver, ed,, Noyes Publications, Park Ridge, NJ, pp. 136 - 152, 1988.

Dixon, R. C., Managing and Motivating Cleanroom Personnel, *Microcontamination*, p. 16, April, 1985.

Dutton, D. A., Select the Right (and Left) Cleanroom Glove for the Job, *Cleanrooms*, p. 18, September, 1988.

Fitch, H. D., Contamination Control Expands our Horizons, *Cleanrooms*, Vol. 8, No. 12, p. 38, December, 1994.

Fitch, H. D., The Unfamiliar, the Unknown, and the Invisible, *Cleanrooms*, p. 10, August, 1992.

Fitton, P., Barrett, G. F. C., Contamination Control Flooring Keeps Dirty Feet out of Clean Areas, *Cleanrooms*, p. 31, September, 1988.

Frick, R. W., and Miller, M. C., Designing NASA's Largest Cleanroom, *Microcontamination*, p. 37, January, 1992.

Gerbig, F. T., Upgrading your Cleanroom, *Microcontamination*, p. 43, January, 1992.

Gianino, R., Understanding Cleanroom Facilities and Functions, *Cleanrooms*, Vol. 8, No. 12, pp. 16, December, 1994.

Goodwin, B. W., Clean Room Garments and Fabrics. *Handbook of Contamination Control in Microelectronics*, D. L. Tolliver, ed, Noyes Publications, Park Ridge, NJ, pp. 110 - 134, 1988.

Greiner, J., Grant, L., Huffman, T., and Patel, W., Designing a High Performance, Low Energy Cost Cleanroom: A Case Study, *Cleanrooms*, p. 14, January, 1992.

Hauenstein, L. R., Cosmetics in the Cleanroom: Is it a Problem?, *Cleanrooms*, p. 17, April, 1991.

Helander, R. D., Certifying a Class 10 Cleanroom Using Federal Standard 209C, *Microcontamination*, p. 45, September, 1987.

Hertzson, L., Garments go to High-Tech Designs to Meet Needs of Today's Cleanrooms, *Cleanrooms*, p. 14, September, 1988.

Huffman, R. T., Patel, W., and Petit, R., Clean Construction Methodology for "Narrow Time Window" Cleanroom Construction Project, *Cleanrooms*, p. 40, February, 1992.

Kraft,R., Build the Clean into Cleanrooms by Enforcing Quality Assurance Protocols During Construction Phase, *Cleanrooms*, p. 18, October, 1988.

LeClerc, M., The Who, What, When, Why, and How of Room Certification, *Cleanrooms*, p. 23, June, 1988.

Low, D. C., Recommended Tests for Nonwoven Cleanroom Garment Materials, *Cleanrooms*, p. 16, January, 1991.

Magdelain, R. S., Maintain the Clean in Cleanrooms with the Proper Tools and Procedures, *Cleanrooms*, p. 39, September, 1988

McCraty, R., Electrostatics in Clean Rooms, *Handbook of Contamination Control in Microelectronics*, D. L. Tolliver, ed, Noyes Publications, Park Ridge, NJ, pp. 153 - 184, 1988.

Mears, E. L., Mini-Environments: No Band-Aid for Contamination Control, *Cleanrooms*, Vol. 8, No. 10, p. 23, October, 1994.

Mitch: K., Glove Performance Reults During Simulated Usage, *Cleanrooms*, p. 18, September, 1991.

Nappi, J. J., Jr., Air Showers: Their Role in the Fight Against Contamination, *Cleanrooms*, p. 26, May, 1991.

Naughton, P., Planning for Facility Expansion, *Microcontamination*, p. 55, November, 1987.

Robertson, J. T., Cleanroom Design Issues for the 1990's, *Cleanrooms*, p. 18, May, 1991.

Salvo, N. M., Practical Considerations in Contamination Source Control: How to Make the Best of a Retrofit Cleanroom, *Microcontamination*, p. 43, April, 1985.

Scott, G. L., The Cleanroom is so Precious, that it Should be Designed with a Bodyguard of Support Facilities, *Cleanrooms*, p. 18, May, 1989.

Seemayer, W., Dress for Cleanliness Using Head-to-Toe Gowning Procedures, *Cleanrooms*, p. 10, April, 1988.

Soules, W. J., Airflow Management Techniques, *Cleanrooms*, p. 17, February, 1991.

Soules, W. J., Considerations in Garment Selection, *Cleanrooms*, p. 18, January, 1993.

Spector, R., Berndt, C., and Burnett, E., Reviewing Methods for Evaluating Cleanroom Garment Fabrics, *Microcontamination*, p. 31, March, 1993.

Stokes, K. H., Change Rooms: Design and Operation, *Microcontamination*, p. 12, June, 1987.

Sullivan, G., and Trimble, J., Evaluation of Face Coverings, *Microcontamination*, p. 65, May, 1986.

Whyte, W., and Donaldson, N., Cleaning a Cleanroom, *Microcontamination*, p. 49, November, 1987.

Wolf, R., Cleanroom 2005 - A Glimpse into the Future, *Cleanrooms*, Vol. 8, No. 12, pp. 6, December, 1994.

Wright, M. W., Criteria and Methods to Evaluating Performance when Comparing Filters to Filters, *Cleanrooms*, p. 26, May, 1989.

5.3.3.2 Controlling Particulates

Donovan, R. P., Locke, B. R., and Ensor, D. S., Measuring Particle Emissions from Cleanroom Equipment, *Microcontamination*, p. 36, Octobe. 1987.

Hamberg, O., Particulate Fallout Predictions for Cleanrooms, *J. Env. Sci.*, p. 15 - 20, May - June 1982.

Hoening, S. A., Keeping Dust off Optical Components, *Applied Optics*, Vol. 18, No. 10, pp. 1471, 15-May, 1979.

Kasper, G., and Wen, H. Y., Particles in Ultrapure Process Gases, *Handbook of Contamination Control in Microelectronics*, D. L. Tolliver, ed, Noyes Publications, Park Ridge, NJ, pp. 301 - 346, 1988.

Khilnani, A., and Matsuhiro, D., Adhesion Forces in Particle Removal from Wafer Surfaces, *Microcontamination*, Vol. , No. , pp. 28 - 30, April, 1986.

Kitagawa, Y., Hayashi, A., and Minami, S., Fiber-Optic Particle Size Monitor, *Applied Optics*, Vol. 27, No. 15, pp. 3068 - 3073, August, 1988.

Lieberman, A., Sampling the Air to Monitor and Validate a Room Under Federal Standard 209C, *Cleanrooms*, p. 16, June, 1988.

Loeb, W. E., Particulate Contamination - Tie-Down with Parylene C, *Proceedings of the USAF/NASA International Spacecraft Contamination Conference*, Vol. NASA CP-2069, No. AFML-TR-78-220, pp. 863 - 879, 7 - 9 March, 1978.

Moore, E. W., Contamination of Technological Components by Human Dust, *Microcontamination*, p. 65, September, 1985.

Rooney, J. L., Pui, D. Y. H., and Grant, D. C., Evaluating Particle Removal Efficiencies of Wafer-Cleaning Techniques using Standard Particles, *Microcontamination*, p. 37, May, 1990.

Strasser, G., and Bader, M., Controlling Particle Contamination During Venting and Pumping of Vacuum Loadlocks, *Microcontamination*, p. 45, May, 1990.

Tullis, B. J., Particle Contamination by Process Equipment, *Handbook of Contamination Control in Microelectronics*, D. L. Tolliver, ed, Noyes Publications, Park Ridge, NJ, pp. 410 - 441, 1988.

Yost, M., and Steinman, A., Electrostatic Attraction and Particle Control, *Microcontamination*, p. 18, June, 1986.

5.3.3.3 Cleaning Techniques

Anon., Cleaning with Supercritical CO2, *NASA Tech Briefs*, MFS-29611, March, 1979.

Barsh, M. K., Second Surface Mirror Cleaning and Verification, *Proceedings of the USAF/NASA International Spacecraft Contamination Conference*, NASA CP-2071, AFML-TR-78-222, pp. 927 - 944, 7 - 9 March 1978.

Deguchi, T. J., and Kalem, C. B., Oxygen Ion Cleaning of Organic Contaminant Films, *Optical System Contamiantion: Effects, Measurment, Control*, SPIE Vol. 777, No. 777-47, pp. 333 - 338, 19 - 22 May 1987.

Feicht, J. R., Blanco, J. R., and Champetier, R. J., Dust Removal from Mirrors: Experiments and Analysis of Adhesion Forces, *Stray Light and Contamination in Optical Systems*, SPIE Vol. 967, No. 967-37, pp. 19 - 29, 17 - 19 August 1988.

Fine, J., and Pernick, B. J., Use of Strippable Coatings to Protect and Clean Optical Surfaces, *Applied Optics*, Vol. 26, No. 16, pp. 3172 - 3173, August, 1987.

Fisher, R. F., George, P. M., Flammang, S. M., and Howard, T. L., Ion-Beam Cleaning of Contaminated Optics, *Optical System Contamination: Effects, Measurement, Control II*, SPIE Vol. 1329, No. 1329-10, pp. 86 - 97, 10 - 12 July 1990.

George, P. M., Lindquist, J. M., and Hankins, M., Ion Beam Removal of Water and Dioctyl Phthalate from Cryogenic Mirrors, *J. Spacecraft*, Vol. 27, No. 3, pp. 253 - 257, May - June, 1990.

Halber, J., Using Ultrasonic Techniques for Wet-Process Cleaning, *Microcontamination*, p. 36, December, 1988.

McDermott, W. T., Ockovic, R. C., Wu, J. J., and Miller, R. J., Removing Submicron Surface Particles Using a Cryogenic Argon-Aerosol Technique, *Microcontamination*, p. 2, October, 1991.

Musselman, R. P., and Yarbrough, T. W., Shear Stress Cleaning for Surface Departiculation, *J. Env. Sci.*, p. 51 - 56, January/February, 1987.

Osiecki, R. A., and Magee, T. J., Ultraviolet Laser Cleaning of Mirror Surfaces, *Optical System Contamination: Effects, Measurement, Control II*, SPIE Vol. 1329, No. 1329-12, p. 127 - 133, 10 - 12 July 1990.

Peterson, R. V., and Bowers, C. W., Contamination Removal by CO2 Jet Spray, *Optical System Contamination: Effects, Measurement, Control II*, SPIE Vol. 1329, No. 1329-13, pp. 72 - 85, 10 - 12 July 1990.

Pierce, V. G., Frish, M. B., Green, B. D., Piper, L. G., Guregian, J. J., and Anapol, M. I., Laser-Mirror Cleaning in a Simulated Space Environment, *Optical System Contamination: Effects, Measurement, Control II*, SPIE Vol. 1329, No. 1329-36, p. 134 - 140, 10 - 12 July 1990.

Piper, L. G., Frish, M. B. Pierce, V. G., and Green, B. D., Laser Cleaning of Cryogenic Optics, *Optical System Contamination: Effects, Measurement, Control II*, SPIE Vol. 1329, No. 1329-09, pp. 110 - 126, 10 - 12 July 1990.

Piper, L. G., Spencer, M. N., Woodward, A. M., and Green, B. D., CROSS: Contaminant Removal off Optical Surfaces in Space, *Optical System Contamiantion: Effects, Measurment, Control*, SPIE Vol. 777, No. 777-46, pp. 320 - 332, 19 - 22 May 1987.

Shaw, C. G., Contamination Removal by Ion Sputtering, *Optical System Contamination: Effects, Measurement, Control II*, SPIE Vol. 1329, No. 1329-08, pp. 98 - 109, 10 - 12 July 1990.

Walter, A. E., Using an Integrated System to Clean and Dry Precision Parts, *Microcontamination*, p. 31, January, 1992.

5.3.3.4 Monitoring Techniques

Aline, K. M., and Dowda[illegible]., Dark Field Photographic Techniques for Documenting Optical Surface Contamination, *Scatter from Optical Components* Vol. 1165, No. 1165-36, pp. 401 - 405, 8 - 10 August 1989.

Amore, L. J., Cariou, F. E., and Riviello, S. J., X-Ray Flourescence Contamination Detection Studies, *RADC-TR-87-299*, January, 1988.

Anon., Pressure Roller for Tape-Lift Tests, *NASA Tech Briefs*, pp. 105, September, 1991.

Anon., Recommended Practice for QCM (Quartz Crystal Microbalance) Measurement of Spacecraft Molecular Contamination, *ASTM Document: E21.05-QCM-90.01*, Draft "C", 20 February 1995.

Arora, A., Surface Contamination Measurement and Control by Nondestructive Techniques, *J. Env. Sci.*, p. 30 - 32, November - December, 1985.

Beck, D. G., et. al, Investigation of Contamination on Optical Surveillance Systems, *RADC-TR-87-230*, November, 1987.

Bennett, J. M., Mattsson, L., Keane, M. P., and Karlsson, L., Test of Strip Coating Materials for Protecting Optics, *Applied Optics*, Vol. 28, No. 5, pp. 1018 - 1026, March, 1989.

Benson, R. C., Bargeron, C. B., Phillips, T. E., and Uy, O. M., Analysis of Mirror Surface after Laser or Ion Removal of Contaminants, *Optical System Contamination: Effects, Measurement, Control II*, SPIE Vol. 1329, No. 1329-11, pp. 141 - 167, 10 - 12 July 1990.

Borson, E. N., An Overview of Contamination Monitoring in Ground Operations, *The Aerospace Corporation*, Workshop on Molecular Contamination Detection/Outgassing, 24 October 1989.

Borson, E. N., Watts, E. J., and To, G. A., Standard Method for Measurement of Nonvolatile Residue on Surfaces, *SD-TR-89-63*, The Aerospace Corporation, 10 August 1989.

Bryson, R. J., Seiber, B. L., Bertrand, W. T., Jones, J. H., Wood, B. E., and Lesho, J. C., Pre-Flight Testing of Thermoelectric Quartz Crystal Microbalances (TQCM) for Midcourse Space Experiment (MSX) Spacecraft, *Arnold Engineering Development Center*, Vol. AEDC-TR-93-24, No. , pp. , February, 1994.

Carre, D. J., and Fleischauer, P. D., Contamination Simulation Facility with in situ Infrared Analysis Capability, *Shuttle Optical Environment*, SPIE Vol. 287, No. 287-18, pp. 116 - 122, 23 - 24 April 1981.

Chuan, R. L., and Bowers, W. D., Nonoptical Real-Time Particle Fallout Monitor, *Optical System Contamination: Effects, Measurement, Control II*, SPIE Vol. 1329, No. 1329-14, pp. 168 - 178, 10 - 12 July 1990.

Cooper, D. W., Analyzing Nonvolatile Residue Using Aerosol Formation and Measurement, *Microcontamination*, p. 29, April, 1992.

Fountain, J. A., Temperature Controlled Quartz Crystal Microbalance Measurements on Space Transportation System (STS-2), *Spacecraft Contamination Environment*, SPIE Vol. 338, p. 24 - 29, 4 - 6 May 1982.

Gause, R. L., A Noncontacting Scanning Photoelectron Emission Technique for Bonding Surface Cleanliness Inspection, *NASA TM-100361*, February, 1989.

Gise, P., Surface Particle Detection Technology, *Handbook of Contamination Control in Microelectronics*, D. L. Tolliver, ed, Noyes Publications, Park Ridge, NJ, pp. 383 - 409, 1988.

Harvey, G. A., Raper, J. L., and Zellers, D. C., Measuring Low-Level Nonvolatile Residue Contamination on Wipes, Swabs, and Gloves, *Microcontamination*, p. 43, November, 1990.

Hass, G., and Hunter, W. R., Laboratory Experiments to Study Surface Contamination and Degradation of Optical Coatings and Materials in Simulated Space Environments, *Applied Optics*, Vol. 9, No. 9, pp. 2101 - 2110, September, 1970.

Jarratt, R. V., Jr., Flink, B. K., Fancy, R. D., and Linton, R. C., Self-Contained Space Qualifiable Optical Contamination Monitor, *Optical System Contamiantion: Effects, Measurment, Control*, SPIE Vol. 777, No. 777-17, pp. 171 - 178, 19 - 22 May 1987.

Judeikis, H. S., Arnold, G. S., Young Owl, R. C., and Hall, D. F., Design of a Laboratory Study of Contaminant Film Darkening in Space, *The Aerospace Corporation*, TR-94 (4935) -3, 1 October 1993.

Koch, W. R., and Moseley, M. J., Preparation and Cleanliness Verification of a Space Simulation Chamber for Contamination Sensitive Test Specimens, *14th Space Simulation Conference*, The Payload - Testing for Success, NASA CP-2341, pp. 343 - 352, 8 - 11 October, 1984.

Kruger, R., Evaluating a Contamination Hazard with a Residual Gas Analyzer, *Proceedings of the USAF/NASA International Spacecraft Contamination Conference*, NASA CP-2061, AFML-TR-78-212, pp. 644 - 656, 7 - 9 March 1978.

Liu, Chang-Keng, and Glassford, A. P. M., Cost-Effective Method for Measuring Contamination Effects, *J. Spacecraft*, Vol. 16, No. 6, pp. 402 - 404, November - December, 1979.

Maag, C. R., and Scott, R. R., Ground Contamination Monitoring Methods, *Proceedings of the USAF/NASA International Spacecraft Contamination Conference*, NASA CP-2064, AFML-TR-78-215, pp. 741 - 762, 7 - 9 March 1978.

Maag, C. R., National Oceanic and Atmospheric Administration (NOAA) Contamination Monitoring Instrumentation, *Optics in Adverse Environments*, SPIE Vol. 216, No. 216-10, pp. 87 - 94, 4 - 5 February 1980.

McKeown, D., and Claysmith, C. R., Quartz Crystal Microbalance Systems for Shuttle Contamination Measurements, *Proceedings of the USAF/NASA International Spacecraft Contamination Conference*, NASA CP-2059, AFML-TR-78-210, pp. 605 - 628, 7 - 9 March 1978.

Muscari, J. A., Rantanen, R.O., and Pugel, N. J., Applicability of Thermogravimetric Analysis to Space Contamination, *Proceedings of the USAF/NASA International Spacecraft Contamination Conference*, NASA CP-2042, AFML-TR-78-193, pp. 107 - 117, 7 - 9 March 1978.

Nuss, H., Molecular Contamination Studies by Molecular Beam Scattering, *Proceedings of the USAF/NASA International Spacecraft Contamination Conference*, NASA CP-2062, AFML-TR-78-213, pp. 657 - 681, 7 - 9 March 1978.

Rhoades, R., Ground Operations, *Proceedings of the USAF/NASA International Spacecraft Contamination Conference*, NASA CP-2081, AFML-TR-78-232, pp. 1159 - 1161, 7 - 9 March 1978.

Shlanger, S. S., and Epstein, G., Aerospace Corporation work with Optically Stimulated Electron Emission (OSEE), *The Aerospace Corporation*, 25 October 1989.

Shlanger, S., and Lockerby, S., Using the CS 9000 Scanning Densiometer to Detect Contamination, *The Aerospace Corporation*, Workshop on Molecular Contamination Detection/Outgassing, 24 October 1989.

Wallace, D. A., and Wallace, S. A., Realistic Performance Specifications for Flight Quartz Crystal Microbalance Instruments for Contamination Measurement on Spacecraft, *AIAA Paper No. 88-2727*, AIAA Thermophysics, Plasmadynamics, and Lasers Conference, San Antonio, TX, 27 - 29 June 1988.

Wallace, D. A., and Wallace, S. A., Use of a Cryogenically Cooled QCM in Conjunction with a Programmable Data Acquisition System to Detect and Examine Accreted Mass on the Sensing Crystal Caused by Environmental Contamination, *Scatter from Optical Components*, SPIE Vol. 1165, No. 1165-39, pp. 424 - 431, 8 - 10 August 1989.

Wallace, D. A., Considerations in the Use of QCM's for Accurate Contamination Measurement, *Proceedings of the USAF/NASA International Spacecraft Contamination Conference*, NASA CP-2060, AFML-TR-78-211, pp. 629 - 643, 7 - 9 March 1978.

Zwaal, A., Outgassing Measurements on Materials in Vacuum Using a Vacuum Balance and Quartz Crystal Balances, *Proceedings of the USAF/NASA International Spacecraft Contamination Conference*, NASA CP-2043, AFML-TR-78-194, pp. 118 - 150, 7 - 9 March 1978.

5.3.3.5 Program Specific Documents

5.3.3.5.1 Shuttle

Bareiss, L. E., Insights into Contamination Control for the Shuttle Payload Integration Facility (SPIF) at the Eastern Launch Site (ELS), *Shuttle Optical Environment*, SPIE Vol. 287, No. 287-17, pp. 79 - 76, 23 - 24 April 1981.

Bareiss, L. E., Shuttle/Payload Contamination Evaluation (SPACE) Program Verification with the Induced Environment Contamination Monitor, *Optics in Adverse Environments*, SPIE Vol. 216, No. 216-05, pp. 40 - 47, 4 - 5 February 1980.

Bareiss, L. E., Spacelab Induced Environment Technical Overview, *Proceedings of the USAF/NASA International Spacecraft Contamination Conference*, NASA CP-2044, AFML-TR-78-195, pp. 152 - 175, 7 - 9 March 1978.

Bareiss, L. E., Payton, R. M., and Papazian, H. A., Shuttle/Spacelab Contamination Environment and Effects Handbook, *NASA CR-4053*, March, 1987.

Barnhart, B. J., Shuttle Contamination and Experimentation: DoD Implications, *Shuttle Optical Environment*, SPIE Vol. 287, No. 287-04, pp. 25 - 34, 23 - 24 April 1981.

Bettini, R. G., Shuttle Environment Effects on Coated Mirrors, *Optical System Contamiantion: Effects, Measurment, Control*, SPIE Vol. 777, No. 777-03, pp. 20 - 25, 19 - 22 May 1987.

Hamberg, O., Prelaunch and Orbiter Bay Contamination Control at KSC, *The Aerospace Corporation*, No. 78-5124, 16 November, 1978.

Jacobs, S., Leger, L., and Ehlers, H. K. F., Shuttle Payload Integration: Contamination Aspects, *Shuttle Optical Environment*, SPIE Vol. 287, No. 287-15, pp. 54 - 58, 23 - 24 April 1981.

Jarossy, F. J., Shuttle/Payload Contamination Evaluation (SPACE) - A Systems Level Contamination Model, *Optics in Adverse Environments*, SPIE Vol. 216, No. 216-04, pp. 31 - 39, 4 - 5 February 1980.

Jarossy, F. J., Pizzicaroli, J. C., and Owen, N. L., Shuttle/Payload Contamination Evaluation (SPACE) Program Improvements, *Shuttle Optical Environment*, SPIE Vol. 287, No. 287-09, pp. 78 - 85, 23 - 24 April 1981.

Jeffrey, J. A., Maag, C. R., Seastrom, J. W., and Weber, M. F., Assessment of Contamination in the Shuttle Bay, *Shuttle Optical Environment*, SPIE Vol. 287, No. 287-07, pp. 41 - 52, 23 - 24 April 1981.

Kohl, J. L., and Weiser, H., Shuttle Contamination Effects on Ultraviolet Coronagraphic Observations, *Shuttle Optical Environment*, SPIE Vol. 287, No. 287-05, pp. 35 - 40, 23 - 24 April 1981.

Lehmann, J., Tanner, S. G., and Wilkerson, T., eds, The Shuttle Environment Workshop, *Systematics General Corporation*, Report No. 24-5087, NASA GSFC Contrac[illegible]AS5-27362, February, 1983.

McKeown, D., Cox, V. H., and Peters[illegible], R. V., Analysis of TQCM Surface Contamination Absorbed During the Spacelab 1 Mission, *AIAA Paper No. 85-7008*, AIAA Shuttle Environment and Operations II Conference, Houston, TX, 13 - 15 November 1985.

Melfi, L. T., Jr., Hueser, J. E., and Brock, F. J., Direct Simulation Monte Carlo Technique for Modeling of the Environment in the Vicinity of the Space Shuttle Orbiter, *Shuttle Optical Environment*, SPIE Vol. 287, No. 287-10, pp. 86 - 94, 23 - 24 April 1981.

Miller, E. R., Introduction: Preliminary Results of the Induced Environment Contamination Monitor (IECM) Measurements of Space Transportation System (STS-2), *Spacecraft Contamination Environment*, SPIE Vol. 338, pp. 2 - 3, 4 - 6 May 1982.

Moss, R. G., Potential for Cross Contam[illegible]ation for Payloads in the STS Bay, *Spacecraft Contamination: Sources and Prevention*, J. A. Roux and T. D. McCay, eds, Progr[illegible] in Astronautics and Aeronautics, Vol. 91, AIAA, pp. 29 - 36, 1984.

Richmond, R. G., and Kelso, R. M., Effectiveness of the Shuttle Orbiter Payload Bay Liner as a Barrier to Molecular Contamination from Hydraulic Fluids, *Proceedings of the USAF/NASA International Spacecraft Contamination Conference*, NASA CP-2068, AFML-TR-78-219, pp. 846 - 862, 7 - 9 March 1978.

Ruff, R. C., Taeusch, D. R., Oran, W. A., and Rathz, T., Mass Spectrometer for IECM, *Proceedings of the USAF/NASA International Spacecraft Contamination Conference*, NASA CP-2058, AFML-TR-78-209, pp. 567 - 604, 7 - 9 March 1978.

Saylor, W. P., Contamination Control Plan for a Shuttle Payload, *AIAA-83-2647*, Shuttle Environment Conference, October, 1983.

Scialdone, J. J., Assessment of Shuttle Payloads Gaseous Environment Contamination and its Control, *Spacecraft Materials in Space Environment*, ESA SP-149, pp. 101 - 116, 2 - 5 October 1979.

5.3.3.5.2 Hubble Space Telescope

Aguilar, L., Kwan, S., Smith, M., Bush, J., Steakley, J., and Kruse, B., Environmental Monitoring Data for the Hubble Space Telescope Clean Room, *Optical System Contamiantion: Effects, Measurment, Control*, SPIE Vol. 777, No. 777-33, pp. 288 - 298, 19 - 22 May 1987.

Bush, J., Lloyd, S., Martin, S., Burdick, L., Liggio, B., and Nerren, B., Hubble Space Telescope Protective Cover System, *Optical System Contamiantion: Effects, Measurment, Control*, SPIE Vol. 777, No. 777-32, pp. 278 - 287, 19 - 22 May 1987.

Cheney, G. D., Cleanliness Maintenance of NASA's Hubble Space Telescope, *Perkin Elmer Optical Group*, PA 10551, November, 1985.

Fong, M. C., Peterson, M. A., and Lee, A. L., Hubble Space Telescope Contamination Analysis, *Optical System Contamiantion: Effects Measurment, Control*, SPIE Vol. 777, No. 777-25, pp. 211 - 225, 19 - 22 May 1987.

Leschly, K., Taylor, D. M., Jenkins, T., and Barengoltz, J. B., Strategy for Contamination Control to Improve Wide-Field Planetary Camera Far-Ultraviolet Performance, *Optical System Contamination: Effects, Measurement, Control II*, SPIE Vol. 1329, No. 1329-06, pp. 42 - 57, 10 - 12 July 1990.

Peterson, M. A., and McCloskey, D. B., Hubble Space Telescope low Pressure Venting: Analysis, Thermal Vacuum Test Solution, Validation, and Flight Prediction, *Optical System Contamiantion: Effects, Measurment, Control*, SPIE Vol. 777, No. 777-29, pp. 252 - 264, 19 - 22 May 1987.

Steakley, J. M., Glassford, P., Osiecki, R. A., Tenerelli, D. J., Burdick, L. A., Jr., Housten, S. J., and Hultquist, A. E., Definition and Implementation of a Thermal Vacuum Bakeout Program for the Hubble Space Telescope, *Optical System Contamiantion: Effects, Measurment, Control*, SPIE Vol. 777, No. 777-28, pp. 246 - 251, 19 - 22 May 1987.

5.3.3.5.3 Other

Abrams, E. M., and Carosso, N. P., Science Objectives lead to Contamination Requirements for the Cosmic Background Explorer, *Optical System Contamination: Effects, Measurement, Control II*, SPIE Vol. 1329, No. 1329-02, pp. 16 - 23, 10 - 12 July 1990.

Andreozzi, L. C., Irace, W., and Maag, C. R., Contamination Control of the [illegible]ed Astronomical Satellite, *Optics in Adverse Environments*, SPIE Vol. 216, No. 216-06, pp. 48 - 60, 4 - 5 February 19[illegible]0.

Carosso, N. J. P., Space Station Users Contamination Requirements, *Optical System Contamiantion: Effects, Measurment, Control*, SPIE Vol. 777, No. 777-12, pp. 138 - 145, 19 - 22 May 1987.

Carosso, P. A., Upper Atmosphere Research Satellite (UARS) Contamination Control Approach, *Optical System Contamiantion: Effects, Measurment, Control*, SPIE Vol. 777, No. 777-13, pp. 146 - 152, 19 - 22 May 1987.

Carre, D. J., Dowling, J. M., Herm, R. R., Harvey, N. M., Peplinski, D. R., Pluchino, A., Borson, E. N., Champetier, R. J., and Peterson, R. V., Contamination Prevention and Control Plan for the Talon Gold Experiment, *The Aerospace Corporation*, TOR-0080 (5755) - 2, 29 September 1980.

Desloire, M., and Jaeger, R., Cleanliness Aspect of the Ariane Payload Bay, *Spacecraft Materials in Space Environment*, ESA SP-150, pp. 117 - 130, 2 - 5 October 1979.

Dyer, J. S., Mikesell, R., Perry, R., Mikesell, T., and Guregian, J. J., Contamination Measurements during Development and Testing of the SPIRIT III Cryogenic Infrared Telescope, , SPIE Vol. 2261, 1994.

Edwards, P. G., and Marcoux, J., METEOSAT Cleanliness Control Principles, *Spacecraft Materials in Space Environment*, ESA SP-148, pp. 91 - 100, 2 - 5 October 1979.

Farren, D. B., Generic Contamination Analysis for the Titan IV Launch Vehicle, *Martin Marietta*, MCR-87-2547, February, 1988.

Guttman, A., Furber, R. D., and Muntz, E. P., Protection of Satellite Infrared Experiment (SIRE) Cryogenic Infrared (IR) Optics in Shuttle Orbiter, *Optics in Adverse Environments*, SPIE Vol. 216, No. 216-26, pp. 174 - 185, 4 - 5 February 1980.

Hall, D. F., ML12 Spacecraft Contamination and Coatings Degradation Flight Experiment, *AFWAL-TR-83-4140*, Interim Report for Period: 23 Dec 74 - 30 Sep 83, December, 1983.

Hoffman, A. R., and Koukol, R. C., Particulate Contamination Control for the Viking and Voyager Unmanned Planetary Spacecraft, *Proceedings of the USAF/NASA International Spacecraft Contamination Conference*, NASA CP-2070, AFML-TR-78-221, pp. 899 - 926, 7 - 9 March 1978.

Linton, R. C., Optical Effects Module and Passive Sample Array, *Spacecraft Contamination Environment*, SPIE Vol. 338, No. , pp. 16 - 23, 4 - 6 May 1982.

Mah, D. L., Preliminary Assessment of the Space Infrared Experiment's (SIRE) Potential for Contamination, *Shuttle Optical Environment*, SPIE Vol. 287, No. 287-13, pp. 108 - 115, 23 - 24 April 1981.

Mauldin, L. E., III, and Chu, W. P., Optical Degradation due to Contamination on the SAGE/SAGE II Spaceflight Instruments, *Spacecraft Contamination Environment*, SPIE Vol. 338, No. 338-05, pp. 58 - 64, 4 - 6 May 1982.

Mrowka, S., Jelinsky, S., Jelinsky, P., and Malina, R. F., Contamination Control Approach for the Extreme Ultraviolet Explorer Satellite Instrumentation, *Optical System Contamiantion: Effects, Measurment, Control*, SPIE Vol. 777, No. 777-05, pp. 34 - 42, 19 - 22 May 1987.

Mullen, C., and Shaw, C. G., Contamination Measurements During IUS Thermal Vacuum Tests in a Large Space Chamber, *15th Space Simulation Conference*, The Payload - Testing for Success, NASA CP-2342, pp. 353 - 371, 8 - 11 October 1984.

Pepi, J. W., Kahan, M. A., Barnes, W. H., and Zielinski, R. J., Teal Ruby - Design, Manufacture and Test, *Optics in Adverse Environments*, SPIE Vol. 216, No. 216-20, pp. 160 - 173, 4 - 5 February 1980.

Ray, D. C., Jelinsky, S. R., Welsh, B. Y., and Malina, R. F., Contamination Control Program Results from Three Years of Ground Operations on the Extreme Ultraviolet Explorer Instruments, *Optical System Contamination: Effects, Measurement, Control II*, SPIE Vol. 1329, No. 1329-03, pp. 24 - 30, 10 - 12 July 1990.

Steakley, J. M., Raar, D. J., and Smith, M. P., Contamination Monitoring During the Hubble Space Telescope Thermal Vacuum/Thermal Balance Test, *Optical System Contamiantion: Effects, Measurment, Control*, SPIE Vol. 777, No. 777-30, pp. 265 - 270, 19 - 22 May 1987.

Steakley, R. C., King, A. D., and Rigney, R. E., Contamination Control of the Cryogenic Limb Array Etalon Spectrometer, *Optical System Contamination: Effects, Measurement, Control II*, SPIE Vol. 1329, No. 1329-04, pp. 31 - 41, 10 - 12 July 1990.

Wheeler, N. B., Nadile, R., Gardiner, H. A. B., Gibson, J., Bates, L., Guregian, J., and Benoit, B., CIRRIS Mirror Cleaning History Review, *Air Force Phillips Laboratory*, PL-TR-91-2166, 8 July 1991.

Yee, J. H., and Abreu, V. J., Optical Contamination on the Atmosphere Explorer-E Satellite, *Spacecraft Contamination Environment*, SPIE Vol. 338, No. 338-11, pp. 120 - 128, 4 - 6 May 1982.

5.3.3.6 Other Contamination Control

Austin, J. D., Contamination Control Plan for Prelaunch Operations, *Spacecraft Contamination Environment*, SPIE Vol. 338, No. 338-01, pp. 42 - 48, 4 - 6 May 1982.

Borson, E. N., Contamination Control Documents for Use in Statements of Work and Contamination Control Plans for Spacecraft Programs, *Aerospace Report No. TOR-93(3411)-5*, 30 September 1993.

Borson, E. N., Spacecraft Contamination Experience, *NASA/SDIO Space Environmental Effects on Materials Workshop*, NASA CP-3035, pp. 331 - 352, 28 June - 1 July 1988.

Borson, E. N., The Control of Contamination - Where are we Going?, *Proceedings of the USAF/NASA International Spacecraft Contamination Conference*, NASA CP-2078, AFML-TR-78-229, pp. 1129 - 1137, 7 - 9 March 1978.

Bowers, W. D., and Chuan, R. L., 200 MHz Surface Acoustic Wave Mass Microbalance, *Optical System Contamination: Effects, Measurement, Control II*, SPIE Vol. 1329, No. 1329-15, pp. 179 - 188, 10 - 12 July 1990.

Bremer, J. C., General Contamination Criteria for Optical Surfaces, *Shuttle Optical Environment*, SPIE Vol. 287, No. 287-02, p. 34,991, 23 - 24 April 1981.

Chen, A. T., Abe, N. D., Mullen, C. R., and Gilbert, C. C., Contamination Sensivity and Control of Optical Sensors, *Optical System Contamiantion: Effects, Measurment, Control*, SPIE Vol. 777, No. 777-10, pp. 97 - 126, 19 - 22 May 1987.

Chen, P., GSFC Contamination Engineering, *The Aerospace Corporation*, Proceedings of the Spacecraft Thermal Control Technology Workshop, Section 3.12 , 3 - 5 February 1993.

Crutcher, E. R., Assemblage Analysis - Identification of Contamination Sources, *Proceedings of the USAF/NASA International Spacecraft Contamination Conference*, NASA CP-2065, AFML-TR-78-216, pp. 763 - 778, 7 - 9 March 1978.

Dauphin, J., European Contamination Concerns, *Proceedings of the USAF/NASA International Spacecraft Contamination Conference*, NASA CP-2079, AFML-TR-78-230, pp. 1138 - 1154, 7 - 9 March 1978.

Enlow, D. L., Klotzbucher, D. M., and Odell, E. L. G., Environmental Test System - Design and Development, *Vol. II*, Air Force Wright Aeronautical Laboratory, AFWAL-TR-83-4031, January, 1984.

Hall, D. F., Spacecraft Contamination Flight Measurement Program, *AIAA 87-1624*, AIAA 22nd Thermophysics Conference, Honolulu, HI, 8 - 10 June 1987.

Hamberg, O., Prelaunch and Orbiter Bay Contamination Control at KSC, *The Aerospace Corporation*, Vol. 78-5124.17-15, 16-Nov. 1978.

Hansen, P. A., Operational Strategies for Contamination Control of Composite Materials, *17th Space Simulation Conference*, Terrestrial Test for Space Success, NASA CP-3181, pp. 251 - 252, 9 - 12 November 1992.

Hansen, P. A., and Maag, C. R., Development of Contamination Requirements for Spaceborne Optical Instrumentation, *Optical System Contamiantion: Effects, Measurment, Control*, SPIE Vol. 777, No. 777-08, pp. 68 - 78, 19 - 22 May 1987.

Lumsden, J. M., and Noel, M. B., Purging Sensitive Science Instruments with Nitrogen in the STS Environment, *AIAA 83-2645*, 1983.

Madden, P. G., Low-Cost Analysis for an Effective Contamination Control Program, *Microcontamination*, p. 20, October, 1986.

Muscari, J. A., and Jacobs, S., Silver-Teflon Contamination UV Radiation Study, *Proceedings of the USAF/NASA International Spacecraft Contamination Conference*, NASA CP-2077, AFML-TR-78-228, pp. 1112 - 1127, 7 - 9 March 1978.

Parker, H. W., Humidity Monitor and Dew Point Hygrometer, *Spacecraft Contamination Environment*, SPIE Vol. 338, p. 4, 4 - 6 May 1982.

Pipes, J. G., Frazine, D. F., Young, R. P., Borson, E. J., and Rachal, L. H., Spacecraft Test Chamber Contamination Study - AEDC Mark I Facility, *Proceedings of the USAF/NASA International Spacecraft Contamination Conference*, NASA CP-2073, AFML-TR-78-224, pp. 971 - 1005, 7 - 9 March 1978.

Ray, D. C., Malina, R. F., Welsh, B. Y., and Battel, S. J., Contaminaiton Monitoring Approaches for EUV Space Optics, *Scatter from Optical Components*, SPIE Vol. 1165, No. 1165-40, pp. 432 - 443, 8 - 10 August 1989.

Schmidt, G., VLS Payload Ground Operations Plan, *Vandenberg Air Force Base*, Vol. VCP-81-254 , 31 January 1983.

Scialdone, J. J., Abatement of Gaseous and Particulate Contamination in a Space Instrument, *AIAA 83-1567*, AIAA 18th Thermophysics Conference, Montreal, Canada, 1 - 3 June 1983.

Shaw, C. G., Thornton, M. M., and Mullen, C. R., Contamination Effects Test Facility, *Optical System Contamiantion: Effects, Measurment, Control*, SPIE Vol. 777, No. 777-20, pp. 189 - 198, 19 - 22 May 1987.

Stowers, I. F., Fundamentals of Contamination Control Technology, *Lawrence Livermore Laboratory*, UCID-19022, 21 April 1981.

Taylor, D. M., Soules, D., and Osborn, D., JPL Molecular Contamination Investigation Facility, *Optical System Contamination: Effects, Measurement, Control II*, SPIE Vol. 1329, No. 1329-20, pp. 233 - 245, 10 - 12 July 1990.

5.3.4 General

Bueker, R., and Willard, M. T., Interplanetary Spacecraft Decontamination Operations and Equipment, *J. Spacecraft*, Vol. 5, No. 8, pp. 990 - 993, August, 1968.

Freniere, E. R., Application of the General Unwanted Energy Rejection Analysis Program (GUERAP) in Evaluating On-Station Optical Performance, *Optics in Adverse Environments*, SPIE Vol. 216, No. 216-12, pp. 102 - 108, 4 - 5 February 1980.

Hale, R. R., An Improved Technique to Predict Space System Contamination, *Proceedings of the USAF/NASA International Spacecraft Contamination Conference*, NASA CP-2046, AFML-TR-78-197, pp. 230 - 249, 7 - 9 March 1978.

Herm, R. R., Johnson, B. R., and Young, S. J., Prevention of Primary Mirror Contamination by Helium Purging, *Optical System Contamiantion: Effects, Measurment, Control*, SPIE Vol. 777, No. 777-14, pp. 154 - 161, 19 - 22 May 1987.

Jeaney, J. B., Comparative Review of Optical Surface Contamination Assessment Techniques, *Optical System Contamiantion: Effects, Measurment, Control*, SPIE Vol. 777, No. 777-18, pp. 179 - 188, 19 - 22 May 1987.

Jemiola, J. M., Spacecraft Contamination - A Now and Future Concern, *Optics in Adverse Environments*, SPIE Vol. 216, No. 216-01, pp. 34,738, 4 - 5 February 1980.

Mittal, K. L., Surface Contamination Control Primer, *Cleanrooms*, p. 10, April, 1993.

Muscari, J. A. Mah, D., and Somers, R. Satellite Contamination - II, Volume I, Analytical Equations, Laboratory Tests, and Space Application, *AFWAL-TR-81-4059*, Vol. 1, August, 1981.

Naumann, R. J., Contamination Assessment and Control in Scientific Satellites, *NASA TN D-7433*, October, 1973.

Simpson, J. P., and Witteborn, F. C., Infrared Radiation From the Space Contaminant Environment, *Proceedings of the USAF/NASA International Spacecraft Contamination Conference*, NASA CP-2045, AFML-TR-78-196, pp. 176 - 207, 7 - 9 March 1978.

Thornton, M. M., Spacecraft Contamination Database, *Optical System Contamination: Effects, Measurement, Control II*, SPIE Vol. 1329, No. 1329-27, pp. 305 - 317, 10 - 12 July 1990.

Tribble, A. C., *The Space Environment - Implications for Spacecraft Design*, Princeton University Press, Princeton, NJ, 1995.

REPORT DOCUMENTATION PAGE

Form Approved
OMB No. 0704-0188

1. AGENCY USE ONLY (Leave Blank)	2. REPORT DATE	3. REPORT TYPE AND DATES COVERED
	May 1996	Contractor Report (Final)

4. TITLE AND SUBTITLE

Contamination Control Engineering Design Guidelines for the Aerospace Community

5. FUNDING NUMBERS

NAS5-32876

6. AUTHOR(S)

A. C. Tribble, B. Boyadjian, J. Davis, J. Haffner, and E. McCullough

7. PERFORMING ORGANIZATION NAME(S) AND ADDRESS(ES)

Rockwell International Corporation
12214 Lakewood Blvd, P. O. Box 7009
Downey, CA 90241-7009

8. PERFORMING ORGANIZATON REPORT NUMBERS

M-810

9. SPONSORING/MONITORING AGENCY NAME(S) AND ADDRESS(ES)

NASA Goddard Space Flight Center*
Greenbelt, Maryland

10. SPONSORING/MONITORING AGENCY REPORT NUMBER

NASA CR-4740

11. SUPPLEMENTARY NOTES

*The report was prepared for the NASA Goddard Space Flight Center as one of the technology development contracts sponsored by the Space Environments & Effects Program managed at the Marshall Space Flight Center, Huntsville, Alabama.

12a. DISTRIBUTION/AVAILABILITY STATEMENT

Subject Category 31

Unclassified-Unlimited

12b. DISTRIBUTION CODE

13. ABSTRACT *(Maximum 200 words)*

Thermal control surfaces, solar arrays, and optical devices may be adversely affected by a small quanitity of molecular and/or particulate contamination. What is rarely discussed is how one: a) quantifies the level of contamination that must be maintained in order for the system to function properly, and b) enforces contamination control to ensure compliance with requirements. This document is designed to address these specific issues and is intended to serve as a handbook on contamination control for the reader, illustrating process and methodology while providing direction to more detailed references when needed. The effects of molecular contamination on reflecting and transmitting surfaces are examined and quantified in accordance with MIL STD 1246C. The generation, transportation, and deposition of molecular contamination is reviewed and specific examples are worked to illustrate the process a design engineer can use to estimate end of life cleanliness levels required by solar arrays, thermal control surfaces, and optical surfaces. A similar process is used to describe the effect of particulate contamination as related to percent area coverage (PAC) and bi-directional reflectance distribution function (BRDF). Relationships between PAC and surface cleanliness, which include the effects of submicron sized particles, are developed and BRDF is related to specific sensor design parameters such as Point Source Transmittance (PST). The pros and cons of various methods of preventing, monitoring, and cleaning surfaces are examined and discussed.

14. SUBJECT TERMS

Contamination, Contamination Guidelines

15. NUMBER OF PAGES

130

16. PRICE CODE

A07

17. SECURITY CLASSIFICATION	18. SECURITY CLASSIFICATION OF THIS PAGE	19. SECURITY CLASSIFICATION OF ABSTRACT	20. LIMITATION OF ABSTRACT
Unclassified	Unclassified	Unclassified	Unlimited